UNIVERSITÀ
DEGLI STUDI
FIRENZE

DOTTORATO DI RICERCA IN
Scienza per la conservazione dei Beni Culturali

CICLO XXVI

COORDINATORE Prof. Piero Baglioni

Study of contemporary artworks and artists' materials by means of spectroscopic techniques

Settore Scientifico Disciplinare FIS/07

Dottorando
Dott.ssa Marchiafava Veronica

Tutore
Prof. Marcello Picollo

Co-Tutore
Prof. Antonella Salvini

Coordinatore
Prof. Baglioni Piero

Anni 2011/2013

INDEX

LIST OF ABBREVIATIONS

ATR: Attenuated Total Reflectance

CoPAC: *Conservazione Preventiva dell'Arte Contemporanea* (Preventive Conservation of Contemporary Art)

FORS: Fibre Optic Reflectance Spectroscopy

FT-IR: Fourier Transform-Infrared

KK: Kramers Krönig

IRUG: Infrared & Raman Users Group

Mid-IR: Mid-infrared

NMR: Nuclear Magnetic Resonance

PLM: Polarised Light MicroscopyPy-GC/MS: Pyrolysis- Gas Chromatography/Mass Spectrometry

SDBS: Spectral Database for Organic Compounds

SDD: Silicon Drift Detector

THM-GC/MS: Thermally assisted Hydrolysis and Methylation-Gas Chromatography/Mass Spectrometry

TMAH: Tetramethylammonium hydroxide

TMS: Tetramethylsilane

TR: Total Reflectance

UV-Vis-NIR: Ultraviolet-Visible-Near Infrared

W&N: Winsor and Newton

XRD: X-Ray Diffraction

XRF: X-Ray Fluorescence

a chi mi vuole bene

"Art does not reproduce what we see; rather, it makes see"

Paul Klee

INTRODUCTION

This research activity was carried out at the "Nello Carrara" Institute of Applied Physics of the National Research Council (IFAC-CNR) within the framework of the *Preventive Conservation of Contemporary Art Project* (CoPAC, 2011-2013).

The increased use of new synthetic materials, as a result of the rapid development that the chemical industry has undergone since the late 19th century, strongly influenced the artistic field. Thus, the 20th century represents a period of rapid change and innovation in the arts. Modern and contemporary artists abandoned the canons of the traditional art in search of new ideas and new ways of making art, which gave rise to the "avant-gardes" artists. Since 1920s-1930s, these new artists started to make full use of the newly available synthetic materials in order to achieve original and creative effects. These modern materials were usually designed for other applications, such as industrial, and thus not for use by artists. As it has become apparent in many cases these new materials did not offer the important characteristics of stability and durability, which are necessary for works of art to be stable over the years. Furthermore, they were often used in combination with the traditional materials, although incompatible with each other. For these reasons, many contemporary artworks are unstable and can quickly show signs of deterioration even shortly after their creation.

A comprehensive understanding of both the chemical composition and physical behaviour of modern materials is important for developing correct conservation treatments for such contemporary artworks. This means that a particular conservation procedure might be appropriate for one kind of material but have disastrous consequences for another.

Scientific research can play a fundamental role, becoming often a prerequisite, in the identification of the various materials constituting an artwork and in the determination of their degradation processes/causes.

In the last decades the spectroscopic techniques have been successfully applied to identify the traditional artists' materials (pigments, dyes, binders, etc.), but only few applications of these scientific methods have been carried out on the contemporary artists' materials.

In the present research some of the spectroscopic techniques (particularly FT-IR and UV-Vis-NIR spectroscopies) were applied both on modern synthetic reference materials and on contemporary artworks. Priority was given to non-invasive analytical techniques, such as FORS, colorimetry, and FT-IR in Total Reflectance configuration, and especially to those that can be performed by using portable devices, making possible rapid *in situ* surveys. Invasive techniques, which require small samples, such as Py–GC/MS or NMR spectroscopy, in some cases were also included because of the high level of detail they can provide on the chemical

composition of the samples. When necessary, the data obtained were integrated with those acquired by means of X-Ray Diffraction, X-Ray Fluorescence, and Raman spectroscopy.

This thesis is divided into three sections. In Section I, the CoPAC Project and the problem of the preventive conservation of contemporary art will be introduced by briefly describing the new materials used by contemporary artists and the analytical techniques that have been applied in this research activity. In section II, the results of the researches carried out on some of the new synthetic materials used by contemporary artists will be reported. Particularly, a study on commercial alkyd paints and their photo-oxidative degradation will be described in Chapter 2. In Chapter 3 a comparative study of IR spectra acquired in the three instrumental configurations (Transmittance, ATR, and Total Reflectance) on a collection of polymeric reference samples will be presented, highlighting the potentials of *in situ* and non-invasive FT-IR analysis. Lastly, section III will deal with the diagnostic investigations carried out on some actual case studies. The selection of the works to be analysed was done in collaboration with curators and conservators focusing on degradation problems noticed during conservation survey. Non invasive and invasive analysis were performed on two polymateric works by Anselm Kiefer (*Die Grosse Fracht* and *The Strip*; Chapter 4), on the original palette by Fernando Melani and on two of his paintings (*La Bandiera Italiana* and *N. Inv. 2625*; Chapter 5), on the Keith Haring *Tuttomondo* mural (Chapter 6) and on some of the canvases constituting the *Caverna dell'Antimateria* by Pinot Gallizio (Chapter 7). The *in situ* investigations and the analysis of the samples taken from selected areas of the said case studies allowed the identification of the main paint constituents (especially pigments/dyes) of the artworks under examination.

SECTION I
SCIENCE AND CONTEMPORARY ART

CHAPTER 1
PREVENTIVE CONSERVATION OF CONTEMPORARY ART

1.1 The CoPAC Project

The Preventive Conservation of Contemporary Art (CoPAC) Project was a 2-year research project (2011-2013) financially supported by the Regione Toscana (Tuscany, Italy) and part of the PAR-FAS program, Disciplinary Framework *Science and Technology for the Safeguard and Valorisation of Cultural Heritage*. The CoPAC Project was a joint effort by research institutions, conservators, city councils, museums, and art collections in Tuscany including the City of Pisa, the Contemporary Art Centre "Luigi Pecci" in Prato, the Fernando Melani's Studio-Home and the San Giorgio Library in Pistoia.

CoPAC activities were mainly focussed on the study of the materials used by contemporary artists to produce their artworks. CoPAC's goals were twofold: (1) define a set of contemporary artists' materials and (2) monitor their degradation over time. In order to achieve these goals the research team developed an experiential plan based on the use of several diagnostic methodologies to study the artist materials of interest. The objectives of this approach were to acquire as much data as possible about these artists' materials, how they were used together, and to monitor both the state- of the artworks and the surrounding environmental conditions. Complementary research activities were designed to collect additional information through interviews with the artists themselves. The interviews included questions to artists about the materials used, the purpose of their artistic creation, and their thoughts about the conservation of their works. At the same time, it was decided to investigate the degradation processes of selecting reference laboratory materials and studying their behaviours after natural and artificial ageing. The ultimate goal of the CoPAC Project was to set up an interactive archive to manage and disseminate the acquired information for the benefit of the curatorial and technical participants (http://copac.sns.it/).

The CoPAC Project consisted of seven work packages (WPs) as shown in Figure 1.1.

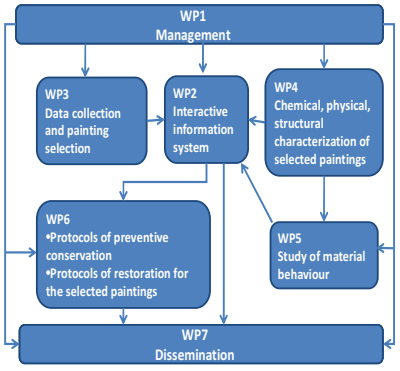

Fig. 1.1 - Diagram of the interaction between the seven WPs of the CoPAC Project.

WP1 and WP7 related to the data "Management" and "Dissemination" targets, respectively. WP2, "Interactive information system", dealt with the creation of an interactive and multimedia archive for all of the diagnostic, conservation, and restoration reports. WP3, "Data collection and painting selection", was a repository for information about artists' materials and painting techniques. WP4, "Chemical, physical structural characterisation of selected paintings" included spectroscopic analysis chromatographic methods and imaging techniques. In WP5, "Study of material behaviours", the research focussed on gaining detailed knowledge about the behaviour of reference artists' materials before, during, and after natural and artificial ageing. WP6, "Protocols of preventive conservation and Protocols of restoration for the selected paintings", defined the conservation practices pertinent to the research activities undertaken.

1.2 New materials, new problems

The preservation of contemporary art presents two fundamental challenges. First, the preservation of the materials used by artists in the creation of the works of art. Second, the preservation of the intention and meaning of the artwork itself, which in most cases goes beyond the conservation of the material structure itself (Althöfer, 1991).

One of the main features of contemporary art is its multiplicity of forms, expressions, techniques, and the artists' materials themselves. In contemporary art often the "matter" carries the message of the work. Indeed, matter is art itself. The artists of the past could count on a limited selection of substances but they were familiar with characteristics and behaviours of these materials with time. In contrast the range of materials utilised by contemporary artists is extremely wide, often containing substances not traditionally used for works of art. In contemporary art, traditional materials are often mixed or replaced with others designed for home or industrial use, or with everyday objects, and assembled in novel ways (Chiantore and Rava, 2005; Pugliese, 2006).

In contemporary art synthetic pigments/dyes and polymers are chosen by artists and designers, not only for creation of unique works of art, but also for their serial production. The reason for this preference lies in the relative cheapness of synthetic materials, due to the ease of production and the flexibility of application. The degradation of contemporary artworks is often accelerated by the presence of these inexpensive materials, mixed in various combinations, and applied by means of original artistic techniques.

Since the 19th century several synthetic pigments/dyes have been introduced by the industry. Till today several chemical compounds and their derivatives are produced and marketed under different trademarks. Pigments based on heavy metals (such as chromium, cadmium,

selenium, manganese and so on) or organic colorants, based on azo compounds, anilines, phthalocyanines etc., are daily used by contemporary artists. Despite this, the artists themselves often ignore the behaviour of these materials. For example, pigments based on cadmium sulphides are faded when combined with pigments based on copper, while the pigments based on molybdenum or zinc chromate are very unstable to light (Scicolone, 1993).
A further class of widespread artistic materials that are very unstable is represented by synthetic resins (e.g. PVA, acrylics, alkyds, polystyrene, etc.). Synthetic polymers (used by artists as binding medium, varnishes, and as plastics for 3D installations) are often designed for purposes other than the artistic creation that requires strength and durability superior to that considered acceptable for other aims. Like traditional materials, also synthetic polymer age and deteriorate, even after few years by their production, even though they are mistakenly considered indestructible (Rava, 1994).
The degradation of a polymer is mainly due to three phenomena that involve the alteration of the chemical-physical, mechanical and optical properties (Borgioli, 2005):
1) Depolymerisation, which is the fragmentation of the polymeric chain into smaller pieces;
2) Cross-linking, which occurs when adjacent chains are joined to each other with the formation of new bonds;
3) Formation of new functional groups with increasing of the polarity and onset of yellowing.
The causes of the polymer degradation are due to chemical factors (e.g. oxygen, water, etc.), environmental conditions (such as temperature, humidity, lighting, and air pollution), biological factors (e.g. micro-organisms) and physical/mechanical factors (e.g. the improper use of materials with different dilatation coefficients). Particularly, the UV/Vis radiation and the heat promote the oxidative processes in the presence of oxygen (Fig. 1.2). The oxidation of the polymer chains and their cross-linking cause the decrease of the solubility (and therefore the removal) of the synthetic resins, sometimes favoring also the yellowing of the polymer resulting in a chromatic alteration of the artwork (Chiantore, 1994).
The extreme variability of behaviour of plastic materials also depends on the fact that several constituents are present in their formulation. Indeed, a plastic is a complex system consisting, in addition to the synthetic resins, of different components such as pigments/dyes, fillers, etc. Thus, the ageing of plastics may depend on the stability of these substances even before from that of the resin. The degradation may also be affected by impurities or by structural abnormalities, formed during the production processes, that can interact synergistically to originate further alteration mechanisms.
The deterioration of polymeric materials causes the loss of their mechanical and optical properties. This loss is manifested by alteration of the colour, loss of gloss, embrittlement,

development of cracking and crumbling. Once triggered, the degradation is often not reversible and can only be slowed or weakened. So it is essential to design a preventive conservation and a routine maintenance of contemporary artworks to avoid conservative interventions that may be harmful, risky and invasive for the work itself.

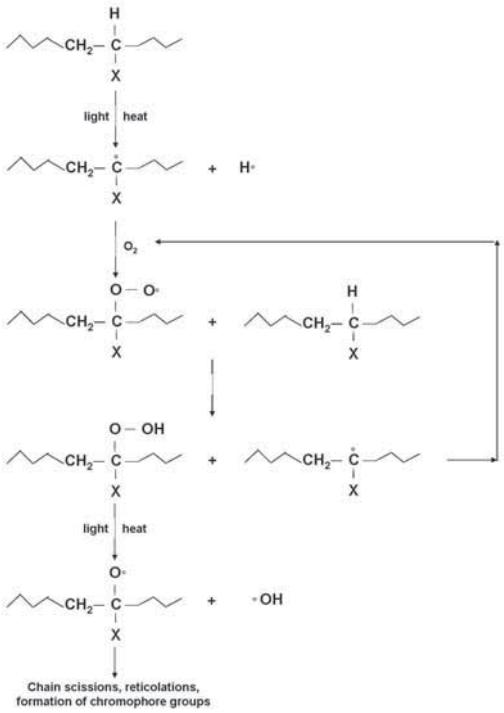

Fig. 1.2 – Polimeric reactions during the oxidative processes (Chiantore, 1994)

Sometimes artists use changeable and perishable substances such as the food used in the *eat art* (Fig. 1.3). In these cases the constituent materials are by nature perishable and temporary. Any possible restoration of these works could not only be difficult, but also anachronistic. It is therefore necessary to understand if the conservative intervention should stop the natural degradation (although the work was conceived as a concrete expression of the idea) or if methods should be developed to slow down/neutralise the degradation, maintaining the aesthetic effect.

Fig. 1.3 – Giovanni Anselmo, *Senza Titolo* (1968), Centre Pompidou, Paris
For this eating sculpture the daily substitution of the salad leaf is prescribed (Veaute and Cottrer ,2010)
[Image from: http://www.scultura-italiana.com/Biografie/Anselmo.htm; last access: 02 January 2014]

Another category of contemporary *oeuvres* that raises some issues with regard to its preservation is the so-called *conceptual art*, which is characterised by the fact that the creative idea is the message rather than the work's entity. In this case, the physical construction of the *oeuvre* is so marginal that the creation, and the assembly are carried out by assistants and collaborators of the artist, which supplies the project and the modalities of execution but not the work itself.

Other contemporary artworks that entail some problems with regard to their conservation are the so-called *performance oeuvres*, which are linked to a transitory event such as a performance, an installation or a happening. In these cases, the photos and the videos that reproduce the extraordinary and unique performances become work of art themselves. Thus, the object of conservation is the record, the memory of the happening. So the creation, maintenance and updating of a conspicuous photographic and video archive should be promoted (Veaute and Cottrer, 2010).

1.3 Scientific methods[1]

The combination of products of diverse nature, their different adaptation to the environment and their different interaction with the materials used in conservation make restoration of contemporary artworks an opportunity for testing new methodologies. In this sense, it becomes essential to have the most complete knowledge of the materials used, of their state of conservation, of their possible transformation over time and of their interaction with the support, other materials and the environment (Zendri, 2010).

The analytical methodologies for the study of Cultural Heritage are divided into invasive and non-invasive techniques. The former require samples taken from the work of art. Invasive techniques, in turn, are divided into:

- non-destructive methods, if the sample is not destroyed during the analysis, thus it can be used for other investigations;
- modificative methods, if the sample is modified during the analysis;
- destructive methods, if the sample is destroyed during the analysis and it cannot be used for other investigations.

Among the techniques used in the present research, FT-IR is probably the most common analytical techniques in the field of Cultural Heritage (Derrick *et al.*, 1991; Casadio and Toniolo, 2001). The main goal of IR analysis is to determine the chemical functional groups constituting the investigated material. Different functional groups, indeed, absorb

[1] A brief description of the scientific methods applied for this research is here illustrated. For more details, see the references shown in brackets.

characteristic frequencies of IR radiation. Thus, IR spectroscopy can allow the identification both of the organic materials (binding media, varnishes, dyes, adhesives, etc.) and of the inorganic ones (pigments, minerals, etc) present in the works of art. FT-IR spectra can be acquired with several instrumental configurations and three of them will be widely described in Chapter 3 (Coates, 1998; Galeotti *et al.*, 2009). The three configurations taken into consideration in the present dissertation are: transmittance, Attenuated Total Reflectance, and Total Reflectance modes. In FT-IR transmittance mode a sample of the artist material is generally embedded in a KBr pellet of 13mm in diameter. In the ATR mode, instead, the sample is analysed as it is without any modifications but the measurement requires an intimate and strong contact between the surface of the sample and the head of the ATR accessory. Only the FT-IR investigation in Total Reflectance mode is completely non-invasive and contactless, allowing the direct analysis of an object by means of portable devices (Fabbri *et al.*, 2001; Bacci *et al.*, 2005), however the spectra obtained are un-correctable and distorted by surface effects.

Another spectroscopic method for the study of Cultural Heritage is the UV-Vis-NIR diffuse reflectance spectroscopy, which is based on the analysis of the radiation diffused by the surface of a material in the 200-2500 nm range when compared with a highly reflecting reference standard (e.g. Spectralon®, barium sulphate). This method is primarily used to identify pigments/dyes, evaluate colour changes and/or to detect alteration products. UV-Vis-NIR reflectance analysis can be performed on samples non-destructively by means of bench-top spectrophotometer (Bacci, 2000). It can be also carried out non-invasively using instruments equipped with fiber optics bundles. The development of portable devices made it possible to perform also *in situ* measurements (Springsteen, 1998; Picollo and Porcinai, 1999; Leona and Winter, 2001; Bacci, 2001; Bacci *et al.*, 2003; Bacci *et al.*, 2009; Cucci *et al.*, 2013).

The colour of an art object and its variations during the time or after conservation treatments can be measured, in a non-invasive way, by means of colorimetry (Rawlins, 1936 and 1937; Bromelle, 1955; Wyszecki and Stiles, 1982; Saunders, 1986; Bacci *et al.*, 2008; Oleari C., 2008). This method is used to determine the colour parameters of an object by measuring the visible spectral reflectance of the object itself. The measurements are carried out using colorimeters or spectrophotometers supported by software capable of processing the reflectance data of the material. The radiation reflected from an object is associated with a set of three numbers (called chromaticity coordinates) that defines the colour values. A colorimetric measuring system includes three basic elements: the illumination source (e.g. lamps, laser diodes, etc.), the object and a detector, typically a CCD (Bacci, 2000).

Considering the chemical analysis performed within this thesis, Py-GC/MS is an invasive method, which can be successfully used for the chemical characterisation of organic materials (varnishes, binding media, adhesives, etc.) (Learner, 2001; Chiavari *et al.*, 1995; Cappitelli *et al.*, 2002; Chiavari and Prati, 2003; Bonaduce and Colombini, 2004; Colombini and Modugno, 2004; Bonaduce and Andreotti, 2009; Scalarone and Chiantore, 2009; Vicente *et al.*, 2009).

Pyrolysis is simply the breaking of complex molecules into smaller fragments by the application of heat. When the thermal energy applied to the compound is greater than the bond energy, the bonds that hold the molecule together break. The composition of the produced low molecular weight fragments is indicative of specific types of macromolecule.

In Py-GC/MS technique the sample consists of a few mg (or <mg, in the case of high organic carbon content compounds) of the original material. If necessary, the analysis could be preceded by an extraction of the sample with an organic solvent to remove any unbound low molecular components that would obscure the fragments of interest detection (Irwins, 1982). In some cases it could be desirable to introduce, during the sample preparation, a chemical agent that directly reacts, upon heating, with the macromolecule, producing a mixture of derivatised low molecular weight fragments in a process known as "thermally assisted chemolysis". Typical chemical reagents used for this purpose are tetramethylammonium hydroxide (TMAH) and trimethylsulfonium hydroxide (TMSH) (Challinor, 2001).

SECTION II
ARTISTIC MATERIALS

CHAPTER 2 – ALKYD PAINTS

In the 20th century, the introduction of new pigments and paints greatly increased the type of materials used by artists. The use of synthetic materials and new formulations enhanced the possibility of developing new artistic techniques. In addition, the ways in which artists expressed themselves were in turn influenced by the discoveries and innovations produced by industrial development, thus leading to a complete renovation of their works of art both materially and conceptually.

Modern paint is a complex mixture of components, such as pigments, binders, additives, and so on. Modern synthetic paints display different characteristics and properties, depending on their composition: for example, with respect their ageing, specific display conditions, and any necessary conservation treatment (Learner, 2007).

Despite the great variety of modern paint formulations, there are only three principal classes of synthetic binders that have been widely used by artists: polyvinyl acetate, acrylic, and alkyd resins.

This chapter is focussed on alkyd paints used for artistic purposes. The reason behind this choice is that many scientific works on this class of binders have been performed mainly in the industrial sector, while very few research projects relative on artistic alkyd paints have been carried out.

The gaining of knowledge regarding this class of resins is not the only reason why it is important to study them. It is just as important to be able to characterise and identify them, in addition to understanding of their durability and degradation over time.

2.1 Alkyd resins

2.1-1 General information

Alkyd resins, which are very versatile polymers, are mainly used in the formulation of paints and coatings. Their success is due to their low cost and to the fact that can be partly synthesized from renewable resources, such as vegetable oils, or from recycled materials (Karayannidis *et al.,* 2005; Varekova *et al*., 2006; Wutticharoenwong *et al.*, 2012; Ye *et al.*, 2012).

Alkyd [1] paints are oil-modified alkyd polyesters made by means of the condensation polymerisation of three types of monomers: polyalcohols, or polyols, (*i.e.,* glycerol, pentaeryhritol, sorbytol, etc.), polybasic acids (*i.e.,* phthalic acid, isophthalic acid, terephthalic

[1]The term *alkyd* originates from the *AL* in polyhydric *ALcohols* and the *CID* (modified to *KYD)* in polybasic *aCIDs*.

acid, etc.), and a source of fatty acids (either siccative oils or free fatty acids). An example of an ideal alkyd resin structure obtained from phthalic anhydride, glycerol, and linoleic acid is shown in Figure 2.1.

Further important components of alkyd paints are pigments (derived from natural or synthetic materials that have been ground into fine powders), which give paint its colour, extenders (inert pigments used to increase the bulk of the paint and/or to adjust the consistency of the paint), and additives, which have widely different functions in a coating formulation (Athawale and Chamanker, 1997; Ávár and Bechtold, 1999; van Gorkum and Bouwman, 2005; Kalenda *et al.*, 2010; Kalendová *et al.*, 2010) (Table 2.1).

Fig. 2.1 - An ideal alkyd resin (containing phthalic anhydride, glycerol and linoleic acid)

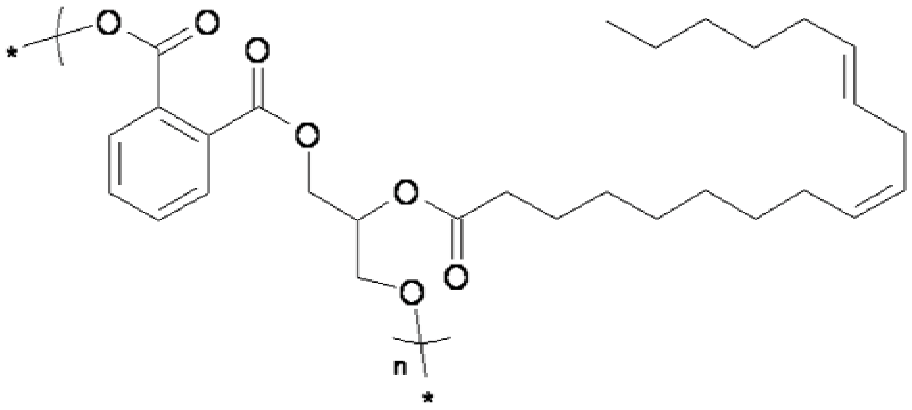

Table 2.1 - Example of a typical composition of an alkyd paint mixture (van Gorkum and Bouwman, 2005)

component	weight %
binder	30
organic solvent	27
water	10
pigments	19
extenders	12
additives	2

The first alkyd resin was synthesised in the 1920s by Roy H. Kienle. He established a classification, still in use today, that is based on “oil length” in the finished resin (Kienle and Ferguson, 1929; Hofland, 2012). The oil length is defined as the weight percent of oil or triglyceride equivalent or, alternatively, as the weight percent of fatty acids in the finished resin (Lin, 2005). Alkyd resins used for artists’ paints are classified as ‘long oil’ alkyds, because they contain between 56-70 weight percent of oil and/or fatty acids. ‘Short oil’ (35-45 weight percent), ‘medium oil’ (46-55 weight percent) and ‘very long oil’ (greater than 70 weight percent) alkyd resins are also manufactured and used in various other coating applications (Schilling *et al.*, 2007; Ploeger *et al.*, 2008 e 2009a; Table 2.2).

Table 2.2 - Classification of alkyd resins (Lin, 2005)

Resin Class	% of Oil	% of Fatty Acids	% of Phthalic Anhydride
Very long oil	>70	>68	<20
Long oil	56-70	53-68	20-30
Medium oil	46-55	43-52	30-35
Short oil	<45	>42	>35

There exists a large variety of ingredients that can be used to obtain an alkyd resin. The selection of each one of the three principal components - polybasic acids, polyalcohols, and fatty acids - affects the final properties, as well as the use and the time of air drying of the resin, and may even affect the choice of the manufacturing processes (Table 2.3).

Table 2.3 - The major types of polybasic acids (or anhydrides), polyhydric alcohols and sources of fatty acids used in alkyd synthesis

Polybasic Acids and Anhydrides	Polyhydric alcohols	Sources of fatty acids
Phthalic anhydride	Pentaerythritol	Linseed oil
Isophthalic acid	Glycerol	Soya oil
Maleic anhydride	Trimethylolpropane	Safflower oil
Fumaric acid	Trimethylolethane	Sunflower oil
Adipic acid	Ethylene glycol	Castor oil
Azelaic acid	Neopentyl glycol	Castor oil dehydrated
Sebacic acid		Coconut oil
Cholerindic anhydride		Tung oil
Trimellitic anhydride		Cottonseed oil

As regards polybasic acids, the most commonly used dibasic acid in the preparation of alkyds is phthalic acid ($C_8H_6O_4$) or its anhydride ($C_8H_4O_3$) (Fig. 2.2) because of both their low cost and the excellent overall properties that are imparted to the final product (van Gorkum and Bouwman, 2005; Ploeger *et al.*, 2008).

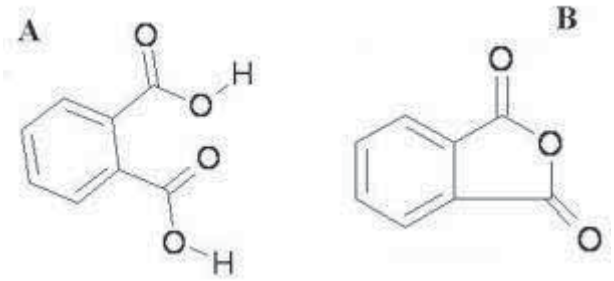

Fig. 2.2 – Chemical structure of phthalic acid (A) and phthalic anhydride (B)

Alkyds prepared with isophthalic acid ($C_6H_4(COOH)_2$) usually have higher molecular weight and greater thermal stability, and show much higher viscosity than do their phthalic counterparts at the same oil length. These are the major reason why resin manufacturers use isophthalic acid for the preparation of long oil alkyds. In spite of these advantages, a production system involving isophthalic acid is much more complicated and difficult than one that uses phthalic anhydride. Maleic anhydride ($C_4H_2O_3$) is sometimes used for the partial replacement for phthalic anhydride in making alkyds. Its presence, even in small amounts, in the resin formula could accelerate an increase in viscosity during the resin manufacturing process. Furthermore, the final product dries more rapidly, and produces harder film that is

characterised by improved colour, adhesion, water resistance, alkali resistance, and exterior durability that are superior to those of traditional alkyd resins Finally, aliphatic dibasic acids (i.e. adipic, azelaic, and sebacic acids) can also be used to produce alkyd resins that have high flexibility and low viscosity (Aydin *et al.*, 2004).

As far as polyalcohols are concerned, the most important products used for alkyd formulations are pentaerythritol and glycerol (Fig. 2.3). The former is a polyol consisting of four methylol groups (CH_2OH) surrounding a centre carbon atom ($C_5H_{12}O_4$). This structure lends stability against heat, light, and moisture. The latter is a triol consisting of two primary alcohol groups and a secondary alcohol group ($C_3H_8O_3$). Glycerol alkyds are more prone to thermal decomposition, which results in a darkening of the resin (Lin, 2005).

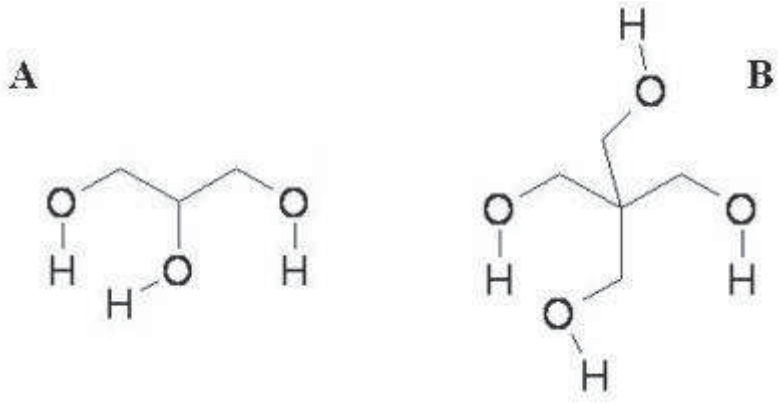

Fig. 2.3 - Chemical structure of glycerol (A) and pentaerythritol (B)

Many alkyd resins are charged with fatty acids derived from vegetable oils: the content of double bonds between the carbon atoms varies, depending on the type of oil used in the formulation of the resin. The fatty acid content also bestows other properties on the resin, including a potential for cross-linking, flexibility, compatibility with the solvents, and solubility (Table 2.4) (Ploeger *et al.*, 2008). For example, if the oil length decreases and the phthalic content increases, the aromaticity and/or the polarity of the solvent will also need to be increased in order to dissolve the resin effectively (Lin, 2005). Linseed, soya, safflower and castor oils are commonly used in 'long oil' applications because of their fatty acid compositions and lower costs (Ploeger *et al.,* 2008).

Table 2.4 - Trends of property changes with oil length of alkyd resins (Lin, 2005)

Oil length	**Long Medium Short**
Requirement of aromatic polar solvent	→
Compatibility with other film formers	→
Viscosity	→
Ease of brushing	←
Air dry time	←
Film hardness	→
Gloss	→
Gloss retention	→
Colour retention	→

Different chemical processes may be used for the synthesis of alkyd resins. The choice is usually dictated by the starting ingredients. Two procedures are mainly used, namely the *alcoholysis process* and the *fatty acids process*. In the former process, there is a transesterification reaction between the polyol and the oil, followed by a condensation reaction with phthalic anhydride and the elimination of water. In the latter, the alcoholysis step is avoided when free fatty acids are used, instead of oil, as the starting component. All of the ingredients can, therefore, be charged into the reactor to start a batch. The reactants are heated together until the desired end point is reached (Lin, 2005; Thanamongkollit and Soucek, 2012). Alkyds prepared using the fatty acid process have a narrower distribution of molecular weight, and produce film that has better mechanical properties (Chen and Kumanotani, 1965).

Alkyds were first introduced on the market by General Electric (GE) in the USA in the 1930s, when the *Glyptal* trademark became an alternative name for them (McIntyre, 2003). The Du Pont line of *Dulux*[2] enamels for automotive and appliance finishes, for example, used alkyd resins that Du Pont manufactured under a GE license (Coe, 2000). The large-scale commercial production underwent exponential growth, arriving at replacing the oils that had been used as binders in paints for centuries and offering better film-forming properties at a lower price. Many artists, such as Pablo Picasso, Jackson Pollock (Fig. 2.4), Frank Stella and Roy Lichtenstein, started to use industrial and household alkyd paints from the time that they were first introduced (Cappitelli, 2004; Cappitelli and Koussiaki, 2006; Ploeger *et al.*, 2008). It was only in 1976 that a series of oil paints based on alkyd resins (*Griffin Alkyd*) was produced for the first time by *Winsor & Newton* (W&N), Middlesex, England (Ploeger *et al.*, 2007 and 2008).

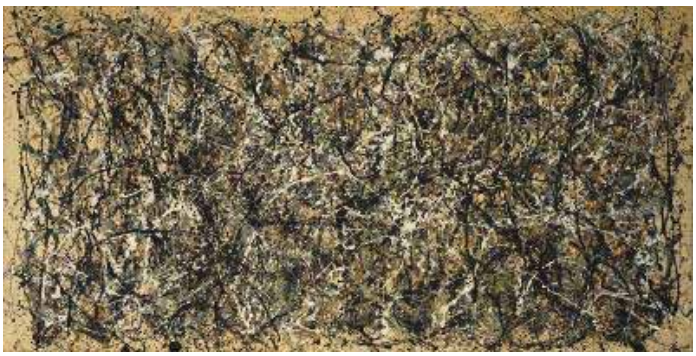

Fig. 2.4 - Jackson Pollock *One: Number 31* (1950), Museum of Modern Art (MoMA), New York (http://www.jackson-pollock.org/one-number31.jsp , last access October 2, 2013)

[2] Dulux actually owes its existence to a flaw in its more famous cousin, Duco. This nitrocellulose lacquer first brought colour to automobiles when General Motors (GM) used it in 1923. It was thick and quick-drying, which pleased carmakers, but was frustrating for consumers, who could not apply it like the oil-based paints that they were used to. DuPont researchers therefore tried mixing synthetic alkyd resins with oil, and found that the resulting drying time for the enamel was slower than for Duco but faster than for traditional oil paint (www2.dupont.com/Phoenix_Heritage/en_US/1923_b_detail.html, last access October 2, 2013).

2.1-2 The drying of alkyd paints

Two different mechanisms can be identified during the drying of artists' alkyd paint (van Gorkum and Bouwman, 2005; Ploeger *et al.*, 2009b):

1- A physical drying of the paint by means of solvent evaporation;

2- Its chemical drying, by means of auto-oxidation (also known as oxydative drying).

After alkyd paint has been applied to a surface at room temperature, the physical drying process starts. The solvent evaporates, and a pictorial film is then formed. The chemical drying subsequently begins, and proceeds by means of a free-radical chain reaction mechanism that can be described in terms of initiation, propagation, and termination, as shown in Figure 2.5. During the initiation step, an initiating free-radical species (I) extracts an H-atom from the substrate, thus producing an alkyl radical (R·). This radical is able to react rapidly with oxygen to form a peroxy radical (ROO·) which, in turn, can extract other hydrogen atoms to form a hydroperoxide (ROOH) and a new alkyl radical. The ROOHs thus formed are decomposed, and radicals such as R·, RO·, and ROO· are created again (propagation step)[3]. These radicals can react by means of recombination (termination step) or via the addition of radicals to C=C double bonds, to form cross-links[4] (van Gorkum and Bouwman, 2005; Soucek *et al.*, 2012).

Initiation

$R–H + I· \rightarrow R· + I–H$

Propagation (the formation of hydroperoxide)

$R· + O_2 \rightarrow ROO·$

$ROO· + R–H \rightarrow ROOH + R·$

Propagation (the decomposition of hydroperoxide and the formation of free radicals)

$ROOH \rightarrow RO· + ·OH$

$ROOH + ROOH \rightarrow RO· + ROO· + H_2O$

$RO· + RH \rightarrow R· + ROH$

Termination (cross-linking via the recombination of radicals)

$2R· \rightarrow RR$

$2RO· \rightarrow ROOR$

$2ROO· \rightarrow ROOR + O_2$

$ROO· + R· \rightarrow ROOR$

$RO· + R· \rightarrow ROR$

$RO· + ROO· \rightarrow ROR$

Fig. 2.5 - Radical reactions that take place during the autoxidation of an alkyd resin (van Gorkum and Bouwman, 2005; Soucek *et al.*, 2012)

[3] The hydroperoxides not only generate free radicals, but also decompose by means of fragmentation to produce by-products that are mainly aldehydes (with lesser amounts of ketones and alcohols). These are responsible for the characteristic pungent smell during the drying process of an alkyd paint.(Chang and Guo, 1998).

[4] Propagation (cross-linking via the addition of radicals):

$R· + C=C \rightarrow R-C-C·$

$RO· + C=C \rightarrow R-O-C-C·$

$ROO· + C=C \rightarrow R-O-O-C-C·$

As the auto-oxidative process is advantageous for the air-drying of alkyd coatings, it may be accelerated by using suitable promoters (catalysts). These products promote the decomposition of hydroperoxides into free radicals, thus favouring the formation of hard cross-linked polymer networks that bind the pigment to the painted surface of the treated object.

Common driers are metal soaps made of carboxylic acids[5]. The metals most commonly used in drier compounds are historically grouped into three categories (Table 2.5):

1 - *primary driers* (*active or oxidation driers*), which are autoxidation catalysts (Muizebelt *et al*. 1994; Kalenda *et al*., 2010; Kalendová *et al*., 2010);

2 - *secondary driers* (*through-driers*), which are active in the cross-linking steps of drying;

3 - *auxiliary driers*, which enhance or alter the activity of the primary drier, and thereby improve the appearance and quality of the paint film (van Gorkum and Bouwman, 2005; Soucek *et al.*, 2012).

One of the most common drier combinations used is Co/Zr/Ca (Ploeger *et al.*, 2009b).

Table 2.5 - Metals used in alkyd paint formulations, in each drier category (van Gorkum *et al*., 2005)

Primary driers	Secondary driers	Auxiliary driers
Cobalt	Lead	Calcium
Manganese	Zirconium	Zinc
Iron	Bismuth	Lithium
Cerium	Barium	Potassium
Vanadium	Aluminium	
	Strontium	

2.2 Commercial alkyd paints: characterisation and UV ageing

2.2-1 Aim of the work

In order to investigate the photo-oxidative deterioration of alkyd paints when these are exposed to UV light, an ageing study on these materials was carried out. For this purpose, alkyd pictorial mock-ups were characterised before and after UV exposure by means of FT-IR spectroscopy, THM-GC/MS, XRF and PLM. UV-Vis-NIR reflectance spectroscopy and colorimetry were also used to evaluate colour changes that may possibly have occurred.

2.2-2 Experimental

Samples

In this study, ten commercial *Winsor & Newton-Griffin Alkyd "fast drying oil colours"* were investigated (Fig. 2.6, Table 2.6). As stated by the manufacturer, *"Griffin Alkyd Fast Drying Oil Colours are milled with an alkyd resin rather than traditional linseed oil. These paints*

[5] The commonly used acids include linoleates, tallates, naphthenates and octoates (Soucek *at al.*, 2012).

offer working properties that are similar to those of a traditional oil colour, yet dry much more rapidly.[…] Just like traditional oils, alkyds dry by oxidation (a linkage achieved with the help of oxygen in the atmosphere), a process that happens much more rapidly for alkyds than for traditional oils. The film is touch dry in 18 to 24 hours (Pyle and Pearce, 2001). The choice to investigate the *Griffin Alkyd "fast drying oil colour"* series made by W&N was due not only to the fact that W&N was the first to introduce this kind of paint on the market of artistic materials, but mainly because it is the leading company in this particular commercial sector. Its catalogue offers a full colour range of artists' alkyd paints, although many other manufacturers have incorporated alkyds into their formulations (Learner, 2004). Hence, the W&N alkyd paints are probably the ones most widely used in their class.

Fig. 2.6 – Tubes of the selected *Winsor & Newton-Griffin Alkyd "fast drying oil colours"*

Table 2.6 - List of the commercial *Winsor & Newton-Griffin Alkyd Fast Drying Oil Colours* investigated and their technical properties as declared by the manufacturer

Sample Number	Colour Name	Chemical Description	Colour Index Name	Permanence rating*	ASTM lightfastness rating**	Transparency/ Opacity***
1	Titanium White	Titanium dioxide	PW6	AA	I	O
2	Cadmium Red Medium	Cadmium sulphoselenide	PR108	A	I	O
3	Winsor Red	Naphtol carbamide, Naphtol As	PR170/PR188	A	-	T
4	Cadmium Yellow Light	Cadmium zinc sulphide	PY35	A	I	O
5	Winsor Lemon	Arylamide yellow	PY3	A	II	T
6	Viridian	Hydrated chromium oxide	PG18	AA	I	T
7	Phthalo Green	Chlorinated copper phtalocyanine	PG7	A	I	T
8	French Ultramarine	Complex sodium alumino-silicate containing sulphur	PB29	A(iii)	I	T
9	Phthalo Blue	Copper phtalocyanine	PB15	A	I	T
10	Ivory Black	Bone black	PBk9	AA	I	O

* Permanence rating: is defined as a colour's 'durability when laid with a brush on paper or canvas, graded appropriately and displayed under a glass frame in a dry room freely exposed to ordinary daylight and an ordinary town atmosphere':
AA , Extremely Permanent; A, Permanent; (iii), Bleached by acids, acidic atmospheres.
** ASTM lightfastness rating: each colour to be rated on a scale from I to V, depending on the medium. In this rating, system I is the highest lightfastness available, al though both ratings I and II are considered permanent for use by artists.
*** T, transparent colours; O, opaque colours.

Samples were cast on glass microscope slides (7.5 cm x 2.5 cm; thickness approximately 0.2 mm) in order to assess their behaviour on an inert material (Fig. 2.7).

During the preparation of the samples, special attention was paid to the creation of surfaces that were as smooth and homogeneous as possible in order to limit morphology effects during the reflection measurements. The samples were partially screened with aluminium foil, to evaluate the difference in behaviour during the ageing between irradiated and non-irradiated areas. Every specimen was analyzed three days after its preparation, when it was definitely dry to touch.

Fig. 2.7 – Mock-ups prepared with *Winsor & Newton-Griffin Alkyd "fast drying oil colours"*

UV ageing[6]

The samples were artificially aged for 150 days in a UV Chamber UVACUBE SOL 2/400F produced by Dr. Hönle GmbH UV-Technology, Germany. The UV light source was a 910 Wm^{-2} Xenon arc solar simulator, with an incorporated H2 filter. This source provides radiation with a spectral range between 295 and 800 nm. Ageing was performed at about 48 °C with a relative humidity (RH) that ranged from 30% to 35%, depending on the ambient RH. The average irradiance was ~400 Wm^{-2} in the visible and ~40 Wm^{-2} in the ultraviolet emission ranges.

FT-IR

All samples were investigated before, during and after the ageing procedure by means of FT-IR spectroscopy.

FT-IR spectra were recorded using three different instrumental configurations: Transmittance, Total Reflectance (TR), and Attenuated Total Reflectance (ATR). IR spectra in transmittance mode were acquired with a *Nicolet - Protégé™ 460 E.S.P.™ spectrophotometer* in the 4000 - 400 cm^{-1} spectral range (64 scans; 4 cm^{-1} resolution). To perform the reflectance measurements, a FT-IR *Alpha Bruker Optics Spectrophotometer*, equipped with an External

[6] UV ageing was performed at the scientific laboratory of the Institute of Science and Technology in Art, Academy of Fine Arts (Vienna, Austria), under the supervision of Prof. Manfred Schreiner and Dr. Valentina Pintus.

Reflection module for the TR spectra and with a Platinum ATR module (single reflection diamond) for the ATR measurements, was used. Spectra were acquired in the 4000 - 375 cm^{-1} spectral range by performing 32 scans at a resolution of 4 cm^{-1}.
Data were evaluated with OPUS 7.0.122 software from Bruker Optics.

THM-GC/MS[7]

All samples were investigated by means of THM-GC/MS before and after UV ageing . This is an extension of Py-GC/MS, which incorporates a derivatisation process.
The reagent used for the THM-GC/MS analyses was a TMAH, 25% (w/w) solution in water, supplied by Sigma Aldrich. About 300 µg of the samples were scraped from the glass slides with a scalpel and placed in a sample cup (ECO-CUP Frontier Lab, Japan) with a 2 µL TMAH drop for analysis.
The THM–GC/MS analyses were performed using a *PY AOC-20i* (Frontier Lab, Japan) pyrolyser unit coupled to a *GCMS-QP2010 Plus* (Shimadzu, Japan) equipped with a capillary column Ultra Alloy-5 (5% diphenyl 95% dimethylpolysiloxane) that had a 0.25 mm internal diameter, 0.25 µm film thickness, and length of 30 m (Frontier Laboratories, Japan). The pyrolysis temperature was set at 600 °C and held for 12 seconds, and the temperature of the pyrolysis interface was set at 280 °C. The carrier gas was helium, the flow of which was set at 1 mL/min. GC temperature programme settings were: an initial temperature of 40 °C, which was held for 5 min; an increase at 10 °C/min to 280 °C; a final temperature of 280 °C, which was held for 5 min. Mass spectra were recorded under electron impact ionisation at 70 eV.

XRF[8]

XRF spectra were recorded using a portable X-Ray Fluorescence analyser, mod. *TRACeR III-SD* (Bruker Optics). The instrument was equipped with an X-ray tube (Rh target), an Ag anode, and a Silicon Drift Detector (SDD) that had a resolution of 190 eV at 10,000 cps. The excitation parameters used during the investigations were: voltage of 40 kV and current of 30 µA. The acquisition time was 20 s.

PLM

The samples were analysed using a *Nikon ECLIPSE E600* optical microscope equipped with a *Nikon DS-Fi1c* video camera and a *Nikon cube UV-2A* (emission range: 330-380 nm,

[7] THM–GC/MS analyses were performed before and after the artificial ageing step at the scientific laboratory of the Institute of Science and Technology in Art, Academy of Fine Arts (Vienna, Austria) under the supervision of Prof. Manfred Schreiner and Dr.Valentina Pintus.
[8] The XRF analysis was performed by Dr. Donata Magrini of the Institute for the Conservation and Valorisation of the Cultural Heritage (Department of Florence) of the National Research Council (ICVBC-CNR).

recovered wavelengths: > 420 nm). Images were acquired in visible and UV light, before and after the artificial ageing on both the covered and uncovered areas, using Nikon NIS-elements D software.

Colorimetry

Colour measurements were performed before, during and after the UV ageing, using a *Konica-Minolta CM-700d* spectrophotometer (400-700 nm, 10 nm steps). The Illuminant D65, Standard Observer 10°, beam of diffuse light of 8 mm diameter, 8° viewing angle geometry, and excluding the specular component of the radiation, were also used.

The data reported were based on an average of three measurements, and colorimetric coordinates were calculated for the CIEL*a*b* 1976 colour space. For each measurement, the instrument was consecutively positioned on exactly the same spot (Ø 8 mm), using a repositioning mask, and was removed immediately afterwards. The total colour differences were calculated on average values as Δ(L*a*b*) and ΔE_{00}, in accordance with the Commission Internationale de l'Eclairage CIEDE2000 formula (Luo *et al.*, 2001; Sharma *et al.*, 2005).

UV-Vis-NIR reflectance spectroscopy

UV-Vis-NIR reflectance spectra were acquired with a *PerkinElmer® LAMBDA1050* spectrophotometer in the spectral range between 200 and 2500 nm. This instrument was equipped with two sources (a pre-aligned tungsten-halogen lamp and a deuterium lamp), and utilised a source doubling mirror for the purpose of improved UV-Vis-NIR energy. Detectors were an R6872 photomultiplier for high energy in the entire UV-Vis wavelength range, and a high performance Peltier-cooled PbS detector for the NIR wavelength range.

2.2-3 Characterisation of the unaged samples

Before the ageing test, the samples were characterised by FT-IR, THM-GC/MS and UV-Vis-NIR reflectance spectroscopy to be sure that their composition was as declared by the manufacturer. The analysis showed that all the samples consisted of an alkyd resin mixed with one or more pigments. Some additives, which were not specified by the manufacturer, were also identified.

Alkyd binder

The THM-GC/MS confirmed the presence of an oil-modified alkyd resin as the binding medium in all the samples studied. For example, in Figure 2.8 the THM-GC/MS pyrogram registered from *French Ultramarine Griffin Alkyd Oil Colour* is reported (Table 2.7). The

polyol used in the formulation of the alkyd resin was pentaerythritol (peak 2, 1,3-dimethoxy-2-(methoxymethyl)-2-methylpropane; peak 3, 3-methoxy-2,2-bis(methoxymethyl)-1-propanol). A small amount of glycerol (peak 1, glycerol trimethyl ether) was also detectable. This is a fragmentation product of triglycerides that constituted the oil component. Peaks 6 and 7 were due to the presence of dimethyl esters of phthalic and isophthalic acid, respectively, which were used as polybasic components during the paint synthesis. Peak 5 and peaks 8-13 revealed the presence of fatty acids, which were detected as methyl esters. In particular, peak 13 (12-hydroxystearic methyl ester) was due to the presence of hydrogenated castor oil (possibly used as a stabiliser or as a rheology modifier, Ploeger and Chiantore, *in press*).

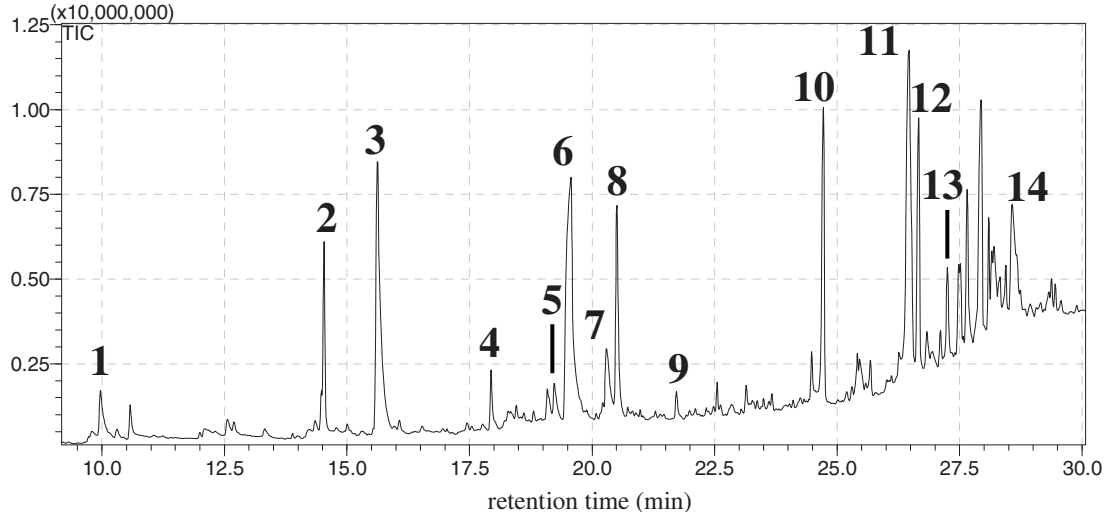

Fig. 2.8 - Pyrogram of *French Ultramarine Griffin Alkyd Oil Colour*. Peak assignments: 1, glycerol trimethyl ether; 2, 1,3-dimethoxy-2-(methoxymethyl)-2-methylpropane; 3,3-methoxy-2,2-bis(methoxymethyl)-1-propanol; 4, 8-methoxyoctanoic acid, methyl ester; 5, suberic acid, dimethyl ester; 6, phthalic acid, dimethyl ester; 7, isophthalic acid, dimethyl ester; 8, azelaic acid, dimethyl ester; 9, palmitic acid, methyl ester; 10, oleic acid , methyl ester; 11, stearic acid, methyl ester; 12, linoleic acid, methyl ester; octadecanoic acid, 12-hydroxy-, methyl ester.

Table 2.7 – THM-GC/MS chromatogram peak assignment for
Winsor & Newton French Ultramarine Griffin Alkyd Oil Colour

Peak n°	Peak assignment	Retention time	m/z	mol wt
1	glycerol trimethyl ether	10.0	59, 89, 106	134
2	1,3-dimethoxy-2-(methoxymethyl)-2-methylpropane	14.5	45, 75, 85, 101, 115, 128, 145	162
3	3-methoxy-2,2-bis(methoxymethyl)-1-propanol	15.6	45, 71, 75, 85, 101, 114, 128, 161	178
4	8-methoxyoctanoic acid, methyl ester	17.9	45, 74, 124, 157	188
5	suberic acid, dimethyl ester	19.2	41, 55, 74, 97, 129, 138, 157, 171, 196	202
6	phthalic acid, dimethyl ester	19.5	50, 64, 77, 92, 120, 133, 163, 185, 194	194
7	isophthalic acid, dimethyl ester	20.3	50, 66, 74, 76, 103, 120, 135, 163, 194	194
8	azelaic acid, dimethyl ester	20.5	55, 74, 111, 152, 185, 194	216
9	sebacic acid, dimethyl ester	21.7	55, 74, 125, 138, 166, 199	230
10	palmitic acid, methyl ester	24.6	43, 74, 87, 129, 143, 171,185, 213, 227, 239, 270	270
11	oleic acid , methyl ester	26.4	55, 69, 97, 111, 123, 137, 180, 222, 264, 296	296
12	stearic acid, methyl ester	26.6	43, 74, 87, 97, 129, 143, 157, 185, 199, 213, 241, 255, 298	298
13	linoleic acid, methyl ester	27.2	41, 45, 55, 67, 95, 133, 150, 163, 187, 207, 220, 262, 294	294
14	octadecanoic acid, 12-hydroxy-, methyl ester	28.6	55, 87, 97, 143,197, 229	314

FT-IR analysis confirmed the presence of an alkyd resin in the formulation of all the *Griffin Alkyd Oil Colour* samples. The main absorptions were due to the (C-H)CH_2 asymmetric stretching at about 2920 cm^{-1}, the (C-H)CH_2 symmetric stretching at about 2850 cm^{-1}, as well as to the strong C=O stretching of esters at about 1730 cm^{-1}. The doublet at 1600 and 1580 cm^{-1} corresponded to the stretching of the double bond in the aromatic ring (phthalic groups), and the absorptions at 1465 cm^{-1} and 1380 cm^{-1} were due to aliphatic CH bending. In the fingerprint region, the C-O stretching of the carbonyl group (1260 cm^{-1}), the O-C-C stretching of esters (1120 cm^{-1}), and the absorption at 1070 cm^{-1} due to aromatic in plane CH bending were visible (Fig.2.9). At 741 cm^{-1} and 706 cm^{-1}, aromatic out-of-plane CH bending vibrations were also present.

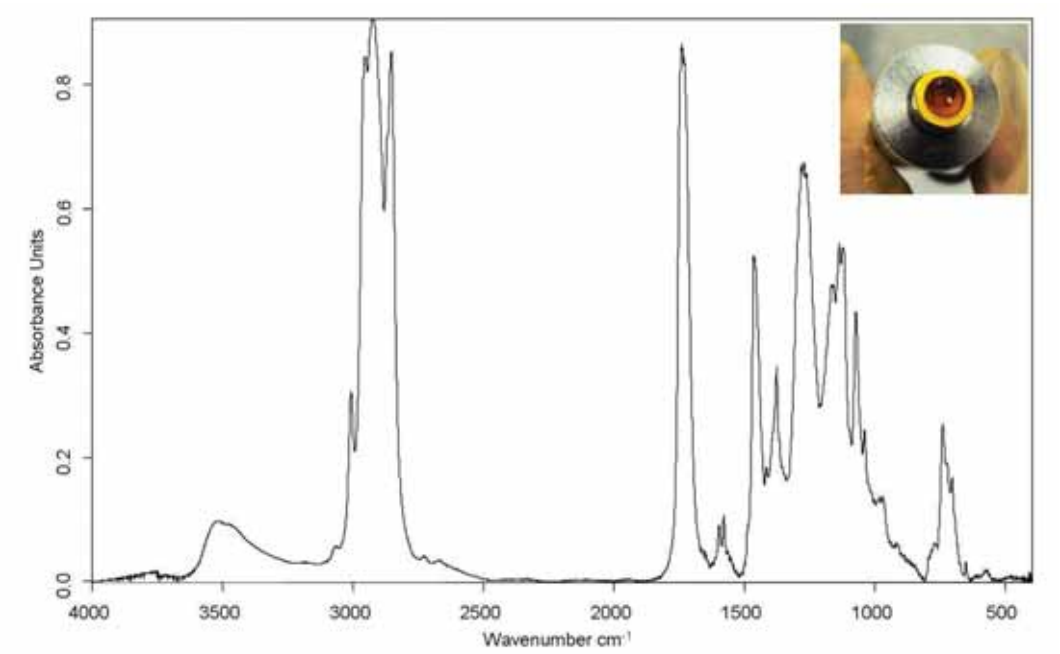

Fig. 1.9 - FT-IR spectrum of the resin casually separated from the paint in the tube (in the upper right box)

UV-Vis-NIR reflectance spectroscopy also confirmed the presence of an alkyd binder. In the reflectance spectra, in fact, the 1st overtone $\nu_s(CH_2)$ at 1727 nm, the 1st overtone $\nu_a(CH_2)$ at 1760 nm, and the combination band $\nu_a(CH_2)+\delta(CH_2)$ at 2308 nm due to the alkyd resin were present.

Pigments/dyes

The combined use of FT-IR and UV-Vis-NIR spectroscopic techniques made it possible to define the pigment/dye composition of each specimen.

Titanium white (TiO_2), PW6. Considering sample 1, the FT-IR spectrum showed strong and broad absorption between 800 cm^{-1} and 450 cm^{-1}, which may have been due to the presence of titanium dioxide in its rutile form (Fig. 2.10).

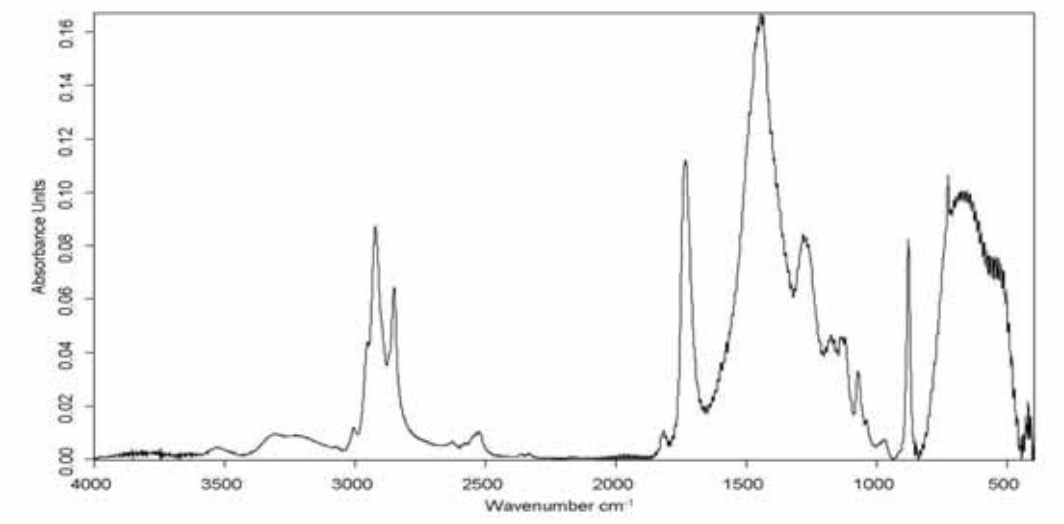

Fig. 2.10 - FT-IR spectrum of *Titanium White Griffin Alkyd Oil Colour*

Since other white pigments (such as zinc white) absorb in this region, the presence of titanium white was readily confirmed by means of UV-Vis-NIR reflectance spectroscopy. Indeed, the UV-Vis-NIR reflectance spectrum of this sample (Fig. 2.11) presented a typical S-type band shape that had an inflection point (identified by calculating the first derivative of the spectrum) at 403 nm (3.07 eV), which confirmed the presence of titanium dioxide in the rutile crystalline form (Bacci *et al.,* 2007; Picollo *et al.*, 2007).

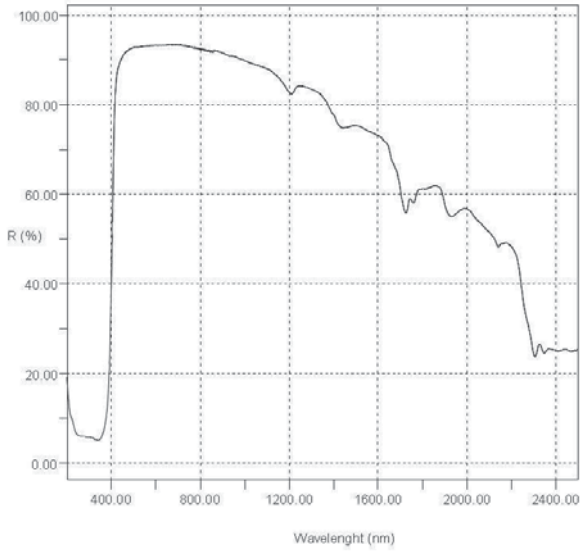

Fig. 2.11- UV-Vis-NIR reflectance spectrum of *Titanium White Griffin Alkyd Oil Colour*

Cadmium sulphoselenide, PR108. No characteristic bands of cadmium red pigment were detectable by means of FT-IR in the medium IR spectral region. The UV-Vis-NIR reflectance spectrum (Fig. 2.12) showed a single absorption band in the UV-Vis region, with the typical "S"-shape of the inorganic pigments being constituted by semiconductors that had an inflection point at 602 nm (2.06 eV). This absorption was due to energy band transitions (Mohammed Noori, 2011).

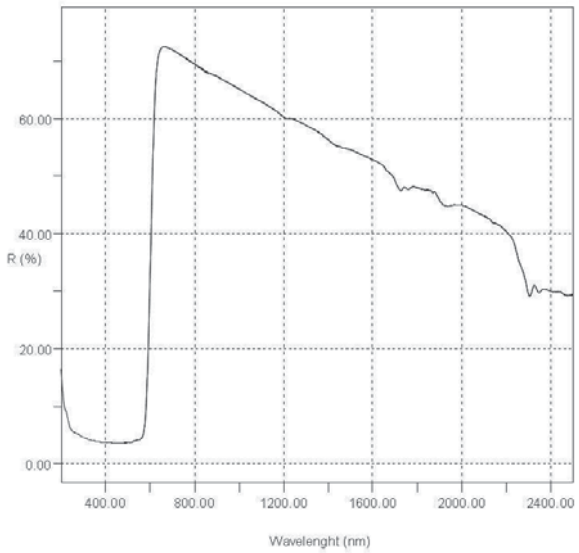

Fig. 2.12 - UV-Vis-NIR reflectance spectrum of *Cadmium red medium Griffin Alkyd Oil Colour*

The XRF[9] elemental analysis showed a peculiar presence of high counts of selenium, calcium and cadmium, in addition to smaller amounts of sulphur and barium. These data permitted us to hypothesize the presence of a red pigment based on Cd(Se,S) and smaller amounts of barium sulphate and calcium carbonate (Fig. 2.13).

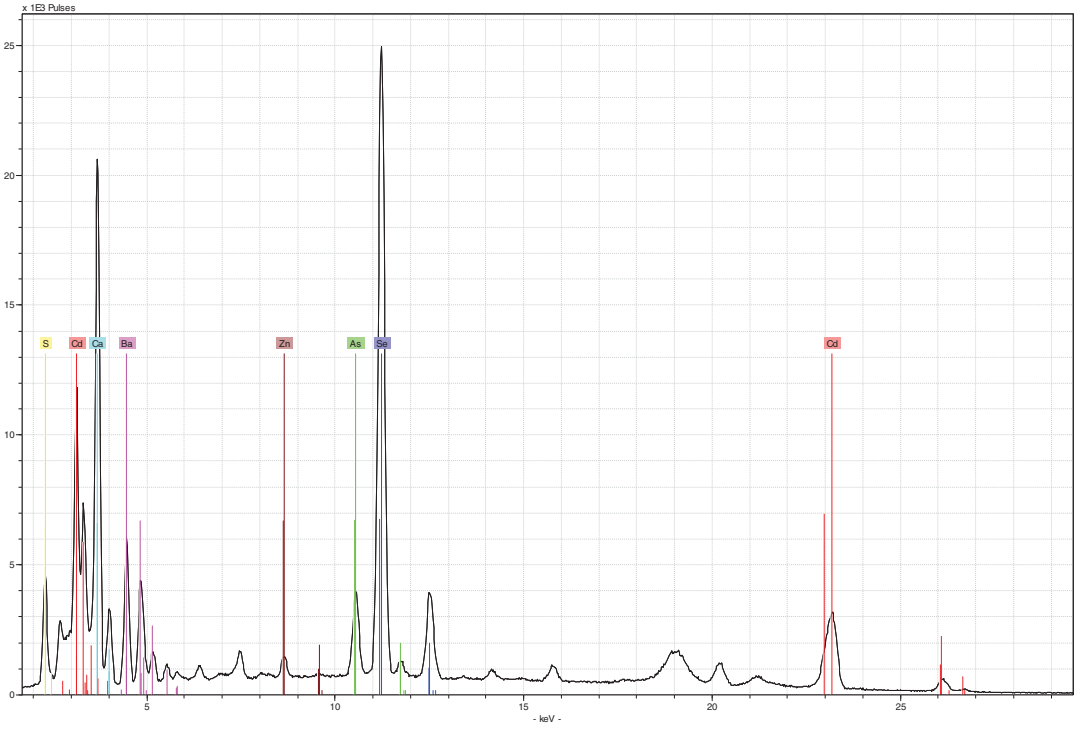

Fig. 2.13 - XRF spectrum of *Cadmium red medium Griffin Alkyd Oil Colour* showing the presence of Se (blue lines), Ca (cyan lines), Cd (red lines), Ba (pink lines), S (yellow lines), and lesser amounts of Zn (brown lines) and As (green lines)

Naphtol carbamide, PR170 - Naphtol As, PR188. The dyes which constituted sample 3 were two red azo dyes that differ from each other only with regard to certain substituents on the

[9] XRF analysis was performed by Dr. Donata Magrini of the Institute for the Conservation and Valorisation of the Cultural Heritage (Department of Florence) of the National Research Council (ICVBC-CNR).

aromatic ring (Fig. 2.14). They therefore have many IR absorption bands that fall at the same frequency or at least at very close frequencies.

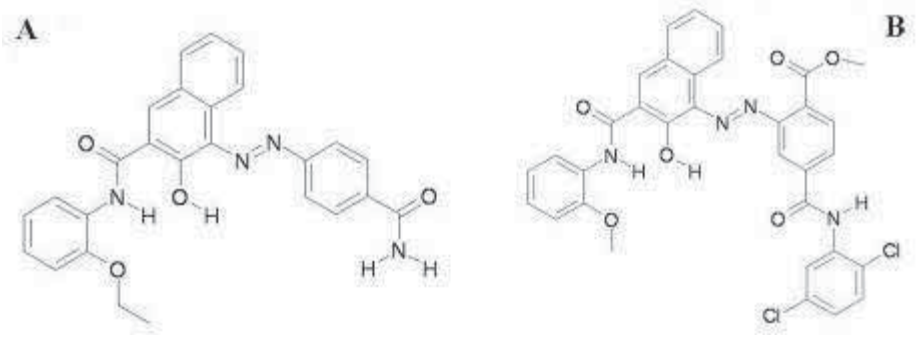

Fig. 2.14– The chemical structures of (A) Naphtol carbamide (PR170) and (B) Naphtol As (PR188)

In fact, by comparing the FT-IR spectrum of sample 3 with the IRUG 2007 reference spectra of PR170 (ref. IOD00271) and PR188 (ref. IOD00432), it was possible to confirm the presence of both the organic dyes (Fig. 2.15). In particular, many absorption bands due only to PR188 (1675 cm^{-1}, 1555 cm^{-1}, 1492 cm^{-1}, 1471 cm^{-1}, 1408 cm^{-1}, 1326 cm^{-1}, 1155 cm^{-1}, 1073 cm^{-1}, 742 cm^{-1}) were easily detectable, while those related to PR170 were extremely low (1386 cm^{-1}) or were superimposed on that of PR188 (3063 cm^{-1}, 1656 cm^{-1}, 1450 cm^{-1}, 1290 cm^{-1}, 1263 cm^{-1}, 1047 cm^{-1}, 1011 cm^{-1}, 752 cm^{-1}) (Learner, 2004).

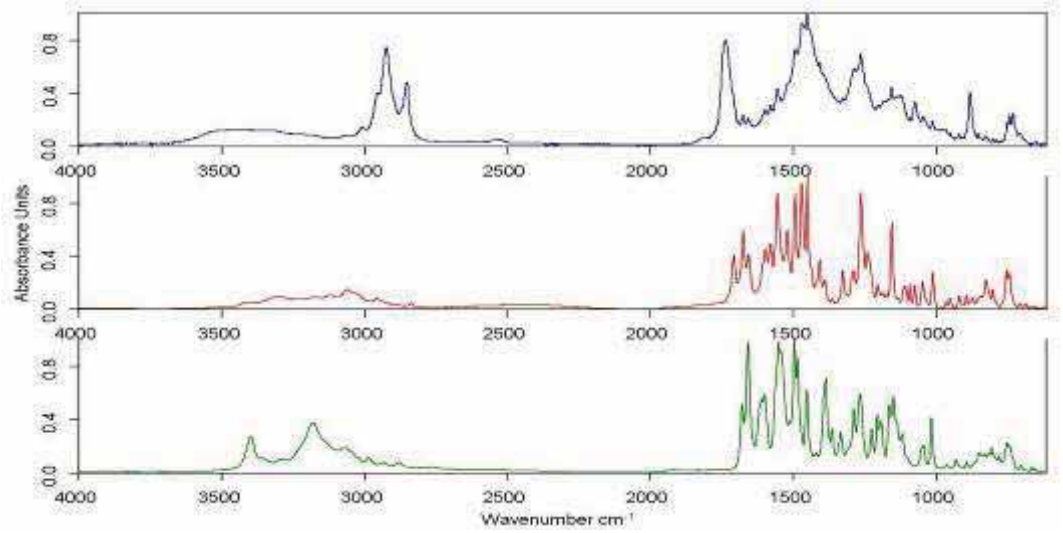

Fig. 2.15 - FT-IR spectra of *Winsor Red Griffin Alkyd Oil Colour* (blue line), references of PR188 (red line, ref. IOD00432) and PR170 (green line, ref. IOD00271) from IRUG 2007 database

The UV-Vis-NIR reflectance spectrum (Fig. 2.16) showed an absorption band "S"-shape, with an inflection point at 603 nm (2.06 eV), due to a *n*(azo)→π* transition (Robin and Simpson, 1962).

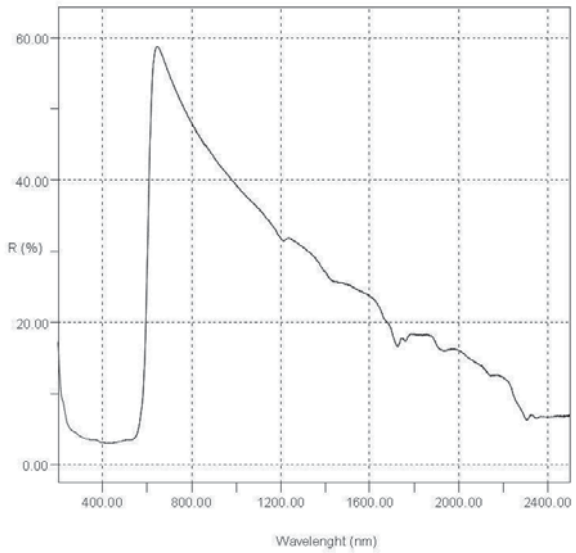

Fig. 2.16 - UV-Vis-NIR reflectance spectrum of *Winsor red Griffin Alkyd Oil Colour*

Cadmium zinc sulphide, PY35. No characteristic bands of cadmium yellow pigment were detectable by FT-IR in the medium IR spectral region. The UV-Vis-NIR reflectance spectrum showed, in the visible region, the typical "S"-shape of the band-band transitions that is characteristic of many inorganic pigments (Fig. 2.17). In this case, the broad absorption due to these transitions was characterised by an inflection point centred at 518 nm (2.39 eV), which is typical of a light yellow brilliant paint (Buxbaum, 1993). A very weak absorption at 728 nm can be attributed to the presence of Co^{2+} as a vicariant of Zn^{2+} in the ZnS lattice (Weakliem, 1962; Van Alphen, 1998).

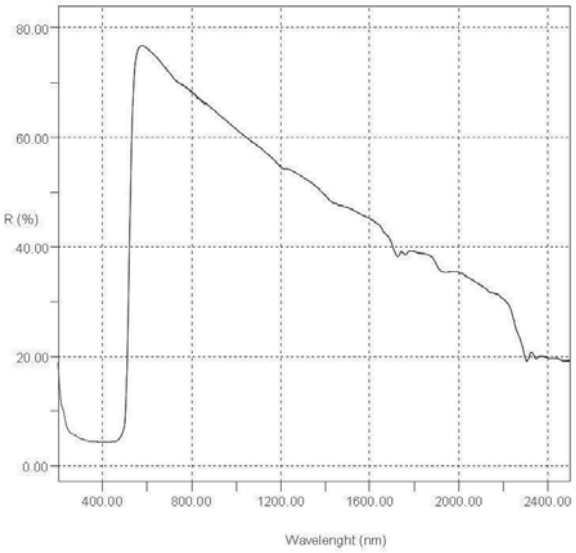

Fig. 2.17 - UV-Vis-NIR reflectance spectrum of *Cadmium yellow light Griffin Alkyd Oil Colour*

The XRF[10] elemental analysis showed a peculiar presence of high counts of calcium, cadmium, zinc, sulphur and barium. These data confirmed the presence of (Cd, Zn)S, $CaCO_3$ and $BaSO_4$ (Fig. 2.18).

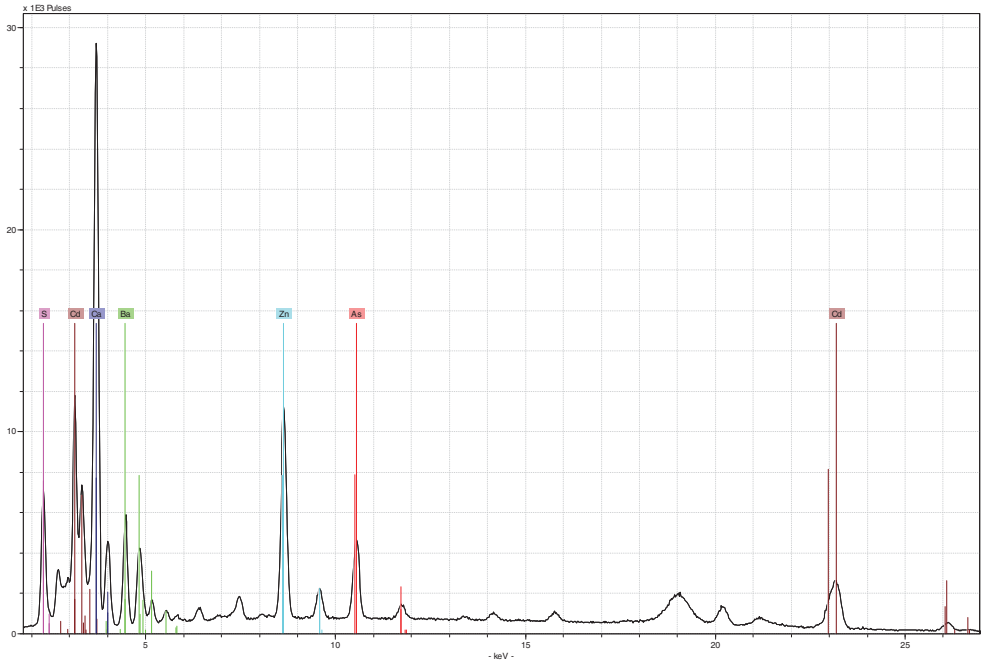

Fig. 2.18 - XRF spectrum of *Cadmium yellow light Griffin Alkyd Oil Colour* showing the presence of Ca (grey lines), Cd (brown lines), Zn (cyan lines), S (pink lines), Ba (green lines) and a lesser amount of As (red lines)

Arylamide yellow, PY3. The FT-IR absorption bands of the PY3 yellow dye (Fig. 2.19) in sample 5 corresponded to those found in the literature (Learner, 2004; Quillen Lomax *et al*., 2007): 3110 cm^{-1} (stretching of the NH bond), 1671 cm^{-1} (C=O stretching), 1592 cm^{-1}, 1583 cm^{-1}, 1535 cm^{-1}, 1502 cm^{-1} (asymmetric stretching of nitro group-NO_2 on the aromatic ring), 1336 cm^{-1}, 1279 cm^{-1}, 1176 cm^{-1}, 1137 cm^{-1}, 1036 cm^{-1} (absorbance due to the aromatic chloro group), 812 cm^{-1}, 749 cm^{-1} and 620 cm^{-1} (Fig. 2.20).

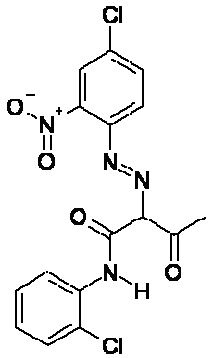

Fig. 2.19 - Chemical structure of arylamide yellow (PY3)

[10] The XRF analysis was performed by Dr. Donata Magrini of the Institute for the Conservation and Valorisation of the Cultural Heritage (Department of Florence) of the National Research Council (ICVBC-CNR).

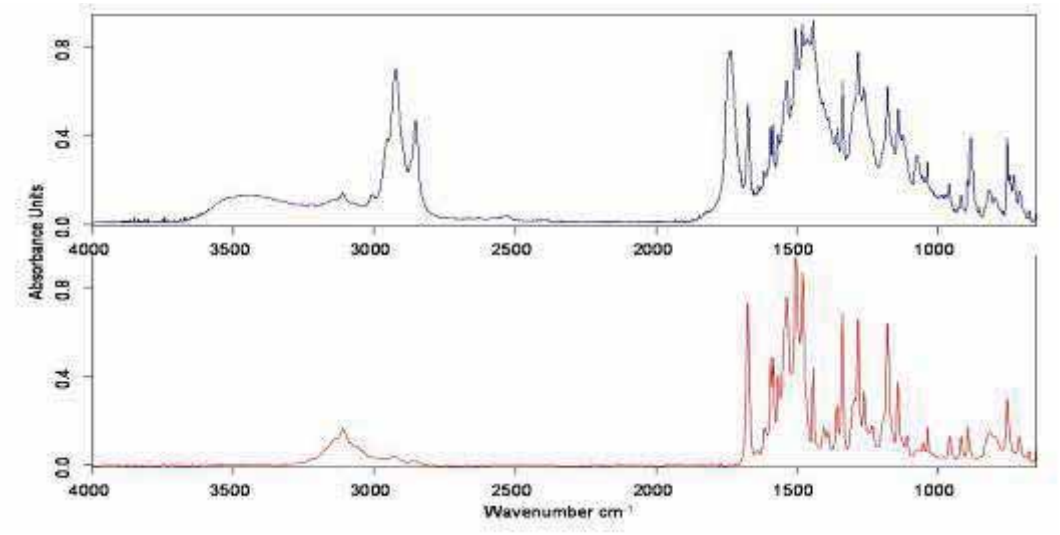

Fig. 2.20 - FT-IR spectra of *Winsor Lemon Griffin Alkyd Oil Colour* (blue line) and of PY3-IRUG 2007 database (ref. IOD00360, red line)

The UV-Vis-NIR reflectance spectrum (Fig. 2.21) showed a strong absorption in the blue-violet region of the Vis, with an inflection point at 493 nm due to a $n(\text{azo}) \rightarrow \pi^*$ transition (Robin and Simpson, 1962).

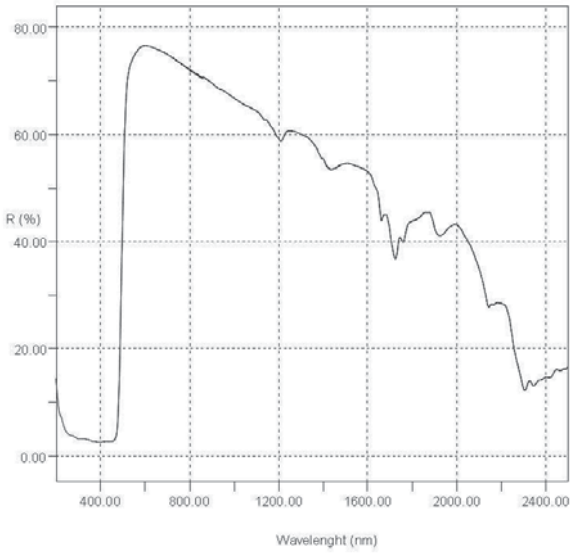

Fig. 2.21 - UV-Vis-NIR reflectance spectrum of *Winsor lemon Griffin Alkyd Oil Colour*

THM-GC/MS also confirmed the composition declared by the manufacturer. In the pyrogram of *Winsor lemon Griffin Alkyd Oil Colour*, the pyrolysis fragments of a monoazo yellow pigment (peak #: o-Chloroaniline; peak *: 3-chloro-N-methyl-benzenamine) were visible, along with the peaks of the alkyd binder (Fig. 2.22).

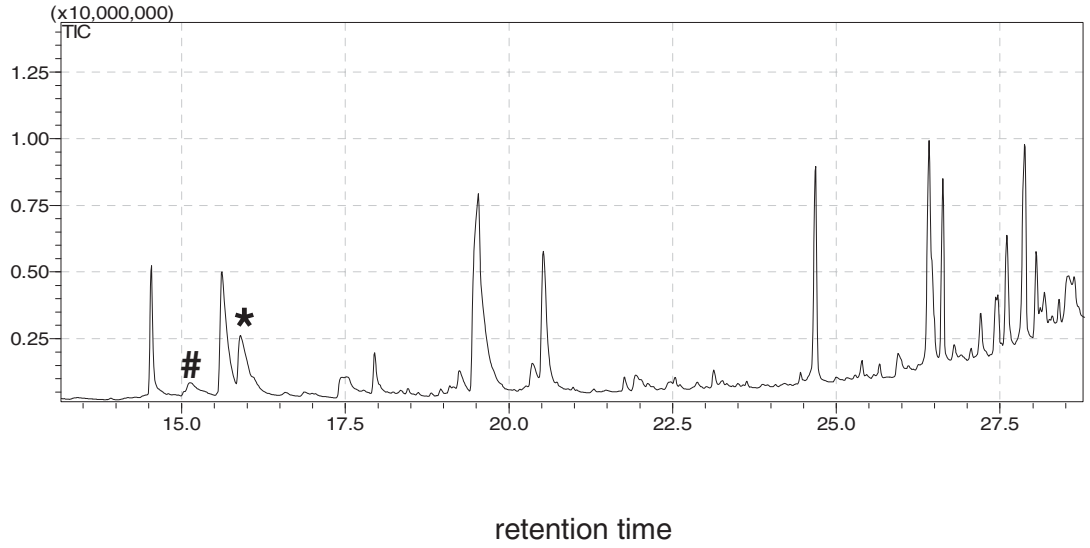

Fig. 2.22 - Pyrogram of *Winsor Lemon Griffin Alkyd Oil Colour* (peak #: o-Chloroaniline m/z 65,92,127 retention time 15.1 min; peak *: 3-chloro-N-methyl-benzenamine m/z 77,140, 142 retention time 15.9 min).

Hydrated chromium oxide green ($Cr_2O_3.xH_2O$), PG18. The FT-IR spectrum of *Viridian Griffin Alkyd Oil Colour* (Fig. 2.23) showed a broad absorption band in the OH stretching region (3600-3100 cm^{-1}) and absorptions at 1062 cm^{-1}, 791 cm^{-1}, 553 cm^{-1} and 470 cm^{-1}, which are referred to the hydrated chromium oxide green pigment used in the formulation of the paint (Bacci, 2000).

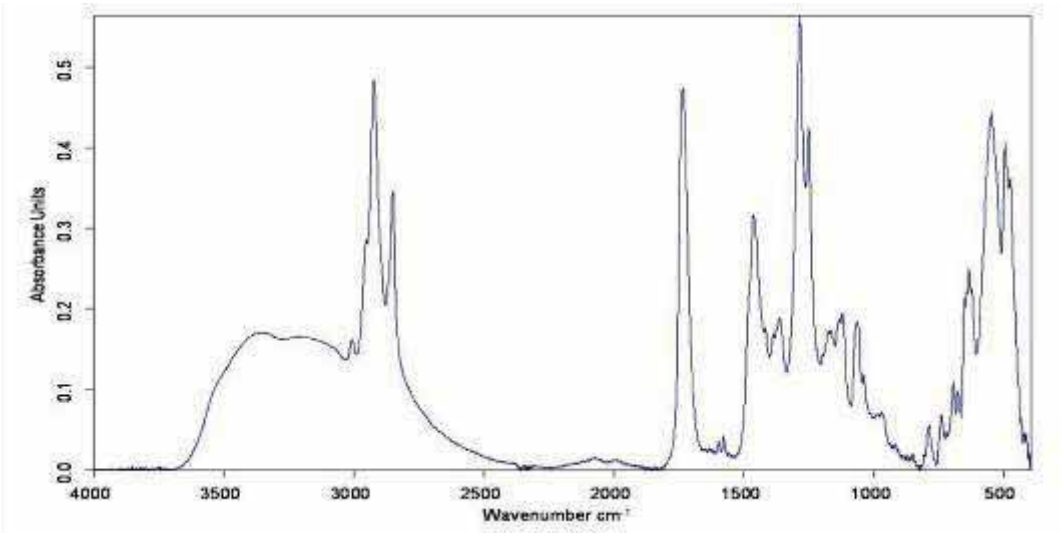

Fig. 2.23- FT-IR spectrum of *Viridian Griffin Alkyd Oil Colour*

The UV-Vis-NIR reflectance spectrum (Fig. 2.24) showed absorption bands at about 435 nm and 700 nm, as well as one in the UV at 300 nm: these are typical of the Viridian pigment. In the visible region, the two reflectance maxima at about 510 nm and 376 nm are responsible for the bluish green hue of this particular pigment (Lewis 1987). The absorptions in the visible range were due to ligand field transition related to the presence of Cr(III), while the UV-absorption may have been caused by electronic charge-transfer transitions between the chromium and the oxygen (Bacci, 2000).

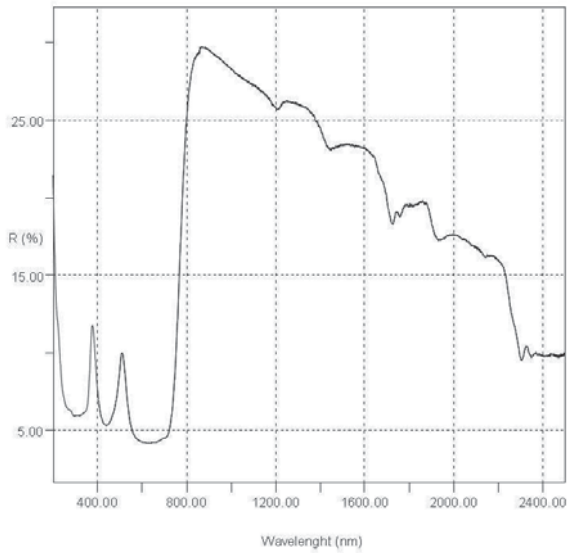

Fig. 2.24 - UV-Vis-NIR reflectance spectrum of *Viridian Griffin Alkyd Oil Colour*

Chlorinated copper phthalocyanine green ($C_{32}H_3N_8Cl_{13}Cu$), PG 7. After considering the FT-IR spectrum of sample 7 (Fig. 2.25), we attributed the bands at 1212 cm^{-1} and 777 cm^{-1} to the presence of a phthalocyanine green dye (PG7), Fig. 2.26.

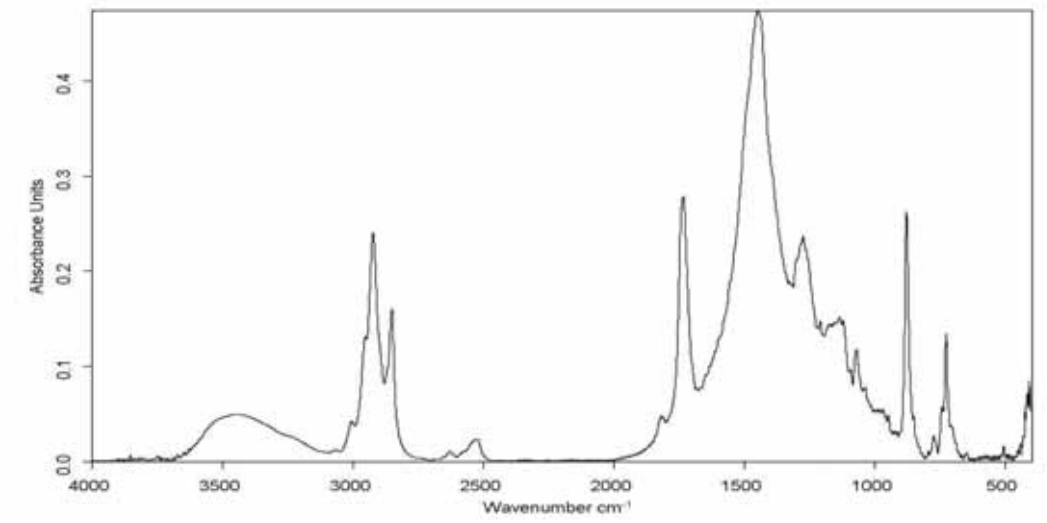

Fig. 2.25 - FT-IR spectrum of *Phthalo Green Griffin Alkyd Oil Colour*

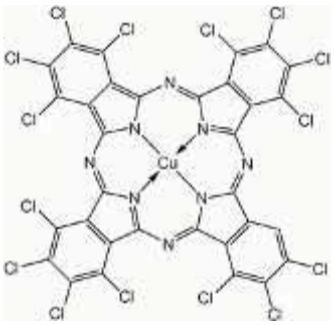

Fig. 2.26 - Chemical structure of copper phthalocyanine green (PG7)

Furthermore, three absorption bands at 640 nm, 721 nm and 797 nm and a maximum of reflectance at 490 nm were present in the UV-Vis-NIR reflectance spectrum (Fig. 2.27). The absorptions were due to $\pi \rightarrow \pi^*$ type electronic transitions (Johnston, 1967).

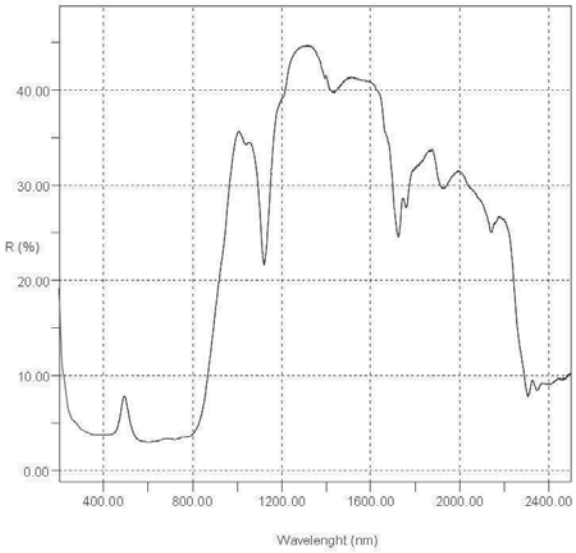

Fig. 2.27 - UV-Vis-NIR reflectance spectrum of *Phthalo Green Griffin Alkyd Oil Colour*

Ultramarine blue ($Na_6Al_6Si_6O_{24}S_4$), PB 29. In the FT-IR spectrum of sample 8 (Fig. 2.28), the absorption bands of the Ultramarine Blue pigment (PB29) were clearly visible. To be brief, the overlapping stretching bands of Si-O-Si and Si-O-Al between 1150 cm^{-1} and 950 cm^{-1} were present, as were four bands at 688, 654, 581 and 445 cm^{-1} that all corresponded to Si-O bond vibrations (Bruni *et al.*, 1999; Learner, 2004; Vahur *et al.*, 2010).

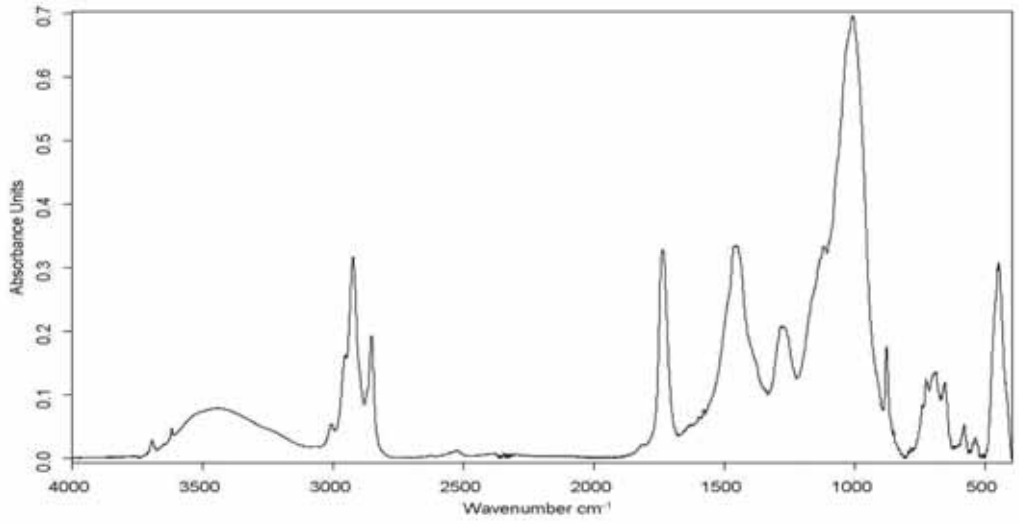

Fig. 2.28 - FT-IR spectrum of *Ultramarine Blue Griffin Alkyd Oil Colour*

The UV-Vis-NIR reflectance spectrum (Fig. 2.29) showed a maximum of reflectance at about 447 nm and one around 770 nm, thus confirming the reddish component in the hue of the blue pigment as reported in the literature (Herbst and Hunger, 1993). The absorption centred

around 600 nm was due to a charge transfer electronic transition that was related to the presence of the S_3^- ion in the crystal structure of the aluminosilicate (Bacci, 2000).

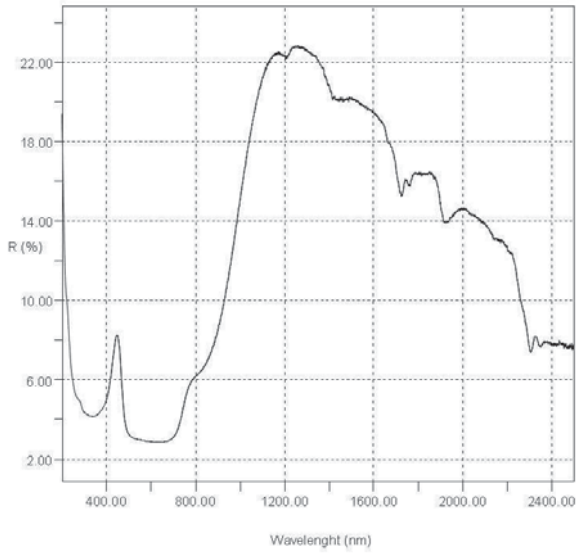

Fig. 2.29 - UV-Vis-NIR reflectance spectrum of *French Ultramarine Griffin Alkyd Oil Colour*

Copper phthalocyanine blue, PB15. In the IR spectrum of sample 9 (Fig. 2.30), the absorption bands of both the resin and the extender partially covered the characteristic peaks of the phthalo dye, which generally presents many sharp bands (mainly below 1700 cm^{-1}). In spite of these interferences, three peaks at 1165 cm^{-1}, 1092 $cm^{-1}$and 722 cm^{-1} could be attributed to the phthalocyanine blue (PB15) (Fig. 2.31). In particular, the sharp band at 722 cm^{-1} (out-of-plane aromatic C-H bending) referred to the α-polymorphic form (Ebert and Gottlieb, 1952; Knudsen, 1966; Newman, 1979).

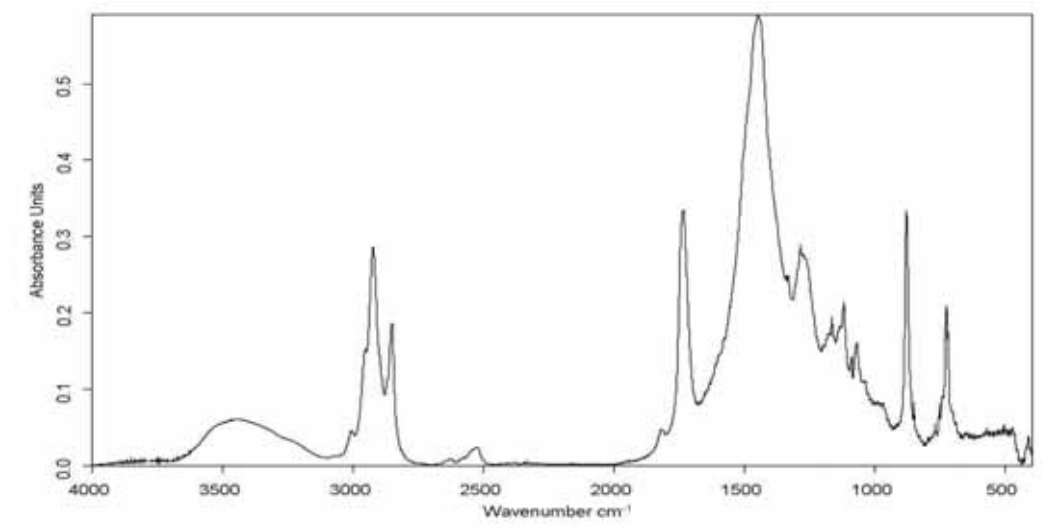

Fig. 2.30 - FT-IR spectrum of *Phthalo Blue Griffin Alkyd Oil Colour*

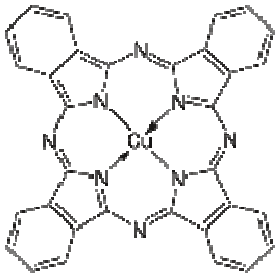

Fig. 2.31 - Chemical structure of copper phthalocyanine blue (PB15)

In the visible region of the UV-Vis-NIR reflectance spectrum (Fig. 2.32), a maximum of reflectance at 458 nm and two main absorption bands at 614 and 692 nm were evident (Johnston, 1967). The relative maximum of reflectance between 600 and 700 nm is characteristic of phthalocyanine blue in the α crystalline form, and is the cause of the reddish tint of the paint. Absorption bands in the UV, between 200 and 350 nm, are due to $\pi \rightarrow \pi^*$ transitions (Johnston, 1967).

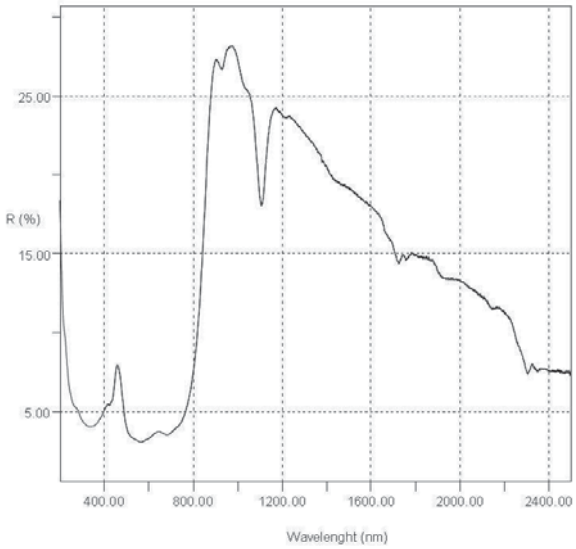

Fig. 2.32 - UV-Vis-NIR reflectance spectrum of *Phthalo Blue Griffin Alkyd Oil Colour.*

Ivory Black, PBk9. In the FT-IR spectrum of sample 10, the absorption bands of apatite $Ca_5(PO_4)_3[F,OH,Cl]$ were present. In particular, a broad band centred at 1025 cm^{-1} referred to phosphate ion stretching was detected; while three sharp peaks (562 cm^{-1}, 599 cm^{-1}, 630 cm^{-1}) were due to phosphate ion bending (Fig. 2.33). Thanks to the fact that ivory black usually contains up to 80% of calcium phosphate and15-20% of carbon, the IR data confirmed the presence of this pigment in the formulation of sample 10.

No useful information was obtained from the UV-Vis-NIR reflectance spectrum due to the presence of a strong absorption band (that was due to the presence of carbon) which covered the entire spectral range investigated.

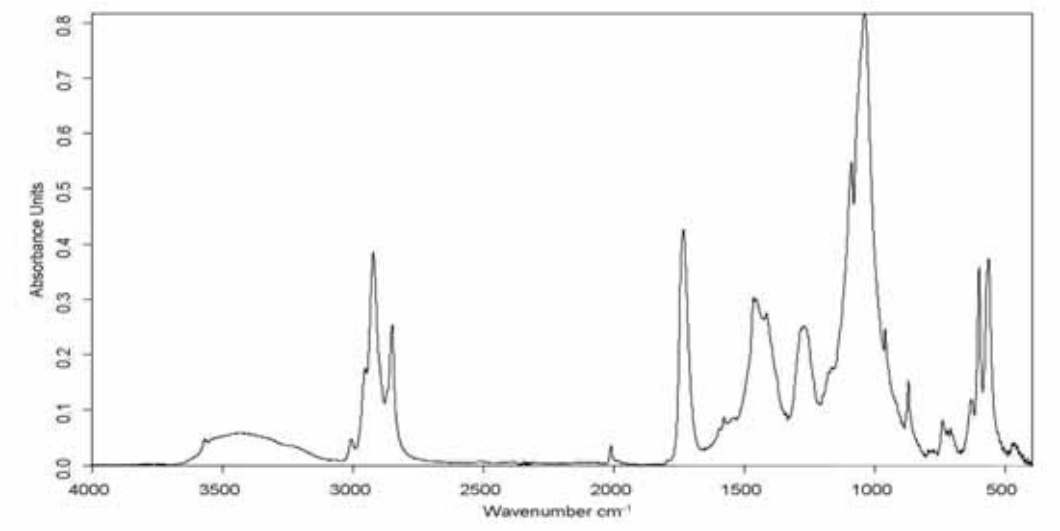

Fig. 2.33 - FT-IR spectrum of *Ivory Black Griffin Alkyd Oil Colour*

Extenders

FT-IR spectra revealed the presence of three inorganic fillers:

- dolomite, $MgCa(CO_3)_2$ (all samples except 6): absorption bands at 2530, 1450, 881, and 730 cm^{-1} (Gadsden, 1975; van der Marel and Beutelspacher, 1976);
- barite, $BaSO_4$ (samples 2 and 4): absorption bands at 1185, 1120, 1082, 635, and 610 cm^{-1} (Gadsden, 1975);
- kaolinite, $Al_2Si_2H_4O_9$ (sample 8), absorption bands at 3695, 3669, 3653 and 3620 cm^{-1} (Madejová, 2003).

The dolomite was also identified by means of UV-Vis-NIR reflectance spectroscopy. In particular, an overtone, at 2350 nm ($3\nu_3$), and two combination bands, at 1900 nm ($\nu_1+3\nu_3$) and 2143 nm ($\nu_1+2\nu_3+\nu_4$), of the carbonate ion of the dolomite were visible in the UV-Vis-NIR reflectance spectra (Gadsden, 1975).

2.2-4 Samples characterisation after UV ageing

PLM

After comparing the images acquired in visible light before and after the UV ageing, we found no relevant changes in any of the samples (covered or uncovered) except for *French Ultramarine Griffin Alkyd Oil Colour*. As can be seen in Figure 2.37, the colour of the un-aged sample was homogeneously deep blue (Fig. 2.34 A). Instead, after the UV exposition, the covered area of this sample (Fig. 2.34 B top) was found to be unchanged, while the uncovered one (Fig. 2.34 B bottom) showed considerable change in colour, resulting as a lighter blue.

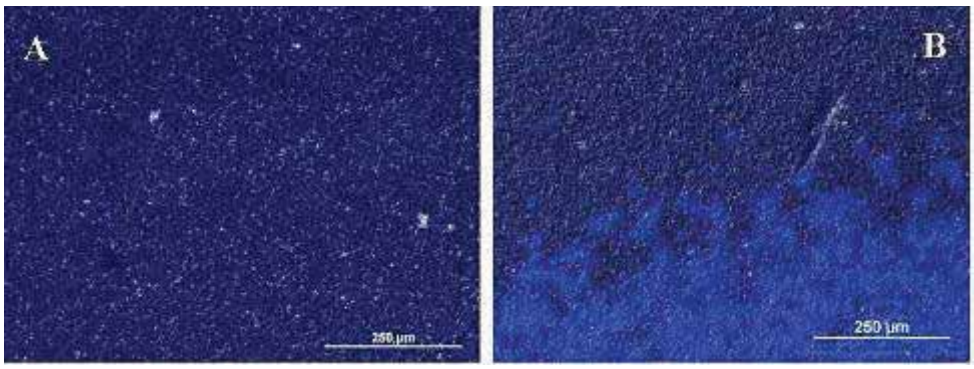

Fig. 2.34 – Visible images acquired on *French Ultramarine Griffin Alkyd oil colour* before (A) and after UV ageing (B) by means of optical microscopy

After considering the images acquired under UV light, the same trend was observed for all the analysed samples. All mock-ups were found to be fluorescent prior to the artificial ageing. After the ageing, the fluorescence of the covered areas had decreased only slightly, while it was extremely low or negligible in the uncovered areas. A typical example of this behaviour is reported in Figure 2.35.

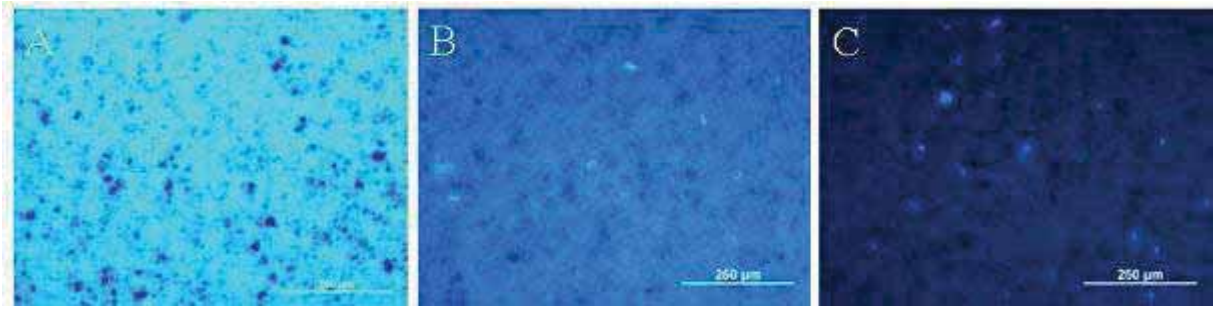

Fig. 2.35 - UV images acquired on *Viridian Griffin Alkyd oil colour* before (A) and after UV ageing on the non-irradiated (B) and irradiated areas (C) by means of optical microscopy

Colorimetry

Tables 2.8 and 2.9 summarise the total colour changes (ΔE_{00}) and the shift in the values of the lightness/darkness (ΔL^*), redness/greenness (Δa^*), yellowness/blueness (Δb^*) of alkyd samples after 90 and 150 days of UV ageing.

The most significant colour changes were recorded for *French Ultramarine Griffin Alkyd Oil Colour*. The total colour difference of the UV radiation exposed area was $\Delta E_{00} = 15.5$. The greatest contribution to the colour variation was made by the b* parameter, which decreased (final $\Delta b* = -35.5$) during the ageing. Furthermore, the L* and a* parameters increased ($\Delta L^* = 8.5$; $\Delta a^* = 13.6$). Thus, during the ageing, both the blueness and lightness of the uncovered area increased. Instead, after a consideration of the un-irradiated area, we found the total colour difference to be $\Delta E_{00} = 2.3$. In this case, a small decrease in the blueness ($\Delta b^* = 3.5$) and in the reddish component ($\Delta a^* = -2.1$) occurred.

The *Phthalo blue Griffin Alkyd Oil Colour* underwent, instead, less pronounced colour changes (uncovered area: $\Delta E_{00} = 2.1$; covered area: $\Delta E_{00} = 2.0$). In this case, both areas

showed the same behaviour under ageing, with an increase in the L* and b* parameters and a decrease in the reddish/greenish parameter.

Table 2.8 – ΔE_{00} colour variations of *Griffin Alkyd Oil Colours* after 90 and 150 days of UV ageing (unc: uncovered area; cov: covered area; ±: maximum error)

Sample	Colour	CIEDE2000			
		ΔE_{00} (90 days)	**±**	**ΔE_{00} (150 days)**	**±**
1	**Titanium White-unc**	**1.14**	0.02	**1.21**	0.04
	Titanium White-cov	**1.77**	0.03	**1.50**	0.02
2	**Cadmium Red Medium-unc**	**1.77**	0.06	**1.98**	0.07
	Cadmium Red Medium-cov	**1.33**	0.04	**1.77**	0.04
3	**Winsor Red-unc**	**2.02**	0.01	**2.77**	0.02
	Winsor Red-cov	**0.92**	0.00	**1.16**	0.01
4	**Cadmium Yellow Light-unc**	**0.59**	0.01	**0.90**	0.02
	Cadmium Yellow Light-cov	**0.63**	0.01	**1.93**	0.05
5	**Winsor Lemon-unc**	**2.02**	0.00	**2.81**	0.02
	Winsor Lemon-cov	**0.45**	0.02	**2.03**	0.02
6	**Viridian-unc**	**1.45**	0.03	**1.85**	0.04
	Viridian-cov	**1.32**	0.02	**1.44**	0.04
7	**Phthalo Green-unc**	**2.73**	0.04	**3.18**	0.04
	Phthalo Green-cov	**1.99**	0.00	**2.21**	0.02
8	**French Ultramarine-unc**	**12.63**	0.09	**15.47**	0.11
	French Ultramarine-cov	**0.10**	0.08	**2.25**	0.16
9	**Phthalo Blue-unc**	**2.08**	0.05	**2.09**	0.10
	Phthalo Blue-cov	**1.37**	0.06	**2.00**	0.04
10	**Ivory Black-unc**	**1.03**	0.00	**1.22**	0.02
	Ivory Black-cov	**0.84**	0.02	**0.85**	0.01

Cadmium yellow light Griffin Alkyd Oil Colour was very stable after 90 days of ageing. After 150 days, a slight decrease in the lightness and a more pronounced decrease in the b* coordinate occurred. In particular, a weak increase in the reddish component also occurred in the un-exposed area.

The colour differences for the *Winsor Lemon Griffin Alkyd Oil Colour* sample after 90 days of artificial ageing were different in both areas (uncovered area: $\Delta E_{00} = 2.02$; covered area: $\Delta E_{00} = 0.45$), with a tendency to increase after 150 days (uncovered area: $\Delta E_{00} = 2.81$; covered area: $\Delta E_{00} = 2.03$). These variations were due to a decrease in the L* and b* coordinates and to an increase in the a* parameter.

In considering the green alkyd samples, we observed in both cases an increase in the L* and a* parameters due to a rise in their brightness and a decrease in the greenish component.

Cadmium red medium Griffin Alkyd Oil Colour showed homogeneous colour differences for both areas due to a decrease in the reddish component (final $\Delta a^* > -2.50$) and in the yellowness (final $\Delta b^* > -3.50$). The other red sample (*Winsor red Griffin Alkyd Oil Colour*) had a total colour change that was more marked on the exposed area. This was due principally to a strong decrease in the red and the yellow components.

Table 2.9 – ΔL*, Δa* and Δb* colour variations of of *Griffin Alkyd Oil Colours* after 90 and 150 days of UV ageing (unc: uncovered area; cov: covered area)

Sample	Colour	90 days			150 days		
		ΔL*	**Δa***	**Δb***	**ΔL***	**Δa***	**Δb***
1	**Titanium White-unc**	**0.40**	**0.42**	**-1.07**	**0.39**	**0.44**	**-1.15**
	maximum error	± 0.04	± 0.02	± 0.06	± 0.16	± 0.03	± 0.05
	Titanium White-cov	**-0.29**	**-0.36**	**2.08**	**-1.02**	**-0.02**	**1.65**
	maximum error	± 0.08	± 0.03	± 0.09	± 0.03	± 0.03	± 0.08
2	**Cadmium Red Medium-unc**	**1.31**	**-1.75**	**-3.26**	**0.16**	**-2.61**	**-3.66**
	maximum error	± 0.06	± 0.15	± 0.23	± 0.04	± 0.12	± 0.17
	Cadmium Red Medium-cov	**0.91**	**-1.44**	**-2.67**	**-0.08**	**-3.45**	**-4.92**
	maximum error	± 0.05	± 0.04	± 0.07	± 0.05	± 0.07	± 0.11
3	**Winsor Red-unc**	**-0.48**	**-3.22**	**-5.26**	**-1.16**	**-4.51**	**-6.75**
	maximum error	± 0.03	± 0.02	± 0.04	± 0.02	± 0.05	± 0.03
	Winsor Red-cov	**0.51**	**-1.24**	**-2.13**	**0.17**	**-2.23**	**-3.18**
	maximum error	± 0.03	± 0.03	± 0.05	± 0.04	± 0.04	± 0.04
4	**Cadmium Yellow Light-unc**	**0.00**	**0.10**	**-2.67**	**-0.64**	**0.34**	**-3.42**
	maximum error	± 0.04	± 0.03	± 0.07	± 0.04	± 0.03	± 0.06
	Cadmium Yellow Light-cov	**-0.36**	**0.22**	**-2.54**	**-1.66**	**1.01**	**-6.26**
	maximum error	± 0.03	± 0.02	± 0.05	± 0.07	± 0.04	± 0.09
5	**Winsor Lemon-unc**	**-2.22**	**2.35**	**-3.29**	**-2.89**	**3.46**	**-4.51**
	maximum error	± 0.02	± 0.04	± 0.09	± 0.06	± 0.05	± 0.12
	Winsor Lemon-cov	**0.31**	**0.66**	**-1.19**	**-1.63**	**2.95**	**-3.71**
	maximum error	± 0.05	± 0.07	± 0.07	± 0.07	± 0.05	± 0.08
6	**Viridian-unc**	**-0.16**	**1.56**	**-0.08**	**-0.92**	**1.80**	**-0.31**
	maximum error	± 0.02	± 0.04	± 0.01	± 0.03	± 0.06	± 0.03
	Viridian-cov	**0.78**	**1.27**	**0.10**	**0.42**	**1.51**	**0.16**
	maximum error	± 0.01	± 0.03	± 0.03	± 0.04	± 0.04	± 0.04
7	**Phthalo Green-unc**	**2.77**	**1.67**	**0.59**	**3.19**	**1.93**	**0.80**
	maximum error	± 0.05	± 0.04	± 0.01	± 0.05	± 0.06	± 0.02
	Phthalo Green-cov	**2.28**	**0.92**	**0.65**	**2.38**	**1.10**	**0.95**
	maximum error	± 0.02	± 0.00	± 0.02	± 0.05	± 0.03	± 0.03
8	**French Ultramarine-unc**	**3.37**	**13.69**	**-31.07**	**8.54**	**13.61**	**-35.52**
	maximum error	± 0.05	± 0.04	± 0.21	± 0.02	± 0.05	± 0.18
	French Ultramarine-cov	**0.02**	**0.09**	**-0.17**	**0.17**	**-2.08**	**3.49**
	maximum error	± 0.04	± 0.12	± 0.21	± 0.05	± 0.17	± 0.27
9	**Phthalo Blue-unc**	**2.56**	**-0.01**	**1.32**	**2.60**	**-0.16**	**1.32**
	maximum error	± 0.04	± 0.04	± 0.28	± 0.42	± 0.42	± 0.63
	Phthalo Blue-cov	**1.38**	**-0.79**	**1.68**	**1.86**	**-1.20**	**2.59**
	maximum error	± 0.06	± 0.04	± 0.27	± 0.08	± 0.06	± 0.32
10	**Ivory Black-unc**	**1.39**	**0.04**	**0.22**	**1.62**	**0.07**	**0.32**
	maximum error	± 0.01	± 0.02	± 0.01	± 0.02	± 0.05	± 0.05
	Ivory Black-cov	**1.14**	**0.01**	**0.11**	**1.16**	**0.03**	**0.14**
	maximum error	± 0.02	± 0.03	± 0.03	± 0.03	± 0.03	± 0.04

After considering *Ivory Black Griffin Alkyd Oil Colour*, we concluded that the colour difference was primarily due to changes in the L* coordinate. There was, indeed, an increase in the value of this parameter, and this fact provided evidence of an increase in the lightness of the original colour.

For *Titanium white Griffin Alkyd Oil Colour*, the total colour differences were due to a decrease in the yellowish component (Δb* ≈ -1) in the exposed area. In the un-exposed area,

instead, an increase in the b* parameter (more yellow) and a decrease in the lightness occurred.

UV-Vis-NIR Reflectance spectroscopy

UV-Vis-NIR reflectance spectra confirmed the results obtained with the colour measurements. In fact, this technique confirmed that the greatest variations registered after UV ageing were those relative to the irradiated area of the *French Ultramarine Griffin Alkyd Oil Colour* sample. As shown in Figure 2.36, the maximum of reflectance centred at 448 nm increased (from 8% to 47%) and broadened after UV ageing. Furthermore, the absorption centred at 600 nm decreased and the spectrum began to rise at wavelengths greater than 660 nm, with an inflection point at 726 nm. This type of evidence is typical of a light blue colour, thus confirming the visual perception of a de-saturated and lighter colour with respect to the unaged one. On the contrary, the spectrum registered on the un-irradiated area, was very similar to the one acquired before UV ageing: only a slight increase in the reflectance in the UV-Vis range and a decrease in the NIR range were detected.

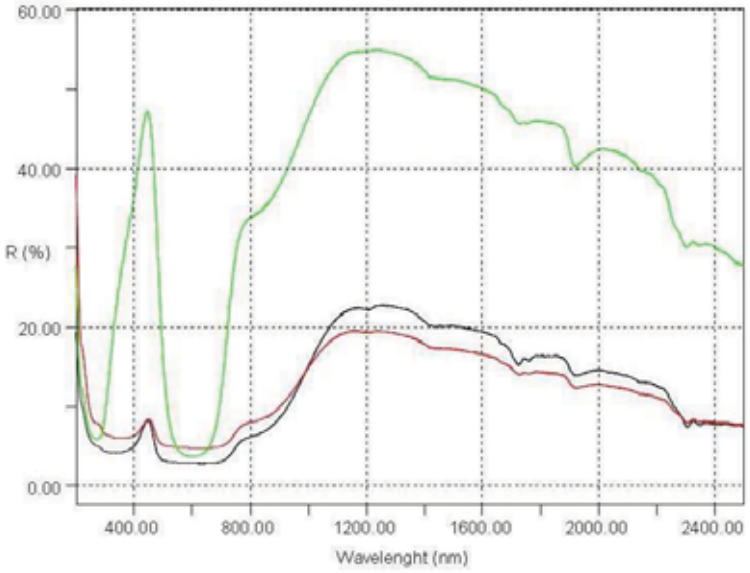

Fig. 2.36 - UV-Vis-NIR reflectance spectra of *French Ultramarine Griffin Alkyd Oil Colour* before (black line) and after UV ageing (irradiated area: green line; un-irradiated area: red line)

Another significant variation was registered for *Titanium White Griffin Alkyd Oil Colour*. For this sample an increase in the reflectance in the UV range was detected. Furthermore, a batochromic shift was observed in the 400-500 nm spectral range. This shift was more evident in the un-irradiated area, indicating a tendency of the sample to turn yellow when not exposed to UV radiation (Fig. 2.37).

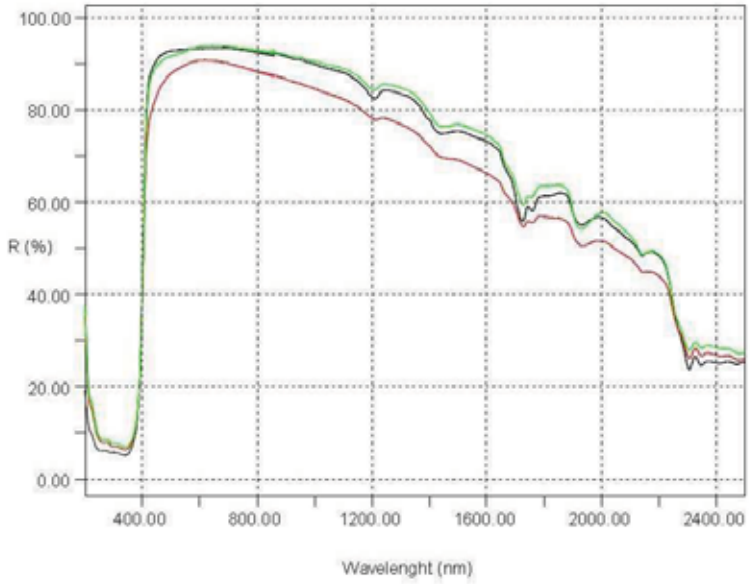

Fig. 2.37 - UV-Vis-NIR reflectance spectra of *Titanium White Griffin Alkyd Oil Colour* before (black line) and after UV ageing (irradiated area: green line; un-irradiated area: red line)

Similar behaviour was observed also for the spectra of the yellow samples (*Winsor lemon* and *Cadmium yellow light*), which presented a batochromic shift towards higher wavelengths (between 530 and 580 nm), thus indicating an increase in the reddish component of the colour (Fig. 2.38). After considering the other samples, we concluded that the variations detected were not very significant and that they involved only slight differences in reflectance, which usually tended to increase after UV irradiation.

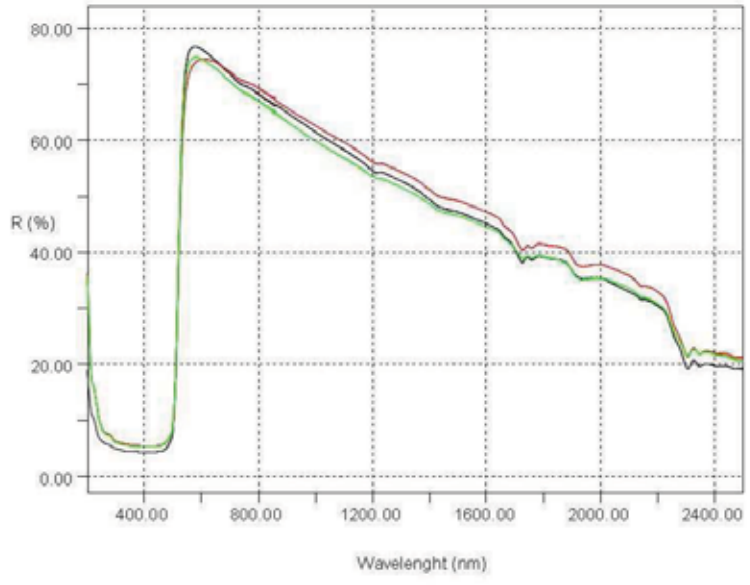

Fig. 2.38 - UV-Vis-NIR reflectance spectra of *Cadmium yellow light Griffin Alkyd Oil Colour* before (black line) and after UV ageing (irradiated area: green line; un-irradiated area: red line)

THM-GC/MS

In addition to pentaerythritol and phthalic and isophthalic acids, the fresh paints, as already described in § 2.2-3, contained typical drying oil compounds: glycerol derivatives, dicarboxylic and unsaturated fatty acids were in fact detected.

Since the formulation of alkyd paint involves the use of free fatty acids or modified siccative oils, the degradation of this binding medium is linked to that of traditional siccative oils. With progressive ageing, the fragmentation of triglycerides has as a direct consequence the formation of shorter fragments. The oxidative scission leads mainly to the formation of dicarboxylic acids, dihydroxy acids and hydroxylated monocarboxylic acids, and the exact size of the products depends on the position in which the scission occurs. For example, azelaic acid (nonanedioic acid) results from the oxidative scission of a double bond at C9 in the C18 unsaturated fatty acids (oleic, linoleic or linolenic acids). Other products of degradation are suberic (octanedioic acid) and sebacic acids (decanedioic acid). Diacids are relatively stable end-products of the autoxidation process (Lazzari and Chiantore, 1999; Colombini *et al.*, 2000 and 2002; van den Berg J. D., 2002; Schilling *et al.*, 2007; Ploeger *et al.*, 2008).

The pyrograms acquired after the UV ageing showed, as expected, a variation in the pyrolitic profile of the alkyd binder (Fig 2.39).

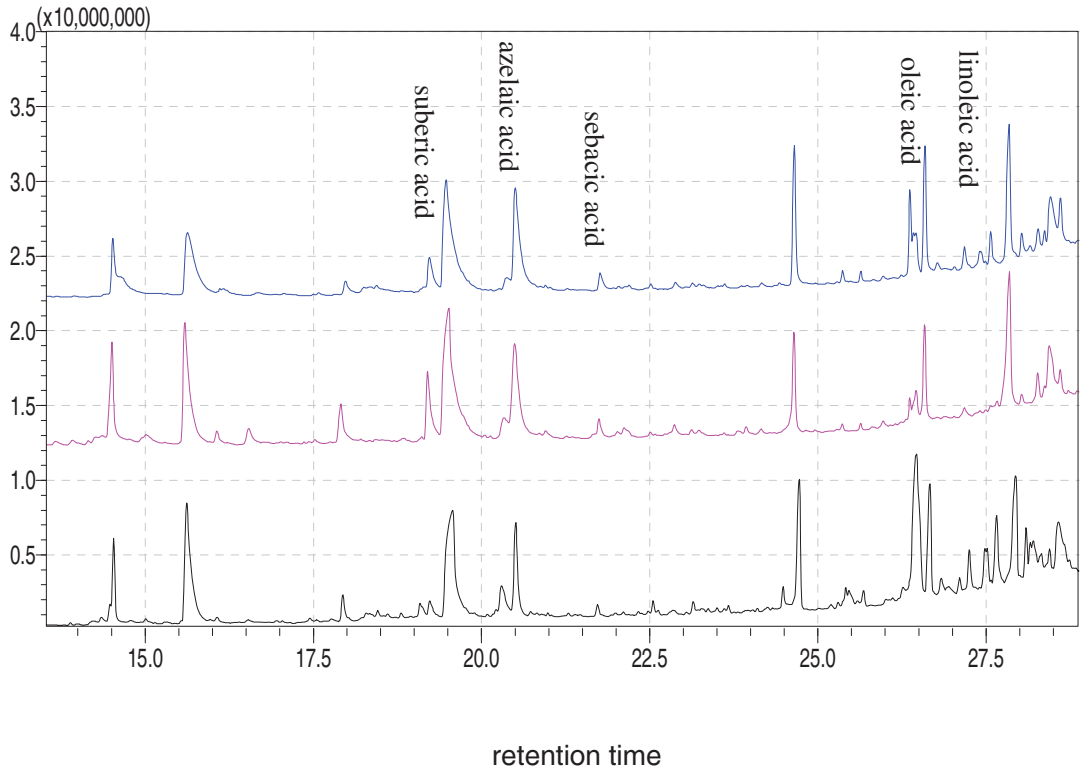

Fig. 2.39 - Comparison between the pyrograms acquired on *French Ultramarine Griffin Alkyd Oil Colour* before ageing (black line) and after UV ageing on the irradiated area (pink line) and on the un-irradiated area (blue line)

In particular, after ageing there was a decrease in the content of unsaturated fatty acids. Linoleic acid completely disappeared in all the covered and uncovered areas. Furthermore all the pyrograms showed a strong decrease in the peak referring to oleic acid. This degradation was generally higher in the exposed areas, and reached a maximum in the case of *French Ultramarine Griffin Alkyd Oil Colour*, where the content of oleic acid was close to zero. At the same time, the decrease in unsaturated fatty acids was accompanied by a significant rise in

the content of free carboxylic mono- and di-acids. A comparison of the pyrograms acquired before and after the UV ageing showed an increase, more marked in the uncovered areas, in azelaic and suberic acids. Although in a smaller quantity, also the content of sebacic acid increased after the artificial ageing.

Ivory Black Griffin Alkyd Oil Colour had proven to be the most stable paint analysed, since it showed the lowest degradation of unsaturated fatty acids. This was confirmed by the very low amount of free carboxylic mono- and di-acids detected in the pyrogram after the ageing.

FT-IR

Significant changes in the IR spectra were documented for the UV-aged samples, thus giving proof of photo-oxidative degradation in the alkyd paints.

FT-IR spectra acquired in transmittance mode (KBr pellets) after accelerated ageing showed certain differences with respect to the ones registered previously. For example, in the *French Ultramarine Griffin Alkyd Oil Colour*, which demonstrated the greatest variation in colour and in the pyrolitic profile (as shown in the previous sections), these differences were mainly due to variations in some absorption bands attributed to the alkyd resins (Fig. 2.40).

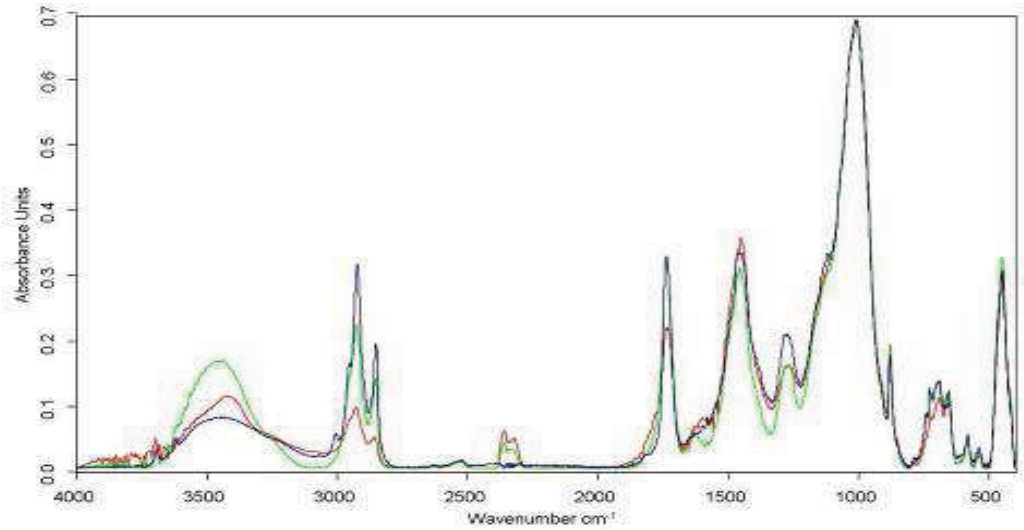

Fig. 2.40 - FT-IR spectra of *French Ultramarine Griffin Alkyd Oil Colour* before (blue line) and after UV ageing (irradiated area: red line; un-irradiated area: green line)

In fact, no significant differences in intensity and shape of the peaks due to the pigment and to the fillers were detected. Instead, the main changes were characterised by a disappearance of the vinyl protons C-H stretching peak (centred at 3008 cm^{-1}; see also §2.3-3) and by a decrease in the asymmetric and symmetric (C-H)CH_2 stretching absorptions, at about 2920 cm^{-1} and 2850 cm^{-1} respectively, of the alkyd resin (Fig. 2.41).

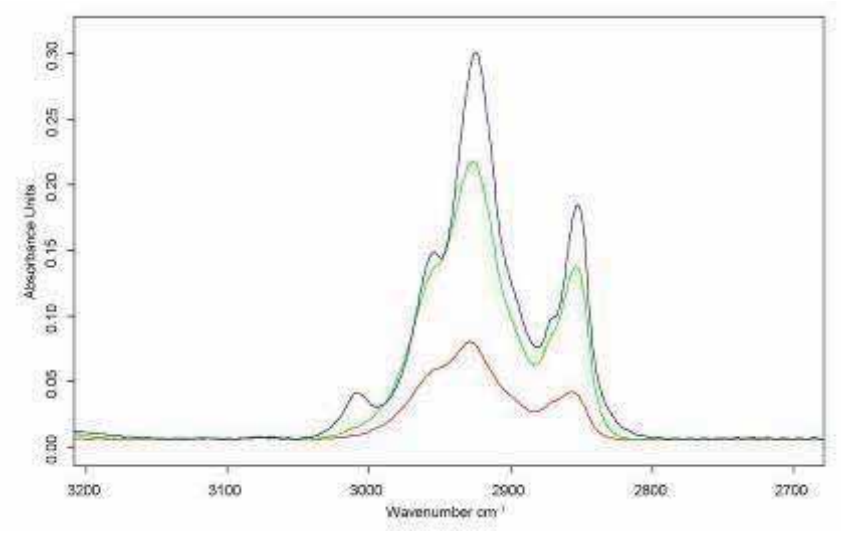

Fig. 2.41 - FT-IR spectra of *French Ultramarine Griffin Alkyd Oil Colour* before (blue line) and after UV ageing (irradiated area: red line; un-irradiated area: green line) in the 3200-2650 cm^{-1} spectral range

Furthermore, there was a decrease in intensity as well as a broadening of the C=O stretching peak at about 1730 cm^{-1}, due to the formation of new oxidised species in the alkyd medium (Fig. 2.42). These variations were mainly relevant in the areas exposed to the UV, thus confirming the degradative action of this radiation.

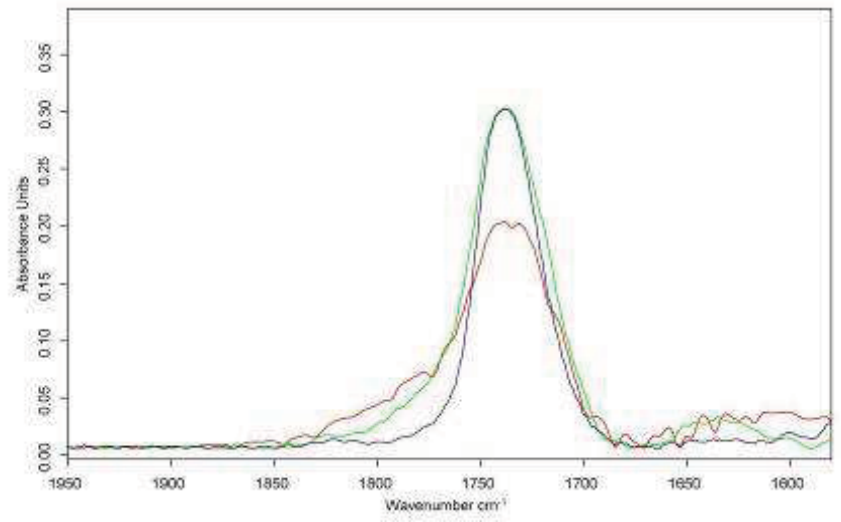

Fig. 2.42 - FT-IR spectra of *French Ultramarine Griffin Alkyd Oil Colour* before (blue line) and after UV ageing (irradiated area: red line; un-irradiated area: green line) in the 1950-1550 cm^{-1} spectral range

The IR spectra acquired in the ATR and Total Reflectance configuration confirmed the results obtained in transmittance mode. Indeed, the main differences detected after UV ageing also in these spectra were due to a modification of the peaks attributed to the alkyd resin. Furthermore, these variations were more evident than the ones registered in transmittance. As shown in Figures 2.43 and 2.44, in fact, the asymmetric and symmetric (C-H)CH_2 stretching absorption bands significantly decreased to the point of almost disappearing in the irradiated area. A change in dimension and shape of the C=O stretching peak was observed also in these spectra, while no significant variations in the bands due to the pigment were registered. Since both ATR and Total Reflectance methods are surface techniques, it was possible to

hypothesise that these phenomena were linked to the degradation in the alkyd medium, with the formation of photo-oxidative species over time mainly on the surface of the samples.

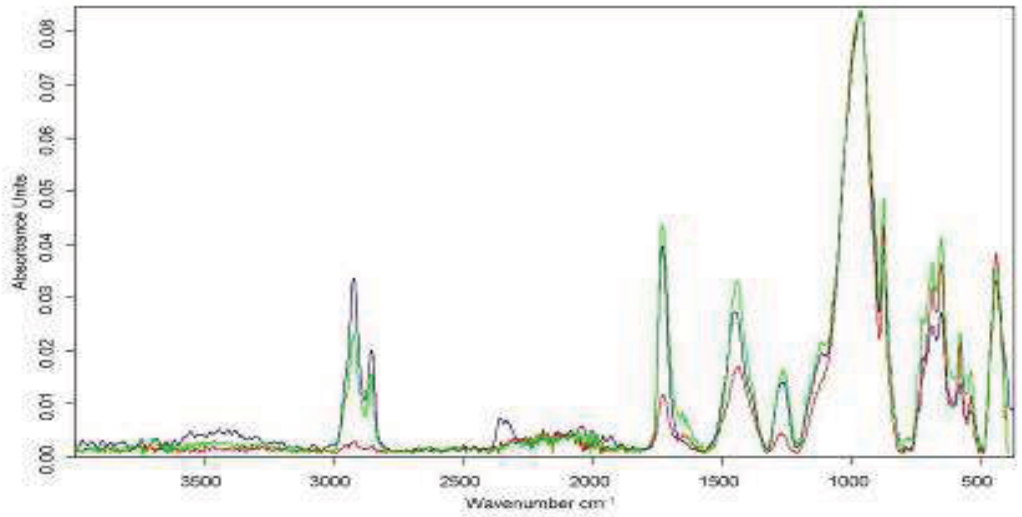

Fig. 2.43 - ATR spectra of *French Ultramarine Griffin Alkyd Oil Colour* before (blue line) and after UV ageing (irradiated area: red line; un-irradiated area: green line)

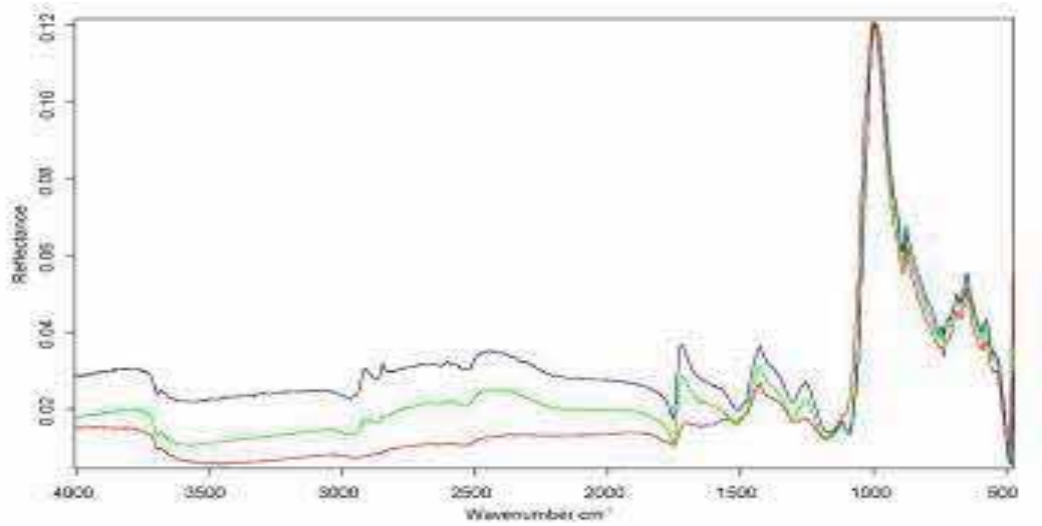

Fig. 2.44 - Total Reflectace spectra of *French Ultramarine Griffin Alkyd Oil Colour* before (blue line) and after UV ageing (irradiated area: red line; un-irradiated area: green line)

2.3 Study of the chemical curing in alkyd paints

2.3-1 Aim of the work

Although much work has already been done on the characterisation of alkyd paints (Loan, 1972; Hodson and Landert, 1987; Mallégol *et al.*, 2001 and 2002; Muizebelt *et al.*, 1994, 1998, 2000; Hubert *et al.*, 1997; van Gorkum *et al.*, 2005; Ploeger *et al.*, 2008, 2009a and 2009b; Caki *et al.*, 2012; Chittavanich *et al.*, 2012; Soucek *et al.*, 2012; La Nasa *et al.*, 2013), very little information is available as regards the time required for an alkyd paint to attain a state of chemical curing, i.e. a state in which most of the cross-linking processes creating the pictorial pattern have been completed. This chemical transformation is of extreme importance, since the curing state can be considered to be the starting point of the ageing processes. In this

study, the chemical curing of French ultramarine alkyd paint (PB29) in the *Griffin Alkyd "fast drying oil colour"* series was followed by means of FT-IR and multinuclear (^{1}H and $^{13}C\{^{1}H\}$) NMR spectroscopic techniques. Their application in the field is already well-established, in particular in the characterisation of binding mediums (Marshall and Lander, 1985; Marshall, 1986; Sacchi *et al.*, 1997; van den Berg *et al.*, 2001; Spyros, 2003; Spyros and Anglos, 2004 and 2006; Cipriani *et al.*, 2009). However, it has never been applied to the study of the curing process of alkyd resins.

2.3-2 Experimental

Samples

A set of 15 mock-ups on glass (50 mm x 110 mm) using *French ultramarine*[11] *Griffin Alkyd "fast drying oil colour"* (PB29) paint was prepared, and a layer of about 1.5 g of paint on 45 cm^2 of glass surface was spread over each sample so as to obtain a homogeneous thickness of about 34 mg/cm^2. The procedure followed in the preparation of the mock-ups was well defined in order to obtain comparable analytical results from each mock-up. In fact, different drying times may be related to diverse thicknesses or concentrations of the paint layers (Erich *et al.*, 2005). The alkyd mock-ups were then kept in the laboratory at room temperature (approximately 23-25°C and 45-55% RH), in an attempt to reproduce the environmental conditions of an artist's studio/atelier. Progress in the cross-linking process was followed by monitoring the composition of the organic extracts in $CHCl_3$ of a fixed amount of paint layer over a period of approximately 1700 h (about 10 weeks), ranging from fresh paint (t_0) to 1656 h (t_9) by using FT-IR and NMR spectroscopies (Fig. 2.45, Table 2.10). An additional measurement was also performed on a one-year-old (t_{10}) mock-up.

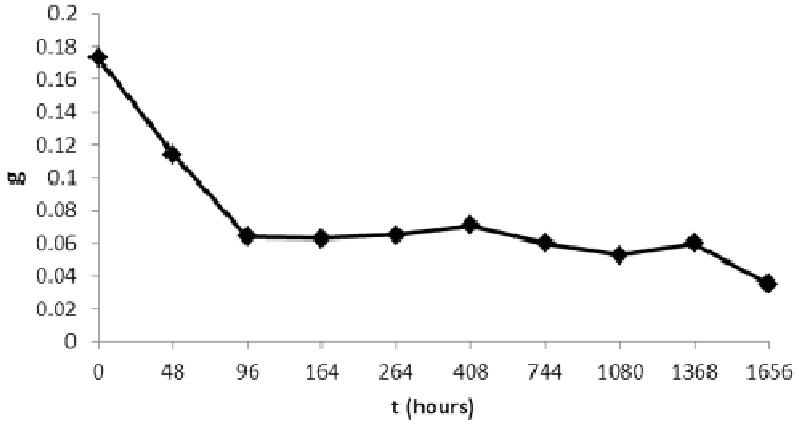

Fig. 2.45 - Weight loss of the extracts from mock-up film over 1656 h (*ca.* 10 weeks)

[11] Our choice of the French ultramarine colour depended on several considerations. The fact that it contains an inorganic pigment, instead of an organic dye, avoid any interference due to the possible presence of a part of the dye itself in the extracted materials. Furthermore, French ultramarine was chosen from among inorganic pigments because it could be easily extracted with the use of chloroform, leaving clear and colourless solutions after filtration.

Table 2.10 - Values of sample weight loss, amount of crude binder, and material extract from the samples at the different steps of the curing study of the alkyd paint mock-ups.

	Time (h)	weight loss of the mock-ups (%)	Crude paint binder (g)	Extracts (g)
t_0	0	0	0.508	0.173
t_1	48	13.6	0.446	0.114
t_2	96	13.6	0.440	0.064
t_3	164	15.3	0.440	0.063
t_4	264	15.6	0.432	0.065
t_5	408	16.2	0.440	0.070
t_6	744	16.4	0.432	0.060
t_7	1080	16.7	0.432	0.053
t_8	1368	16.7	0.440	0.060
t_9	1656	16.8	0.438	0.035

The decrease in weight and in content of the double bonds of the extracted material with time was monitored, because the double bonds present in the fatty-acid chains were involved in the cross-linking reactions. The lack of significant variation in weight and in the presence of double bonds is a good indicator of the absence or, at least, of the drastic reduction in the cross-linking reactions that are directly related to the attaining of chemical curing.

For every mock-up analysed, a sample (starting with 508 mg of fresh paint, t_0) of the previously layered French ultramarine paint was put into a 50-ml flask equipped with a magnetic bar, and was then extracted using $CHCl_3$ (25 ml). The suspension was stirred for six hours at room temperature. The insoluble materials were subsequently removed by filtering the suspension through a chromatography column (20 mm diameter) filled with celite (15 g). The celite was thoroughly mixed with $CHCl_3$, loaded onto the glass column, and packed with the use of a glass rod (0.5 mm diameter). The extraction mixture was poured slowly into the column, and this was followed by washings with $CHCl_3$ until 60 ml of eluted clear and colourless solution were collected in a flask. Removal of the solvent by using a rotary evaporator produced a crude residue, which was weighed and used for the FT-IR and NMR analyses.

FT-IR

In the case of FT-IR, about 1 mg of paint or of rotary evaporator residue was mixed with 100 mg of powdered KBr in order to prepare a pellet for measurement.

FT-IR spectra were recorded using two different instruments:

1) A FT-IR Nicolet *Nexus 470 E.S.P.*^{TM} spectrophotometer equipped with a SiC Globar and a DTGS detector. The IR spectra were acquired in transmittance mode in the 4000-400 cm^{-1} range (acquisition of 64 scans with 4 cm^{-1} resolution), using KBr matrix pellets.

2) A Bruker Optics *ALPHA* FT-IR spectrophotometer equipped with a SiC Globar source and a DTGS detector. Measurements were acquired in transmittance in the 7500-375 cm^{-1} range (acquisition of 64 scans with 4 cm^{-1} resolution), using KBr matrix pellets. The IR spectra collected were processed using OMNIC 7.3.94 and OPUS 7.0.122 software.

NMR[12]

About 10 mg of the crude residue from the rotary evaporator were dissolved in 0.5 ml chloroform-D for the purpose of collecting NMR spectra. The solution was directly inserted in a 5-mm NMR tube without any further manipulation.

The ^{1}H and $^{13}C\{^{1}H\}$ NMR spectra were recorded on a Bruker *Advance 300 MHz* spectrometer, using standard instrument software and pulse sequences. In particular, for ^{1}H NMR spectra the experimental setup was: recycle delay (D1) = 2,000 sec, pulse length = 4,0 µsec, AQ time = 1,60 sec, NS = 64 and TD = 16K.

The following parameters were used for $^{13}C\{^{1}H\}$ NMR spectra: recycle delay (D1) = 2,000 sec, pulse length = 11,0 µsec, AQ time = 1,97 sec, NS = 8K and TD = 64K. The peak positions, which were relative to tetramethylsilane (TMS), were calibrated against the residual solvent resonance (^{1}H, ^{13}C) or the multiplet deuterated solvent.

The solvent selected for the acquisition of the spectra was deuterochloroform ($CDCl_3$), which was used as purchased from a commercial supplier (Aldrich).

2.3-3 FT-IR analysis

FT-IR spectra were first recorded on samples taken directly from the paint layer of each mock-up. The main data acquired from these first-round measurements regarded the evident and progressive reduction in the absorption band centred at 3008 cm^{-1}, which corresponded to the C-H stretching of the vinyl protons. The same behaviour was detected in the spectra recorded on the chloroform extracts. To be more precise, the intense absorption band at 3008 cm^{-1} in the spectrum of the fresh paint rapidly decreased and eventually disappeared at the end of the ageing test (t_{10}), as reported in Figure 2.46.

[12] NMR analysis was performed by Dr. Vincenzo Mirabello of the Institute of Chemistry of Organometallic Compounds of the National Research Council (ICCOM-CNR).

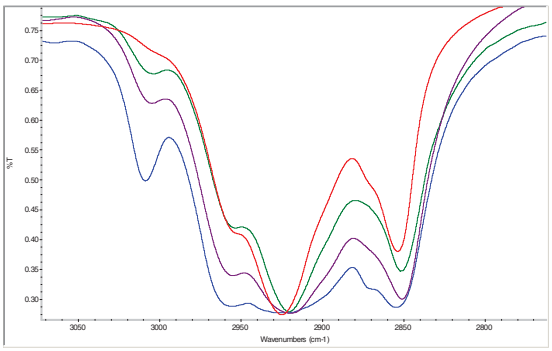

Fig. 2.46 -. Comparison of FT-IR spectra of the $CHCl_3$ extracts at different times: t_0 (blue line), t_4 (violet line), t_7 (green line), t_{10} (red line)

Furthermore, from the IR spectra of the extracts it was possible to obtain further important information on the progress of the cross-linking reactions. Thus, an examination of the 1650-1550 cm^{-1} spectral range showed two peaks centred at 1600 and 1580 cm^{-1}, which corresponded to the C=C stretching of the aromatic ring of the phthalic groups belonging to the alkyd resin (Fig. 2.47), (Ploeger *et al.*, 2008).

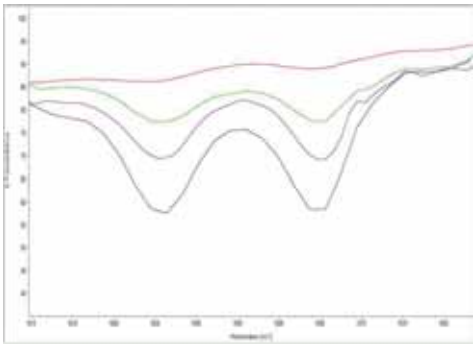

Fig. 2.47 -. Comparison of FT-IR spectra of the $CHCl_3$ extracts at different times: t_0 (red line), t_4 (violet line), t_7 (blue line), t_{10} (green line)

Once again, the intensity of these bands progressively decreased from t_0 to t_{10}. Unfortunately, although it proved useful for checking the progress of the chemical curing, the FT-IR technique did not enable us to refine our evaluation, due to its low sensitivity level.

2.3-4 NMR analysis

^1H and ^{13}C NMR spectroscopies were therefore employed in order to better quantify the time necessary for attaining a chemical curing of the alkyd paint under study. The NMR measurements, which were performed on the chloroform extracts, confirmed the trend highlighted by the FT-IR analysis, and made it possible to have a more accurate assessment of the process under investigation. Even more important, a series of simple markers, ones that can be found in ^1H-NMR spectra, were identified, and their change over time was correlated to the progress in the paint curing. Since the cross-linking reactions involved in the formation of the pictorial film mainly affect the amount of carbon-carbon double bonds, the decrease in allyl, diallyl and vinyl protons and carbons was monitored.

The ^{1}H-NMR spectra of the tested material extracted at t_0 (a) and t_9 (b) showed all the signals typical of an alkyd binding medium (Fig. 2.48 and 2.49, Table 2.11) (Marshall and Lander, 1985; Spyros and Anglos, 2004 and 2006; Cipriani *et al.*, 2009).

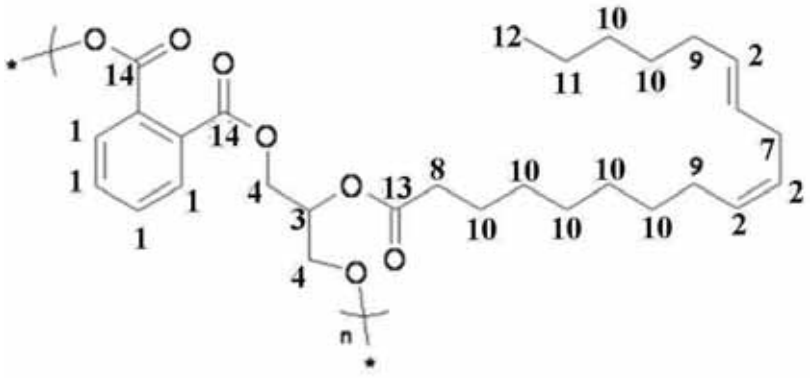

Fig. 2.48 -Structure of a generic alkyd resin.
The numbers correspond to the different types of H or C, as reported in Table 2.11

The chemical drying of the paint by means of cross linking resulted in a reduction in the intensity of all the peaks originating from the vinyl bond position (Sacchi *et al.*, 1997). Observing the ^{1}H and ^{13}C NMR spectra run over the $t_0 - t_2$ time (96 hours), a decrease in intensity of the peaks due to vinyl (**2**), allyl (**9**), and diallyl (**7**) protons and carbons was observed, together with an increase in the weight loss of each single extract. This time range corresponded to the physical drying of the painting, but this phenomenon was clearly accompanied by the beginning of the cross-linking process. As reported in Table 2.10, during the following two weeks ($t_3 - t_5$), no relevant weight change was detected in the paint samples or in the corresponding extracts. Conversely, in the same time range, the analyses of both the ^{1}H and ^{13}C NMR showed a progressive reduction in the intensity of the vinyl protons and carbon peaks, thus confirming the continuation of the chemical curing reactions.

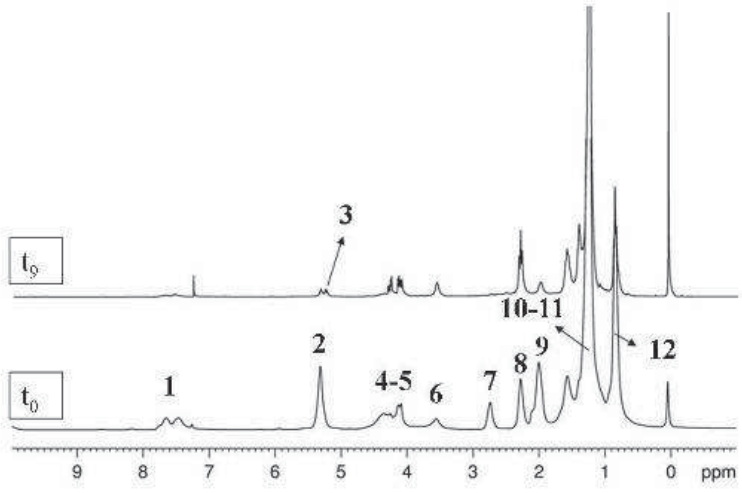

Fig. 2.49 - ^{1}H NMR spectra of t_0 (bottom) and t_9 (10 weeks) of French Ultramarine extracts in chloroform.
(Peak numbers are in agreement with Figure 2.51 and Table 2.11)

Table 2.11 - Chemical shift (δ) of the main ^{1}H and ^{13}C NMR resonances in the t_0 sample extracted in $CDCl_3$

Peak number	δ ^{1}H	δ ^{13}C	Group	assignment
1	7.8 – 7.4	131.7 – 129.9; 129.5 – 128.5	*Ph*CO	aromatic phthalate
2	5.31	129.9; 129.7; 128.3; 128.1; 127.9; 127.8	*CH=CH*	unsaturated vinyl protons
3	5.25	69.0	*CH*OCOR	triglycerides
4	4.34 – 4.18	62.8	CH_2OCOR	triglycerides
5	4.34 – 4.13	62.4	CH_2OCOR	1,2-diglycerides
6	3.57	71.9	CH_2OH	1,2-diglycerides
7	2.76	25.6	CH=CHCH_2CH=CH	diallyl
8	2.30	34.1	CH_2COOR	mono- and diesters
9	2.00	27.2	CH_2CH=CH	unsaturated fatty acids
10	1.37 -1.20	30 - 28.8; 31.9; 31.5	$(CH_2)_x$	fatty acids and diacids
11	1.37 -1.20	22.7 – 22.6	C-n-1 CH_2CH_3	acyl chains
12	0.91 - 0.87	14.2	CH_3	acyl chains
13		173.9 – 172.5	CH2*CO*OR	aliphatic carbonyl ester
14		168.0 – 166.0	Ph*CO*OR	/

No changes occurred in either the number of protons of the end-chain methyl groups of fatty acid during the chemical curing or in the intensity of their peaks. Thus, the integral of **12** signal (δ 0.91 ÷ 0.87 in Table 2.11) was used as a normalisation factor for the other peaks of the same spectrum (van den Berg *et al.*, 2001). These normalised intensities made it possible to establish the percentage decrease in the curing markers (peaks **2**, **7** and **9**), as indicated in eq. (1):

$$\% = \frac{\mathbf{I_{max} - I_x}}{\mathbf{I_{max}}} \qquad \text{eq. (1)}$$

where:

I_{max} = the normalised intensity of peaks **2**, **7** and **9** calculated at t_0 as compared to peak **12**.

I_x = the normalised intensity of peaks **2**, **7** and **9** as compared to peak **12**, at different extraction times.

In the δ 5.4 ÷ 5.1 region, the ^{1}H NMR spectrum of the chloroform extract of the fresh paint showed a single peak, because of an overlap of the absorptions that was due to the unsaturated

vinyl (**2**) and the *CH*OCOR protons (**3**). For this analysis, the intensity of peak 3 was assumed to be essentially unchanged, since no hydrolysis was detected at all during the curing process. It was possible to clearly distinguish bands **2** and **3** only in the final spectrum recorded at t_{10}. The area of peak **3** at t_{10} was therefore considered as the correction value to be subtracted from the envelope of the **2**+**3** at t_0-t_9 peak, in order to obtain a more realistic value of the intensity of peak **2** (Fig. 2.50).

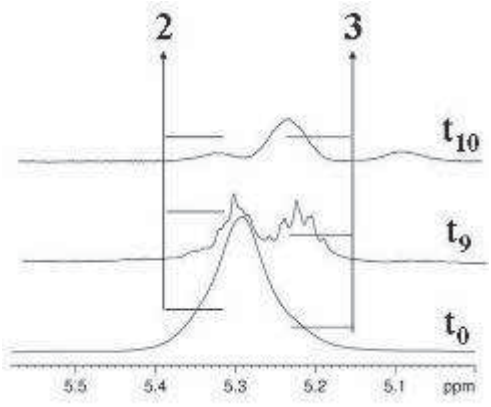

Fig. 2.50 - Progressive decrease in the signal due to the vinyl proton (**2**) in ^{1}H-NMR spectra over one year of ageing

The intensity of the peak at δ 5.31 (**2**) was reduced by 33% within the first 48 hours (t_1). The cross-linking process seemed to be completed after about 70 days (t_9, 1656 hours), when the number of double bounds decreased and was drastically reduced by 78.2%. After about 52 weeks (t_{10}), the amount of unsaturated protons was approximately 0% (0.5%, Fig. 2.51). These results proved unequivocally that the most important changes in the organic composition of an alkyd paint occurred within a short time, mostly as a consequence of the evaporation of the volatile components as well as of the rapid continuation of the cross-linking reactions.

The evidence of the rapid ageing of the organic binder was also analysed following the drastic decrease in two other sets of signals featuring ^{1}H NMR spectra. The first of these additional indicators was that of the diallyl protons (peak **7**), the number of which decreased as soon as the cross-linking processes went ahead. The intensity of this peak was reduced by 41% after 48 hours, while the signal reduction slowed down after 96 hours, and took about 57 days (1368 hours) to arrive at zero.

The second proton marker used to follow the curing process was the reduction in the intensity of peak **9**, which was ascribed to the allyl protons. The time-dependence of this marker clearly confirmed the behaviour already observed for both the vinyl (**2**) and the diallyl (**7**) protons (Fig. 2.51). The different rate at which the allyl and diallyl protons decreased was explained, as reported in the literature (van Gorkum and Bouwman, 2005; Wexler, 1964), by their different activities with respect to all the radical reactions involved in the cross-linking process.

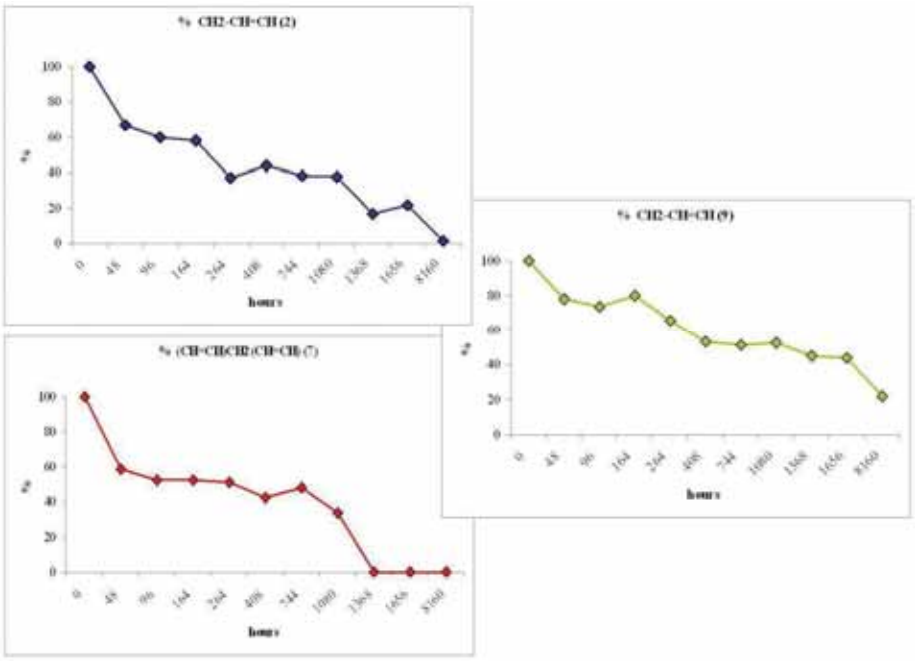

Fig. 2.51 **-.** Percentage decrease in vinyl protons (peak **2**), in the double allyl protons (peak **7**), in allyl protons (peak **9**) in ^{1}H NMR spectra over 1 year

The data on the allyl protons seemed to be in contrast, as regards the absolute values, with those related to the vinyl protons. For instance, for the allyl protons, percentages at 1656 and 8160 hours were found to be about 20% higher than expected. The hypothesis of a contribution to the integrals of the allyl peaks seemed to be the most realistic one, although it was not possible to identify the chemical species responsible for it. This hypothesis was strengthened by the analyses of the $^{13}C\{^{1}H\}$ NMR spectra. It is well known that the variability in the ^{13}C-relaxation time makes the analysis of carbon NMR resonances realistic only for a semi-quantitative analysis. However, the reduction in the amount of double bonds was also monitored by running $^{13}C\{^{1}H\}$ NMR experiments over the same samples used for the ^{1}H-NMR spectra. The drastic reduction in intensity for both the vinyl and allyl sets of signals from t_0 (fresh paint) to t_9 (after 1656 hours at RT) was in perfect agreement with the trend observed in the analysis of the proton spectra (Fig. 2.52).

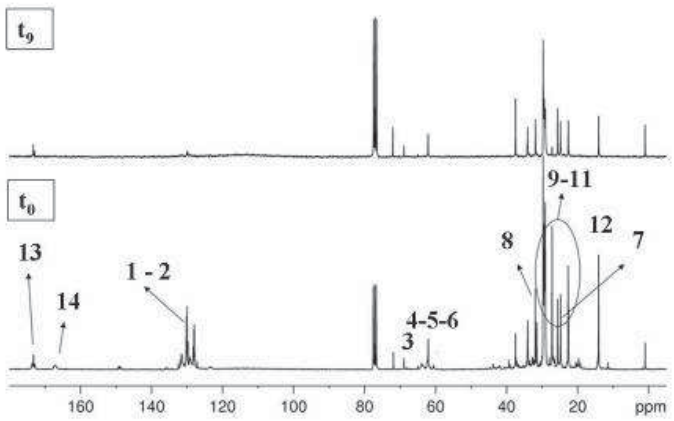

Fig.2.52 **-** $^{13}C\{^{1}H\}$ NMR spectra of French Ultramarine Alkyd paint extracted in chloroform at t_0 (bottom) and t_9 (10 weeks). (Peak numbers are in agreement with Figure 2.51 and Table 2.10).

As for the ^{1}H spectra, if the number of end-chain methyl groups of fatty acid was considered to be unchanged during the chemical curing, peak **12** (14.2 ppm) was used as an internal reference in order to evaluate the percentage of decrease in the allyl carbon **9** (27.2 ppm), (Fig. 2.53).

The trend of the decrease in the double bonds was therefore confirmed and, more important, the percentages at 1656 and 8160 hours (27% and 0%, respectively) were in good agreement with those of the vinyl protons (22% and 0%, respectively).

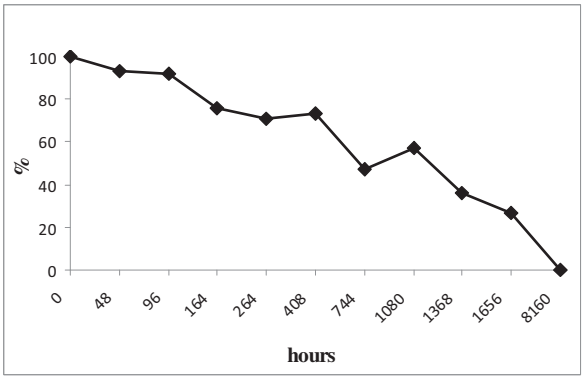

Fig. 2.53 - Percentage decrease in the allyl carbon (peak **9** in ^{13}C-NMR spectra) over 1 year

This experimental finding clearly confirmed that the data obtained for the allyl protons were not realistic, and were probably increased by the presence of variable amounts of oxidized or cyclic fragments in the extracted materials.

2.4 Case study

2.4-1 The artwork

Within the framework of the CoPAC Project it was possible to study an artwork by the Italian painter Patrizia Zara, who had used alkyd paints to create some of her works.

Patrizia Zara, who graduated in Stage Design from the Academy of Fine Arts of Brera (Milan, Italy) in 1992, is a young artist who defines herself a "hyperrealist painter". Her quest for perfection of detail is evident in her works where the main subject is the hand (www.patriziazara.com; last access: November 17, 2013). One of these artworks is *Salto di qualità* (2008), a painting on canvas (50 cm x 50 cm) that was created using *Winsor & Newton Griffin Fast Drying Alkyd Colours*. In the work are illustrated a human hand and its shadow, which stand out from a monochrome background (Fig. 2.54).

During a visit to Zara's atelier, on 18 July 2012, it was possible to study this painting by means of the non-invasive *in situ* FORS technique. Although no useful information about the alkyd binder was obtained, it was possible to make a tentative identification of the pictorial palette used by the artist.

Fig. 2.54 - *Salto di qualità*, Patrizia Zara (2008)

2.4-2 Experimental

FORS measurements in the UV-Vis-NIR spectral range (350–2200 nm) were performed using two single-beam *Zeiss* spectroanalysers, model *MC601* (190-1015 nm range) and model *MC611 NIR 2.2WR* (910-2200 nm range), housed together in a compact and portable chassis for the purpose of *in situ* analyses. The data acquisition step was 0.8 nm/ pixel for the 1024-element silicon photodiode array detector (*MCS601*), and 6.0 nm/pixel for the 256-element InGaAs diode array detector (*MCS611 NIR 2.2 WR*). The radiation between 320 nm and 2700 nm, which was provided by a voltage-stabilized 20W halogen lamp (mod. CLH600), was

conveyed to the sample by means of a quartz optical fibre bundle that also transported the reflected radiation to the detectors. The geometry of the probe head was 8°/8°. Calibration was performed by means of a 99% Spectralon® diffuse reflectance standard. Spectra were processed using Aspect Plus® 1.80 software.

2.4-3 Results

The identification of some of the paints used by the artist was possible thanks to a comparison with the UV-Vis-NIR reflectance spectra acquired on the reference samples (§ 2.2-2).

The canvas was prepared with a white layer of *Titanium white Griffin Alkyd Oil Colour* (spot 13; Fig. 2.55). In fact, the spectrum presented a typical "S"-shape band with an inflection point at 403 nm (3.07 eV), which confirmed the presence of titanium dioxide in the rutile crystalline form (Bacci *et al.,* 2007; Picollo *et al.*, 2007).

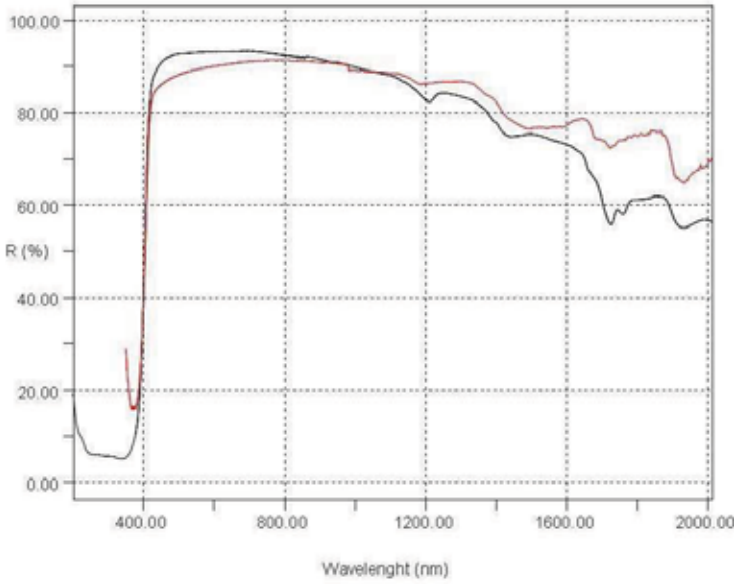

Fig. 2.55 – FORS spectra of the preparation layer (red line) and of *Titanium white Griffin Alkyd Oil Colour* (black line)

This colour was also used, mixed with other paints, in order to obtain different nuances. For example, the pink areas was found to be a mixture of *Titanium white Griffin Alkyd Oil Colour*, *Cadmium red medium Griffin Alkyd Oil Colour*, and an unidentified yellow colour (Fig. 2.56).

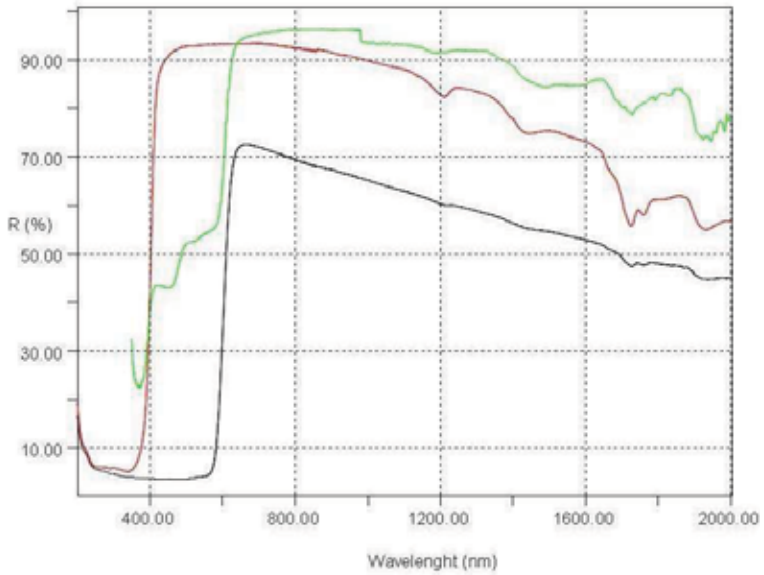

Fig. 2.56 - FORS spectra of a pink area (green line), *Titanium white Griffin Alkyd Oil Colour* (red line) and *Cadmium red medium Griffin Alkyd Oil Colour* (black line)

The orange areas seemed to be painted with a mixture of *Cadmium yellow light Griffin Alkyd Oil Colour* with an unidentified red paint (Fig. 2.57).

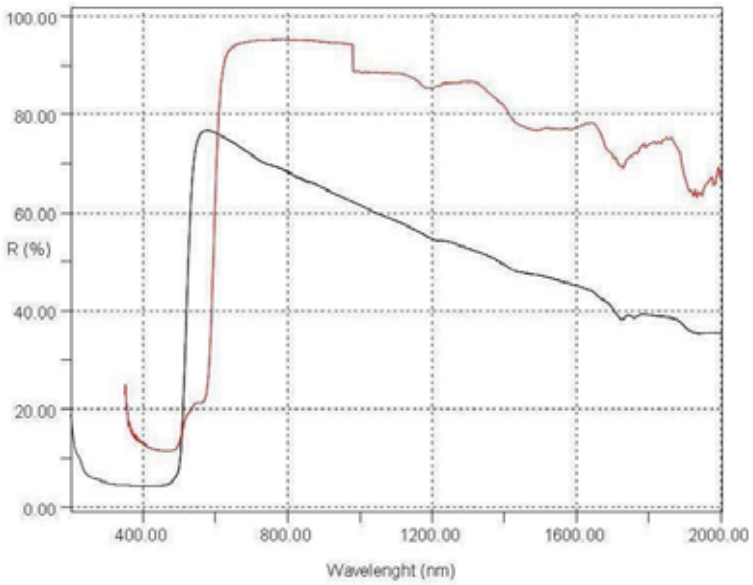

Fig. 2.57 - FORS spectra of an orange area (red line) and of *Cadmium yellow light Griffin Alkyd Oil Colour* (black line)

Lastly, the green area was painted using the *Viridian Griffin Alkyd Oil Colour* (Fig. 2.58).

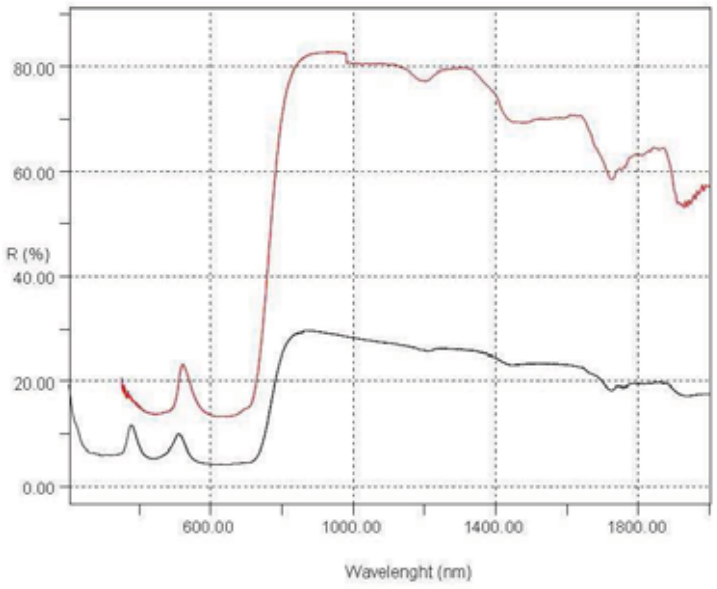

Fig. 2.58 - FORS spectra of a green area (red line) and of *Viridian Griffin Alkyd Oil Colour* (green line)

2.5 Conclusion

In this chapter, a study on alkyd paints was presented. In particular, a characterisation of ten commercial *Winsor & Newton* alkyd paints was carried out. The integrated use of THM-GC/MS, FT-IR, UV-Vis-NIR reflectance spectroscopy and XRF (when necessary) enabled us to identify the principal components present in the formulation.

From a consideration of the THM-GC/MS analysis, the binder was found to be an oil modified alkyd resin made from penthaerythritol, phthalic acid and free fatty acids. The pigments/dyes and the fillers were identified by means of FT-IR, UV-Vis-NIR reflectance analysis and XRF (only for pigments based on cadmium). The main FT-IR and UV-Vis-NIR absorption band are reported in Table 2.12.

Chromatographic and spectroscopic techniques were successfully used to evaluate the photo-oxidative behaviour of alkyd paints exposed to UV radiation. Useful information about the degradation process of the organic fraction of the resin was obtained. The profile of the fatty acids was carefully investigated by means of THM-GC/MS. Unsaturated acids (oleic and linoleic) were found to be subject to an oxidation process which quickly leads to the formation of hydroxides and dicarboxylic acids (e.g. azelaic acid). Colour differences in the surface of the samples were also detected after the accelerated ageing, thanks to colorimetry, UV-Vis-NIR reflectance spectroscopy, and PLM. The formulation that was found to be the most unstable was *French Ultramarine Griffin Alkyd Oil Colour*, which was characterised by an intense chromatic variation, in addition to a high degree of oxidation, after UV exposure.

FT-IR and NMR spectroscopies were successfully applied also to follow the process of chemical drying (curing) that occurred in the alkyd paint binder. To this end, the reduction in

the signals that was attributed to the vinyl, allyl, and diallyl protons and carbons during the natural drying was monitored. All data acquired led us to conclude that, in the selected experimental conditions, the chemical curing required about 70 days to be completed.

Table 2.12 – FT-IR and UV-Vis-NIR absorption band positions in the spectra acquired on the *Griffin Alkyd Oil Colours* samples

Sample	Identification	Main FTIR absorption bands (cm^{-1})	UV-Vis-NIR absorption maxima (nm)[a]
1	Titanium dioxide (PW6)	800-450	$\lambda < 403$ (ip)
	Alkyd resin	2923, 2851, 1735, 1600, 1578, 1285 1074	1727 (w), 1760 (sh), 2308 (w)
	Dolomite	1448, 882, 729	2143 (w), 2350 (w)
2	Cadmium sulphoselenide (PR108)	/	$\lambda < 602$ (ip)
	Alkyd resin	2923, 2850, 1287, 1070	1727 (w), 1760 (sh), 2308 (w)
	Dolomite	2530, 1440, 880, 729	2143 (w), 2350 (w)
	Barite	1185, 1122, 636, 606	/
3	Naphtol As (PR188)	1675, 1555, 1492, 1471, 1408, 1326, 1155, 1073, 742	$\lambda < 603$ (ip)
	Naphtol carbamide (PR170)	3063, 1656, 1450, 1290, 1263, 1047, 1011, 752	$\lambda < 603$ (ip)
	Alkyd resin	2924, 2852, 1736, 1598, 1579, 1469, 1263, 1072	1727 (w), 1760 (sh), 2308 (w)
	Dolomite	2530, 1451, 881, 729	2143 (w), 2350 (w)
4	Cadmium zinc sulphide (PY35)	/	$\lambda < 518$ (ip)
	Alkyd resin	2924, 2852, 1736, 1260, 1123, 1072	1727 (w), 1760 (sh), 2308 (w)
	Dolomite	2530, 1449, 881, 729	2143 (w), 2350 (w)
	Barite	1181, 1123, 636, 611	/
5	Hansa Yellow (PY3)	3110, 1671, 1592, 1583, 1535, 1502, 1336, 1279, 1176, 1137, 1036, 812, 749, 620	$\lambda < 493$ (ip)
	Alkyd resin	2924, 2852, 1734, 1281, 1072	1727 (w), 1760 (sh), 2308 (w)
	Dolomite	1442, 882, 729	2143 (w), 2350 (w)
6	Viridian (PG18)	3600-3100, 1062, 791, 553, 470	300 (s), 435 (s), 700 (s)
	Alkyd resin	2924, 2852, 1737, 1600, 1580, 1466,	1727 (w), 1760 (sh), 2308 (w)
7	Phthalo Green (PG7)	1212, 777	640 (s), 721 (s), 797 (s), 1121 (sh)
	Alkyd resin	2925, 2852, 1736, 1260, 1072	1727 (w), 1760 (sh), 2308 (w)
	Dolomite	1449, 881, 729	2143 (w), 2350 (w)
8	Ultramarine Blue (PB29)	1150, 950, 688, 654, 581, 445	600 (s)
	Alkyd resin	2925, 2853, 1737, 1460	1727 (w), 1760 (sh), 2308 (w)
	Dolomite	2530, 1456, 881, 729	2143 (w), 2350 (w)
	Kaolinite	3695, 3653, 3620	/
9	Phthalo Blue (PB15)	1165, 1092, 722	614 (m), 692 (m), 1105 (sh)
	Alkyd resin	2925, 2852, 1735, 1121, 1070	1727 (w), 1760 (sh), 2308 (w)
	Dolomite	2530, 1440, 881, 729	2143 (w), 2350 (w)
10	Ivory Black (PBk9)	1025, 562, 599, 630	/
	Alkyd resin	2924, 2851, 1735, 1467	/
	Dolomite	1440, 880, 730	/

[a]sh (sharp), m (medium), s (strong), w (weak) and ip (inflection point)

CHAPTER 3 – PLASTICS

3.1 Synthetic polymers

3.1-1 What is plastic?

The word "plastic" (from the Greek πλαστικός) literally means "able to be moulded". This term is commonly used to indicate synthetic and semi-synthetic organic macromolecules that have a high molecular weight and are made up of specific units (monomers) linked to form long chains.

The reaction that generates the macromolecules is called polymerisation. When only one type of monomer is used as starting material, the product is called *homopolymer*. It is possible to obtain macromolecules also by mixing two, three or more different monomers, and these products are called *copolymers*, *terpolymers* and simply *polymers*, respectively.

The main polymerisation processes are divided into two categories:

- *addition polymerisation* (or *chain-growth polymerisation*), in which unsaturated monomer units (those containing at least one double or triple carbon-carbon bond) are joined together to produce a linear polymer. The most common polymers formed in this way are polyethylene, polypropylene, polystyrene and polyvinylchloride.
- *condensation polymerisation* (or *step-growth polymerisation*), which comprises stepwise intermolecular reactions that usually involve more than one monomer incorporating alcohol, amine or carbonyl functional groups. Condensation polymers include polyesters, polycarbonates, nylons, formaldehyde polymers and epoxies.

There are two main categories of plastic materials: thermoplastics and thermosetting polymers. Thermoplastic materials become flexible or mouldable above a specific temperature, and return to a solid state upon cooling. If re-heated, they soften and melt again. Unlike thermoplastic materials, thermosetting plastics can be melted to take a shape, but once solidified, they cannot be re-melted.

The chemical-physical properties of plastics may be designed by varying the production processes and the formulations. Indeed, by starting from the same basic resin, the final formulation may be varied by adding several types of additives (e.g. colorants, fillers[1], plasticisers[2], etc.), which then make it possible to control precisely the characteristics of the finished material.

[1] Fillers are used to modify, during the polymerisation, the flow properties of plastic, as well as their tensile and compressive strength, abrasion resistance, dimensional and thermal stabilities (Shoshua, 2008).

[2] Plasticisers are generally low volatile substances used to increase the flexibility of rigid polymers, in order to make them more suitable for mechanical processes of forming or for specific applications (Shoshua, 2008).

3.1-2 Historical notes

The first attempts to exploit the natural polymers for the production of common objects date back to the 19th century, when it was possible to transform polymers as natural rubber, gutta-percha, shellac, etc. into shapes that were useful for the desired functions by means of appropriate moulding processes.

Thanks to discoveries in the field of chemistry, semi-synthetic plastics were gradually replaced by entirely synthetic products. In 1839 Eduard Simon discovered the styrene monomer. That same year, Goodyear discovered the "vulcanisation process" by which natural rubber latex (derived from the bark of *Hevea brasiliensis*) is joined with sulfur at a high temperature, resulting in a product with mechanical and physical properties superior to those of rubber in its raw state (Waentig, 2008).

In 1861, Alexander Parkes discovered *Parkesine*®, an organic material derived from cellulose, which, once heated, could be moulded, and retained its shape when cooled (Ciardelli *et al.*, 1983).

In 1868, John Wesley Hyatt invented *Celluloide*® by hot mixing cellulose nitrate and alcoholised camphor, as a substitute for ivory in billiard balls. In addition to this use, *Celluloide*® became famous as the first flexible photographic film used for still photography and motion pictures (Alferj and Cernia, 1983).

Over the next few decades, more and more plastics were introduced, including some modified natural polymers, such as rayon, which were made from cellulose products. In 1907, Leo Hendrik Baekeland, a Belgian-American chemist, by improving phenol-formaldehyde reaction techniques, developed the first fully synthetic resin to become commercially successful, tradenamed *Bakelite*®. This plastic attained rapid growth in the production of objects for daily use, such as telephones, radios, fountain pens, and so on (Waenting, 2008).

In 1920, a major breakthrough occurred in the development of plastic materials. A German chemist, Hermann Staudinger, hypothesised that plastics were made up of very large molecules held together by strong chemical bonds. This assumption spurred an increase in research in the field of plastics. Many new plastic products were designed during the 1920s and 1930s, including nylon, methyl methacrylate (also known as *Lucite* or *Plexiglas*), and polytetrafluoroethylene, which was marketed as *Teflon* in 1950 (Ciardelli *et al.*, 1983).

Advances in the plastics industry continued after the end of World War Two. In the 1950s, two of today's most commonly used plastics were discovered. Indeed, the German chemist Karl Ziegler developed polyethylene in 1953, and the following year Giulio Natta, an Italian chemist, invented polypropylene. Today, the search for new plastics still continues. New ways

to use existing plastics are constantly being developed, for example as a replacement for other materials such as wood and glass.

3.1-3 Plastic in art: brief history

The exceptional versatility of plastics is the reason for their pervasive and capillary diffusion in every field and aspect of human lives. Nowadays, as culture and art reflect and dip into the historical context and into daily life, plastics have also become a part of the cultural heritage and are widely found in museums, art collections and galleries.

The first documented use of plastics as artistic materials dates back to the pioneer works of Naum Gabo in the early 1900s (Derrick *et al*., 1993). One of his important works, which was created by means of *Celluloide*®, is *Head of Woman* (Fig. 3.1), currently on display at the Museum of Modern Art (MoMA, New York) (Bordini, 2007).

Fig. 3.1 - Naum Gabo, *Head of Woman* (1917-20), celluloid and metal
[Image from: http://www.moma.org/collection/object.php?object_id=81440]

It is no wonder that artists more sensitive to experimentation have tried to take advantage of the new synthetic polymers ever since their first appearance, especially as materials for sculptors. In this way, they could avoid difficult shaping techniques in wax and plaster, expensive bronze casting, or the hard work required for sculpting in stone or wood. Furthermore, plastic materials possessed qualities of transparency, lightness and brightness that are greatly appreciated by artists.

In the mid-1930s, artists replaced cellulose materials with more resistant plastics, such as *Plexiglass*®, or *Perspex*® (polymethylmethacrylate), owing to the instability of the former.

The pioneering phase for the use of plastics in art ended after World War Two, when the introduction of new synthetic polymers and the birth of the post-avantgarde artistic

movements led to a rapid spread of plastics also among artists. The works of Piero Gilardi can be inserted within this context. He achieved great fame, in the mid-1960s, with his *Tappeti-Natura* (Carpets-Nature), made of painted polyurethane foam (Fig. 3.2), which represented natural landscapes in a hyper-realistic way (Chiantore and Rava, 2005).

Fig. 3.2 - Piero Gilardi, *Tappeto-Natura "Mais"* (1966), polychrome polyurethane foam
[Image from: http://www.centrostudipierogilardi.org/it/opere-e-attivita/1963-2010/anni-60; last access: 23 November, 2013]

Another famous artist of that period was the American Bruce Beasley, who, in 1967, started to explore the idea of creating transparent sculptures. He soon ruled out glass as a medium, finding that it was impractical for the large dimensions in which he wanted to work, and discovered that he should use plastic. One of his most famous works is *Apolymon* (Fig. 3.3), which he created in 1968-70 using polymethylmethacrilate. It is now on display in Sacramento (California, USA).

Fig. 3.3 - Bruce Beasley, *Apolymon* (1968-70), cast in acrylic
[Image from: http://www.flickr.com/photos/kidmd/7797559860/; last access: 23 November, 2013]

Since then, recourse to synthetic polymers in the artistic field has constantly increased. Today, along with "traditional" objects contemporary art museums, foundations, and galleries collect , works in transparent plastic (*e.g.* by A. Archipenko, L. Nevelson), in both polyester and polymethylmethacrylate (*e.g.* by F. Arman), in polystyrene foam (*e.g.* by J. Dubuffet, S. Arienti), in polychrome resin (*e.g.* N. de Saint Phalle, D. Hanson, G. Segal), and so on (Chiantore and Rava, 2005).

3.1-4 FT-IR spectroscopy for the study of plastics in the cultural heritage field

At present, resorting to synthetic polymers is an ubiquitous practice among artists, and plastics are definitively considered to constitute a class of artistic materials. In addition to artistic production, the presence of plastics in museums and galleries is also related to design, ethnographic, and technical collections, as well as to film archives. Consequently, a notable percentage of artworks and valuable objects consisting of synthetic and semi-synthetic polymers is kept in museums, and these are classified as items to be preserved for future generations. Despite this fact, the problem of the conservation of plastics in art collections had been disregarded until recently, since for a long time, and due to a widespread misconception, plastics have been considered to be imperishable materials. The need for adopting systematic strategies for the conservation of plastic objects, analogously to other more traditional materials in collections, has had total recognition only in recent decades. Such an increased awareness has given rise to a new research area that is aimed at filling in the lack of knowledge, practices and methodologies for preserving plastics in collections (Albus *et al.*, 2007; Shashoua, 2008; Waentig, 2008). Several projects devoted to the safeguarding of contemporary art have recently been launched – such as INCCA[3], POPART[4], and CoPAC[5]– and studies on the care of plastics in collections have been published (Chalmers *et al.*, 1996; Pastorelli *et al.*, 2012; Cucci *et al.*, 2013; Lattuati-Derieux *et al.*, 2013; Littlejohna *et al.*, 2013). Within these research projects, particular attention has been paid to the development of new tools and techniques that are specifically tailored to the *in-situ* and non-invasive identification of polymers that compose museum objects. In fact, a knowledge of the materials constituting an artwork is the essential first step in understanding the causes of its degradation, and, if necessary, in setting up a correct approach to its preservation.

Most of the best-established analytical techniques for the identification of plastics are borrowed from other application sectors (industrial, chemical, manufacturing, etc.), in which the requirements of portability and non-invasiveness are not usually deemed necessary. A state-of-the-art of the analytical methods usable for the identification of plastics in museum collections was drawn up within the POPART Project, in which a comparative evaluation between well-established methods and novel techniques was carried out (Van Oosten *et al.*, 2012). Several analytical methods were examined within this study, and those based on vibrational spectroscopies - in particular, on FT-IR techniques - were found to be among the most effective and suitable ones for identifying synthetic resin blends in artworks.

[3] http://www.incca.nl/ (Last Access date: 5 July 2013)
[4] http://popart.mnhn.fr/ (Last Access date: 5 July 2013)
[5] http://copac.sns.it/ (Last Access date: 5 July 2013)

In fact, FT-IR analysis in the Mid-IR spectral region offers a considerable ability to distinguish and identify polymers, and meets requirements such as micro-destructivity (and, in certain circumstances, non-destructivity), cost-effectiveness, and the availability of a wide range of commercial instrumentation. At present, FT-IR spectroscopy is well established in several applicative sectors, such as industry, quality controls, etc. (Naranjo *et al.*, 2008), as well as in the cultural heritage field (Derrick *et al.*, 1999; Casadio and Toniolo, 2001). However, reports on FT-IR being applied to the identification and characterisation of plastics in art collections are relatively scarce in the literature (Shearer, 1990; Keneghan, 1995; Paris *et al.*, 2005; Chércoles Asensio *et al.*, 2009), and certain fundamental issues still need to be investigated in greater depth.

A first open question regards the lack of suitable spectral databases of reference materials set up specifically to interpret data acquired on plastics artworks. Indeed, although several FT-IR spectral libraries of synthetic polymers are available, only a few of those include a significant number of polymers of interest in art collections. In recent years, this question has been tackled partially, and spectral archives of plastics of specific interest in the art conservation field are being assembled, such as the "SamCo" archive developed under POPART[6] or the "IRUG" database (Laganà and Keneghan, 2012; www.irug.org). Nevertheless, extensive further work is still needed in order to obtain rich and statistically-meaningful databases for practical applications.

A second question of great interest concerns the feasibility of non-invasive FT-IR measurements on museum objects and the quality of FT-IR spectra acquired *in-situ*. In recent decades, in fact, a new generation of high-resolution portable FT-IR devices has been marketed at affordable prices (Mukhopadhyay, 2004). In addition to their portability, these devices offer the possibility of operating in Total Reflectance (TR) configuration by recording spectra in a contactless mode and without any need for sampling. It should be pointed out that until recently the only way to perform non-invasive FT-IR analysis in the Mid-IR region was by means of optical fibres coupled with FT-IR benches (Scott Williams' works; Fabbri *et al.*, 2001a; Fabbri *et al.*, 2001b; Miliani *et al.*, 2010; Ploeger *et al.*, 2011). However, the use of optical fibres in the Mid-IR region involves several drawbacks, such as the elevated cost of the equipment and the need for liquid nitrogen in order to cool down the MCT detectors. In addition, chalcogenide glass fibres, which are commonly used to produce Mid-IR fiber bundles, strongly attenuate the IR radiation, and have their own absorption bands. The latter may mask spectral features of interest for the identification of materials. Thus, the recent

[6] POPART Conference Highlights. http://popart-highlights.mnhn.fr/identification/what-plastics-are-in-my-collection/index.html (Last Access date: 5 July 2013)

availability of portable FT-IR instrumentation equipped with reflectance mode accessories has opened up new applicative perspectives, especially in the field of art conservation, where *in situ* and non-invasive analyses are in great demand.

Despite this fact, TR FT-IR spectroscopy is still far from being fully exploited as a routine technique for large-scale surveys and *in situ* investigations of art collections. This is mainly due to the lack of databases of FT-IR data acquired in TR mode on reference materials, which are essential for a correct interpretation of spectra acquired on real objects. Commercial FT-IR spectral libraries are usually built using other FT-IR configurations, such as the Transmission and/or the ATR modes. In the TR FT-IR configuration, both diffuse and specular components of the reflected radiation are acquired and contribute to the spectrum registered. For this reason, TR FT-IR spectra are intrinsically more complex, and are not always directly comparable with the data included in commercial spectral archives, unless suitable data pre-treatments are made.

3.2 Comparative study of FT-IR spectra acquired on plastics with different instrumental configurations

3.2-1 Aim of the work

This research aims to investigate the effectiveness of TR FT-IR spectroscopy, implemented by means of portable spectrophotometers, as a non-invasive analytical technique for routine and large-scale investigations on plastic objects to be found in contemporary art museums.

A collection of polymeric samples, which are commercially available as ResinKit™, was analysed in order to create a reference spectral archive. All the spectra were recorded using three FT-IR configurations: Transmittance (Trans), Attenuated Total Reflectance (ATR), and Total Reflectance (TR). A comparative evaluation of the data acquired in the three instrumental configurations was presented, together with an evaluation of the similarity percentages and a discussion of the critical cases.

3.2-2 Preliminary considerations

The choice of an experimental FT-IR configuration (Trans, ATR, and TR) depends on the features of the objects and on the materials examined. As regards plastics, in principle all three of these methodologies are usable.

The most well-established method for the analysis of solid plastic samples is the conventional Trans mode, which can be used whenever sampling is possible. Trans spectra are usually acquired on pellets prepared by mixing a small amount (about 0.5-1mg) of ground sample with potassium bromide (KBr, about 100mg). Since plastics are highly variable in their

softness, flexibility, and consistency, in some cases they can barely be transformed into a thin powder, thus making it impossible to obtain a homogeneous pellet or, consequently, a well-resolved transmittance spectrum. When it is difficult or impossible to obtain homogeneous sample/KBr dispersions, less straightforward preparation processes have to be adopted in order to perform measurements in Trans mode. If the samples are soluble in a volatile solvent, they can be dissolved and analysed by depositing a few drops of the solution on an IR transparent material. When the polymer is not easily soluble, Trans spectra may be recorded by resorting to specific instrumental accessories, such as diamond cells. Thus, provided that suitable technical expedients are adopted for the preparation of the samples, high-quality Trans FT-IR spectra may in principle be acquired from any type of specimen.

Another well-established method for performing FT-IR analysis is use of ATR mode. This configuration, the use of which is widespread for the characterisation of polymers, makes it possible to overcome any drawbacks related to the preparation of KBr pellet samples. However, ATR-mode spectra may be less easy to interpret than ones recorded in a conventional Trans-mode.

In ATR-mode, the penetration depth of the evanescent wave within the sample depends on the optical thickness of the sample. This fact may cause spectral band distortions, due to broadening or peak shifts at the longer wavelengths (Boulet-Audet *et al.*, 2010). These effects have to be taken into account when ATR spectra are compared with those acquired in Trans-mode. Suitable algorithms are available to correct such systematic spectral differences. It should be recalled that, in ATR mode, high-quality spectra may be obtained only by applying high unit pressures, so as to ensure an intimate contact between the sample and the ATR crystal. Therefore, even if in principle the ATR is non-invasive, this method cannot be used to analyse fragile or precious objects without risking damage to them. On very soft materials, as is the case with some common plastics (*e.g.* expanded polystyrene), the ATR mode cannot be used advantageously. The use of an ATR configuration for distinguishing between similar classes of plastics has been reported in a work by Enlow (Enlow *et al.*, 2005), while an application to semi-synthetic resins of interest in museum applications is reported in a work by Paris (Paris *et al.*, 2005).

Lastly, whenever sampling has to be avoided, as is often the case in museum contexts, FT-IR spectra can be acquired in TR mode. As mentioned, one of the main drawbacks of TR FT-IR measurements involves the complexity of the spectra acquired. Indeed, these are often affected by distortions, both in the band shape and in the absorption frequency, which depend mainly on the variable balance between the diffuse and specular reflectance components. These spectral anomalies are due to different factors, such as the concentration of the sample,

the surface texture, the refractive-index of the materials, etc. (Kortüm, 1969). For example, when a strong specular component is present, as is the case with materials that have high refractivity, anomalous spectral bands (usually known as "derivative-like" bands) are observed. These anomalies in the FT-IR reflectance spectra are usually treated by applying specific data processing algorithms, such as the Kramers-Kroenig (KK) transform (Lucarini *et al.*, 2005). The KK algorithm makes it possible to reconstruct a pseudo-absorption spectrum, thus rendering it comparable with those acquired in the Trans and/or ATR modes. However, the use of correction algorithms is not always sufficient to make TR spectra superimposable or comparable with those registered in Trans and/or ATR modes on the same specimen. For example, when undiluted materials with a strong absorption coefficient are analysed in TR mode, intense distortions may appear in the FT-IR spectra. The most evident case is the so-called *reststrahlen* band, in which a reflectance maximum occurs in place of the absorption band. In this case, spectral distortions cannot be corrected by resorting to mathematical algorithms (Fabbri *et al.*, 2001b).

3.2-3 Experimental

Samples

A collection that included 50 specimens of thermoplastic resins, in representation of some of the most popular plastics, was analysed by means of FT-IR spectroscopy. This sample collection is marketed under the name ResinKit™ (Supplier: The ResinKit™ Company[7], Woonsocket, RI, USA). Each ResinKit™ specimen, moulded as a 10 cm x 4 cm chip with a variable thickness ranging from 1 to 3 mm, is catalogued by means of a numerical index on its surface, and is accompanied by technical information on its properties. Each chip has two lateral combs, the teeth of which are removable for the purpose of different kinds of destructive analysis (Fig. 3.4). The list of materials included in the ResinKit™ set analysed is reported in Table 3.1.

Fig. 3.4 - Resin Kit™, A) polystyrene medium impact; B) pholyphenylene oxide; C) polyphenylene sulphide

[7] The Plastics Group of America http://www.plasticsgroup.com/resin_kit (Last Access date: 5 July 2013)

Table 3.1 – List of the Resin Kit™ samples

Number	Name
1	Polystyrene - General Purpose (GPPS)
2	Polystyrene - Medium Impact
3	Polystyrene - High Impact (HIPS)
4	Styrene Acrylonitrile (SAN)
5	ABS – Transparent
6	ABS - Medium Impact
7	ABS - High Impact
8	Styrene - Butadiene Block Copolymer (SBR)
9	Acrylic
10	Modified Acrylic
11	Cellulose Acetate (CA)
12	Cellulose Acetate Butyrate (CAB)
13	Cellulose Acetate Propionate (CAP)
14	Nylon - Transparent
15	Nylon (polyammide) - Type 66
16	Nylon (polyammide) - Type 6
17	Thermoplastic polyester (PBT)
18	Thermoplastic polyester (PETG)
19	Polyphenylene Oxide (PPO)
20	Polycarbonate (PC)
21	Polysulfone (PSU)
22	Polybutylene (PB)
23	Ionomer
24	Polyethylene - Low density (LDPE)
25	Polyethylene - High density (HDPE)
26	Polypropylene – Copolymer
27	Polypropylene – Homopolymer
28	Polypropylene - Barium Solfate Reinforced
29	Polyvinyl Chloride- Flexible
30	Polyvinyl Chloride- Rigid
31	Acetal Resin – Homopolymer
32	Acetal Resin – Copolymer
33	Polyphenylene Sulfide (PPS)
34	Ethylene Vynil Acetate (EVA)
35	Synthetic Elastomer
36	Polypropylene - Glass Filled
37	Urethane Elastomer, Thermoplastic (TPU)
38	Polypropylene - Flame Retardant
39	Polyester Elastomer (PE)
40	ABS - Flame Retardant
41	Polyallomer
42	Styrenic Terpolymer
43	Polymethylpentene (PMP)
44	Polypropylene - Talc Reinforced
45	Polypropylene - Calcium Carbonate Reinforced
46	Polypropylene - Mica Reinforced
47	Nylon – Type 66-33% glass
48	Thermoplastic Rubber (TPV)
49	Polyethylene - Medium density (MDPE)
50	ABS - Nylon Alloy

Methods

FT-IR spectra of all the specimens were recorded using an *Alpha Bruker Optics* spectrophotometer equipped with accessories for the three configurations, Trans, ATR, and TR modes (Fig. 3.5), as explained below.

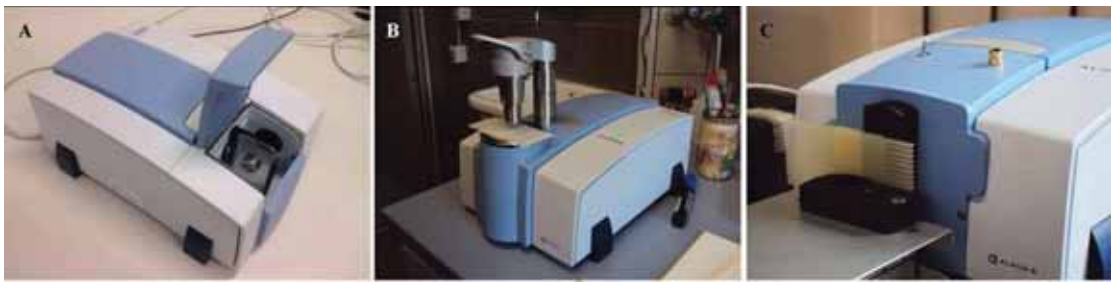

Fig. 3.5 - *Alpha Bruker Optics* spectrophotometer equipped with Trans (A), ATR (B) e TR (C) accessories

Transmittance mode. All 50 samples were prepared using the same procedure. A small sample scraped out from a lateral tooth of the chip was finely ground and mixed with KBr (Sigma-Aldrich Potassium Bromide 99% FT-IR grade) in order to prepare a pellet. In some cases, depending on the nature (e.g. hard or gummy) of the polymer, it was difficult to obtain a homogeneous dispersion of the material in the KBr matrix. Although this aspect could affect the final spectral quality, it was decided to adopt the same preparatory procedure for all the materials analysed in order to facilitate their comparison with the FT-IR data acquired using other instrumental configurations.

The spectral range investigated was 4000-375 cm^{-1}, with a resolution of 4 cm^{-1}, and 64 scans. The Trans spectra are reported in absorbance scale, in order to facilitate the comparison with the ATR and TR data.

Attenuated Total Reflectance mode. ATR spectra were non-invasively recorded on the surface of the thickest part of each specimen, using a diamond crystal. The spectral range investigated was 7000-375 cm^{-1}, with a resolution of 4 cm^{-1}, and 64 scans. All spectra were processed by using the ATR correction tool for ATR diamond crystal with the Opus 7.0.122 software from Bruker Optics. Other post-spectroscopic manipulations (such as normalisation) were avoided.

Total Reflectance mode. As for the ATR configuration, spectra were non-invasively registered on the central area of the specimen, where the thickness was 3mm. The 7000-375 cm^{-1} range was investigated, with a 4 cm^{-1} resolution. Spectral acquisition was usually made using 64 scans. In some cases, it was necessary to acquire 128 scans in order to optimise the signal-to-noise ratio.

All the TR spectra were processed using the KK algorithm. This procedure was usually applied in the 4000-375 cm^{-1} range, and the KK was applied solely to selected regions of the spectra in only a few cases.

3.2-4 Results and discussion

Since acquisition in Trans mode is traditionally the most widespread FT-IR technique for identifying the materials under investigation, and since most FT-IR spectral libraries are based on transmittance spectra, the 50 samples were first characterised in transmittance in order to

build a reference spectral archive. Subsequently, these spectra were compared with the ones acquired in both ATR and TR modes, so as to analyse differences and similarities. Based on the results obtained, five different case-typologies were singled out, as illustrated in detail here as follows.

Case 1. Spectra acquired in Trans, ATR, and TR modes are all comparable

This is the most desirable condition, because TR spectra are superimposable on both ATR and Trans spectra, and this fact makes it possible to make a reliable identification of the polymeric material by means of TR. In the collection of plastic samples analysed, 17 specimens fell within this typology (34% of the cases). Among these, not only polymers with similar composition were present (e.g. ABS polymers, Nylons), but also plastics having a completely different nature (e.g. PSU, PETG).

For example, in the spectra acquired on Resinkit™ N. 5 (*ABS-transparent*), it could be observed that all the spectra had a similar shape and were in good agreement with each other (Fig. 3.6).

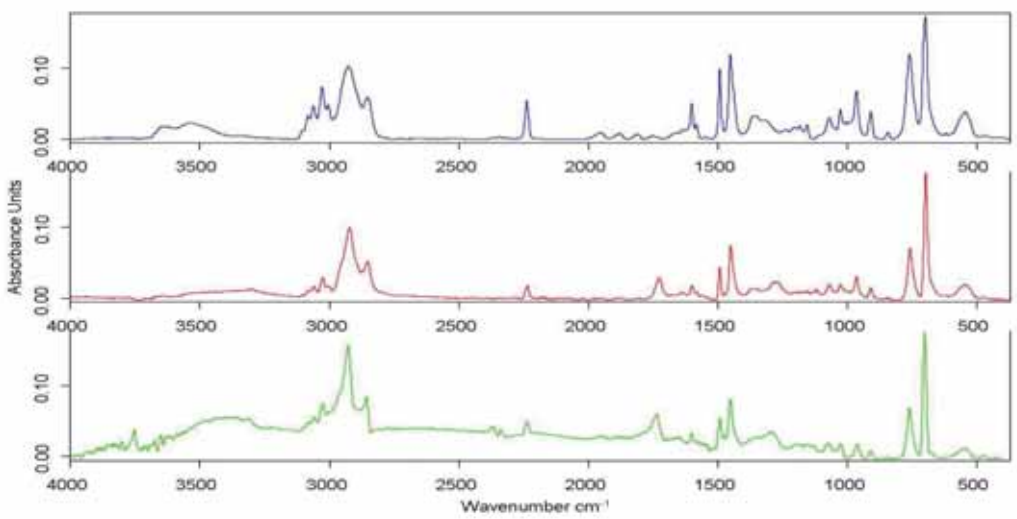

Fig. 3.6 - Trans (blue line), ATR (red line) and TR (green line, after KK transformation) spectra of sample 5 (*ABS-transparent*)

Another example is represented by sample N. 25 (*polyethylene high density*). Indeed, all the characteristic absorptions of the material were easily detectable in all three spectra, thus enabling an unambiguous identification (Fig. 3.7). The slight difference in intensity, which was mainly observed for the absorption bands at 1468 and 721cm^{-1}, did not affect the spectral interpretation.

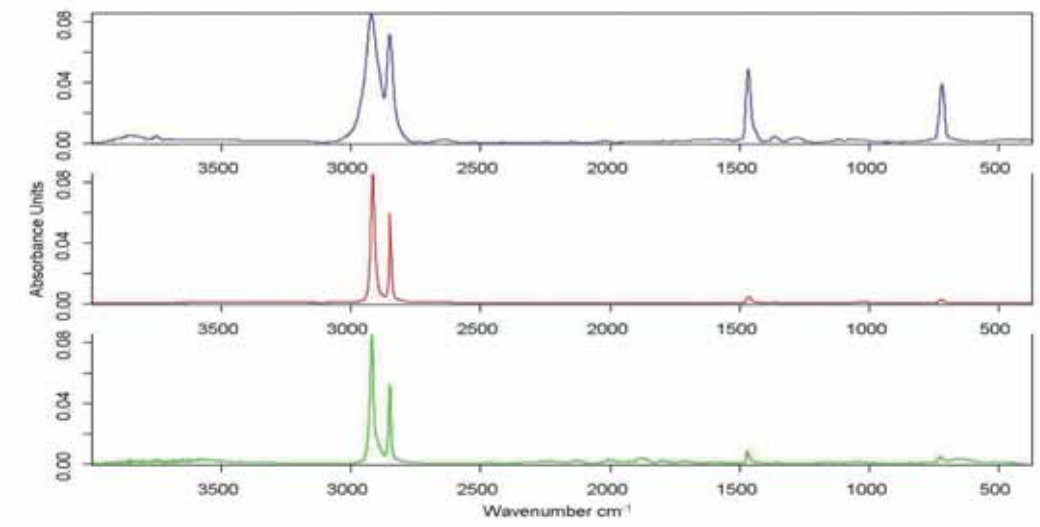

Fig. 3.7 - Trans (blue line), ATR (red line) and TR (green line, after KK transformation) spectra of sample 25 (*polyethylene high density*)

Case 2. Spectra acquired in TR and ATR modes are comparable with each other, and differ from the ones acquired in Trans mode.

In this case, spectra acquired in ATR and TR modes evidenced a higher signal-to-noise ratio as compared with those acquired in Trans. Therefore, the Trans spectra were less resolved, although all the most significant bands of the polymers under examination were still evident. Fifteen specimens were placed in this class (30% of the cases). A typical example is reported in Figure 3.8, where the three types of FT-IR spectra of the sample N. 14 (*nylon transparent*) are shown. The most intense peaks of the amide I and amide II bands at 1640 cm^{-1} and 1540 cm^{-1}, respectively, were intense and sharp in the ATR and TR spectra, whereas in the Trans spectrum these bands appeared to be much broader. Furthermore, the band at about 3300 cm^{-1}, which corresponded to the N-H stretching, was clearly evident in the ATR and TR spectra, while it was hidden by the broad band of the water in the Trans spectrum.

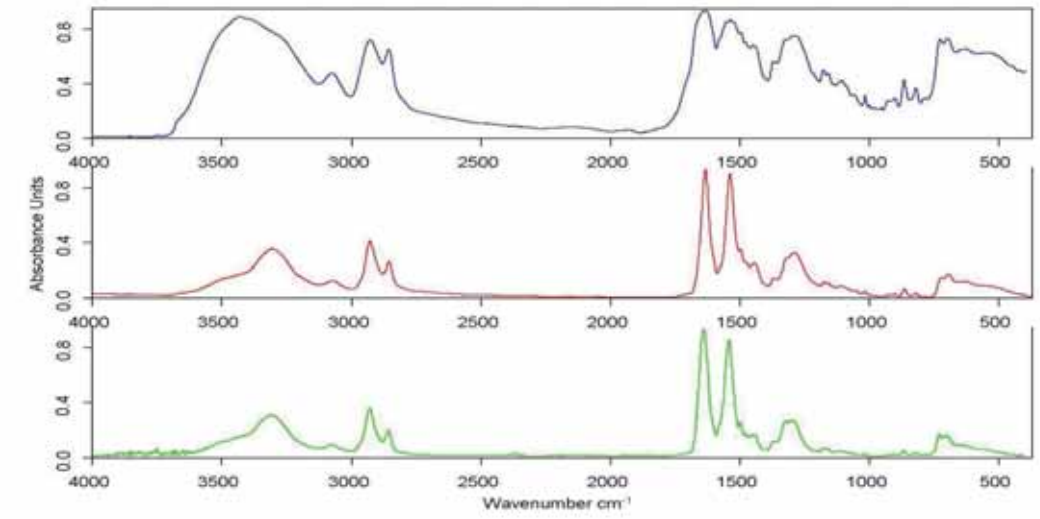

Fig. 3.8 - Trans (blue line), ATR (red line) and TR (green line, after KK transformation) spectra of sample 14 (*nylon transparent*)

Another representative example is that of sample N. 11 (*Cellulose Acetate*). Also for this specimen, the ATR and TR spectra were perfectly superimposable. The Trans spectrum, instead, was less resolved. Despite this fact, it showed, mainly in the fingerprint region, some absorption bands that had a very low intensity in ATR and TR spectra (Fig. 3.9).

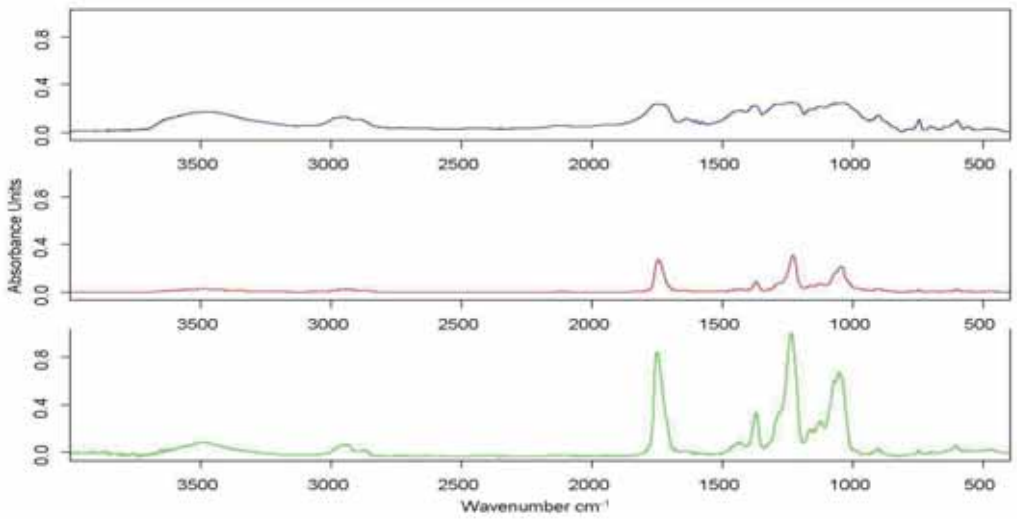

Fig. 3.9 - Trans (blue line), ATR (red line) and TR (green line, after KK transformation) spectra of sample 11 (*Cellulose Acetate*)

In some cases, due to the complexity of reducing the plastic material to a fine powder, the difficulty in obtaining a homogeneous dispersion of the analysed polymer in the KBr pellet was the main cause of the differences encountered in the Trans-mode spectra, as compared to those acquired in the ATR and TR modes.

This is a typical example of polymers that would necessitate resorting to different types of sample preparations in order to increase the quality of the spectral data, such as diamond cells, ATR, and TR measurement modes.

Case 3. Spectra acquired in ATR and Trans modes are comparable with each other, but different from the ones acquired in TR mode

This is one of the most critical cases to be considered. In the present study, this condition occurred in 9 out of the 50 samples investigated (18%). An example of such an occurrence was specimen N. 44 (*polypropylene - talc reinforced*). Indeed, no practical differences were found between the ATR and Trans spectra. When considering the TR spectrum, it could be observed that the absorptions bands falling within the 1500-500 cm^{-1} range were acceptably comparable with those acquired in the ATR and Trans modes. All spectra, in fact, showed similar absorption bands at the same wavelengths, although the general shape of the spectra was slightly different. In contrast, curves were appreciably different in the 3000-2700 cm^{-1} and 500-375 cm^{-1} ranges. In these cases, application of the KK spectral transform algorithm on the TR spectrum made it possible to obtain a good comparability with the Trans and/or ATR spectra (Fig. 3.10).

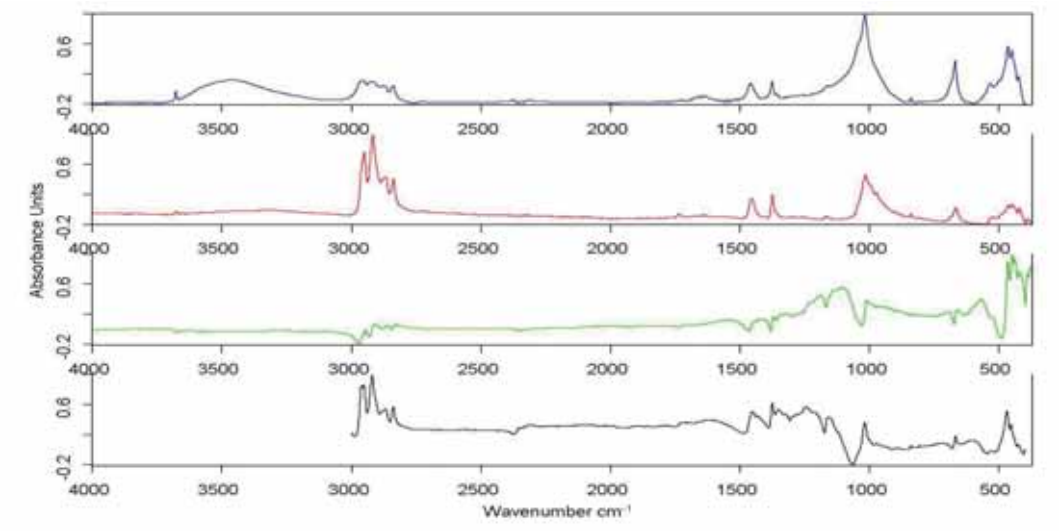

Fig. 3.10 - Trans (blue line), ATR (red line) and TR (green line, before KK transformation; black line, after KK transformation) spectra of sample 44 (*polypropylene talc reinforced*)

Therefore, no direct comparison between TR and Trans and/or ATR spectra was possible for this typology of samples for the entire frequency range: a suitable spectral matching could be obtained between the data acquired in the different configurations only after application of the KK algorithm in selected spectral regions.

In contrast with the previous example, different behaviour was shown by sample N. 32 (*acetal resin copolymer*). Indeed, the TR spectrum was not favourably comparable with the ATR and Trans spectra, either before or after application of the KK algorithm. In particular, the main differences were detected in the fingerprint region (Fig.3.11).

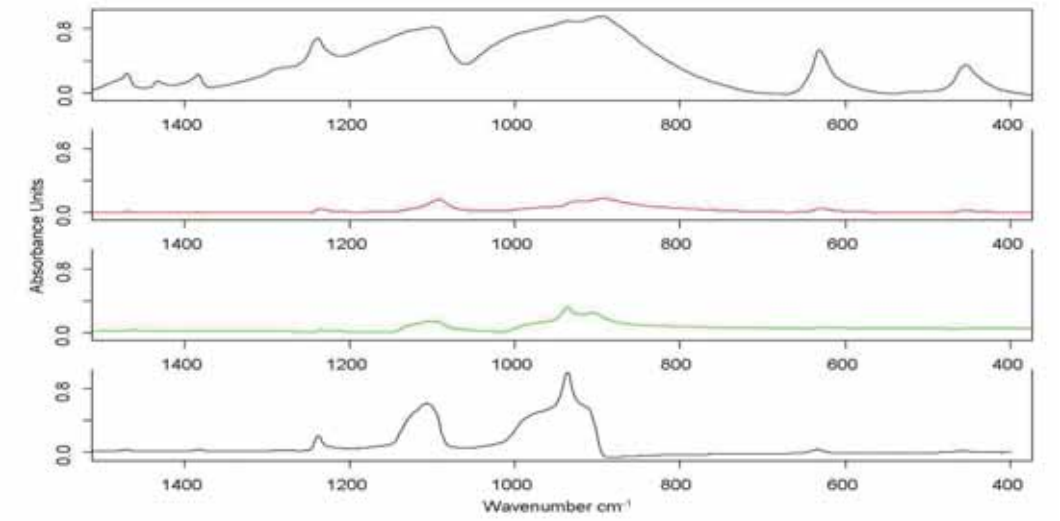

Fig. 3.11 - Trans (blue line), ATR (red line) and TR (green line, before KK transformation; black line, after KK transformation) spectra of sample 32 (*acetal resin - copolymer*)

Case 4. Transmittance, ATR, and TR mode spectra are all different, and are not comparable with each other.

This was the least common case, and this condition occurred in five specimens (10%). In Figure 3.12 the Resinkit N. 37 (*urethane elastomer thermoplastic*) is reported as an example. In this case, the Trans spectrum appeared to be quite unusual, due to the presence of

broadened and poorly-resolved bands with anomalous intensities. This spectral behaviour may be related to the extreme difficulty in obtaining a homogeneous dispersion of the material in the KBr matrix, a difficulty that was due to the soft and gummy consistency of the polymer sample. Instead, the typical spectral features of polyester-based thermoplastic polyurethane were present in the ATR spectrum (Wang and Luo, 2004). The TR spectrum presented absorption bands that could be utilised to correctly identify the polymer.

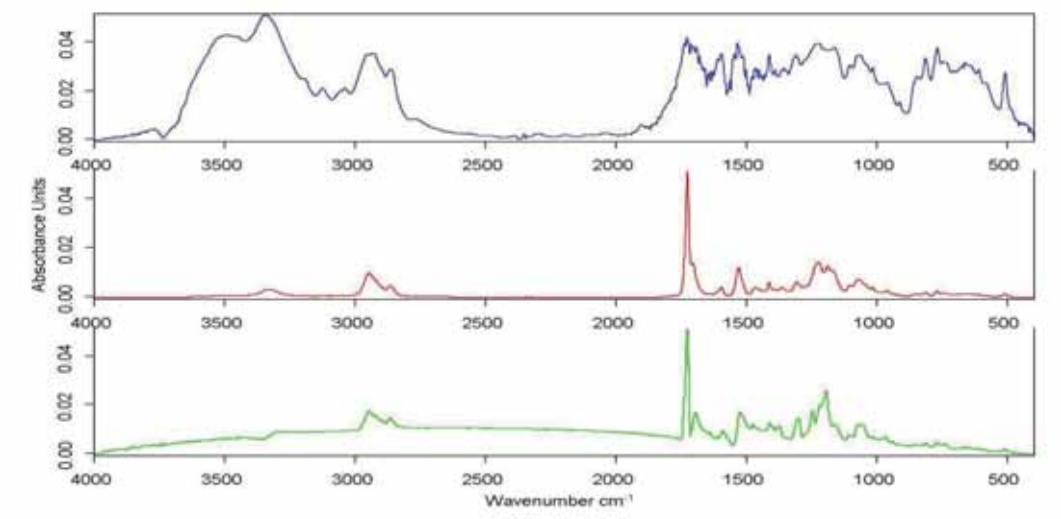

Fig. 3.12 - Trans (blue line), ATR (red line) and TR (green line, after KK transformation) spectra of sample 37 (*urethane thermoplastic elastomer*)

It should be noted, however, that in this case the application of KK did not make the TR spectra more comparable with those of the Trans and ATR. Five different specimens with diverse compositions and appearances were grouped in *Case 4*.

Case 5. Spectra acquired in ATR and TR modes are comparable, but fail to reveal the presence of additives, which are detectable only in Trans mode.

In principle, this condition could be considered as a sub-group of Case 3; in fact, however, it deserved particular attention, since it pointed out a substantially different circumstance, one in which the Trans spectrum was more informative than both ATR and TR. In the present study, this condition occurred in four cases (8%), all of them on polymers containing inorganic additives. An example is represented by the spectra of sample N. 28 (*polypropylene - barium sulfate reinforced*) (Fig. 3.13).

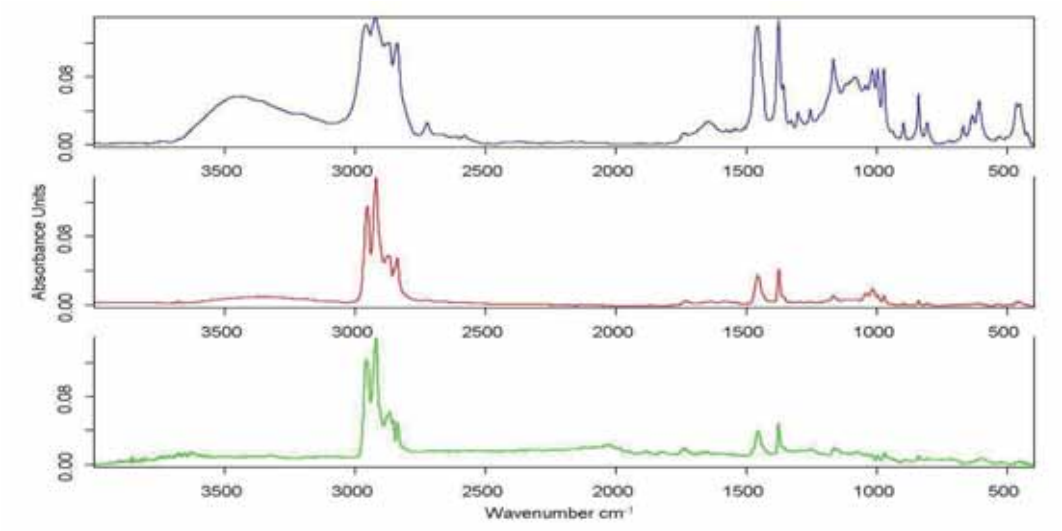

Fig. 3.13 - Trans (blue line), ATR (red line) and TR (green line, after KK transformation) spectra of sample 28 (*polypropylene barium sulphate reinforced*)

In the Trans spectrum, the absorption bands attributed to $BaSO_4$ in the 1200-1050 cm^{-1} range (SO_4^{2-} asymmetric stretching) and the bands at 640 and 615 cm^{-1} (SO_4^{2-} bending vibrations) were present. In contrast, these spectral features were absent or showed very weak intensities in both the ATR and TR mode spectra, thus preventing a complete identification of the additives included in the polymer formulation. This occurrence might be explained by the fact that, depending on the portion of the specimen sampled, the Trans mode technique was able to detect the bulk composition of the investigated samples more easily (if the specimen was adequately ground), while the penetration depth of the other two techniques was limited to the first microns of the sample analysed. Thus, additives used for reinforcement purposes, such as many inorganic fillers/additives, may have a minimal concentration on the surface and hence are not easily revealed by means of both ATR and TR modes. Therefore, for the specimens in Case 5 the FT-IR technique in Trans mode was found to be decisive for identifying the fillers/additives, such as calcium carbonate, barium sulphate, mica, glass, etc., included in the formulation of the polymer.

Another example is represented by spectra acquired on specimen N. 36 (*Polypropylene - glass filled*). Once again, the broad absorption band at 1200-900 cm^{-1} due to the presence of glass is detectable only in the Trans spectrum (Fig. 3.14).

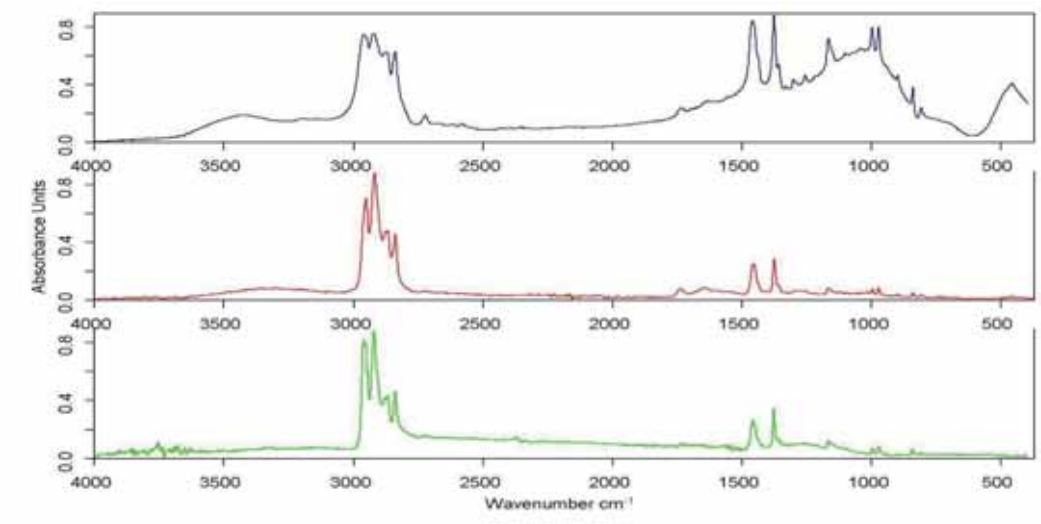

Fig. 3.14 - Trans (blue line), ATR (red line) and TR (green line, after KK transformation) spectra of sample 36 (*polypropylene-glass filled*)

As a general comment with regard to the comparability of the three techniques, it can be stated that the spectra recorded with both the ATR and TR techniques were often in poor agreement with those obtained in Trans mode as regards the intensity and shape of the absorption bands, but this fact usually does not affect the correct identification of the materials. However, for a relatively small number of cases (14 specimens, falling within categories 2 and 3, respectively) of the 50 analysed, TR could not be considered as being interchangeable and as reliable as Trans and ATR. This indicated that portable FT-IR devices may be used to implement a non-invasive identification of constituent polymers in plastic artworks, provided that a certain margin of inexact attributions is taken into account when comparing TR spectra with libraries built using different techniques (Trans and/or ATR). However, the reliability and good quality of the TR spectra acquired without sampling has been confirmed in most cases.

A side outcome of this study performed on the ResinKit^{TM} set was the demonstration that, in a few cases, FT-IR analysis succeeded in highlighting some discrepancies between the declared composition and the actual formulation of the specimens analysed. For example, the FT-IR spectrum of sample N.18 classified in the ResinKit^{TM} set as *thermoplastic polyester-PETG* had the spectral features of an alloy of polyethylene terephthalate and polycarbonate (Fig. 3.15). This material is available commercially, and is used to manufacture such items as greenhouse roofs, automobile instrument panels, wheel covers, snowmobiles, and cellular phones.

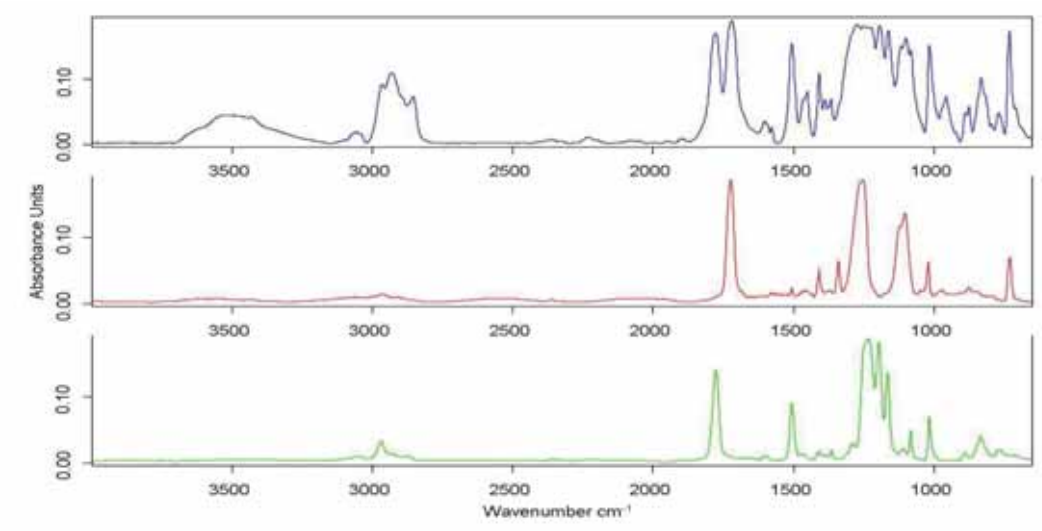

Fig. 3.15 - Trans spectrum (blue line) of sample 18 (*thermoplastic polyester-PETG*); reference spectra of polyethylene terephthalate (ref. ISR00120, red line) and polycarbonate (ref. ISR00122, green line) from IRUG 2007 database

Another general consideration concerns the possibility of distinguishing polymers that belong to the same polymeric class but have a different density. Based on the results obtained, it was found that, irrespective of the instrumental configuration used, FT-IR techniques were not suitable for this finer discrimination. This was indeed the case of the following polymeric classes: *polyethylene* (N. 24 Low density, N. 25 High density), *polystyrene* (N. 1 General purpose, N. 2 Medium impact, N. 3 High impact), and *ABS* (N. 5 Transparent, N. 6 Medium impact, N. 7 High impact).

3.3 Conclusion

In this study, the potentials of non-invasive FT-IR spectroscopy, implemented by means of portable devices that operate in reflectance mode, were investigated. A pilot study on a commercial set of 50 reference samples of thermoplastics resins was carried out. The samples was analysed by means of three different FT-IR instrumental configurations, namely in Trans, ATR and TR modes. The ultimate aim was to investigate the quality and reliability of FT-IR spectra acquired non-invasively in the TR mode by means of portable FT-IR spectrometers. The TR spectra were then compared with those acquired in the Trans and ATR modes, and the resulting data were classified into different categories on the basis of their agreement level. Based on the analysed set it was found that the spectra recorded with using both the ATR and TR techniques were sometimes in poor agreement with those obtained in the Trans mode, in both the intensity and the shape of the absorption bands. Conversely, in most cases the spectra acquired by means of the ATR and TR techniques were found to be definitely comparable, in particular after processing the TR spectra by means of the KK algorithm. However, the results obtained pointed out that the application of the KK algorithm has to be considered case by case, by means of a careful evaluation of the frequency range in which the KK correction has

to be made. Moreover, in a few cases the TR spectra were not comparable with those collected in the ATR and/or Trans modes.

Table 3.2 - List of the Resin Kit™ samples and corresponding case-typologies

Number	Name	Case
1	Polystyrene - General Purpose (GPPS)	3
2	Polystyrene - Medium Impact	2
3	Polystyrene - High Impact (HIPS)	2
4	Styrene Acrylonitrile (SAN)	1
5	ABS – Transparent	1
6	ABS - Medium Impact	1
7	ABS - High Impact	1
8	Styrene - Butadiene Block Copolymer (SBR)	2
9	Acrylic	1
10	Modified Acrylic	1
11	Cellulose Acetate (CA)	2
12	Cellulose Acetate Butyrate (CAB)	2
13	Cellulose Acetate Propionate (CAP)	2
14	Nylon - Transparent	2
15	Nylon (polyammide) - Type 66	1
16	Nylon (polyammide) - Type 6	1
17	Thermoplastic polyester (PBT)	2
18	Thermoplastic polyester (PETG)	1
19	Polyphenylene Oxide (PPO)	1
20	Polycarbonate (PC)	1
21	Polysulfone (PSU)	1
22	Polybutylene (PB)	3
23	Ionomer	2
24	Polyethylene - Low density (LDPE)	2
25	Polyethylene - High density (HDPE)	1
26	Polypropylene – Copolymer	2
27	Polypropylene – Homopolymer	3
28	Polypropylene - Barium Solfate Reinforced	5
29	Polyvinyl Chloride- Flexible	1
30	Polyvinyl Chloride- Rigid	1
31	Acetal Resin – Homopolymer	2
32	Acetal Resin – Copolymer	3
33	Polyphenylene Sulfide (PPS)	4
34	Ethylene Vynil Acetate (EVA)	2
35	Synthetic Elastomer	4
36	Polypropylene - Glass Filled	5
37	Urethane Elastomer, Thermoplastic (TPU)	4
38	Polypropylene - Flame Retardant	3
39	Polyester Elastomer (PE)	2
40	ABS - Flame Retardant	3
41	Polyallomer	4
42	Styrenic Terpolymer	1
43	Polymethylpentene (PMP)	3
44	Polypropylene – Talc Reinforced	3
45	Polypropylene - Calcium Carbonate Reinforced	3
46	Polypropylene – Mica Reinforced	5
47	Nylon - Type 66-33% glass	5
48	Thermoplastic Rubber (TPV)	4
49	Polyethylene - Medium density (MDPE)	2
50	ABS - Nylon Alloy	1

The results obtained revealed that, in the majority of cases, the TR mode may be used advantageously *in situ* in order to obtain a non invasive identification of constituent polymers in plastic objects, especially for large-scale and preliminary surveys of plastic artworks. However, a certain margin (18% according to the results presented here) of inexact attributions has to be taken into account when comparing TR spectra with spectral libraries built using different techniques (Trans and/or ATR).

A collection of TR FT-IR spectra based on this comparative evaluation has been singled out, so as to provide a first nucleus for a TR FT-IR spectral archive of some of the most common synthetic resins, to be used as a guide in interpreting the data acquired in the field.

To conclude, if the fact that TR FT-IR technique is a non-invasive and portable methodology for *in situ* measurements is considered, the results reported indicate a promising perspective for its application in the cultural heritage field and, in particular, in the analysis of plastic artworks.

SECTION III
CASE STUDIES

CHAPTER 4 – ANSELM KIEFER

4.1 Anselm Kiefer

4.1-1 Short biography

Fig. 4.1 – Anselm Kiefer
[Image from: http://www.c4gallery.com/artist/database/anselm-kiefer/anselm-kiefer.html (last access: august 7, 2013)]

Anselm Kiefer (Fig. 4.1) was born in Donaueschingen (Germany) in 1945. After secondary school he studied law but in 1966, after a seminal stay in La Tourette, he devoted himself to art full time. Kiefer studied at the Academy of Fine Arts in Karlsruhe, and later in Düsseldorf, where he became a student of the artist Joseph Beuys. In 1969 he had his first exhibition at the Kunstverein in Hanover.

Already in the early 1980s he was considered one of the greatest exponents of German contemporary art. Today, his curriculum is that of a famous master who has exhibited in the most important museums and galleries of the world. Kiefer has been appreciated mostly out of Germany where, initially, he was associated with the neo-Nazi movement by several art critics because of his provocative actions. As reported in the literature (Albano, 1998), he photographed himself with the *heil* salute in front of some historical German buildings. He later explained that it had been an intuitive and mechanical act dictated only by irony. Kiefer has tried to interpret the aesthetics of the Nazi years with the will of redeeming German history and freeing it from the shadows of the past. Unfortunately many people have not comprehended his artworks' real meaning and for a very long time Kiefer suffered from being associated to the Nazi movement. Due to this misunderstanding he moved from Germany to Barjac, in southern France, in 1992. Since then, the countryside of Provence has been the primary source of inspiration for a new creative phase that set the look on his vision of the fragile human condition that he compares with the power of nature. From 2007 he lives and works in Paris.

Kiefer's artworks are found in the permanent collections of some of world's most important museums, such as "The Metropolitan Museum" (New York), the "Centre Georges Pompidou" (Paris), the "Hamburgher Bahnof" (Berlin) and the "Israel Museum" (Jerusalem). In 2007, the "Guggenheim Museum Bilbao" presented a great retrospective of his works (March 28-September 3, 2007), and, in the same year, the *Louvre Museum* in Paris has commissioned

him, unique living artist since the days of Georges Braque, an artwork for its permanent collection.

In Italy he has the permanent installation *The Seven Heavenly Palaces* at the "Hangar Bicocca" (Milan) and some works in the collections of the "Galleria d'Arte Moderna" (Rome), the "MART" (Rovereto), the "Castello di Rivoli" (Rivoli, Turin), Biblioteca San Giorgio (Pistoia) and the "Fattoria di Celle" (Santomato, Pistoia).

4.1-2 The artistic technique

Kiefer's style, highly innovative and unconventional, is characterised by the use of very diverse materials that he selects and combines according to the emotions that they stir in him. To quote the artist: "*I only use materials that speak to me. […] I don't believe that the Idea can be found everywhere - the Idea in the sense of spirit is already present in the material. For example, lead: it's the material of melancholy, of black rancor. Once, in an old house, I saw a lead drainpipe and that material -lead- literally fascinated me*" (Rumma *et al*., 2006).

In most of his works, Kiefer employed lead, in its solid form or dropped after melting, alone or in combination with other materials (Cacciari and Celant, 1997; Eccher, 1999; Celant, 2008).

Fig. 4.2 - *Cette obscure clarté qui tombe des étoils*, Gori Collection, Fattoria di Celle (Santomato, Pistoia)
[Images from: http://www.goricoll.it/index.php?file=oneopere&id_cell_opera=68&from=opere]

The artist has also made particular use of photographs, vegetable items (*e.g*. straw, dried plants or flowers, burnt wood), shellac, ash, sand, volcanic earths, and iron wire. He has used materials picked up from the land around his studio or collected from around the world. He created an archive of plants and flowers from which restorers have to draw in case they have to replace components in his works (Chiantore and Rava, 2005). However, he is not concerned about the ageing of his artworks because he intends them as dynamic objects aimed to inspire different feelings and interpretations in future viewers. Speaking about his artwork *Cette obscure clarté qui tombe des étoils* (Fig. 4.2) installed at Fattoria di Celle (Santomato, Pistoia) Kiefer said: *"…History for me is matter. In my works I use events, occurrences,*

places, the life of those who have worked and lived there. I'm not interested in technique. I use substances and matter. And by matter I mean history as well as lead, paint, iron and clay" (Gori and Serafini, 2009).

His enormous production has included permanent installations as well as paintings on canvas and wood, usually characterised by large dimensions. Kiefer's preferred painting technique has involved the use of an emulsion of oil colours in a cellulose paste, which he has produced in his *atelier*. The emulsion is applied in thick layers on a support and left to dry for at least one year. In this way, the surface acquires the cracked appearance typical of his paintings and "*becomes the ideal foundation for the application of colour which, on the whole, is painted on with the idea of glazing rather than the application of a consistent substance"* (Chiantore and Rava, 2005).

The transport, installation, and conservation of Kiefer's artworks are problematic because of their large size, heterogeneity and, in some cases, the incompatibility of the materials used. The risk of degradation is high due to the possible detachment of the components, organic matter decomposing or coming under biological attack, and the quality of the support that can easily suffer deformation (Lindner *et al*., 2004). To eliminate or, at least, to minimise these problems it is necessary to characterise and identify these components, their compatibility and their modes of deterioration.

4.2 Case studies: *The Strip* and *Die Grosse Fracht*

4.2-1 The artworks

The Strip

The first object under investigation was a large piece (measuring approximately 18 cm x 300 cm) cut by the artist himself from a large polymateric in progress work on canvas and, for the sake of simplicity, called the *Strip* in the text (Fig. 4.3).

Fig. 4.3 – The *Strip* as supplied by the conservator (on the left) and the unrolling procedure (on the right)

The object arrived at the laboratory of the Institute of Applied Physics “Nello Carrara” of the National Research Council (IFAC-CNR) at the hand of the conservator Antonio Rava who had received the *Strip* by Kiefer himself during a visit to his studio in Barjac. Despite the fragment has no economic/artistic value, macroscopically it looks very similar to other finished artworks, such as *Für Saint-John Perse. Étroits sont les vaissaux* (2003) recently exposed in the exhibition "Anselm Kiefer" organied by the Fondazione Palazzo Albizzini of Città di Castello (Perugia, Italy), Fig. 4.4).

Fig. 4.4 – Two particulars of the *Strip* (on the left)
and a particular of *Für Saint-John Perse. Étroits sont les vaissaux* (on the right)

Die Grosse Fracht

Fig. 4.5- *Die Grosse Fracht* in the San Giorgio Library of Pistoia

Die Grosse Fracht (2006-07) is one of the most prestigious contemporary artworks of city of Pistoia, Tuscany. The artwork was donated by Fondazione della Cassa di Risparmio di Pistoia e Pescia to the San Giorgio Library (Fig. 4.5). Placed on the back wall of the main reading room on the first floor, the large canvas (460 cm x 690 cm) has been designed specifically for the library’s space (Calabrese and Corà, 2007). The title Kiefer gave it, *Die Grosse Fracht*

(The Heavy cargo), is borrowed from a poem of the Austrian modernist poetess Ingeborg Bachmann (June 25, 1926 – October 17, 1973):

The Heavy Cargo

The summer's heavy cargo has been loaded,
waiting in the harbor a sun ship lies,
as at your back the sea gull dips and cries.
The summer's heavy cargo has been loaded.
Waiting in the harbour a sun ship lies,
And there upon the lips of figureheads,
The lemur's mocking smile appears and spreads.
Waiting in the harbour a sun ship lies.
As at your back the sea gull dips and cries,
From the western horizon comes the order to sink,
You'll drown, open- eyed, in the light you'll drink,
As at your back the sea gull dips and cries.

Ingeborg Bachmann

In this artwork Kiefer materialises a sort of "ghost ship", carrying a cargo of books (and therefore of memories and century-old culture), that looms against a dark backdrop, under a sky that does not stand out from the land to which streams of molten lead overlap.

4.2-2 Experimental

Samples

Four principal painted areas distributed throughout the *Strip* were recognised. Their colours ranged from black and pale pink to pale yellow. Since the object is considered destitute of any artistic value five samples were removed. A single sample was collected from each area with the exception of the pale yellow from which two contiguous fragments were scraped out (Fig. 4.6, Table 4.1).

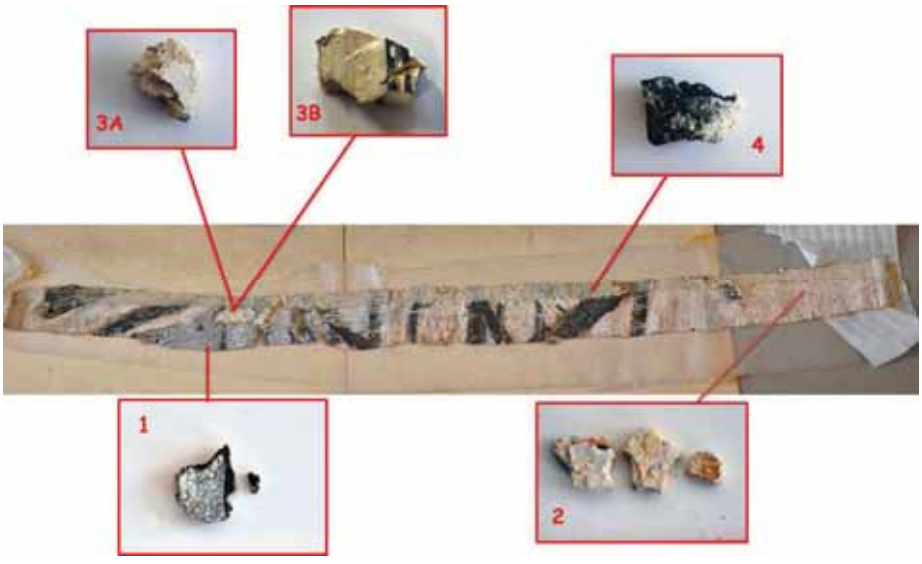

Fig. 4.6 – The samples from the *Strip*

Notwithstanding its young age, *Die Grosse Fracht* was subjected to a partial restoration in 2011 due to the detachment of paint from the canvas support. During the conservative intervention, performed by the conservator Antonio Rava, four samples from this artwork were taken and analysed (Fig. 4.7, Table 4.1).

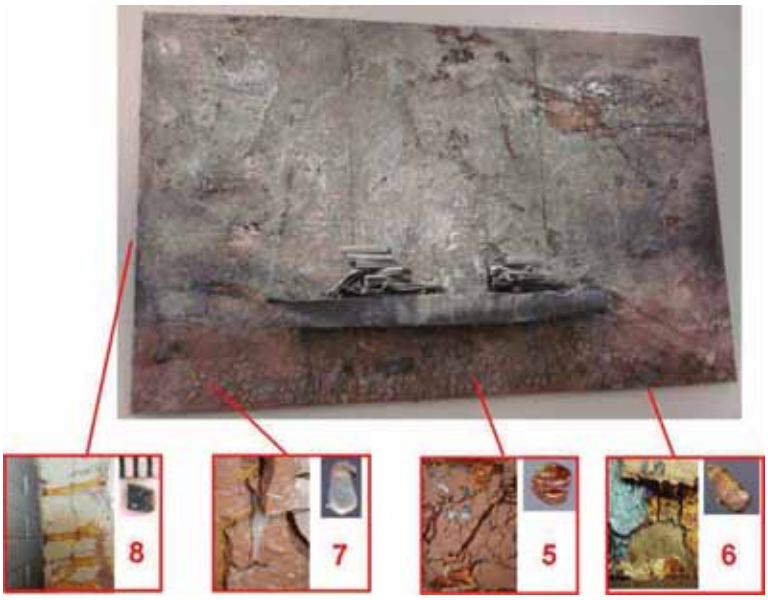

Fig. 4.7 – The samples of *Die Grosse Fracht*

Table 4.1 - List of the analysed samples and their brief description

Sample	Colour	Description
1*	black	black material (10mmx15mm) covered by a thin layer of white paint
2*	pale pink	pale pink material (10mmx13mm) with little brown spots on the surface
3A*	pale yellow	pale yellow material (15mmx20mm)
3B*	pale yellow	pale yellow material (18mmx22mm) partially covered with black paint
4*	black	black material (14mmx20mm) covered by granular material of a light color
5**	brown	drop like shape (3mmx3mm)
6**	brown	brown earthy material (7mmx5mm)
7**	semi-transparent	tacky material (7mmx3mm)
8**	off-white	off-white solid material (7mmx3mm)

* Sample from the *Strip*
**Sample from *Die Grosse Fracht*

Imaging

Visible and UV images were recorded on the *Strip* using a *Nikon D70* camera and two special low-wattage compact fluorescent lamps emitting long wave UV radiation (Philips PL-S 9W/08 2P). To avoid the visible and part of the near infrared component of the radiation a DUG11 filter was mounted on the lens.

FORS

FORS measurements in the UV-Vis-NIR spectral range (350–2200 nm) were performed using two single-beam *Zeiss* spectroanalysers, model *MC601* (190-1015 nm range) and *model MC611 NIR 2.2WR* (910-2200 nm range), housed together in a compact and portable chassis for *in situ* analyses. The data acquisition step was 0.8 nm/ pixel for the 1024-element silicon photodiode array detector (*MCS601*), and 6.0 nm/pixel for the 256-element InGaAs diode array detector (*MCS611 NIR 2.2 WR*). The radiation between 320 nm and 2700 nm, which was provided by a voltage-stabilized 20W halogen lamp (mod. CLH600), was conveyed to the sample by means of a quartz optical fibre bundle that also transported the reflected radiation to the detectors. The geometry of the probe head was 8°/8°. Calibration was performed by means of a 99% Spectralon® diffuse reflectance standard.

To investigate the 270-800 nm (UV-Vis) range a *Zeiss* spectrum analyzer model *CLX 500* equipped with a xenon lamp was used.

Spectra were processed using Aspect Plus® 1.80 software.

FT-IR

FTIR spectra in transmittance mode were recorded using two different devices: a *Nicolet Protégé® 460 E.S.P®* spectrophotometer equipped with a SiC Globar source and a DTGS detector, and a *Bruker Vertex70®* spectrometer coupled to a Hyperion® microscope equipped with a cryogenic mercury-cadmium telluride (MCT) detector.

With the Nicolet instrument, 64 scans were acquired on the samples mounted in KBr pellets, in the 4000-400 cm^{-1} spectral range with a 4 cm^{-1} resolution. The spectra were processed using the software OMNIC 7.3.94.

For measurements with the Bruker Vertex70® spectrometer, the samples were placed between the windows of a diamond anvil cell and observed with a 30x objective, 128 scans and a spectral resolution of 4 cm^{-1}.

TR FTIR spectra in the 7500-375 cm^{-1} range were acquired with an *ALPHA Bruker Optics* spectrophotometer, equipped with a SiC Globar source and a DTGS detector. Spectra (128 scans with 4 cm^{-1} resolution) were processed using the software OPUS 7.0.122. The Kramers-Krönig (KK) algorithm was applied in the 4000-375 cm^{-1} range to rebuild absorbance spectra.

XRD[1]

Samples 1 and 6 were investigated by means of X-Ray Diffraction (XRD) using two different instruments:

- a PanAnalytical X'Pert Pro *X-Ray diffractometer* (40 kV, 30 mA) with Cu K radiation (λ =1,545 Å), for the analysis of sample 1;
- a *Philips X-Ray diffractometer 1979* (40 kV, 24 mA) with Cu K radiation (λ = 1.5406 Å), for the analysis of sample 6.

NMR[2]

Samples 1, 2 and 3A were analysed by means of ^{1}H Nuclear Magnetic Resonance (^{1}H-NMR). Spectra were recorded with a *Varian VXR 200* spectrometer operating at a frequency of 199.985 MHz. For this experiment, the powder samples were subjected to a chloroform (10 ml) extraction at room temperature under magnetic stirring for 30 minutes. After the removal of the insoluble fraction by filtration on paper, the filtrates were dried at 30 °C with reduced pressure in a Büchi rotavapor. The residues were analysed by ^{1}H-NMR using deuterochloroform ($CDCl_3$) as solvent. The spectra were processed using the software iNMR 3.3.7.

4.2-3 Study of the artistic materials

The Strip

The surface of the *Strip* was photographed under visible and UV (365 nm) illuminations for documentation purposes as well as to better define the sampling areas (Aldrovandi and Picollo, 2007). The visible images permitted to identify the four principal paint areas distributed throughout the object, facilitating the sampling. It was also possible to distinguish an area located near the upper end of the *Strip* which is characterised by a granular surface texture. Several metal staples applied by the artist over the paint surface were observed too (Fig. 4.8).

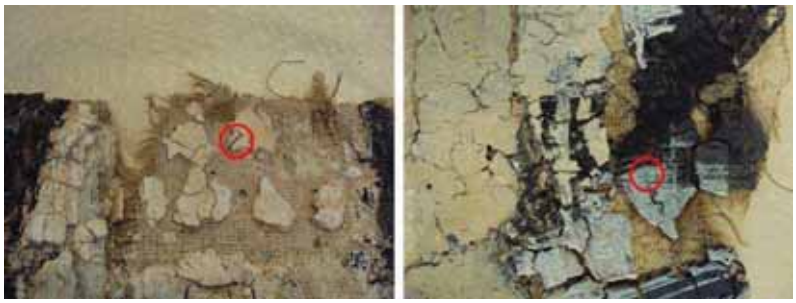

Fig. 4.8 – Metal staples on the surface of the *Strip*: two details

[1] XRD analysis was performed by Dr. Emma Cantisani of the Institute for the Conservation and Valorisation of Cultural Heritage (Department of Florence) of the National Research Council (ICVBC-CNR).
[2] The NMR analysis was performed in the scientific laboratories of the Department of Chemistry "Ugo Schiff" of the University of Florence under the supervision of Prof. Antonella Salvini and Prof. Donatella Giomi.

The UV examination of the *Strip* allowed visualising and localising florescent spots or 'stains', that look organic in nature, on its surface (Fig. 4.9). These stains were generally extremely thin; but it was possible to take a small amount of this material from an area where it appeared relatively thick by using a cotton swab and acetone.

The dried residue in the swab was analysed in a KBr pellet by FTIR in the transmission mode.

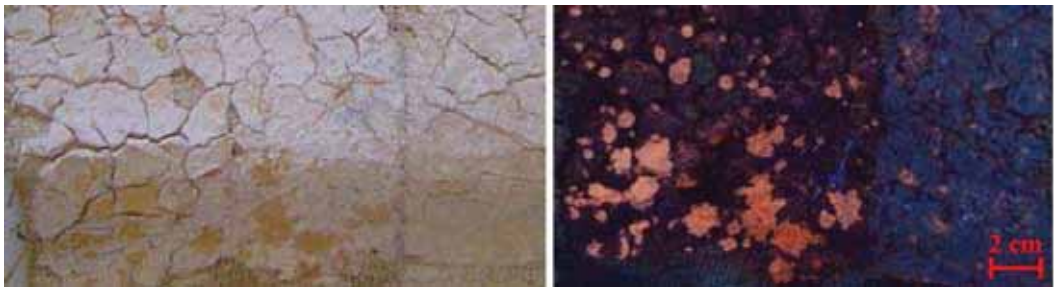

Fig. 4.9 - Images acquired with visible (left) and UV (right) illuminations, respectively, of an area of the *Strip* located near the right edge

Total reflectance FT-IR spectra were also acquired on other dense stains *in situ* on the surface of the *Strip*. All the spectra recorded consistently indicated the presence of shellac as illustrated in Figure 4.10.

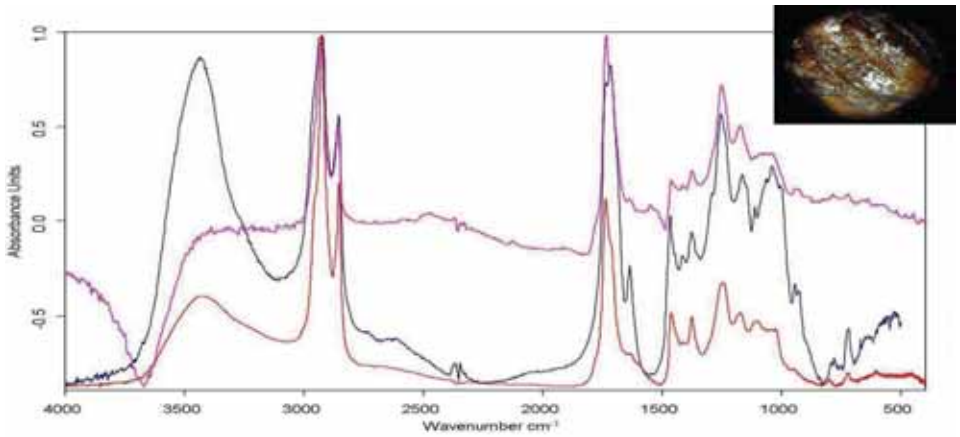

Fig. 4.10 - FTIR spectrum of an acetone extract of a sample removed with a cotton swab (red line), total reflectance spectrum of a 'stain' acquired *in situ* (pink line, after the Kramers-Kronig algorithm application), reference spectrum of shellac from the IRUG2007 database (blue line, ref. INR00273). In the box on the right an image of the measurement area obtained with the on board camera of the Alpha Bruker spectrophotometer is shown

In the picture, the transmittance spectrum of the dried residue (red line) and the reflectance spectrum registered on *in situ* stains (pink line, after Kramers-Kronig algorithm application) were comparable to each other and to the reference spectrum of shellac (blue line, IRUG2007 database, ref. INR00273) They presented, indeed, the spectral features of shellac natural resin: 3600-3200 cm^{-1} (OH stretching), 2930 and 2855 cm^{-1} (CH stretching), 1737 cm^{-1} (C=O stretching), 1637 cm^{-1} (C-C stretching) 1465 and1376 cm^{-1} (CH bending), 1252 cm^{-1} (CO stretching), (Derrick *et al.*, 1991). The obtained result was unequivocally confirmed by means of Py-GC/MS performed within the framework of the CoPAC Project at the SCIBEC[3]

[3] Chemical Science for the Safeguard of Cultural Heritage

laboratory of the University of Pisa (Colombini, 2012). Py-GC/MS analysis showed indeed the presence of butolic acid, characteristic molecular marker for shellac resin (Bonaduce *et al.*, 2003).

The samples detached from the *Strip* were firstly analysed by means of UV-Vis-NIR Fibre Optic Reflectance Spectroscopy. The 350-2200 nm spectra of the samples 1 (white film on the surface), 2, and 3B (Fig. 4.11) showed the typical features of titanium white (TiO_2) in its rutile crystalline form, that has an inflection point at 400 nm (3.09 eV) in its first derivative spectrum (Picollo *et al.*, 2007). This result was confirmed by FT-IR spectra that showed the typical absorption bands at *ca.* 600 and 523 cm^{-1}.

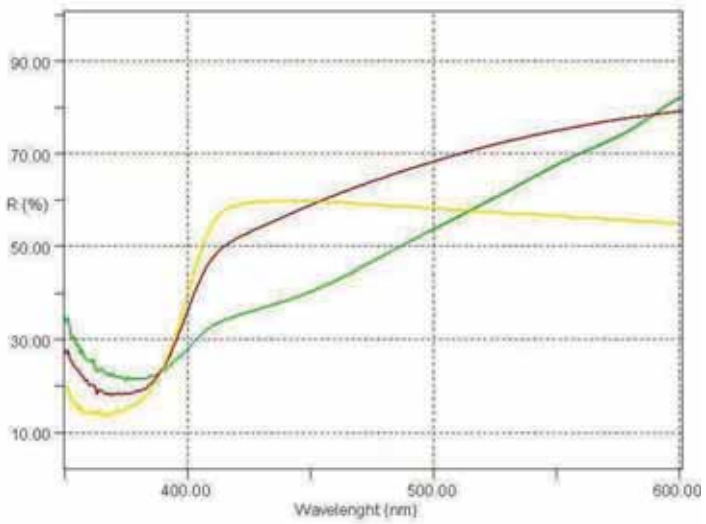

Fig. 4.11 – FORS spectra of samples 1 (yellow line), 2 (green line) and 3B (red line) in the 350-600 nm spectral range

The reflectance spectrum of sample 3B showed, in addition, two absorption bands at 670 nm and 728 nm typical of Co^{2+} ion in pseudo-tetrahedral coordination as a vicariant of Zn^{2+} in the structure of ZnS. The presence of this ion has been associated with the lithopone pigment ($BaSO_4$ + ZnS) produced after the mid-1920s (Weakliem, 1962; Van Alphen, 1998). The presence of ZnS in this sample was confirmed by its FORS spectrum in the 270-800 nm range. The typical strong absorption in the UV region below 350 nm with an inflection point at 340 nm ascribable to ZnS was observed in this sample (Picollo *et al.*, 2007)(Fig. 4.12).

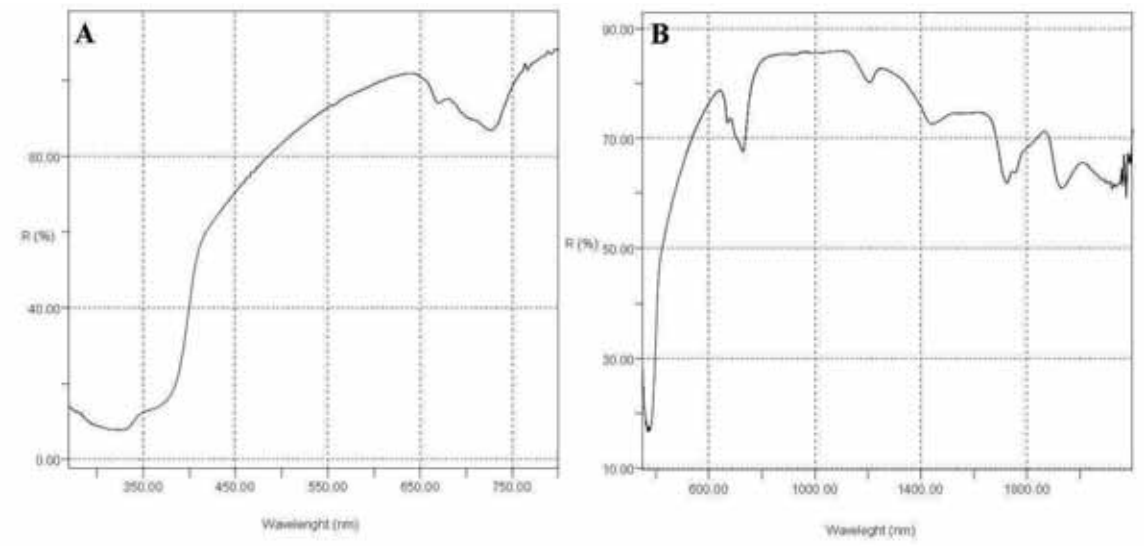

Fig. 4.12 - FORS spectra of sample 3B in the 278-800 nm (A) and 350-2200 nm (B) spectral range

Since the IR spectrum of sample 3B showed the typical absorption bands of barium sulphate (Ramaswamy *et al.*, 2010) at *ca*. 1187, 1124, 1077 (SO_4^{2+} asymmetric stretching), 982 (ν_1 SO_4^{2+} in plane bending), 637 and 611 cm^{-1} (doublet, ν_4 SO_4^{2+} out of plane bending), the presence of lithopone in this sample was univocally confirmed. Furthermore, in all the analysed samples, calcite was identified by its IR bands at 2520 cm^{-1} ($\nu_1 + \nu_3$ CO_3^{2-} combination band), 1794, 1429 (CO_3^{2-} asymmetric stretching), 876 (CO_3^{2} out of plane bending), and 712 cm^{-1} (CO_3^{2} in plane bending) (Gadsden, 1975). In addition, the presence of an organic material with bands at *ca.* 2925, 2850, and 1742 cm^{-1} was observed but this compound could not be unambiguously identified only by FT-IR (Fig. 4.13).

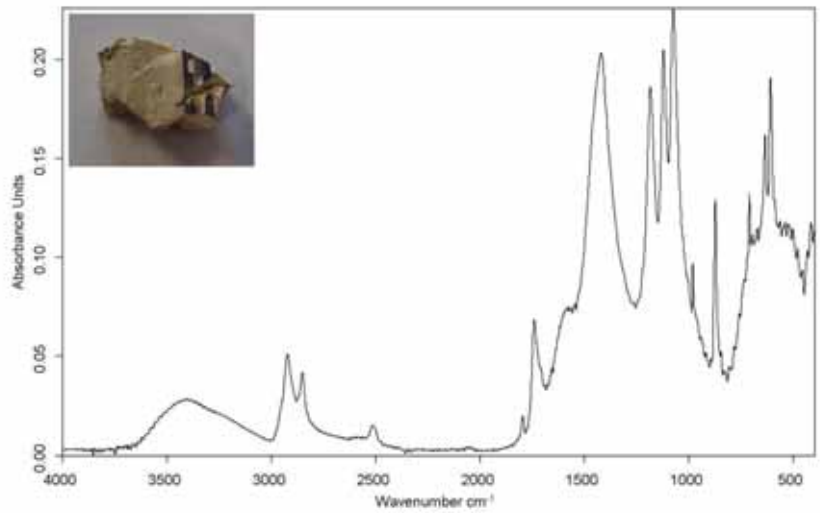

Fig. 4.13 – FT-IR spectrum of sample 3B

To further characterise this organic material, chloroform extracts from samples 1, 2, and 3A were analysed by ^{1}H-NMR using deuterochloroform ($CDCl_3$) as solvent. In all cases a drying oil was detected (Fig. 4.14 and Table 4.2). Due to the relatively low intensity of the NMR signals attributed to the protons in the residual double bonds (5.34 ppm) and in the methylene

groups in α position to the double bonds (2.02ppm), it can be stated that the drying oil was greatly aged.

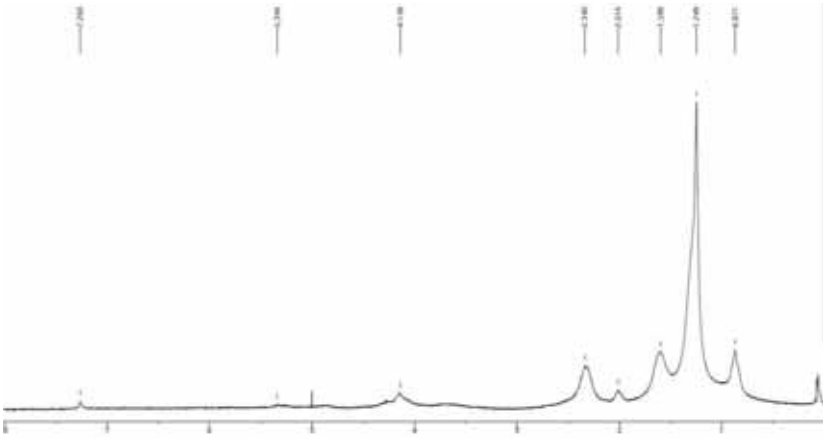

Fig. 4.14 - ^{1}H-NMR spectrum of sample 1

Table 4.2 - ^{1}H-NMR chemical shifts of the chloroform extracts in samples 1, 2, and 3A

Frequencies (ppm)	Attribution
5.33	CH of residual double bonds
4.15	CH_2 glyceric residue
2.34	CH_2 in α position to carbonyl
2.02	CH_2 in α position to double bonds
1.61	CH_2 in β position to carbonyl
1.25	CH_2 chain
0.87	CH_3 terminal

This result was also confirmed by the FT-IR analysis of the extracts. In the case of samples 1 and 2, the FT-IR spectra showed, besides the bands characteristic of glyceric esters (3000-2700 cm^{-1}, and at *ca.* 1734 cm^{-1}), the spectral features of the OH group (in the 3300 - 2500 cm^{-1} range) and C=O group stretchings of the free fatty acids from the hydrolysis of triglycerides (*ca.* 1717 cm^{-1})(Fig. 4.15).

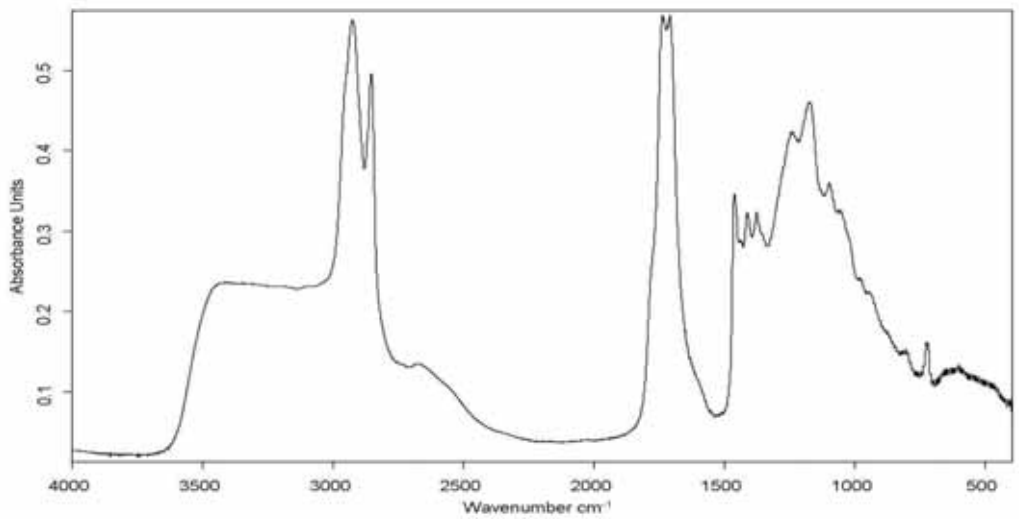

Fig. 4.15 – FT-IR spectrum of the $CHCl_3$ extract of sample 1 showing the presence of free fatty acids

In the sample 3A, any IR bands due to free fatty acids were detected but, in addition to the C=O stretching of the ester, an absorption in the 1650 – 1500 cm^{-1} range was present and due to the CO_2^- asymmetric stretching of carboxylic acid salts (Fig. 4.16). No significant changes were detected in the FT-IR spectra of the insoluble residues of the extractions.

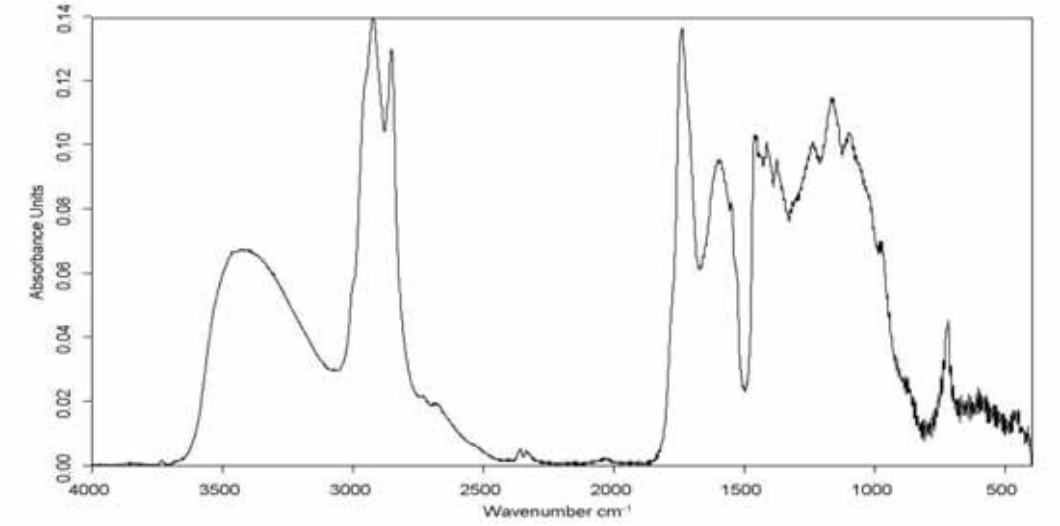

Fig. 4.16 – FT-IR spectrum of the $CHCl_3$ extract of sample 3A showing the presence of carboxylic acid salts

The black insoluble fraction of sample 1 showed a peculiar behaviour: it was attracted by a magnetic stirrer such as a ferromagnetic compound would. The FT-IR spectrum of this black powder was characterised by a very strong absorption band at 566 cm^{-1} attributable to the Fe-O stretching of the magnetite (FeO x Fe_2O_3, CI 77499/Pigment Black 11) (Gasden 1976). This result was confirmed by XRD analysis[4] (Fig. 4.17). Magnetite, indeed, is reported in the literature as a ferromagnetic mineral (Hunt *et al.*, 1995).

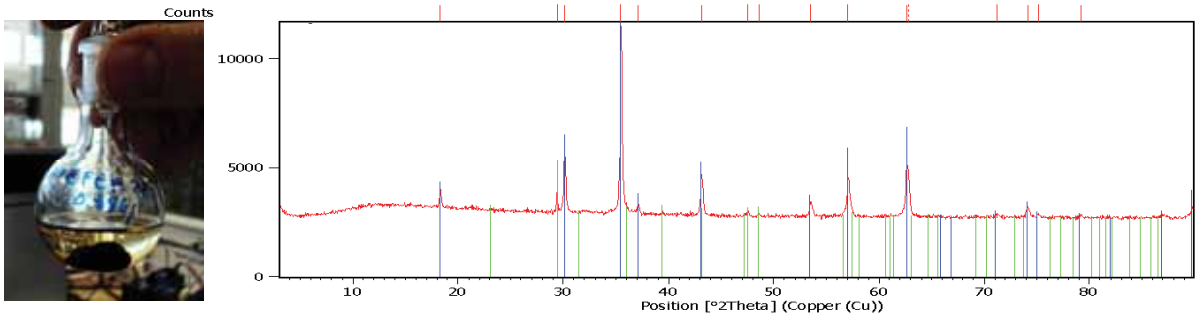

Fig. 4.17 – Black insoluble fraction of sample 1 (on the left) and its XRD powder diffractogram (on the right)

It was not possible identify the pigment responsible for the light yellow colour of samples 3A and 3B. It was assumed that the artist added to the white pigments a yellow colorant in extremely small quantities below the detection limits of the techniques used.

The presence of a silicate based sand, macroscopically visible over the entire upper end of the *Strip*, was confirmed by means of FT-IR spectroscopy. The IR spectrum acquired on sample 4 (Fig. 4.18) showed the spectral features of crystalline quartz (SiO_2), with absorption bands at

[4] XRD analysis was performed by Dr. Emma Cantisani of the Institute for the Conservation and Valorisation of Cultural Heritage (Department of Florence) of the National Research Council (ICVBC-CNR).

1164 and 1084 cm^{-1} (ν_3 Si-O asymmetric stretching), 795 and 777 cm^{-1} (ν_1 Si-O symmetric stretching), 695 cm^{-1} (ν_2 Si-O symmetric bending), 464 cm^{-1} (ν_4 Si-O asymmetric bending) (Saikia *et al*., 2008). The mineral kaolinite was also detected through its characteristic absorption bands at 3697 and 3620 cm^{-1} (OH stretching) and at 694 cm^{-1} (Si-O-Al stretching) (Gadsden, 1975).

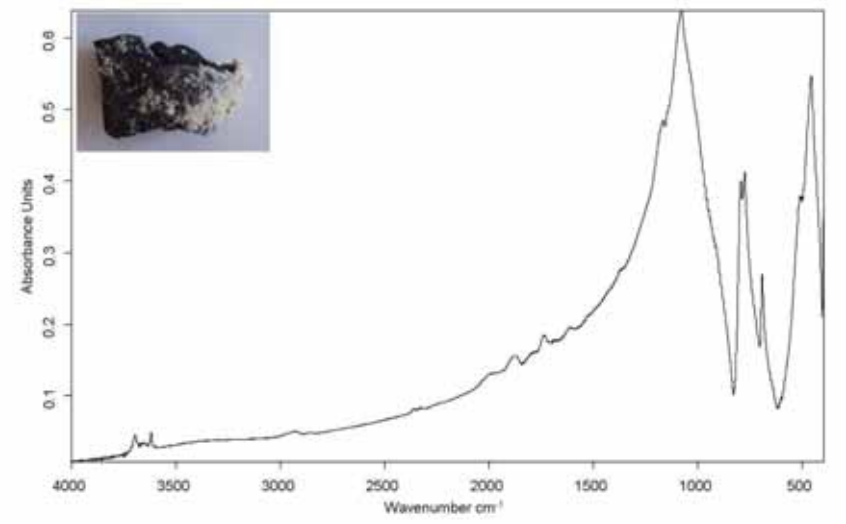

Fig. 4.18 – FT-IR spectrum of sample 4 showing the presence of quartz and kaolinite

Die Grosse Fracht

The photographic documentation of the surface of *Die Grosse Fracht* allowed the identification of areas made with different materials.

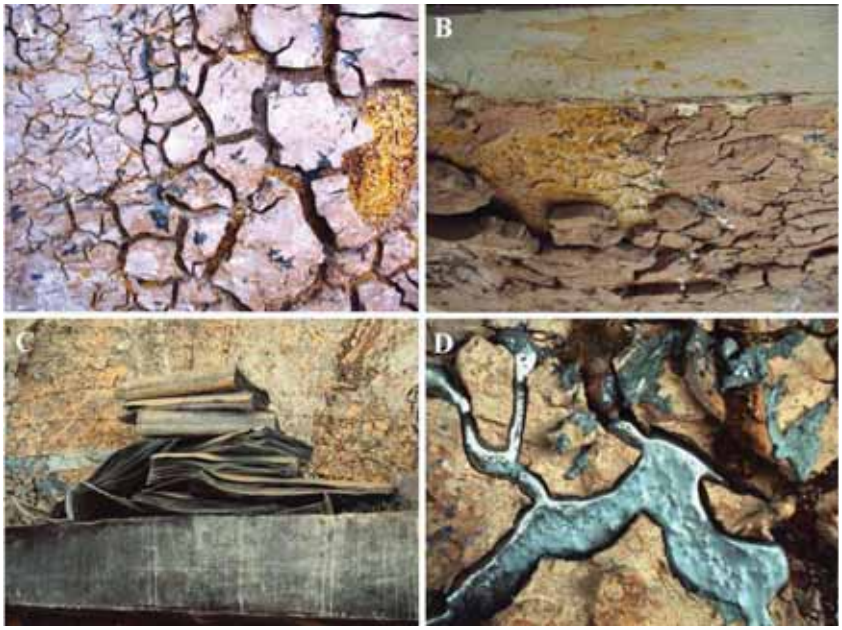

Fig. 4.19 - *Die Grosse Fracht*: cracks (A), resinous material (B), solid lead (C) melted lead (D)

The thick layer of materials, applied on a canvas support, presents itself as a cracked, flaky quality surface typical of some Kiefer's artworks and of his artistic technique (Fig. 4.19A). The craquelures, which appeared to be of various length, depth and width, are often filled

with a resinous material (Fig. 4.19B) or a metal. As reported in the literature, indeed, Kiefer employed in large quantity lead not only in the solid state (Fig. 4.19C) but also melted (Fig. 4.19D), (Albano, 1998; Calabrese and Corà, 2007). During the inspection performed on April 20, 2011 a lot of lacks and detachments of painting materials were noticed (Fig. 4.20).

Fig. 4.20 – Some particulars of *Die Grosse Fracht* showing lacks and detachments of the pictorial surface

Since it was not possible to mount a scaffold to closely study the artwork with non-invasive techniques, the study was focused only on the 4 samples collected during the conservative intervention (May 2011). Although the small number of samples, their analysis gave data that resulted very representative of the different painting materials constituting the artwork, as explained below.

Sample 5 had a brown colour, a glassy consistency, and a drop-like shape. This material is spread all over the surface of the artwork. In Figure 4.21 the FT-IR spectrum of sample 5 is reported. The main IR absorptions were due to the OH stretching of alcohols and carboxylic acids (3500-2500 cm^{-1}), the CH aliphatic stretching (2920 and 2850 cm^{-1}), and the C=O (1715 cm^{-1}) and C-O (1252 cm^{-1}) stretchings of carboxylic acids. These absorption bands are typical of shellac; as confirmed by the comparison with a reference spectrum from the IRUG2007 database (ref. INR00054).

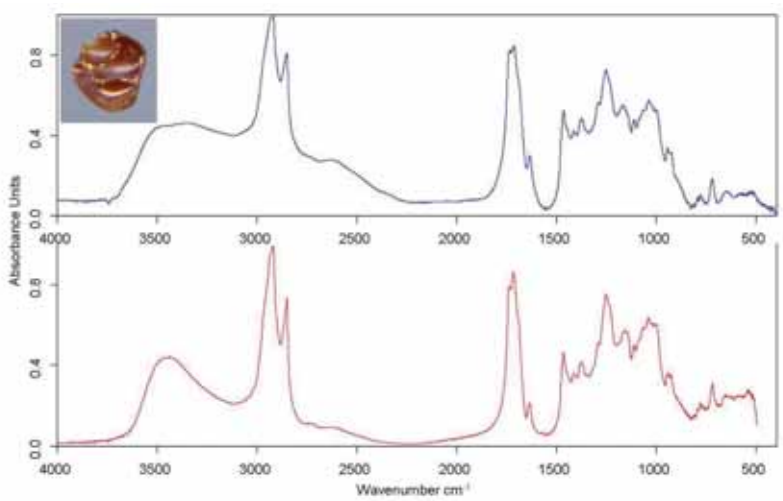

Fig. 4.21 – FT-IR spectrum of sample 5 (blue line) and reference spectrum of shellac from the IRUG2007 database (ref. INR00054, red line)

Sample 6 was removed from the thick paint layer which presented large cracks intentionally made by the artist. This layer is quite fragile, so the paint detached easily from the support. The FT-IR analysis of this sample revealed the spectral features of four inorganic compounds that are commonly present in clays, namely muscovite, kaolinite, quartz, and nitrates. However, in the analysed sample it was not possible to detect the presence of any organic materials. All the characteristic absorption bands of muscovite were observed in the IR spectrum (*ca.* 3625, 1076, 1025, 926, and 748 cm^{-1}) and they are in agreement with those reported in the reference spectra of the IRUG 2007 database (ref. IMP00112). Kaolinite was easily identified in this sample by its features at *ca.* 3695, 3620, 1100-900, 796, 748, 695, 468, and 432 cm^{-1}; these absorption bands were found to be consistent with those observed in the FT-IR spectrum recorded in a kaolinite sample provided by the Department of Mineralogy of the University of Pisa. In the spectrum of the sample 6 (Fig. 4.22) the peak at 1384 cm^{-1} could be attributed to the presence of nitrates, while there was any traces of the presence of organic materials (Fig. 4.22).

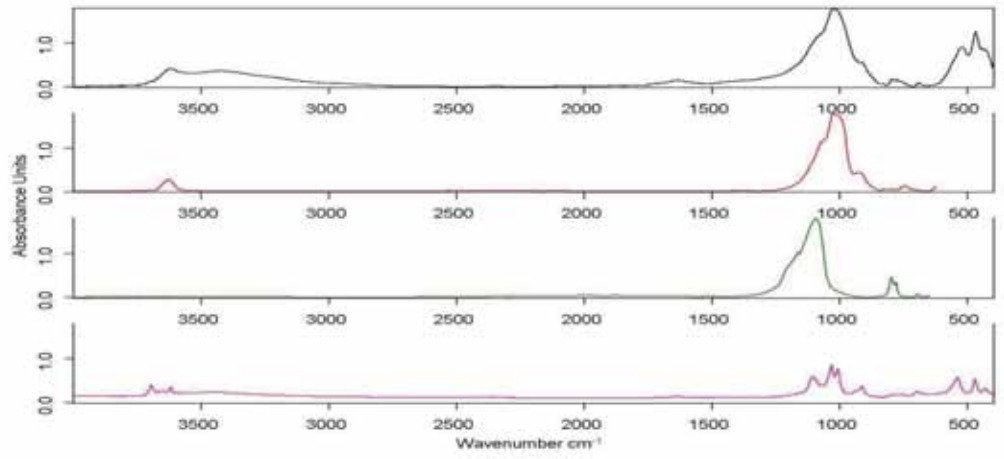

Fig. 4.22 - FTIR spectrum of sample 6 (blue line) and reference spectra of: muscovite (red line, IRUG2007 database ref. IMP00112), quartz (green line, IRUG 2007 database ref. IMP00322) and kaolinite (pink line, Departement of Mineralogy of the University of Pisa)

Even though the absorption bands expected for quartz were not visible in the sample 6 FT-IR spectra, its presence along with muscovite and probably kaolinite was observed in the XRD diffractogram (Fig. 4.23).

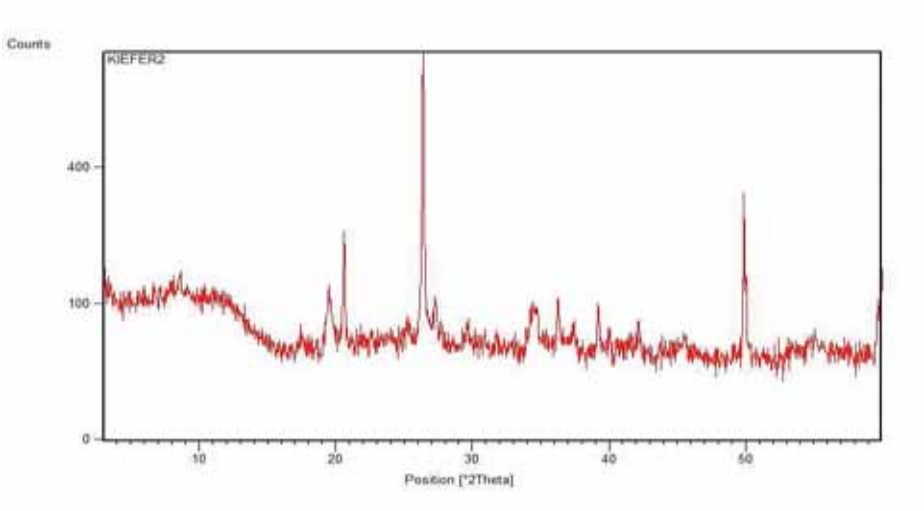

Fig. 4.23 – XRD diffractogram of sample 6

Sample 7 was constituted by a tacky material and was observed mainly in the paint cracks of the entire surface of the artwork. The FT-IR analysis of this sample suggested the presence of a synthetic resin composed of polyvinyl lacetate. The spectrum displayed, indeed, absorption bands at 2969, 2875 cm^{-1} due to aliphatic CH stretching and a rather broad feature due to the carbonyl at 1738 cm^{-1} (C=O stretching). In the fingerprint region two very distinct peaks at 1434 cm^{-1} and 1372 cm^{-1} (CH bending) were visible. In this region a very strong rounded peak centred at 1245 $cm^{-1}$was also present with a broad absorption band between 1120 and 1000 cm^{-1} with its maximum at about 1020 cm^{-1} (C-O stretching). The absorption bands at 947, 794 and 605 cm^{-1} (CH bending) were also visible (Derrick *et al.*, 1991; Learner, 2004). In the IR spectrum, two sharp absorption peaks at 1600 and 1580 cm^{-1}, characteristic of a phthalo group were also shown and their presence could be due to a plasticiser, such as diethylphthalate (Fig. 4.24). The obtained result was unequivocally confirmed by means of Py-GC/MS performed within the framework of the CoPAC Project at the SCIBEC laboratory of the University of Pisa (Colombini, 2012).

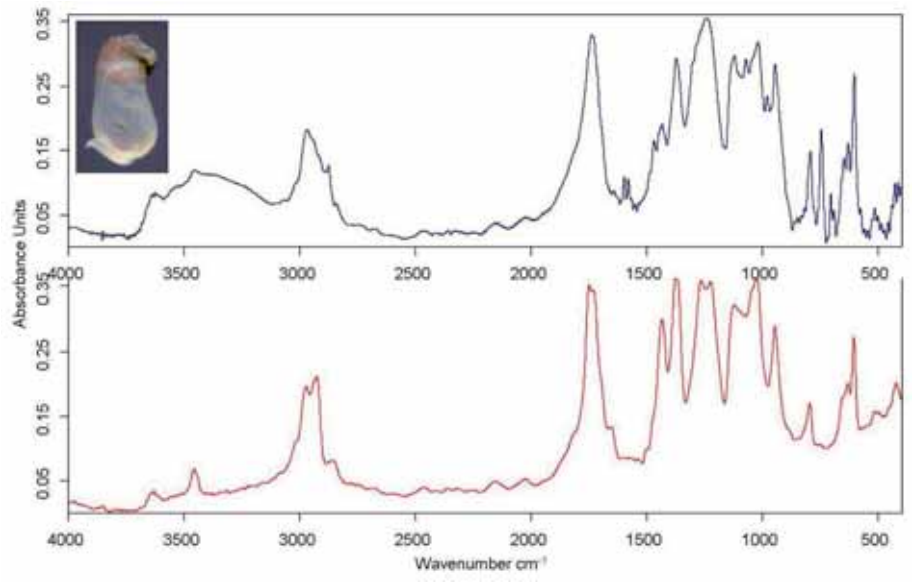

Fig. 4.24 – FT-IR spectrum of sample 7 (blue line) and reference spectrum of polyvinylacetate from the IRUG2007 database (ref. ISR00048, red line)

Fragment 8 was collected from the frame on the left edge of the artwork. FT-IR analysis revealed that its principal component was calcite. Absorption bands at 2980, 2830, and 1740 cm^{-1}due to an unidentified organic compound were also visible. The composition of this organic material was further investigated by GC/MS analysis at the SCIBEC laboratory of the University of Pisa. The chromatogram of the lipid and resinous fraction of the sample showed the presence of monocarboxylic and dicarboxylic acids. The high value of the A/P ratio, together with the amount of dicarboxylic acids detected, clearly demonstrated the siccative nature of the lipid material (probably linseed oil) (Colombini, 2012).

4.3 Conclusion

The combine used of non-invasive and micro-invasive analytical techniques made it possible to firmly identify most of the materials used by the contemporary artist Anselm Kiefer in two of his works: a large *Strip* cut by the artist himself from a polymateric artwork on canvas, and the *Die Grosse Fracht* exhibited at the San Giorgio Library (Pistoia, Italy). The detected materials are reported in Table 4.3.

The *Strip* consists of a mixture of calcite, siccative oil and pigments of various nature: white pigments in common use in the 20th century, such as titanium white (TiO_2 in the rutile crystalline form) and lithopone ($ZnS + BaSO_4$), and the dark pigment magnetite ($FeO \times Fe_2O_3$), less frequently used and encountered as artists' material. Other original materials such as silica sand and metal staples were also observed. Shellac, applied as a coating, was detected in many areas of the surface both of the *Strip* and of *Die Grosse Fracht*, where it is present also in the form of brown drops. Different areas of *Die Grosse Fracht* are formed with various mixtures such as calcite and siccative oil, or clay blocks glued to the support with a

polyvinyl acetate adhesive. The apparent absence of binder media in the clay layers, the use of a hot-melt adhesive, and the fact that the work is exposed on the south wall (with wide daily and seasonal fluctuations in temperature and relative humidity) partly explain its fragility which caused the detachments of fragments, despite its recent creation.

Table 4.3 – List of materials detected in each sample

Sample	Detected materials	Main FTIR absorption bands (cm^{-1})	UV-Vis-NIR absorption maxima (nm)[a]
1*	Calcite	2520, 1794, 1429, 876, 712	/
	Magnetite	566	/
	Titanium dioxide (rutile)	600, 523	$\lambda < 400$ (ip)
	Siccative oil	3300 – 2500, 3000-2700, 1734, 1717	
2*	Calcite	2520, 1794, 1429, 876, 712	/
	Titanium dioxide (rutile)	600, 523	$\lambda < 400$ (ip)
	Siccative oil	3300 – 2500, 3000-2700, 1734, 1717	
3A*°	Lithopone	/	ZnS: λ <340, 670, 728
	Calcite	2520, 1794, 1429, 876, 712	
	Siccative oil	1717, 1650-1500	
3B*	Titanium dioxide (rutile)	600, 523	$\lambda < 400$ (ip)
	Lithopone	$BaSO_4$: 1187, 1124, 1077, 982, 637 611	ZnS: λ <340 (ip), 670, 728
	Calcite	2520, 1794, 1429, 876, 712	/
4*	Sand (quartz),	1164,1084, 795, 777, 695, 464	/
	Kaolinite	3697, 3620, 694	/
5**	Shellac	3500-2500, 2920, 2850, 1715, 1252	/
6**	Clay	Muscovite: 3625, 1076, 1025, 926, 748 Kaolinite: 3695, 3620, 1100-900, 796, 748, 695, 468, 432 Nitrates: 1384	/
7**	Polyviny lacetate	2969, 2875, 1738, 1434,1372,1245, 1020, 947, 794, 605	/
8**	Calcite	2520, 1794, 1429, 876, 712	/
	Siccative oil	980, 2830, 1740	/

[a]sh(sharp), br (broad), m (medium), s (strong), w (weak), sd (shoulder), ip (inflection point)
* Sample from the *Strip*
**Sample from *Die Grosse Fracht*

The obtained data highlight the originality and diversity of the materials used by Anselm Kiefer in his artistic production.

This research provides a starting point for understanding the techniques and materials used by the artist in his works, especially in view of assessing future conservation and/or restoration interventions.

CHAPTER 5 – FERNANDO MELANI

5.1 Fernando Melani

5.1-1 Short biography

Fernando Melani (Fig. 5.1) was born on 25 March 1907 in S. Piero Agliana (Pistoia, Italy). The second of two children, Melani was still a boy when his parents separated, thus he spent his adolescence with his grandmother and an unmarried aunt in the family home, in the building where his Studio-Home is still located (Corà, 1990; §5.1-2).

Fig. 5.1 – Fernando Melani in his studio-home
[Image from: http://www.chiavaccifotografo.it/CCF2009/Melani.html#20, last access:October 18, 2013]

After leaving high school, he turned to sports, particularly tennis which he played at a semi-professional level (Ranaldi *et al*., 2009). The war forced him to leave home, to which he returned at the end of the evacuation period to the countryside around Pistoia, and it was here that he began his activity as a painter. His approach to art was unusual from the very beginning, since it was based on his interest in scientific knowledge.

Today, Fernando Melani is considered one of the precursors of what has become known as the "Poor Art" movement. He did not consider his objects to be finished artworks in themselves. Instead, he called them ''experiences'' (Melani, 1971), which he himself numbered consecutively. The main goal of these ''work-in-progress' artworks was a pure form of abstraction. Melani painted on stretched and un-stretched canvas, on different kinds of paper, and on the slatted covers of wooden crates. He also used wood, little squares of metal joined by welding to create three-dimensional sculptures, and thin wire looped into springy spirals or welded onto delicate structures that resemble molecular models (Celant, 2011).

His artistic activity has been documented by a series of events including many exhibitions and publications. Among these, in 1954 he held his first solo exhibition, which marked the beginning of his abstract exhibition activity, at the "Galleria Numero"(Florence). In the same period, in defence of Abstractism, he published at his own expense a pamphlet *Davanti alla pittura* (In front of painting), the first in a long series of contributions that appeared in catalogues and other publications (for a full report on the subject, see Corà, 1990).

Starting from 1959 he studied the potential of metals (*FM 1557*), in an attempt to capture the secret resonances of matter, according to suggestions taken from the field of modern physics. He produced works consisting of aluminium foil, iron plate (*FM 1986*) and nails (*Error*), and copper wires (Fig. 5.2).

Fig. 5.2 – Aluminium foil applied on the door of the attic of Melani's Studio-Home (image acquired on April 20, 2011)

In 1960 Melani published *Un'analisi critica di Fernando Melani, Quadri di John Forrester* (A critical analysis by Fernando Melani, Paintings by John Forrester) as evidence of his opening to the figurative productions of his times (Giuntoli, 2010).

In 1972 he held a one-man exhibition in Milan at the "Gallery Borgogna" (where he exhibited also in 1976 and 1979). In 1976 he created and exhibited in various locations (Pistoia, Milan, Vinci) the *Progetto di Lettura Globale* (Project for a Global Reading), an installation made up of 31 monochromes of different colours made from unusual materials (emery, carborundum, etc.). Meanwhile, his artistic path took a more conceptual way, which led him, in 1978 , to put on display, at the "La Torre" studio (in Pistoia), everyday items, such as the *Sacco di fiammiferi spenti* (Sack of used matches). At the end of the 1970s, he used repainted and assembled bicycle frames to create strange sculptures.

On 28 March 1985 Fernando Melani died unexpectedly in his Studio-Home in Pistoia. Many posthumous exhibitions were organised after his death, including the anthological ones in Pistoia (1990) and in New York (1991) (Giuntoli 2004).

5.1-2 The Studio-Home

Fernando Melani's Studio-Home represents an original and unique space that harmoniously reflects the artist's creative experiences. It is an ideal environment in which visitors can immerse themselves in his research and follow his career, which reflected the major art movements of the second half of the 20th century, including Conceptual and Minimalist Art (Corà, 1990; Giuntoli, 2010).

The Studio-Home is located at Corso Gramsci 159 in Pistoia (Fig. 5.3). Since 1987 the house has belonged to the City of Pistoia, but it has not been modified in any way. Nor have erroneous restorations been carried out since the artist's death. Indeed, the Studio-Home has brought together all of his artworks, providing an ideal and definitive location for them.

Fig. 5.3 – Melani's Studio-Home at number 159 Corso Gramsci in Pistoia (images acquired on April 20, 2011)

After the war, Melani continued to live, think and work in his home until he died, in 1985. Up to the early Seventies, he used only the attic, where he began to collect his works in particular those made of metal (Fig. 5.4A). Over time, each work found its own place in the rooms of the house: for example, *I giornali sulla scala* (Newspaper on the stair) are a collection of daily newspapers piled up on the steps along the wall of the stairs (Fig. 5.4B). In the Eighties, the artworks descended to occupy the entre first floor, where the sofa in the living room was the only furniture. Here, works related to the Seventies prevail, while the adjacent "library" has been occupied, since 1980-81, by *Bucati* (Laundry) in which variously-shaped, monochromatically-painted scraps of canvas are hung from three laundry lines strung from wall to wall across the room, (Fig. 5.4C) (Giuntoli, 2004).

The artworks occupy both the walls and the floors, arranged within the environment with extreme simplicity. The presence of such a large amount of works attenuates the value of each object by giving precedence to their relationship with the whole background.

Fig. 5.4 - Fernando Melani's Studio-Home: sculpture created from assembled bycicle frames (A), *I giornali sulla scala* (Newspaper on the stair) (B), *Bucati* (Laundry) (C) (images acquired on April 20, 2011)

Between 1987 and 1990, Fernando Melani's Studio-Home was the subject of a renovation project designed by the architect Alessandro Andreini in order to allow its safety for the public (Rinaldi et al., 2009). In August 2005, Donatella Giuntoli left, in her final will, a bequest to the City of Pistoia that consisted of artworks by Melani that she had collected during the course of her life. Thus, one hundred and forty works integrated the "experiences" already present in the experimental laboratory that was Fernando Melani's Studio-Home.

5.2 Study of the pictorial palette

5.2-1 Pigments/Dyes

During a site inspection of Fernando Melani's Studio-Home (on 20 April 2011), a box containing fifteen pigments/dyes (stored in jars or bags) was found in the attic (Fig. 5.5). These consisted of eight yellow (FM1–FM7, FM14), two red (FM8 and FM9), two green (FM10 and FM11), two blue (FM12 and FM13), and one dark-coloured (FM15) materials.

A few grams of each powder were sampled and then analysed by means of FT-IR and UV-Vis-NIR-FORS spectroscopies. In some cases, XRD and NMR spectroscopies were also used to substantiate the results obtained.

Fig. 5.5 – The box containing the fifteen pigments/dyes found in the attic of Melani's Studio-Home (image acquired on 20 April 2011)

5.2-2 Experimental

FT-IR

The IR spectra of the samples were recorded in transmission mode (13-mm diameter KBr pellet technique, 64 scans, 4 cm^{-1} resolution, 4000–400 cm^{-1} range), using a *Nicolet Protégé™ 460 E.S.P.™* spectrophotometer equipped with a SiC Globar source and a DTGS detector. All spectra were processed using OMNIC 7.3.94 software.

For some of the powders consisting of organic materials (samples FM3, FM8, FM10 and FM11), the presence of inorganic fillers, such as calcite ($CaCO_3$) and barite ($BaSO_4$), partially masked the absorption bands of the dyes. Thus, to avoid any problems in interpreting these data, it was decided to investigate also the part of the material extracted with acetone (1 ml), as reported in Fig. 5.6. A few drops of the extracted materials were deposited on a KBr pellet and analysed by means of a *Perkin Elmer System 2000* spectrophotometer (128 scans, 2 cm^{-1} resolution, 4000–400 cm^{-1} range).

Fig. 5.6 - Solutions of sample FM3, FM8, FM10 and FM11 after extraction with acetone

FORS

FORS measurements in the UV-Vis-NIR spectral range (350–2200 nm) were performed using two single-beam *Zeiss* spectroanalysers, model *MC601* (190-1015 nm range) and model *MC611 NIR 2.2WR* (910-2200 nm range), housed together in a compact and portable *chassis* for *in situ* analyses. The data acquisition step was 0.8 nm/ pixel for the 1024-element silicon photodiode array detector (*MCS601*), and 6.0 nm/pixel for the 256-element InGaAs diode array detector (*MCS611 NIR 2.2 WR*). The radiation between 320 nm and 2700 nm, which was provided by a voltage-stabilized 20W halogen lamp (Model CLH600), was conveyed to the sample by means of a quartz optical fibre bundle that also transported the reflected radiation to the detectors. The geometry of the probe head was 8°/8°. Calibration was performed by means of a 99% Spectralon® diffuse reflectance standard. Five spectra were acquired for each sample, and were then processed using Aspect Plus® 1.80 software.

XRD[1]

Samples FM8 and FM15 were investigated by means of X-Ray Diffraction (XRD) using two different instruments:

- a *PanAnalytical X'Pert Pro X-Ray diffractometer* (40 kV, 30 mA) with Cu K radiation (λ =1,545 Å), for the analysis of sample FM8;
- a *Philips X-Ray diffractometer 1979* (40 kV, 24 mA) with Cu K radiation (λ = 1.5406 Å), for the analysis of sample FM15.

NMR[2]

The FM12 sample was analysed by means of ^{1}H and ^{13}C Nuclear Magnetic Resonance (^{1}H-NMR, ^{13}C-NMR). The powder was dissolved in deuterochloroform ($CDCl_3$) and then analysed with a *Varian VXR 200* spectrometer operating at a frequency of 199.985 MHz. The spectra were processed using the software iNMR 3.3.7.

[1] XRD analysis was performed by Dr. Emma Cantisani of the Institute for the Conservation and Valorisation of Cultural Heritage (Department of Florence) of the National Research Council (ICVBC-CNR).
[2] The NMR analysis was performed in the scientific laboratories of the "Ugo Schiff" Department of Chemistry of the University of Florence under the supervision of Prof. Antonella Salvini and Prof. Donatella Giomi.

5.2-3 Results and discussion

Yellow samples

The analysis of the eight yellow powders (Fig. 5.7) showed that Melani used both organic dyes (FM1–FM3) and inorganic pigments (FM4–FM7 and FM14) in the creation of his artworks.

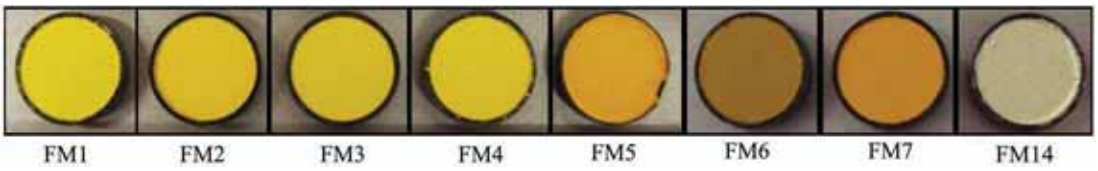

Fig. 5.7 – Yellow powder samples

Spectral analysis demonstrated that the organic dyes belong to the class of Hansa Yellows, synthetic organic monoazo dyes which have a chemical structure characterised by the presence of the azo group (N=N) as chromophore. In particular, sample FM1 consisted of an arylamide yellow (PY3) while FM2 and FM3 were identified as an arylide yellow (PY1).

As reported in Figure 5.8, PY1 and PY3 differed only in the substituent positioned in R2 and R4 places. In PY1, R2 and R4 are, respectively, a methyl group and hydrogen, while in PY3 they are both chloro-atoms (Lake and Lomax, 2007).

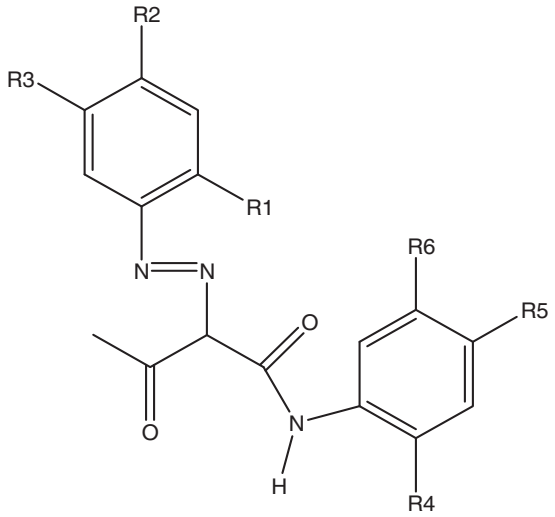

Fig. 5.8 - Chemical structure of arylide yellows,
where R1=NO_2, R2=CH_3(PY1)/Cl(PY3), R3=H, R4=H(PY1)/Cl(PY3), R5=H, R6=H (Lake e Lomax, 2007)

The FT-IR spectra of FM1 (Fig. 5.9) and FM2 (Fig. 5.10) were in perfect agreement with the spectra reported in the IRUG 2007 database for PY3 (ref. IOD00487) and PY1 (ref. IOD00441), respectively. The spectra of the two samples were characterised by a single carbonyl absorption in the 1666–1674 cm^{-1} region, and by a strong absorbance around 1500 cm^{-1} due to the presence of the nitro group. In addition, the FT-IR spectrum of the FM1 powder showed an absorption band at 1036 cm^{-1} that was due to the chloro-carbon bond (Lake and Lomax, 2007).

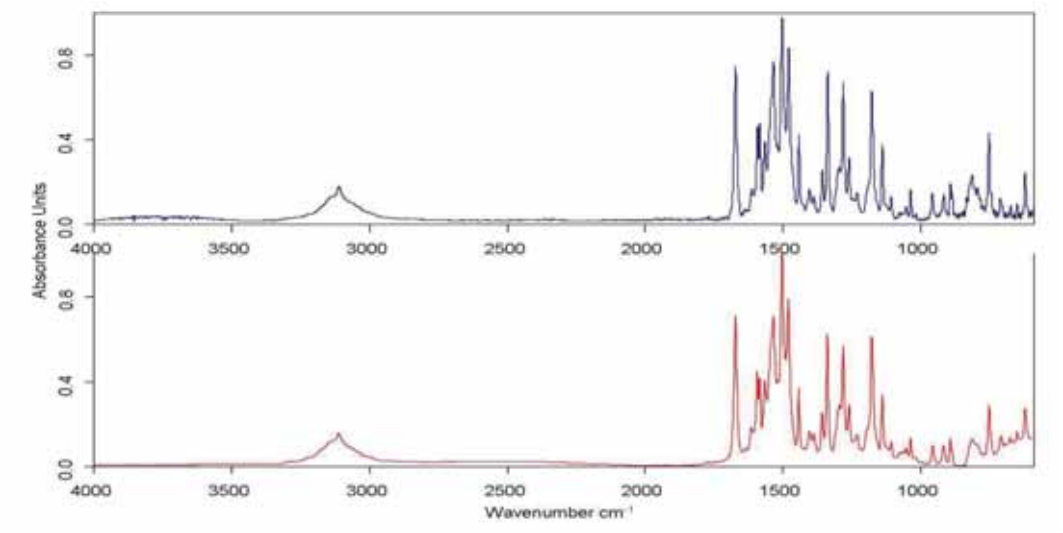

Fig. 5.9 - FT-IR spectrum of FM1 sample (blue line) and reference spectrum of PY3 from IRUG database (ref. IOD00487, red line)

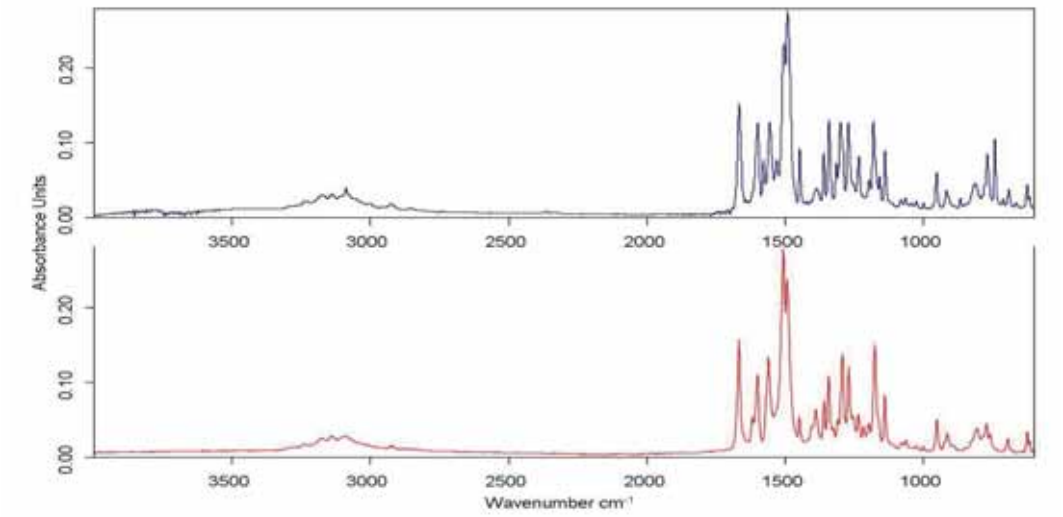

Fig. 5.10 - FT-IR spectra of FM2 sample (blue line) and PY1 reference from IRUG 2007 database (ref. IOD00441, red line)

The FT-IR spectrum of the FM3 sample (Fig. 5.11) showed the presence of two inorganic compounds, i.e. calcite (combination of CO_3^{2-} symmetric and asymmetric stretching at 2512 cm^{-1}; CO_3^{2-} asymmetric stretching at 1424 cm^{-1}; CO_3^{2-} out of plane bending at 875 cm^{-1}; and CO_3^{2-} in plane bending at 712 cm^{-1}) and barite (SO_4^{2-} asymmetric stretching at 1176, 1123 and 1081; SO_4^{2-} in plane bending at 635 and 610 cm^{-1})(van der Marel and Beutelspacher, 1976; Nakamoto, 1978; Feller, 1986).

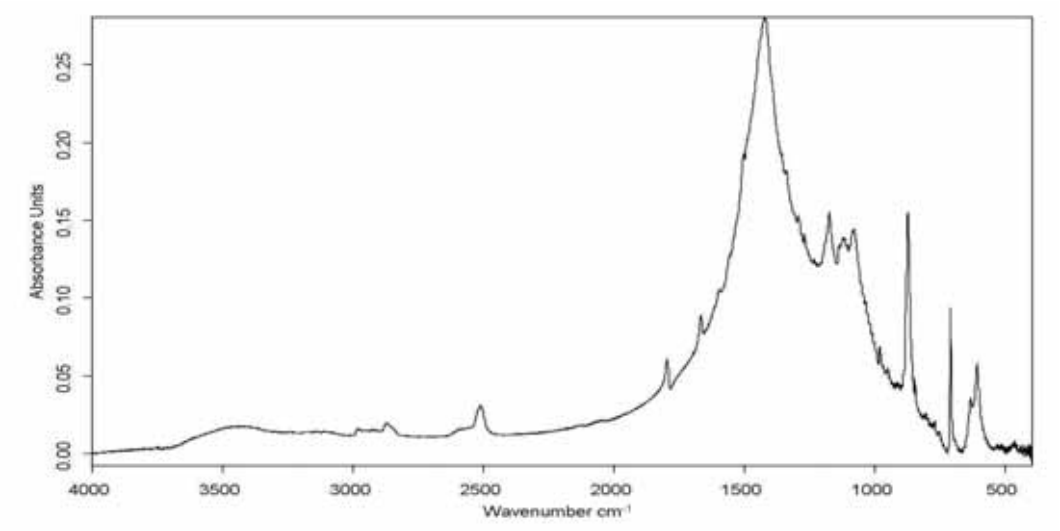

Fig. 5.11 - FT-IR spectrum of FM3 powder sample

The presence of the intense bands due to calcite and barite made it impossible to identify the compound responsible for the yellow colour. Thus, the sample was subjected to an extraction with 1 mL of acetone, and the solution obtained was analysed using FT-IR spectroscopy. The FM3 extracted solution showed the same spectral features as the FM2 sample, thus confirming the presence of PY1 (Fig. 5.12).

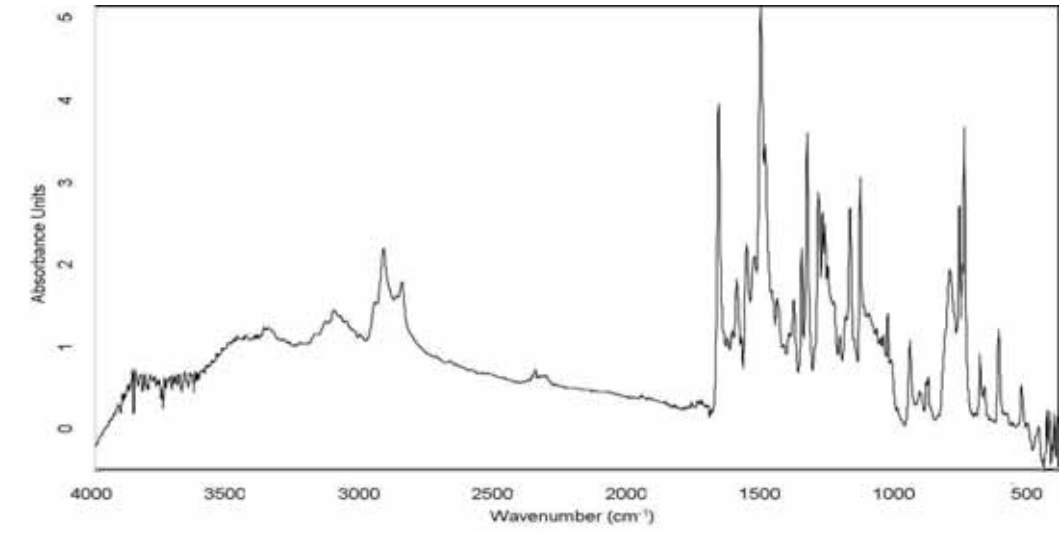

Fig. 5.12- FT-IR spectrum of FM3 extracted solution

The FORS spectra of these three samples (Fig. 5.13) showed an intense absorption band in the UV–Vis region due to a n(azo) → π* transition (Robin and Simpson, 1962).

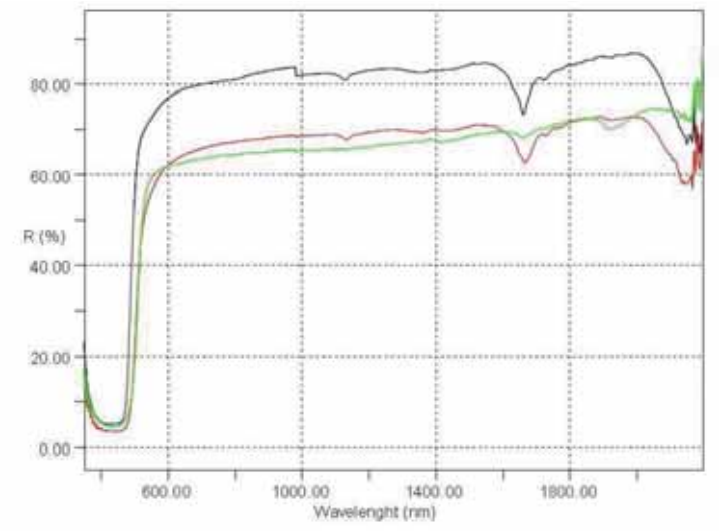

Fig. 5.13 - FORS spectra of FM1 (black line), FM2 (red line), FM3 (green line) samples

The hues of the two dyes (PY1 and PY3) were influenced by their different substituents in the R2 and R4 positions. This difference was emphasised by the inflection points (identified by calculating the first derivative of FM1 and FM2/FM3 spectra, Fig. 5.14), which were placed at 486 nm and at 504 nm, respectively. Indeed, the chloro substituent (an electron donator) produced a hypsochromic green shift in the hue (as for FM1), while a methyl group (an electron acceptor) produced a bathochromic red shift (as for FM2–FM3) in the position of the inflection point of the spectral shape (Christie *et al.*, 1988; Lake and Lomax, 2007).

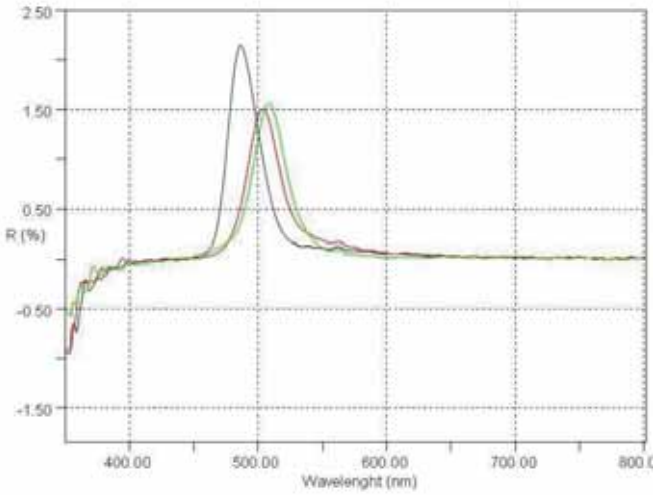

Fig. 5.14 - First derivative spectra of FM1 (green line), FM2 (red line), FM3 (yellow line) samples

In addition, the spectral features in the 850–2200 nm region could be tentatively attributed to ν(C=O) or ν(C=C) overtones (2150 nm), ν(C-H) overtones at 1662 nm, and ν(C-H) 2nd overtones at 1130 nm (Bacci, 2000). In the FM3 reflectance spectrum of the NIR absorption band at around 1100 nm was absent, while the two bands at 1662 nm and 2150 nm were less intense than those of the FM1 and FM2 samples. The broad band at 1930 nm in the FM3

powder was attributed to vibrational combinations of the ν(O-H) and δ(H-O-H) fundamental bands, which in turn were due to absorbed water molecules in the sample (Bacci, 2000).

As regards the five inorganic yellow powders, the FM6 sample was identified as Mars yellow, a hydrated iron oxide pigment (PY42). In fact, in the FT-IR spectrum, only absorption bands characteristic of goethite, α-FeOOH, were evident (Fig. 5.15). The absorption band at 3132 cm^{-1} and the doublet at 904 and 796 cm^{-1} were attributable to OH stretching and OH bending, respectively, while the two peaks centred at 613 and 463 cm^{-1} were due to asymmetric Fe-O stretching (Afremow and Vanderberg, 1966; Schwertmann *et al.*, 1985; Cambier, 1986).

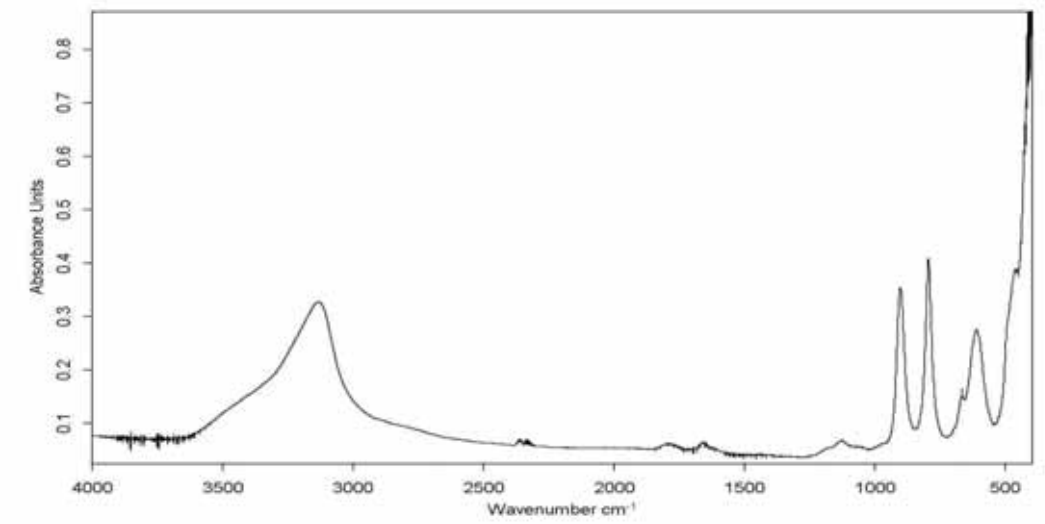

Fig. 5.15 - FT-IR spectrum of FM6 sample

The FORS spectrum (Fig. 5.16) was again in agreement with the occurrence of goethite being due to the presence of charge transfer transitions absorption bands at 400 and 480 nm, as well as those at about 649 and 917 nm, which were due to ligand field transitions (Sherman and Waite, 1985; Cornell and Schwertmann, 1996).

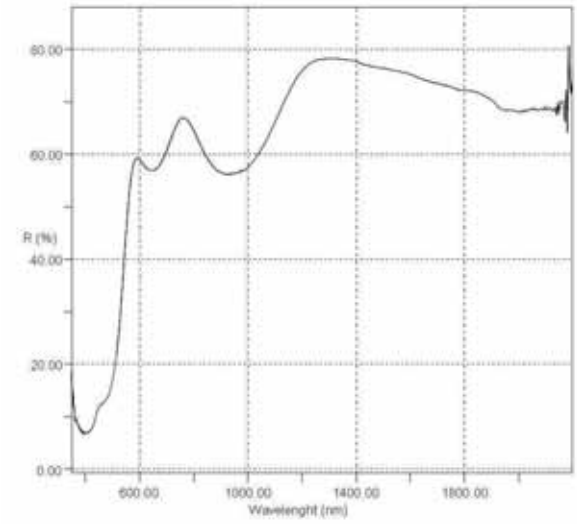

Fig. 5.16 - FORS spectrum of FM6 sample

FM4, FM5, and FM7 were mainly composed of lead chromate ($PbCrO_4$) mixed with different amounts of lead sulphate ($PbSO_4$). In this case, the FT-IR spectrum of each powder (Fig.

5.17) showed the characteristic absorption bands of lead chromate (Cr-O asymmetric and symmetric stretching at 870 cm^{-1} with a shoulder at 833 cm^{-1}) and of lead sulphate (SO_4^{2-} asymmetric stretching at 1180, 1103 and 1060 cm^{-1}; SO_4^{2-} in plane bending 628 and 600 cm^{-1}) (Gadsden, 1975; Kühn and Curran, 1986). The presence of nitrates (1384 cm^{-1}) in these spectra was most probably due to the process used to synthesise the chrome yellow pigment (Kühn and Curran, 1986).

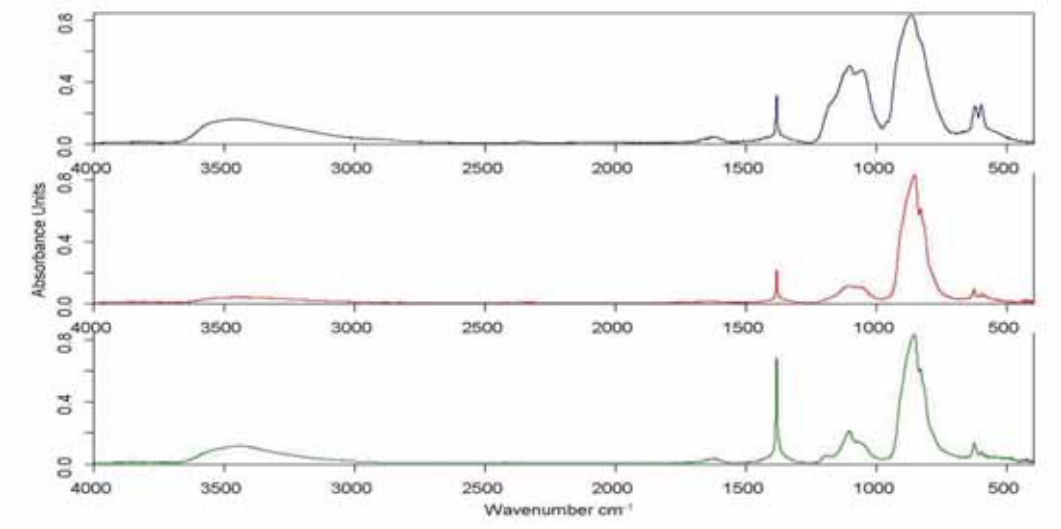

Fig. 5.17 - FT-IR spectra of FM4 (blue line), FM5 (red line), FM7 (green line) samples

Furthermore, the FORS spectra of the FM4, FM5, and FM7 samples (Fig. 5.18) showed the typical "S"-shape spectral feature with a strong absorption in the UV-blue region of the lead chromate based pigments (Bacci, 2000).

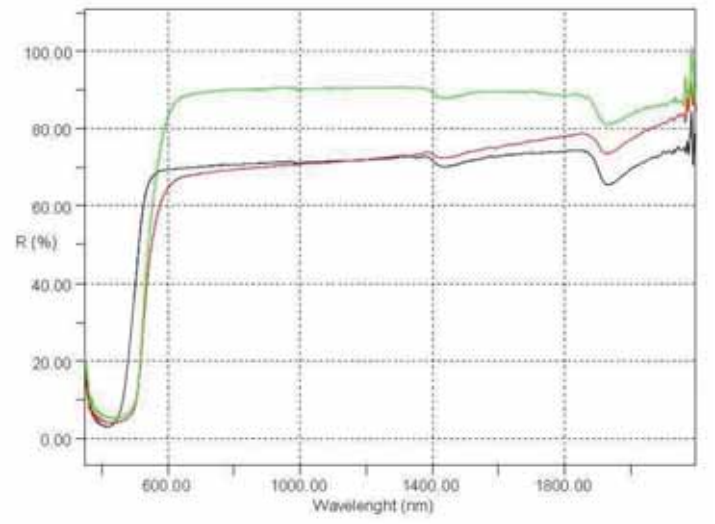

Fig. 5.18 - FORS spectra of FM4 (black line), FM5 (red line), FM7 (green line) samples

The inflection points of these spectra were found by calculating the first derivative of the reflectance spectra of the FM4 and FM5/FM7 samples (Fig. 5.19), which were positioned at 500 nm (2.47 eV) and at 528 nm (2.35 eV), respectively.

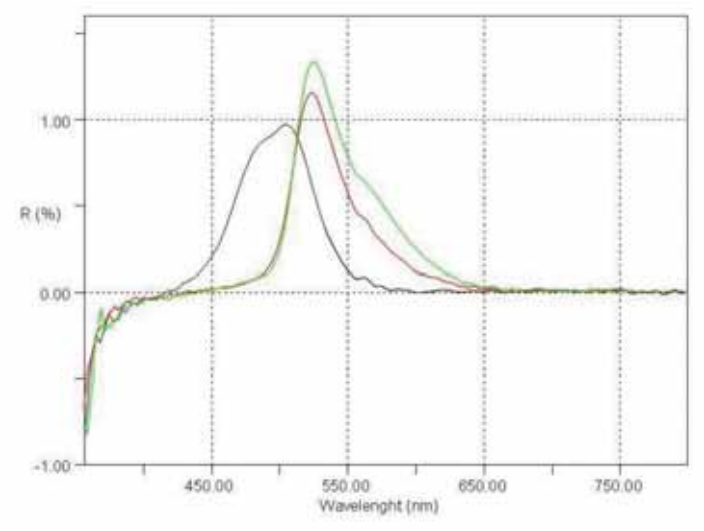

Fig. 5.19 - First derivative spectra of FM4 (green line), FM5 (red line), FM7 (yellow line) samples

Lastly, the final yellow sample (FM14) was identified as monoclinic sulphur. Its FT-IR spectrum exhibited only a weak absorption band 470 cm^{-1}. At first glance, the hypothesis of the presence of sulphur among Melani's materials was suggested by the pale yellow hue of the FM14 powder and, furthermore, by what the artist himself reported with regard to some of the artworks he created in the 1970s (Corà, 1990; Giuntoli, 2010). To be sure that the powder found in his attic was pure monoclinic sulphur, a sample of monoclinic sulphur (bi-sublimate, purity 99.99% by Aldrich) was analysed using the FT-IR (Fig. 5.20) and FORS techniques (Fig. 5.21).

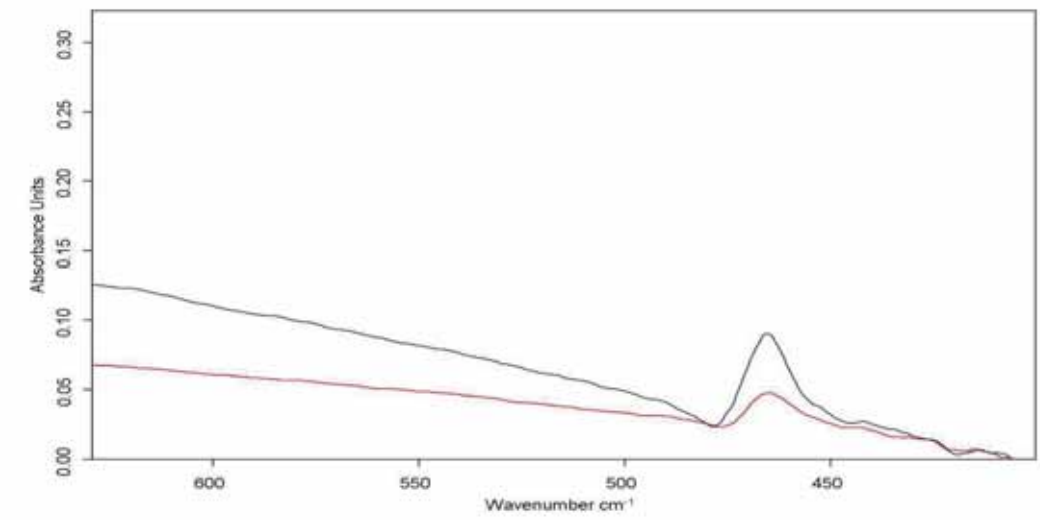

Fig. 5.20 - FT-IR spectra of the FM14 sample (blue line) and of a monoclinic bi-sublimate sulphur (purity 99.99% by Aldrich; red line) in the 650-400 cm^{-1} spectral range

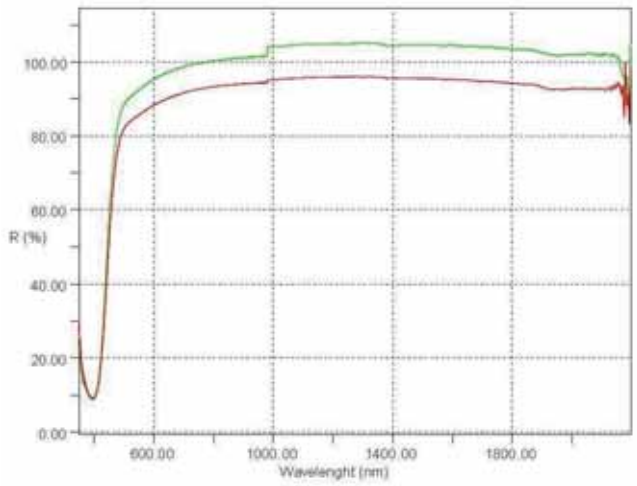

Fig. 5.21 - FORS spectra of the FM14 sample (green line) and of a monoclinic bi-sublimate sulphur (purity 99.99% by Aldrich; red line)

The spectra acquired with both techniques were in total agreement with those collected on the FM14 sample. A further confirmation of the presence of monoclinic sulphur was acquired by means of the 'mixed melting point' test. A mixture of 50% FM14 and 50% bi-sublimate 99.99%-pure sulphur showed a melting point (119–120 °C) that was not depressed when compared with that of the pure components of the mixture. In addition, this melting point confirmed that this particular sulphur was in monoclinic form, just as reported in the literature (McQuarrie *et al.*, 1991).

Red samples

The two red powders are shown in Figure 5.22.

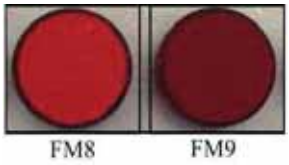

Fig. 5.22 – Red powder samples

The FM8 sample was identified as a mixture of an organic dye and an inorganic pigment.

FT-IR spectrum of the FM8 powder (Fig. 5.23) presented only the absorption bands of calcite (2511 cm^{-1}, combination of CO_3^{2-} symmetric and asymmetric stretching; 1423 cm^{-1}, CO_3^{2-} asymmetric stretching; 875 cm^{-1}, CO_3^{2-} out of plane bending, and 712 cm^{-1}, CO_3^{2-} in plane bending) and barite (1188 cm^{-1}, 1117 cm^{-1} and 1085 cm^{-1}, SO_4^{2-} asymmetric stretching; 712 cm^{-1} and 611 cm^{-1}, SO_4^{2-} in plane bending)(van der Marel and Beutelspacher, 1976; Nakamoto, 1978; Feller, 1986).

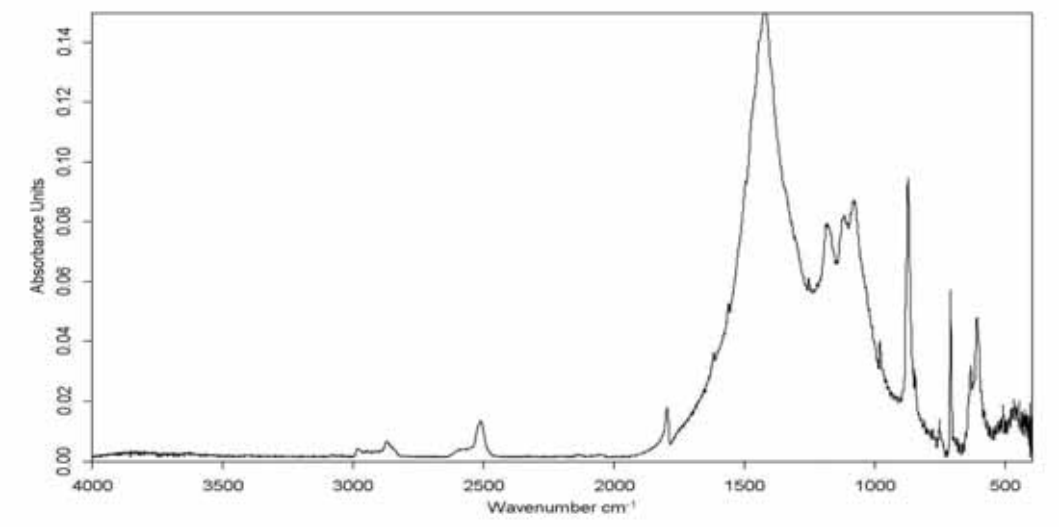

Fig. 5.23 - FT-IR spectrum of FM8 powder sample

Owing to the presence of the intense bands of calcite and barite, it was not possible to identify the compound responsible for the red colour. Thus, the sample was subjected to an extraction with 1 mL of acetone, and the solution obtained was then analysed using FT-IR spectroscopy. The main absorption bands found in the FT-IR spectrum of the extracted part (Fig. 5.24) were at 3150-3000 cm^{-1} (NH, OH and aromatic CH stretchings), 2920 cm^{-1} (aliphatic CH asymmetric stretching), 2820 cm^{-1} (aliphatic CH symmetric stretching), 1600 cm^{-1} (C=C stretching), 1505 cm^{-1} (NO_2 asymmetric stretching) and 1346 cm^{-1} (NO_2 symmetric stretching) (Socrates, 1998). These spectral features are typical of toluidine red (PR3), a synthetic organic dye, as resulted also from a comparison with the IRUG2007 database (ref. IOD00466).

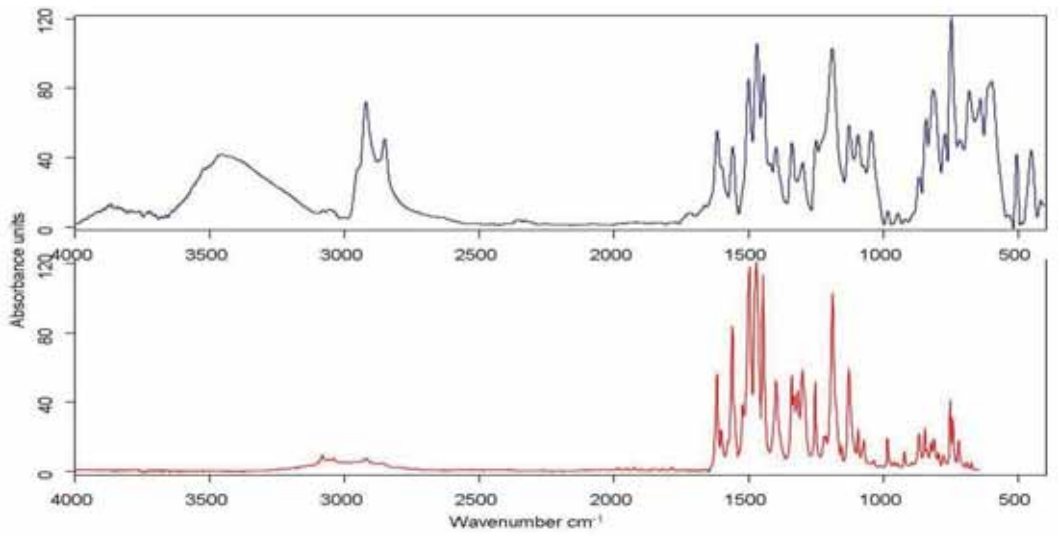

Fig. 5.24 - FT-IR spectrum of the FM8 extracted solution (blue line) and
reference spectrum of PR3 from IRUG 2007 database (ref. IOD00466, red line)

Toluidine red (Fig. 5.25) is obtained by coupling a diazotised primary aromatic amine on the α position of β-naphtol generating an azo bond (N=N) that represents the chromophore group (Potdar, 1988).

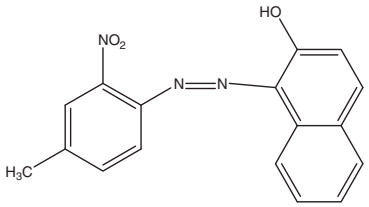

Fig. 5.25 - Chemical structure of toludine red, PR3 (Potdar, 1988)

The FORS spectrum (Fig. 5.26) did not (as expected) show the characteristic profile of the PR3 dye with a strong absorption in the blue-region and with an inflection point at 620 nm (Johnston, 1967; Potdar, 1988). It was, in fact, characterised by a strong absorption band in the UV–Vis region, starting from its inflection point at about 600 nm (2.07 eV). These data, together with the "S"-shape profile of the spectrum, made it possible to attribute the strong UV–Vis absorption band tentatively to the presence of cinnabar (Bacci, 2000).

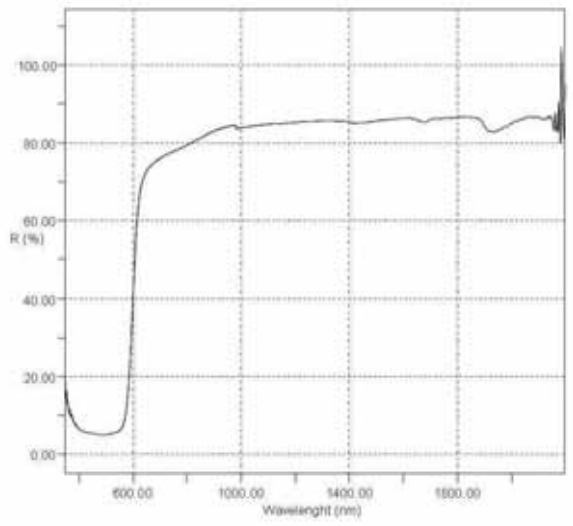

Fig. 5.26 - FORS spectrum of FM8 sample

Subsequently, the presence of cinnabar, as well as two other inorganic compounds (barite and calcite), was unquestionably confirmed by means of the XRD technique (Fig. 5.27).

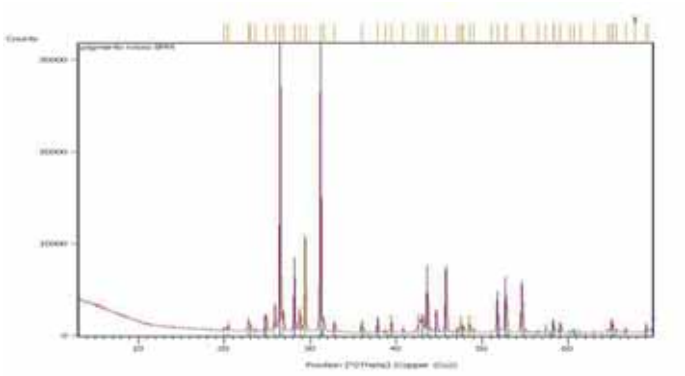

Fig. 5.27 - XRD diffractogram of the FM8 sample showing the presence of cinnabar (blue lines), barite (grey lines) and calcite (green lines)

Thus, the FM8 sample was identified as a mixture of toluidine red and cinnabar, with calcite and barite as fillers.

The composition of the second red powder (FM9) was ascertained as being composed of iron(III) oxide, or hematite (α-Fe_2O_3), which is the fundamental compound of the synthetic red earth class of pigments, namely Mars red or iron oxide (PR101). Indeed, the FT-IR spectrum (Fig. 5.28) showed the characteristic absorption bands of hematite at 544 and 472 cm^{-1} due to asymmetric and symmetric Fe-O stretchings, respectively (Afremow and Vanderberg, 1966; Helwig, 2007). Moreover, absorption bands attributable to silicates were also detected (asymmetric Si-O-Si stretching at 1096 cm^{-1}, with a shoulder at around 1200 cm^{-1})(Helwig, 2007).

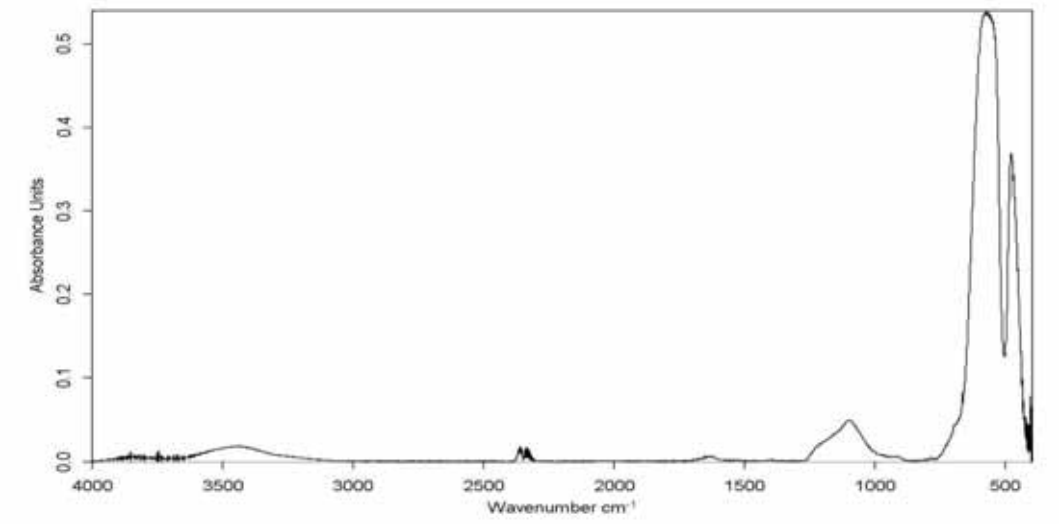

Fig. 5.28 - FT-IR spectrum of FM9 sample

The FORS spectrum showed the typical intense absorption band of hematite at 445 nm due to the charge transfer transition of the Fe-O bond. Two absorption bands at 649 nm and 870 nm, which were due to ligand field transitions of the Fe^{3+} ion (Sherman and Waite, 1985; Cornell and Schwertmann, 1996), were also found (Fig. 5.29).

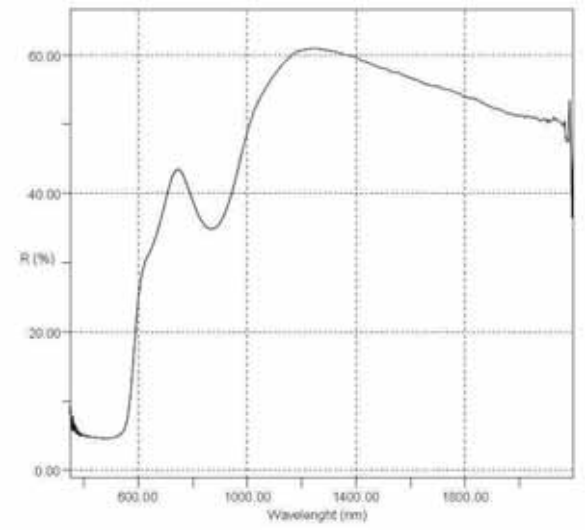

Fig. 5.29- FORS spectrum of the FM9 sample

Green samples

The two yellowish green powders (FM10 and FM11) were found to have identical spectral features (Fig. 5.30).

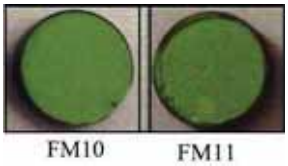

Fig. 5.30 – Green powder samples

The FT-IR spectra of the powder samples (Fig. 5.31) showed distinctly only the absorption bands of calcite (combination of CO_3^{2-} symmetric and asymmetric stretching at 2511 cm^{-1}; CO_3^{2-} asymmetric stretching at 1425 cm^{-1}; CO_3^{2-} out of plane bending at 876 cm^{-1}, and CO_3^{2-} in plane bending at712 cm^{-1}) and barite (SO_4^{2-} asymmetric stretching at 1178 cm^{-1}, 1103 cm^{-1} and 1083 cm^{-1}; SO_4^{2-} in plane bending at 635 cm^{-1} and 610 cm^{-1})(van der Marel and Beutelspacher, 1976; Nakamoto, 1978; Feller, 1986).

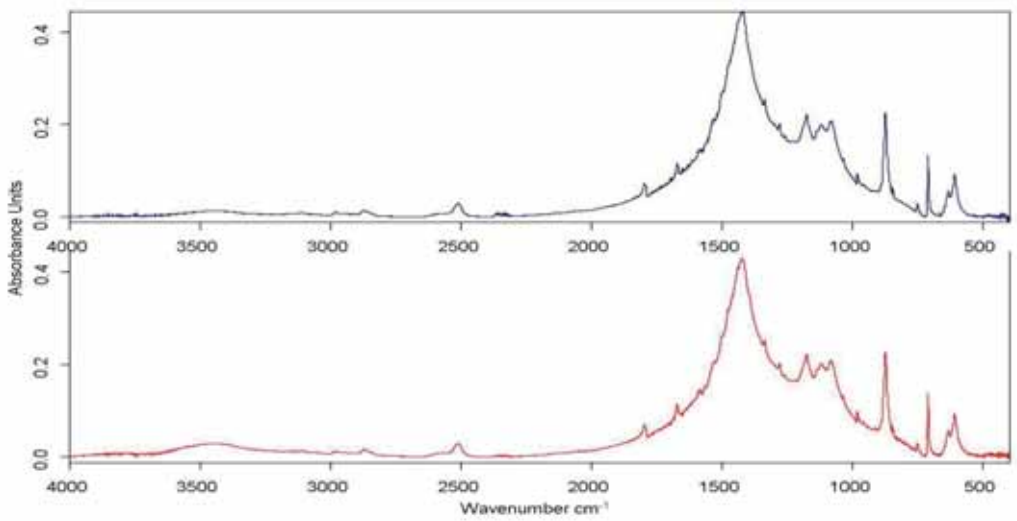

Fig. 5.31- FT-IR spectra of FM10 (blue line) and FM11 (red line) powder samples

As for samples FM3 and FM8, it was not possible to identify the compound responsible for the colour owing to the presence of the intense bands of calcite and barite. Thus, the samples were subjected to an extraction with 1 mL of acetone, and the solutions obtained were analysed by means of FT-IR spectroscopy. The FT-IR spectra of the extracted parts (Fig. 5.32) showed only the distinctive and sharp absorption bands of the yellow organic PY3 pigment: 3106 cm^{-1} (NH stretching), 1670 cm^{-1} (C=O stretching), 1583 cm^{-1}, 1535 cm^{-1}, 1502 cm^{-1} (NO_2 asymmetric stretching), 1336 cm^{-1} (NO_2 symmetric stretching), 1279 cm^{-1}, 1186 cm^{-1}, 1138 cm^{-1}, 1038 cm^{-1} (C-Cl^- stretching), 810 cm^{-1}, 749 cm^{-1} and 620 cm^{-1} (Learner, 2004; Quillen Lomax *et al*., 2007).

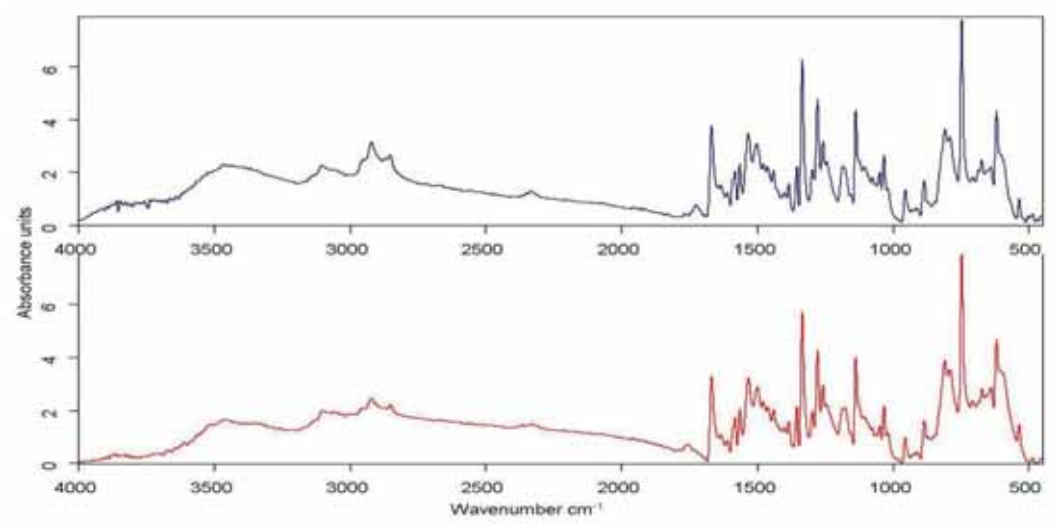

Fig. 5.32 - FT-IR spectra of the FM10 (blue line) and FM11 (red line) extracted solutions

A blue component must also have been present, therefore, to provide the green hue of the samples under analysis. The tentative identification of the blue component was possible thanks to the FORS technique. In fact, in the FORS spectra (Fig. 5.33), two additional absorption bands at 614 and 692 nm were evident in addition to the intense absorption in the UV-blue region given by the PY3 dye. The two absorption bands in the red region were due to the presence of a phthalocyanine blue pigment (Johnston and Feller, 1963; Johnston, 1967). These bands are part of the characteristic spectral features of this compound, which consisted of four intense π–π* transitions in the UV–Vis region. Those below 486 nm (the inflection point of arylide) were masked by intense absorption due to the yellow dye. On the other hand, those in the 600–700 nm range, which corresponded to $a_{1u}(\pi) \rightarrow e_g(\pi^*)$ transitions (Christie and Freer, 1994), were still visible in the spectrum. In addition, the absorptions in the 850–2000 nm region could tentatively be attributed to an electronic charge transfer, $a_{1u}(\pi) \rightarrow e_g(d_{xz},d_{yz})$ or n(azo) → π* transitions, as well as to vibrational overtones of ν(C-H) at 1660 nm and ν(C-H) 2nd overtones at 1100 nm. The NIR spectral features at 1660 nm and 2150 nm may also have been due to the presence of PY3 (Bacci, 2000).

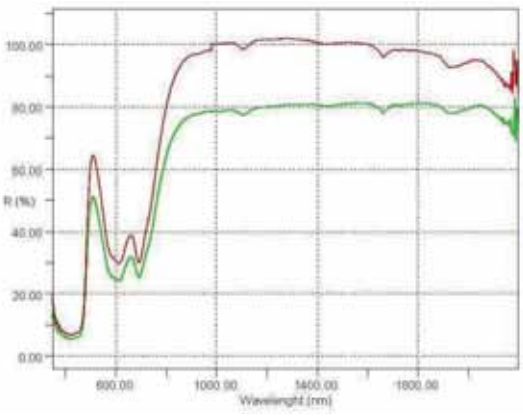

Fig. 5.33 - FORS spectra of FM10 (green line) and FM11 (red line) samples

It should be noted that, in 1959, Di Bernando and Resnick reported that phthalocyanine blue showed an anomalous behaviour when mixed with aromatic yellow dyes, such as arylide yellow (PY3), and also modified its spectral features in the UV–Vis–NIR region (Di Bernando and Resnick, 1959). However, despite this fact, the reflectance spectrum collected on the two green pigments, FM10 and FM11, showed that the two absorption bands of the blue dye at 615 and 690 nm were still present. Thus, in order to experimentally verify the spectral features of the mixture of phthalocyanine blue and arylide powders, as found in the FM10 and the FM11 samples, it was decided to prepare in the laboratory a powder mixture consisting of 0.3% phthalocyanine blue (PB15 by Winsor & Newton), 5% PY3 (FM1), and 94.7% of calcite (Aldrich) by weight. This concentration was chosen by using the data reported by Di Bernardo and Resnick (1959) and by Johnston and Feller (1963) as a starting point. The FT-IR and FORS spectra acquired in this mixture were both in good agreement with those obtained on the FM10 and FM11 samples.

In this case, the use of the two analytical techniques was crucial in order to obtain a complete identification of all the compounds in the FM10 and FM11 samples. The FORS and FT-IR spectra identified them as a mixture of arylide yellow (PY3) and phthalocyanine blue (PB15), in addition to calcite and barite as fillers.

Blue samples

The analysis of the two blue samples (FM12 and FM13) showed that Melani's palette comprised both traditional items and modern compounds rarely used as artists' materials (Fig. 5.34).

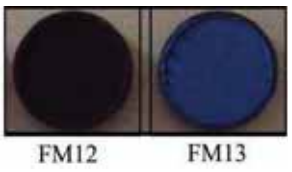

Fig. 5.34 – Blue powder samples

The FM12 sample was identified as the basic dye Victoria Blue B (basic dye number 26). This dye belongs to the triarylmethane chemical class, and is characterised by the fuchsonimine group as its chromophore (Di Bernardo, 1959; Ballard, 1991)(Fig. 5.35).

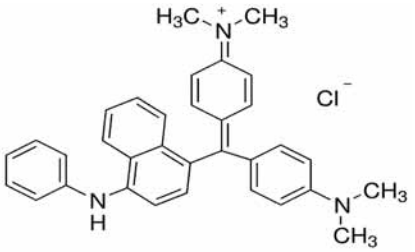

Fig. 5.35 - Chemical structure of Victoria Blue B (basic dye number 26)
[image from http://www.sigmaaldrich.com/catalog/product/sigma/94890?lang=it&region=IT, last access 24 October, 2013]

In this case, its identification was possible by comparing the FT-IR spectrum of the sample (Fig. 5.36) with the one reported in the IRUG 2007 database (ref. IOD00049), as well as with the FT-IR spectrum obtained from a reference sample of Victoria Blue B supplied by Sigma–Aldrich® (CAS number: 2580-56-5, basic blue 26). The main absorption bands were at 3150-3000 cm^{-1} (NH and aromatic CH stretchings), 2920 cm^{-1} (aliphatic CH asymmetric stretching), 2820 cm^{-1} (aliphatic CH symmetric stretching), 1590 cm^{-1} (aromatic C=C stretching), 1337 cm^{-1} (aromatic CH bending)(Socrates, 1998).

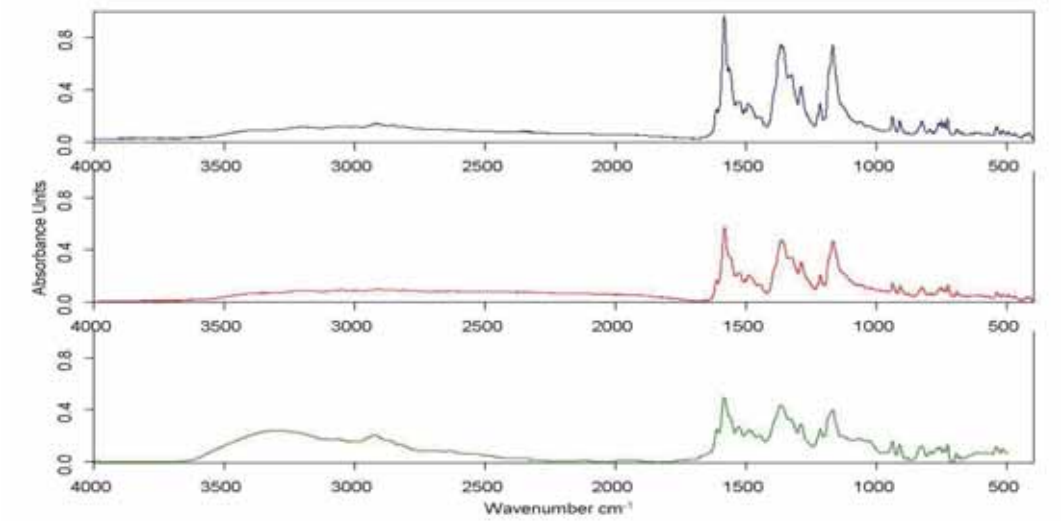

Fig. 5.36 - FT-IR spectra of the FM12 sample (blue line), reference sample of Victoria Blue B supplied by Sigma–Aldrich® (red line), reference of Victoria Blue B from IRUG 2007 database (ref. IOD00049, green line)

The FORS spectrum acquired on the FM12 sample (Fig. 5.37) showed the typical features of a deep blue hue compound with a weak reflectance maximum at 447 nm. In the near infrared region the principal absorption bands were at 1140 and 1200 nm (2nd overtones of aliphatic CH stretching), 1440 nm (1st overtone of OH stretching), 1680 nm (1st overtone of aromatic CH stretching) and 1910 nm (combination band of OH stretching and OH bending).

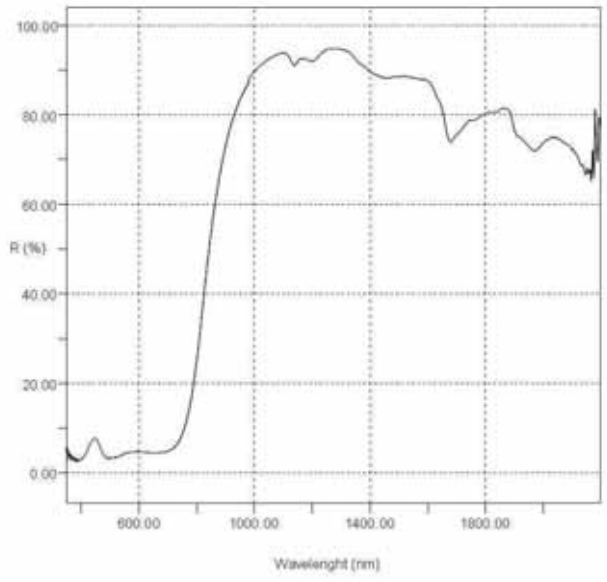

Fig. 5.37 - FORS spectrum of the FM12 sample

A further confirmation of the presence of this blue dye was obtained by means of ^{1}H-NMR and ^{13}C-NMR spectroscopies.

The ^{1}H-NMR spectrum (Fig. 5.38) presented the signals attributable to protons located on the aromatic rings in the 6.7-7.7 ppm range, while signals of the methyl protons were found in the 2.8-3.5 ppm range. The other peaks were attributed to impurities present in the sample.

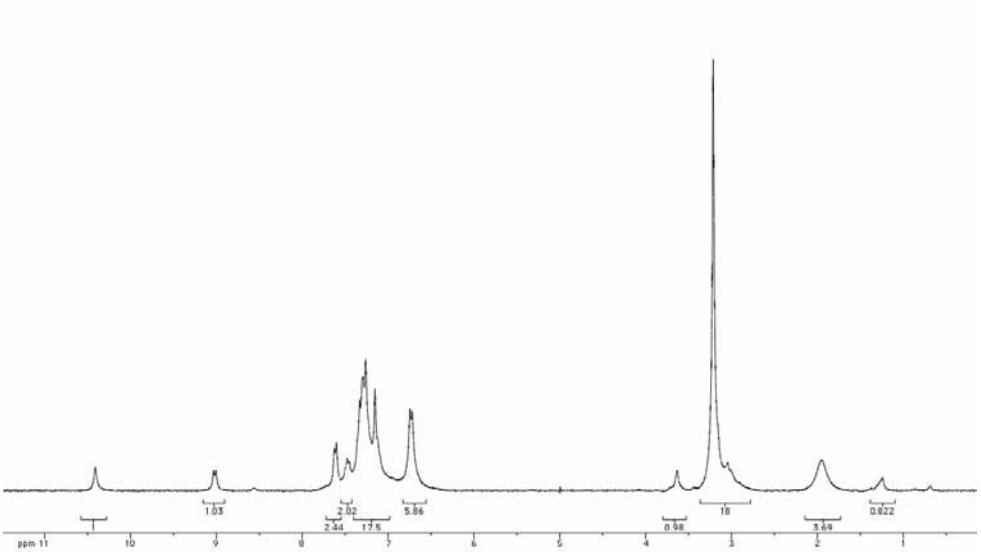

Fig. 5.38 - ^{1}H-NMR spectrum of the FM12 sample

The ^{13}C-NMR spectrum of FM12 sample (Fig. 5.39) was comparable to the reference spectrum of Victoria Blue B reported on the SDBS database (ref. N° 21266CDs-01-347; http://sdbs.riodb.aist.go.jp/sdbs/cgi-bin/direct_frame_top.cgi, last access October 24, 2013).

In Fig. 5.40, the assignments of the FM12 ^{13}C-NMR spectrum are reported.

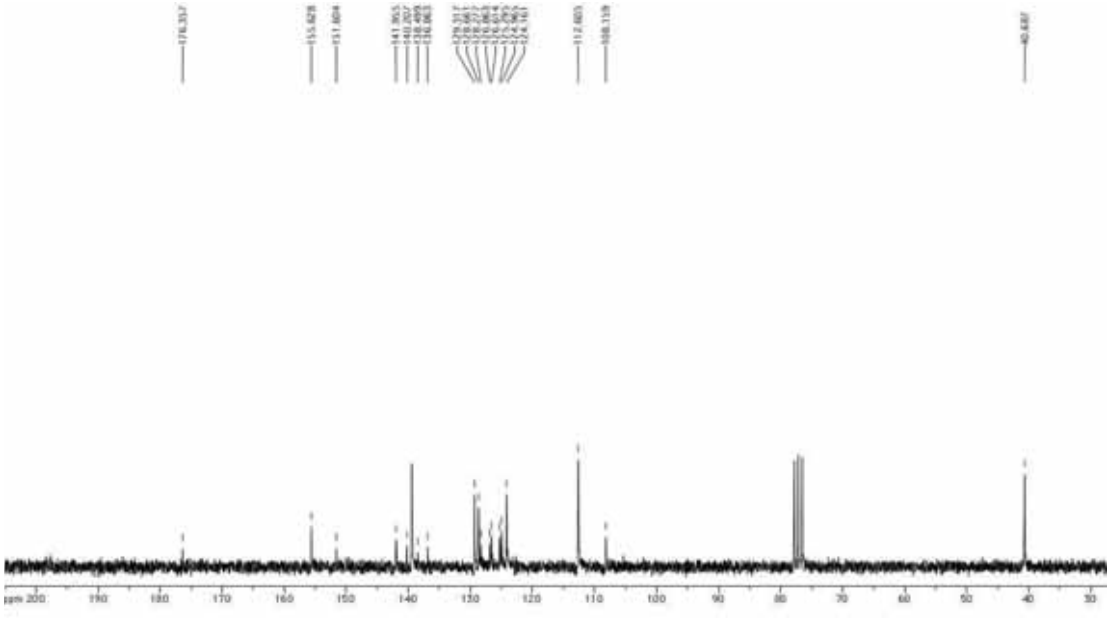

Fig. 5.39 - ^{13}C-NMR spectrum of the FM12 sample

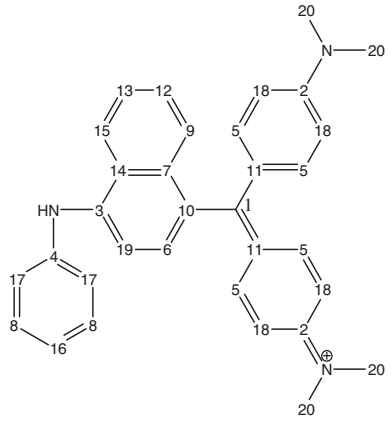

ppm	I	Ass.	ppm	I	Ass.
174.50	139	1			11
155.72	501	2	126.26	262	12
147.57	306	3	125.50	247	13
140.62	416	4	124.16	327	14
139.12	961	5	123.81	247	15
138.60	267	6	123.43	165	16
135.50	350	7	122.47	655	17
129.31	753	8	113.26	1000	18
127.94	295	9	107.16	236	19
127.50	958	10	44.70	88	20

Fig. 5.40 - Assignments of the FM12 ^{13}C-NMR spectrum

The FM13 sample was a light blue powder, and was identified as being a mixture of three inorganic materials. In the FT-IR spectrum (Fig. 5.41) the absorption bands due to Si-O-Si asymmetric (1010 cm^{-1}) and symmetric stretching (694 cm^{-1}, 659 cm^{-1}), and to Si-O-Si bending (451 cm^{-1}) were found (Plesters, 1993). These absorptions could be attributable to the presence of ultramarine blue in the sample. Absorptions due to vibrational modes of the sulfate ion (SO_4^{2-} asymmetric stretchings at 1188, 1121 and 1082 cm^{-1}, SO_4^{2-} symmetric stretching at 983 $cm^{-}1$, SO_4^{2-} in plane bending at 634 and 610 cm^{-1}) and water (OH asymmetric and symmetric stretchings at 3566 and 3413 cm^{-1}, H-O-H bending at 1635 cm^{-1}) were also present. Lastly, the weak absorption at 2089 cm^{-1} may have been due to the stretching of the C≡N bond, which is usually attributable to the presence of Prussian Blue.

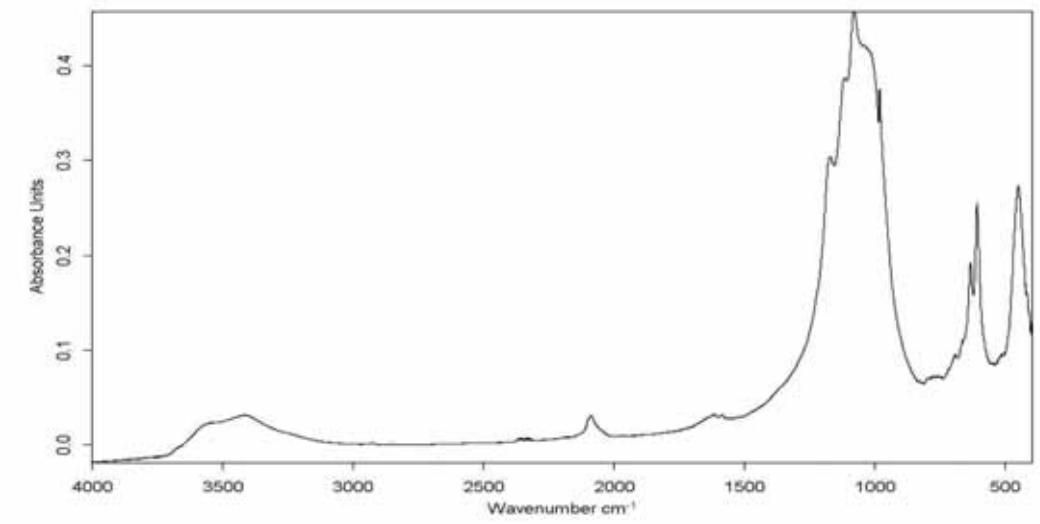

Fig. 5.41 - FT-IR spectrum of the FM13 sample

The reflectance spectrum of the FM13 sample (Fig. 5.42) resembled that of the ultramarine blue, since it showed a strong absorption centred at 600 nm due to the charge-transfer transition of ion S_3^- (Aceto *et al.*, 2013). The maximum of reflectance at 442 nm was, instead, weakly shifted toward lower wavelengths if compared with the value found in the literature

(460 nm). This shift may be caused by the presence of a second blue pigment, such as Prussian blue, which is characterised by a maximum of reflectance at 440 nm (Clark and Cobbold, 1978; Bacci, 2000). The high reflectance value and the considerable intensity of the maximum at 442 nm, enabled us to suppose the presence of a white compound mixed with the two blue pigments.

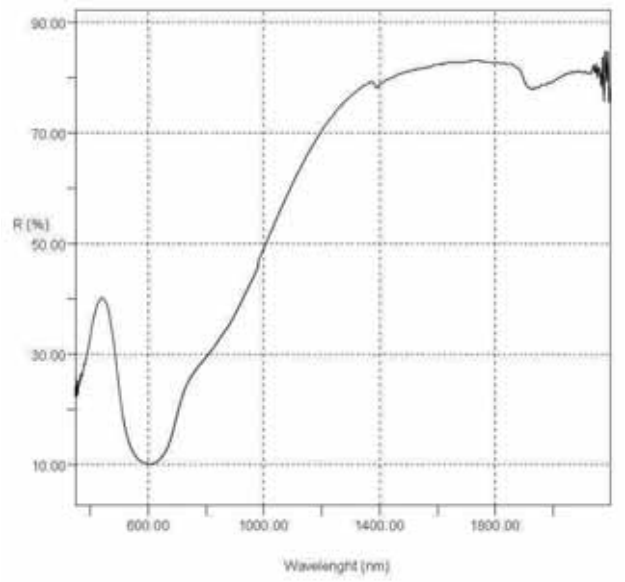

Fig. 5.42 - FORS spectrum of the FM13 sample

From a comparison with the data found in the literature (Clark and Cobbold, 1978; Kulesza, 1996; Berrie, 1997; Bacci, 2000) it can be stated that the FM13 sample was a mixture of ultramarine blue ($Na_6Al_6Si_6O_{24}S_4$), Prussian blue ($Fe_4[Fe(CN)_6]_3$) and barium sulfate ($BaSO_4$).

Dark sample

The FM15 sample was identified as an abrasive powder (Fig. 5.43).

Fig. 5.43 – Dark sample

The FT-IR spectrum (Fig. 5.44) showed absorptions bands due to the presence of a mixture of aluminium oxides and hydroxides, such as diaspore, α-AlO(OH), and corundum, α-Al_2O_3. In particular, the absorption bands at 2910 cm^{-1} (OH asymmetric stretching), 2117 cm^{-1} and 1984 cm^{-1} (OH symmetric stretchings), 963 cm^{-1} (OH bending) and 753 cm^{-1} (Al-O stretching) were attributable to the presence of diaspore, while the absorptions at 642 and 454 cm^{-1} (Al-O bending) were due to corundum. The FT-IR bands at 1080 (OH bending), 575–600 and 520 cm^{-1} (Al-O stretchings) were attributed to both components (Feller, 1986; Demichelis *et al.*, 2008).

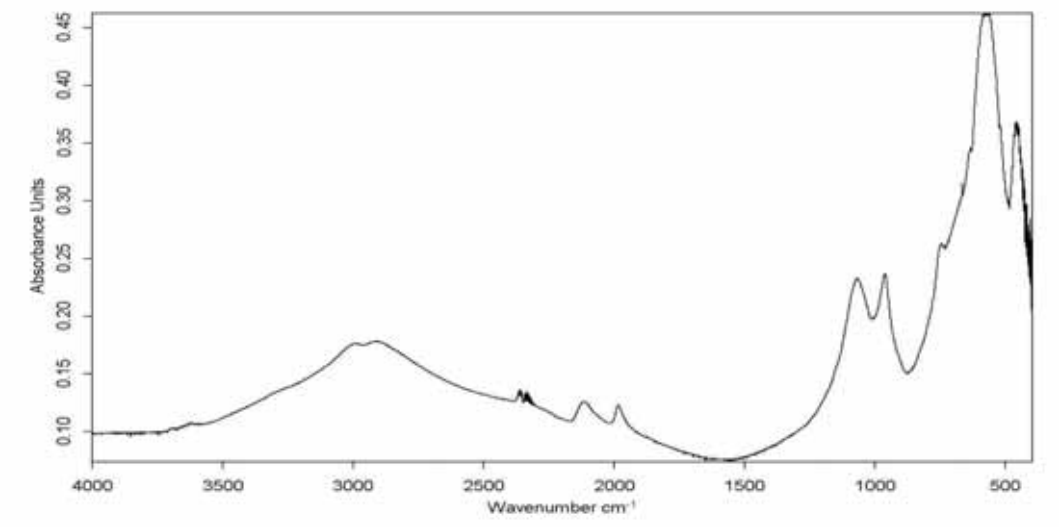

Fig. 5.44 - FT-IR spectrum of the FM15 sample

The results obtained were also corroborated by XRD[3] analysis, which confirmed what has been reported on certain artworks by Melani, such as the *Progetto di Lettura Globale*. As declared by the artist (Corà, 1990; Giuntoli, 2010), he used 'emery', an abrasive powder consisting of aluminium oxides and hydroxides, in addition to pumice as one of the pigments for the creation of this artwork.

[3] XRD analysis was performed by Dr. Emma Cantisani of the Institute for the Conservation and Valorisation of Cultural Heritage (Department of Florence) of the National Research Council (ICVBC-CNR).

5.3 *La Bandiera Italiana*

5.3-1 The artwork

At the end of the corridor that leads to the rooms of Melani's Studio-Home, practically inserted into the space between two doors facing one another, there is *La Bandiera Italiana* (The Italian Flag, Fig. 5.40), which was created by Fernando Melani between 1955 and 1960 for the centenary celebrations of the founding of Italy (1861). The artwork displays an Italian flag (dimensions: 107.5 cm x 142 cm x 16 cm) attached by means of two purple wooden laundry-pegs to a sheet of plywood, painted white in front and black on the back. The canvas, which is made rigid by layers of glue and paint, is divided into three coloured areas: green, white, and red, in recalling the Italian flag. Blue and yellow patterns are painted below the green and red areas, respectively.

Fig. 5.40 - *La Bandiera Italiana* (image acquired on 20 April 2011)

5.3-2 Experimental

FORS

The FORS technique in the 350-2200 nm range was employed in order to obtain data on the composition of the paint layers. The non-invasive measurements were performed *in situ*. The experimental set-up of the instrumentation was the same one used for the analysis of Melani's powdered pigments/dyes found in the Studio-Home (§ 5.2-2).

FT-IR

FT-IR spectroscopy was performed on three small samples detached from the three areas of the flag (A red-yellow, B white, and C green-blue) to substantiate and/or refine the non-invasive *in situ* identification of the pigments and dyes.

The experimental set-up of the instrumentation was the same one used for the analysis of Melani's pictorial palette (§ 5.2-2).

5.3-3 Study of the artistic materials

Within the framework of the CoPAC Project, the composition of the organic compounds present in the artwork was investigated using the Py-GC/MS technique at the SCIBEC laboratory of the University of Pisa. The analysis identified both a vinyl resin and an acrylic resin, which probably consisted of a copolymer based on styrene-2-ethylhexyl-acrylate (La Nasa, 2011). The information found in the museum datasheet and in the literature (Giuntoli, 1987-1991; Giuntoli, 2010), made it possible to hypothesise that Melani used the vinyl resin to shape the canvas into the form of a flag and the acrylic one as a paint binder.

Green area

All FORS spectra in the green area (Fig. 5.41) showed four strong absorptions in the UV-Vis region (405 nm, 640 nm, 721 nm and 797 nm) that were due to intense $\pi \rightarrow \pi^*$ transitions, together with absorptions in the 850-2200 nm region that were attributed to charge transfer $a_{1u}(\pi) \rightarrow e_g(d_{xz},d_{yz})$ or $n(azo) \rightarrow \pi^*$ transitions typical of phthalocyanine based pigments (Johnston and Feller, 1963; Christie and Freer, 1994). In addition, ν(C-H) 1st and 2nd overtones at 1120 nm at 1758 nm, respectively, were also visible (Bacci, 2000). Instead, the absorptions at 1395 nm and 1415 nm, which were due to ν(O-H) overtones, were attributable to the presence of kaolinite (Crowley and Vergo, 1988).

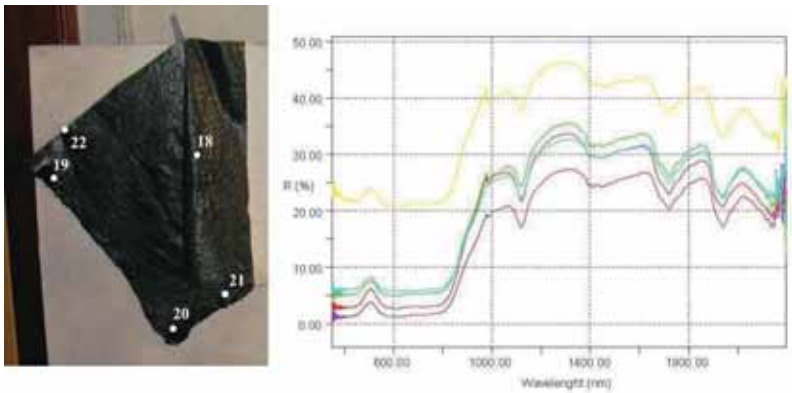

Fig. 5.41 - FORS spectra of spot 18 (green line), spot 19 (red line), spot 20 (yellow line), spot 21 (violet line), and spot 22 (cyan line)

The FT-IR analysis of sample C (Fig. 5.42) confirmed the presence of kaolinite (absorption bands collocated at 3696 cm^{-1}; 3623 cm^{-1}; 1090 cm^{-1}; 1030 cm^{-1}; 944 cm^{-1}; 916 cm^{-1}; 542 cm^{-1} and 472 cm^{-1}) (Gadsden, 1975), while no bands due to the pigment were detectable. The latter were probably covered by the intense absorptions due to barium sulphate (667 cm^{-1} and 603 cm^{-1}), to calcite (2520 cm^{-1}, 1448 cm^{-1}, 873 $cm^{-1}$and 713 cm^{-1}) (van der Marel and Beutelspacher, 1976; Nakamoto, 1978) and to the vinyl binder (2961 cm^{-1}, 2930 cm^{-1}, 2875 cm^{-1}, 1742 cm^{-1}, 1243 cm^{-1}, 1022 cm^{-1}, 608 cm^{-1}).

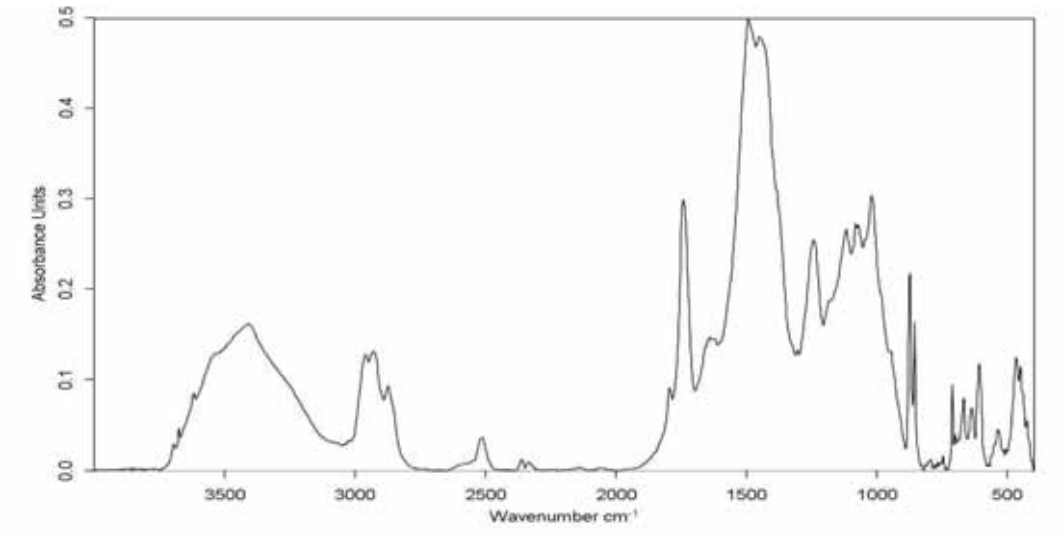

Fig. 5.42 - FT-IR spectrum of sample C

White areas

White areas of the flag and the plywood, which was used as a support, were coated with two different white paints. FORS spectra (Fig. 5.43) registered on spots 10-14 of the canvas showed the typical absorption feature of titanium white in its rutile crystalline form as demonstrated by its inflection point, which was positioned at around 400 nm, due to an electronic band-gap transition (energy gap: 3.09 eV) (Bacci *et al.*, 2007; Picollo *et al.*, 2007).

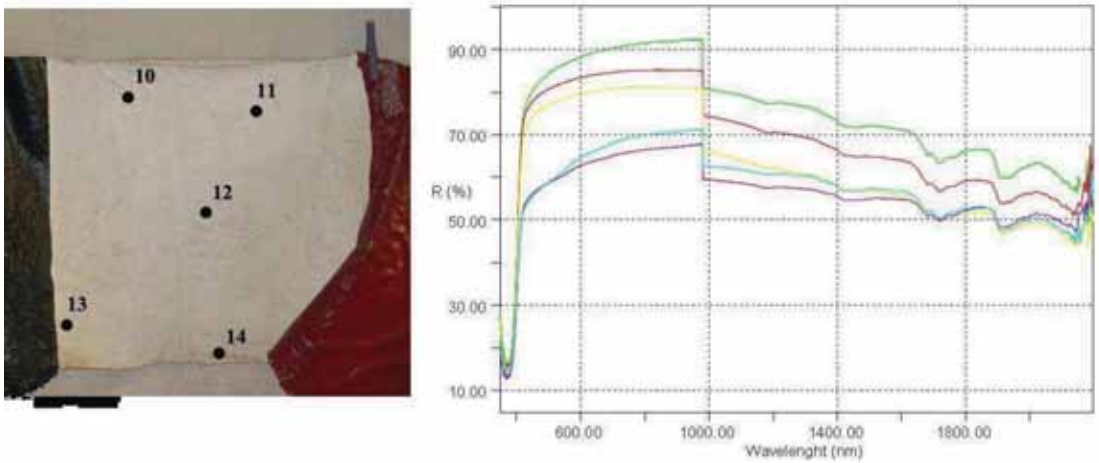

Fig. 5.43 - FORS spectra of spot 9 (green line), spot 10 (red line), spot 11 (yellow line), spot 12 (violet line), and spot 13 (cyan line)

The presence of titanium dioxide was confirmed by the strong absorption in the 800-400 cm^{-1} (Laver, 1997) found in the FT-IR spectrum of sample B (Fig. 5.44). The absorption bands of calcite (2520 cm^{-1}; 1448 cm^{-1}; 873 $cm^{-1}$and 713 cm^{-1}) (van der Marel and Beutelspacher, 1976; Nakamoto, 1978) and of the vinyl binder (2963 cm^{-1}, 2927 cm^{-1}, 2874 cm^{-1}, 1742 cm^{-1}, 1374 cm^{-1}, 1243 cm^{-1}, 1024 cm^{-1}, 608 cm^{-1}) were also detected.

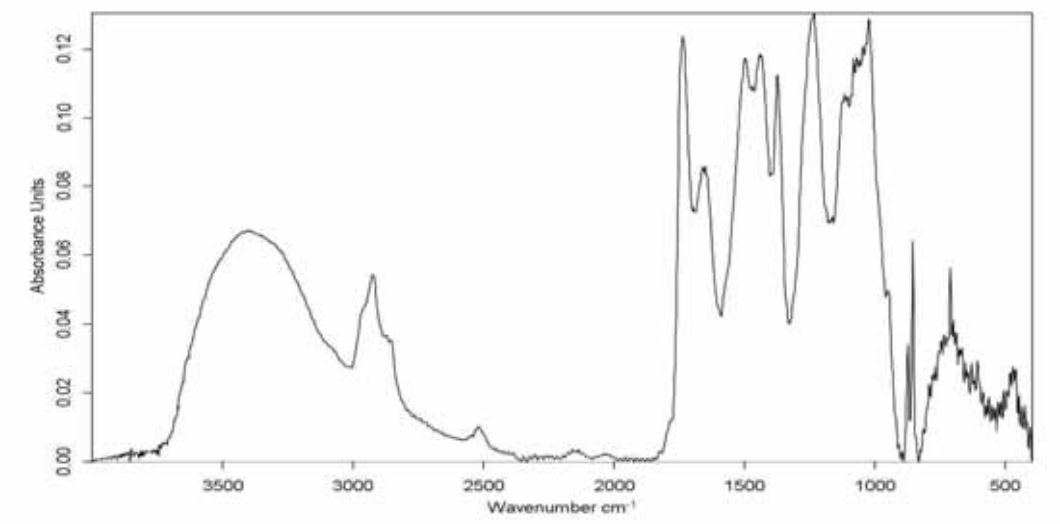

Fig. 5.44 - FT-IR spectrum of sample B

The FORS spectra of points 26 and 27 of the plywood, instead, showed an intense absorption band centred at 358 nm with an inflection point at 372 nm (3.33 eV) that could be attributed to an electronic band gap transition of titanium dioxide in the anatase crystalline form (Fig. 5.45) (Bacci *et al.*, 2007; Picollo *et al.*, 2007).

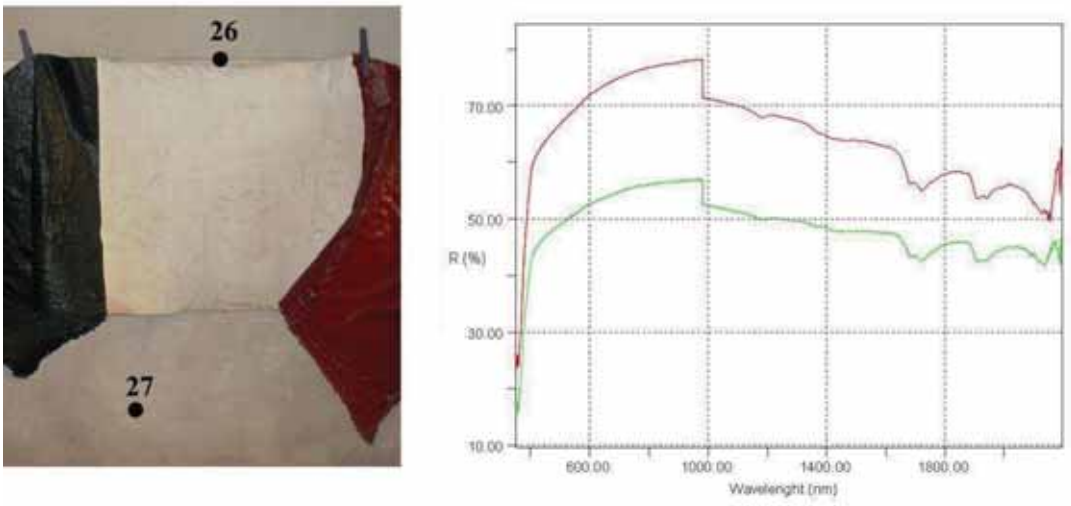

Fig. 5.45 - FORS spectra of spots 26 (green line) and 27 (red line)

Red area

The FORS spectra acquired on the red pattern (spots: 1-4; Fig. 5.46) showed a strong absorption centred at 488 nm, with an inflection point at 620 nm (1.99 eV), together with an "S"-shape spectral feature. These features made it possible to exclude the presence of traditional inorganic pigments, such as cinnabar and cadmium red (their inflection points are positioned at about 600 nm). However, these could have been attributable to an organic dye such as toluidine red PR3. This dye, in fact, shows a characteristic reflectance profile with a strong absorption in the blue region and an inflection point at 620 nm due to a n(azo) → π* transition. All spectra also revealed the presence of kaolinite, with two absorptions at 1382 nm and 1418 nm that were due to ν(O-H) overtones (Crowley and Vergo, 1988).

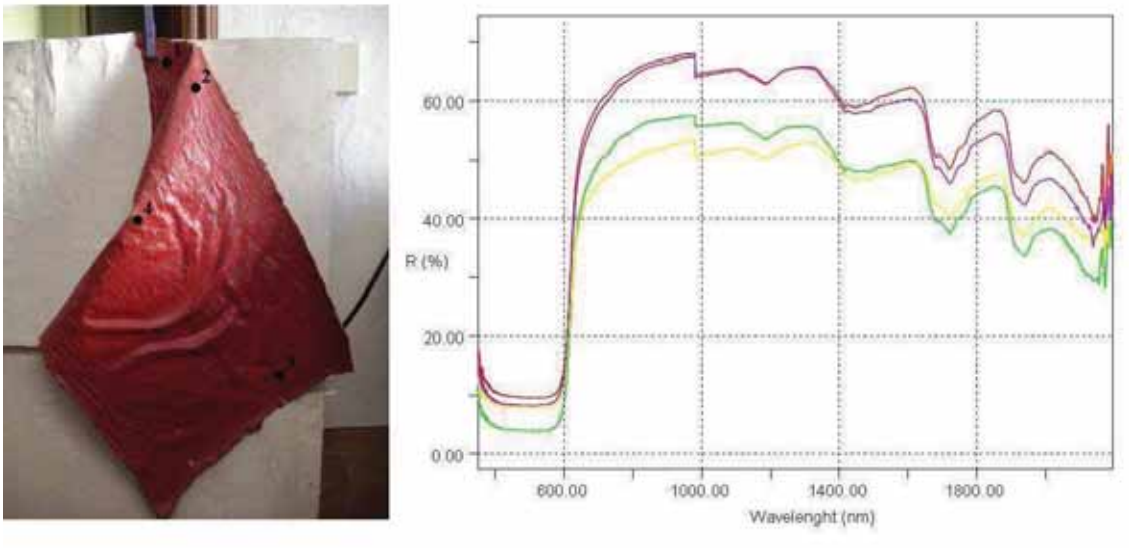

Fig. 5.46 - FORS spectra of spot 1 (green line), spot 2 (red line), spot 3 (yellow line) and spot 4 (violet line)

FT-IR analysis performed on sample A (Fig. 5.47) enabled us to identify unequivocally the presence of kaolinite (3696 cm^{-1}, 3623 cm^{-1}, 1090 cm^{-1}, 1030 cm^{-1}, 944 cm^{-1}, 916 cm^{-1}, 542 cm^{-1} and 472 cm^{-1}) and calcite (2520 cm^{-1}, 1448 cm^{-1}, 873 $cm^{-1}$and 713 cm^{-1}), which were probably used as fillers (van der Marel and Beutelspacher, 1976; Nakamoto, 1978; Johnston and Feller, 2001). As for samples B and C, the absorption bands of the vinyl medium were identified (2962 cm^{-1}, 2927 cm^{-1}, 2875 cm^{-1}, 1739 cm^{-1}, 1377 cm^{-1}, 1244 cm^{-1}, 1023 cm^{-1}, 946 cm^{-1} and 608 cm^{-1}).

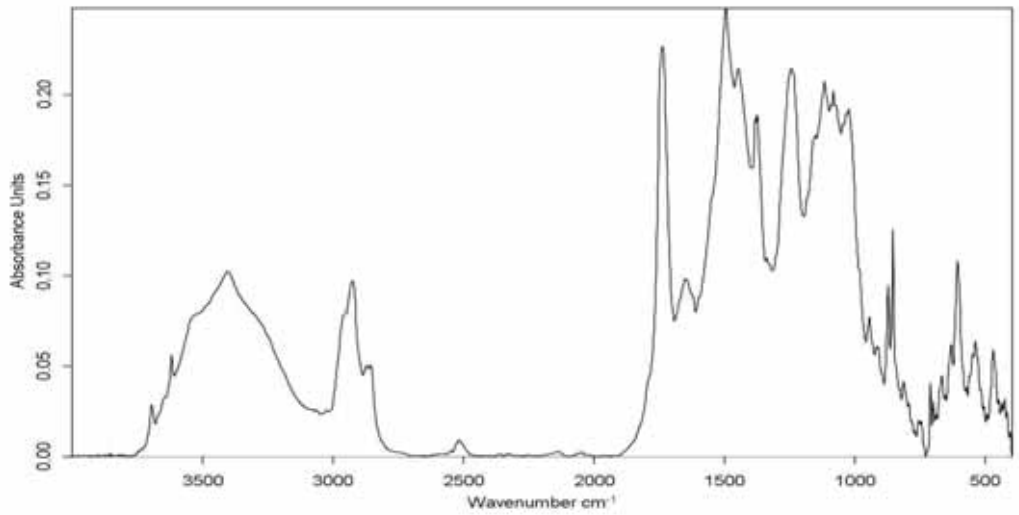

Fig. 5.47 - FT-IR spectrum of sample A

Yellow area

In the UV-blue region, FORS spectra acquired on spots 6 and 7 (Fig. 5.48) showed the typical "S"-shape strong absorption that is characteristic of the lead chromate based pigments. This absorption is due to a ligand-to-metal charge-transfer transition from oxygen to chromium into the chromate ion CrO_4^{2-}. The inflection point of these spectra was positioned at 522 nm (237 eV), with a shoulder at 555 nm (Bacci, 2000). Furthermore, the absorption in the UV

region with the inflection point at around 400 nm (3.09 eV) was due to the presence of titanium white in the rutile crystalline form (Bacci *et al.*, 2007; Picollo *et al.*, 2007).

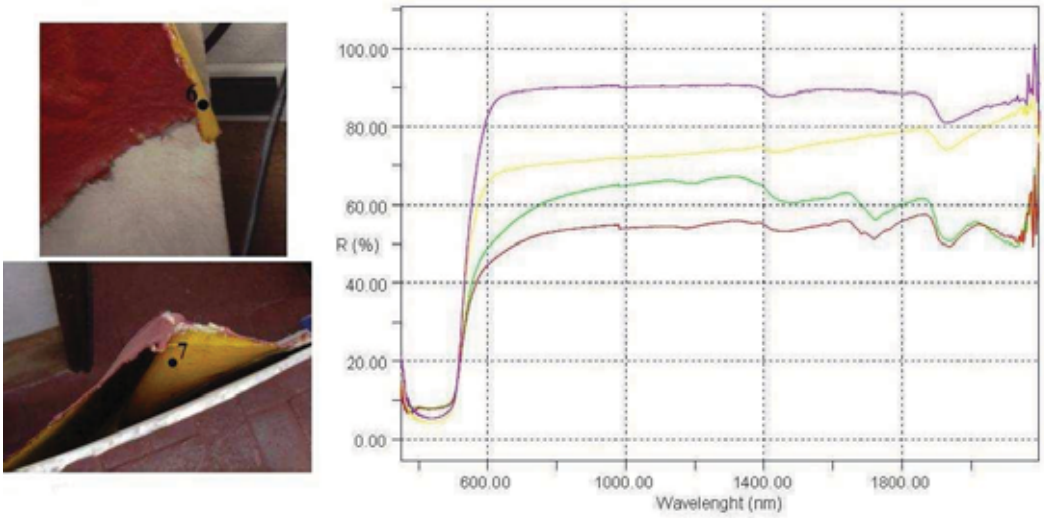

Fig. 5.48 - FORS spectra of spot 6 (green line), spot 7 (red line), FM5 sample (yellow line), FM7 sample (violet line),

FT-IR analysis was not performed, since it was impossible to separate the yellow layer from the red layer in sample A.

Blue Area

FORS spectra performed on spots 15 and 17 (Fig. 5.49) showed a strong absorption centred at 600 nm that was due to charge transfer S_3^- anion transitions in a crystal structure, together with a reflectance maximum at 450 nm with a shoulder at around 770 nm. These features were attributable to the ultramarine blue inorganic pigment (Clark and Cobbold, 1978; Bacci, 2000). Two absorptions at 1394 nm and 1418 nm, due to the presence of kaolinite (Crowley and Vergo, 1988), were also detected.

FT-IR analysis was not performed, since it was impossible to separate the blue layer from the green layer in sample C.

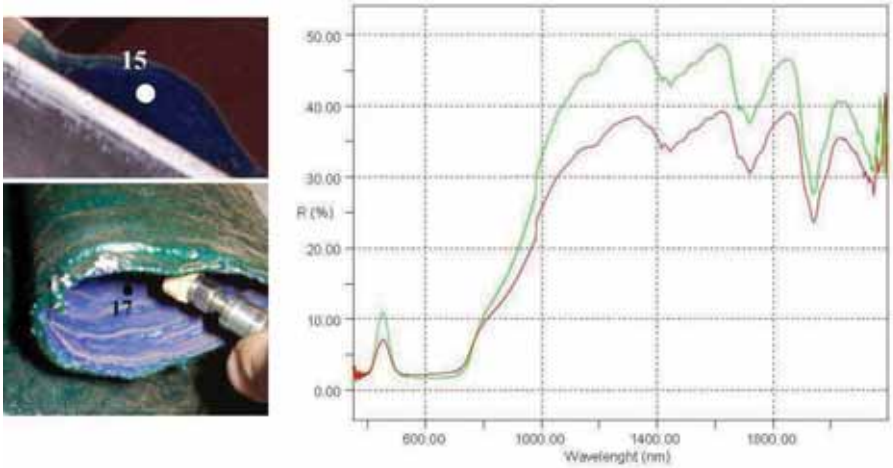

Fig. 5.49- FORS spectra of spot 15 (green line) and spot 17 (red line)

Purple Area

The two purple wooden laundry-pegs were exclusively analysed using FORS. Both reflectance spectra acquired on spots 24 and 25 (Fig. 5.50) showed four absorption bands in the UV-Vis region (530 nm, 569 nm, 627 nm and 697 nm) with two maxima of reflectance at 450 nm and 607 nm. This reflectance profile is typical of a violet organic dye named "carbazole violet" (PV 23) (Kaul and Wihan, 1988).

The absorption in the UV region at around 372 nm was attributable to the presence of titanium white in the rutile crystalline form (Bacci *et al.*, 2007; Picollo *et al.*, 2007).

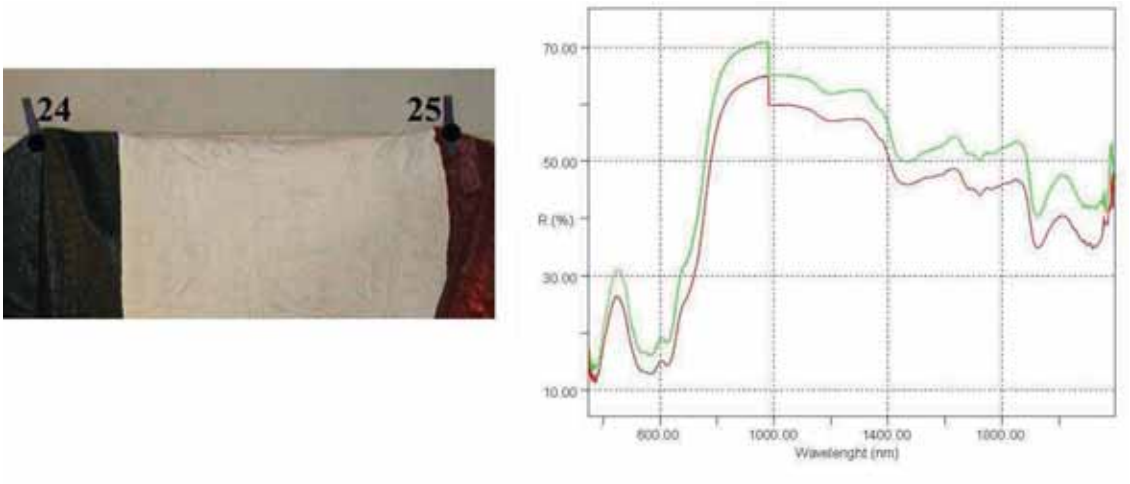

Fig. 5.50 - FORS spectra of spot 25 (green line) and spot 25 (red line)

5.4 Case study: *N. Inv. 2625*

5.4-1 The artwork

The artwork named with its inventory number *N. Inv. 2625* (68.8 cm x 83 cm) is a polychrome painting on straw paper created during the summer of 1981. It belongs to what Melani had named "folder U" (Fig. 5.51), which was one of the artist's own studies on the use of colours on paper (Giuntoli, 2010). The painting is characterised by a yellowish-based hue. The colours were applied using wide, oblique brushstrokes that were repeated one over the other, thus producing yellow, green, blue, red, purple and white colour fields that created a complex superficial coloured texture.

Fig. 5.51 - *N. Inv. 2625* within "folder U" (image acquired on 20 April 2011)

5.4-2 Experimental

FORS

The study of this painting was performed *in situ*, using the non-invasive FORS technique. The experimental set-up of the instrumentation was the same one used to analyse Melani's pictorial palette (§ 5.2-2) and *La Bandiera Italiana* (§ 5.3-2). In Figure 5.52 the analysed spots are reported.

Fig. 5.52 - FORS measurement points on *N. Inv. 2625*

5.4-3 Study of the artistic materials

UV-Vis-NIR reflectance spectroscopy was successfully used to identify the pigments/dyes used by the artist, while no useful information on the paint binding media were obtained.

In considering the yellow areas, the FORS spectra registered on spots 8 and 26, which had an intense and warm colour, were found to be similar to those obtained on the FM5 and FM7 samples (Fig. 5.53). This result intimated the possible use of a lead chromate ($PbCrO_4$) mixed with a lead sulphate-based ($PbSO_4$) pigment. Indeed, the inflection point of spectrum of spot 26 was positioned at 526 nm (2.36 eV), with a shoulder at around 558 nm, similar to those of the FM5 and FM7 powders (§5.2-3). The first derivative FORS spectrum of point 8 showed an intense maximum at 526 nm, while the shoulder was more intense than those found in the spectra of the other lead chromate pigments. It also resulted in a shift to wavelengths longer than 560 nm. This behaviour could also be attributed to the presence of an orange pigment/dye in the area measured.

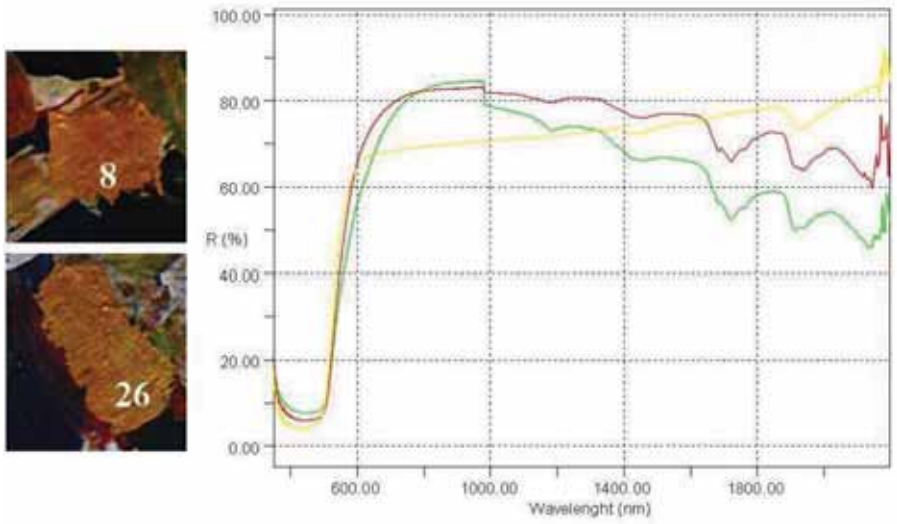

Fig. 5.53 - FORS spectra of area 8 (green line), area 26 (red line) and FM5 sample (yellow line)

The other four yellow colour spots (9, 11, 13 and 16) were made with PY3 arylide yellow. In fact, an intense absorption was found at around 425 nm, with its inflection point at 486 nm (2.55 eV), thus revealing the same spectral features registered for the FM1 powder (Fig. 5.54; §5.2-3). In addition, these spectra showed other absorption bands in the region below 1000 nm that may have been due to the other coloured materials present below the yellow paint layer, which consisted mainly of phthalocyanine green (absorptions at 614 nm, 726 nm e 786 nm). On spots 9, 13 and 16, two absorption bands at 1392 nm and 1418 nm (1st overtones of OH stretching, which may be due to the presence of kaolinite) were also present.

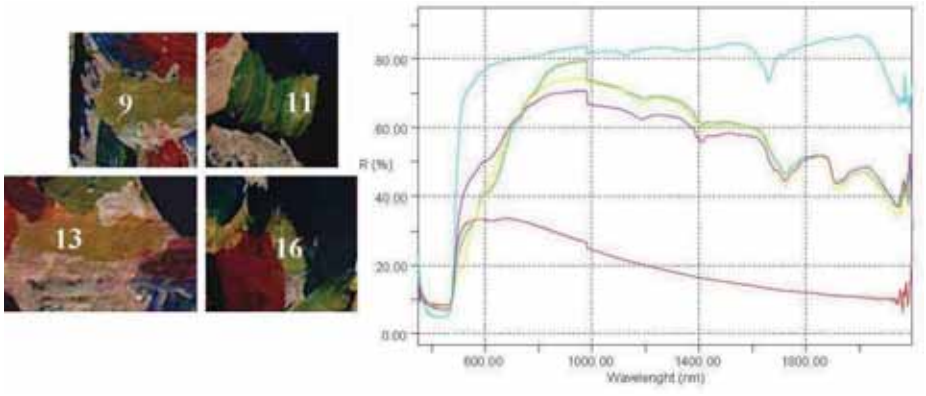

Fig. 5.54- FORS spectra of area 9 (green line), area 11 (red line), area 13 (yellow line), area 16 (violet line), and FM1 sample (cyan line)

The FORS spectra recorded on white, green, blue, purple, orange and red areas showed several absorptions bands that were due to the complex coloured texture of this particular artwork. However, the spectral features made it possible to tentatively identify the main compounds that colour the different chromatic spots.

The reflectance spectra of the white areas (spots: 10, 23 and 25; Fig. 5.55) showed the typical absorption feature of titanium white (in the rutile crystalline form), with an inflection point at around 400 nm that could be attributed to an electronic band-gap transition (energy gap: 3.09 eV) (Bacci *et al.,* 2007; Picollo *et al.,* 2007).

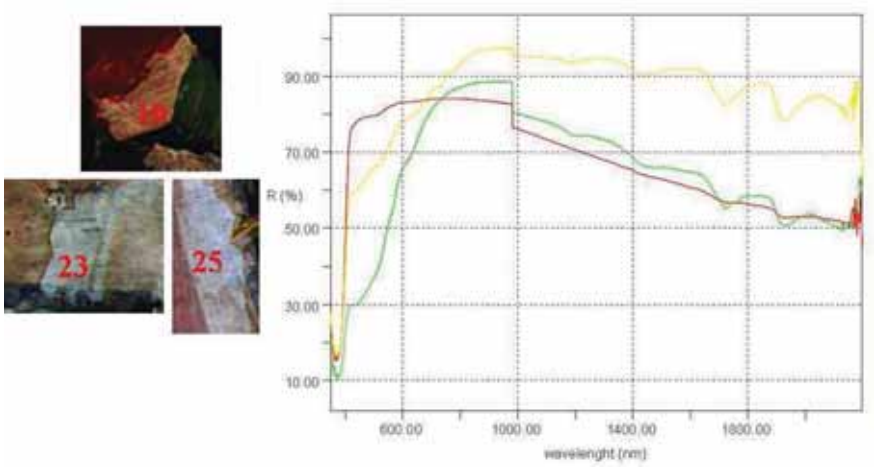

Fig. 5.55 - FORS spectra of area 10 (green line), area 23 (red line), area 25 (yellow line)

In the FORS spectrum of the blue areas (spots: 5, 6, 19 and 22; Fig. 5.56), two main absorption bands at 614 and 692 nm were evident. These features could possibly be attributed to the phthalocyanine blue dye, due to the intense π–π* transitions in the Vis region (Johnston, 1967). Other π–π* transitions were also responsible for the strong absorption in the UV region. The absorption in the UV with the inflection point at about 400 nm (3.09 eV) was also attributable to the presence of titanium white in the rutile crystalline form (Bacci *et al.*, 2007; Picollo *et al.,* 2007).

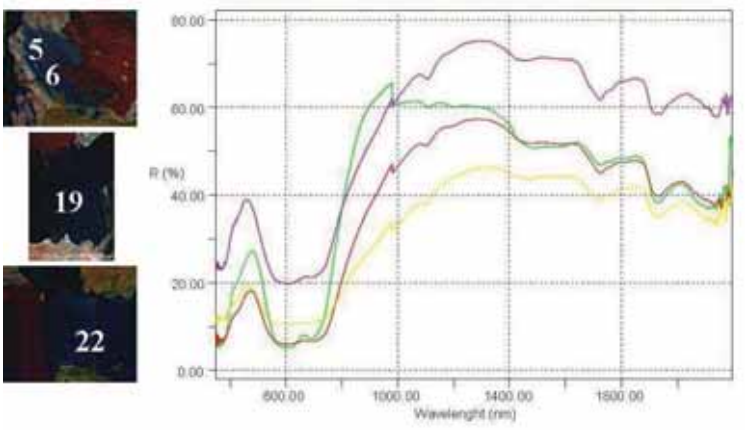

Fig. 5.56 - FORS spectra of area 5 (green line), area 6 (red line), area 19 (yellow line) and area 22 (violet line)

Spectra acquired on the green areas (spots: 3, 4, 12, 17, 27; Fig. 5.57) resembled the one of the phthalo green, since they showed four strong absorptions in the UV–Vis region (405 nm, 640 nm, 721 nm and 797 nm), that were due to intense π–π* transitions, together with absorptions in the 850–2200 nm region that were attributed to charge transfer, $a_{1u}(\pi) \rightarrow e_g(d_{xz},d_{yz})$ or n(azo) $\rightarrow \pi^*$ transitions (Johnston, 1967). The brushstroke of spot 4 may have been performed by mixing the green with a white pigment, showing the spectrum an intense absorption at 374 nm, due to the presence of titanium white in its rutile crystalline form (Bacci *et al.*, 2007*;* Picollo *et al.*, 2007), as well as the characteristic absorption bands of the chlorinated copper phthalocyanine.

Spectra of spots 12 and 17, instead, showed in the UV-Vis region, an intense absorption centred at 423 nm that was attributable to the presence of a PY3 arylide yellow. In all the green areas (except for spot 4), two absorption bands at 1392 and 1418 nm (1st overtone of OH stretching), due to the presence of kaolinite as a filler, were also evident.

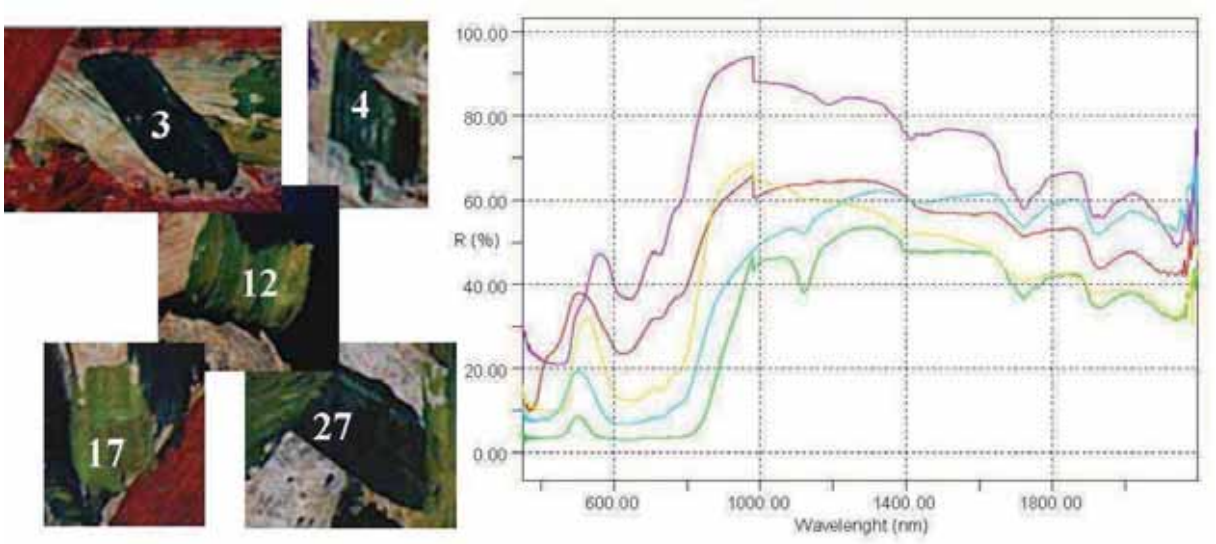

Fig. 5.57 - FORS spectra of area 3 (green line), area 4 (red line), area 12 (yellow line), area 17 (violet line) and area 27 (cyan line)

The reflectance spectra of the purple areas (spots: 20, 21, 28, 29 and 30) are shown in Fig. 5.58. These spectra had a similar profile and maybe the artist had used the same pigment (or mixture of pigments) to create the purple brushstrokes. All spectra were characterised by two maxima of reflectance in the UV-Vis regions: one was centred at 450 nm and the other, less intense, at 662 nm. The spectrum of spot 28 also presented a third maximum at 614 nm. From the data obtained it was possible to hypothesise that Melani did not use a pure purple pigment, but a mixture or superimposition of red and blue colours. Most likely, the blue used was a phthalocyanine blue. Furthermore, in the spectra of points 21, 28 and 30, an absorption at 1392 nm, due to the presence of kaolinite, was observed (1st overtone of OH stretching).

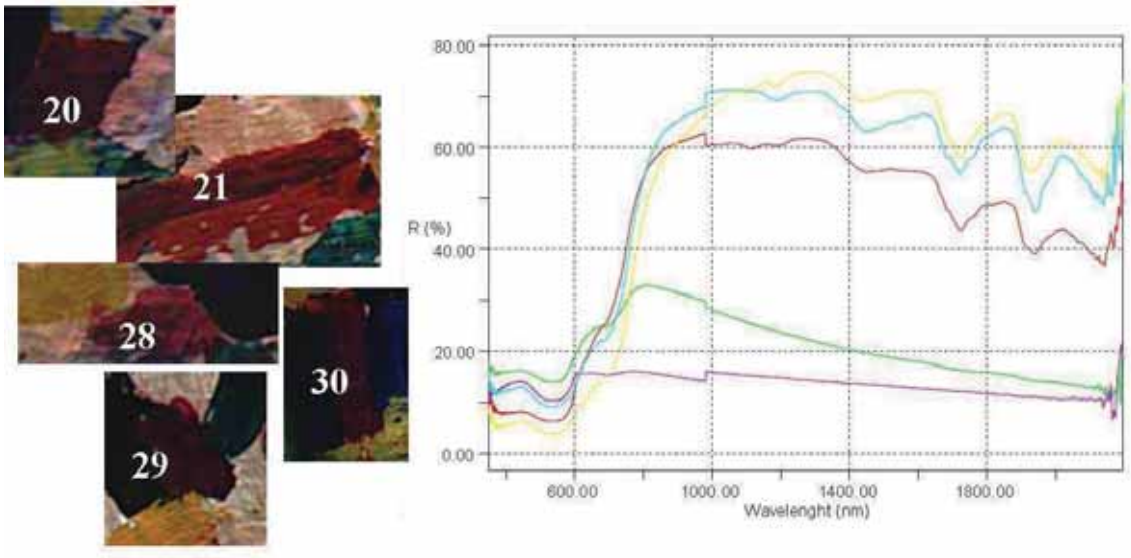

Fig. 5.58 - FORS spectra of area 20 (green line), area 21 (red line), area 28 (yellow line), area 29 (violet line) and area 30 (cyan line)

Moreover, the orange areas (spots: 14, 15 and 31) were created by using a mixture of pigments/dyes or overlapping a yellow and a red colour. In particular, an intense absorption was observed in the UV-Vis centered at 423 nm and due to the PY3 arylide yellow pigment (Fig. 5.59).

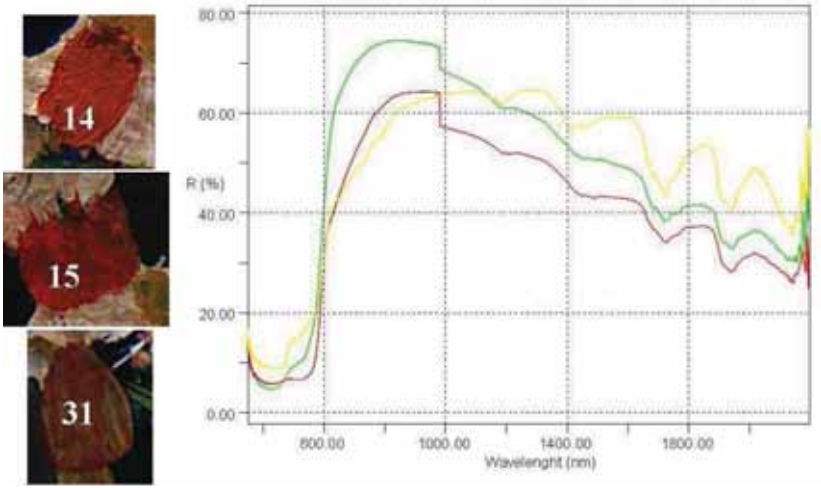

Fig. 5.59 - FORS spectra of area 14 (green line), area 15 (red line), area 31 (yellow line)

Finally, the Fig. 5.60 shows the reflectance spectra of the 1 and 2 red areas. The spectral features suggested the use of a toluidine red (PR3): indeed, a strong absorption was evident in the blue-region (centred at 488 nm, with an "S"-shape), with an inflection point at 620 nm (Johnston, 1967; Potdar, 1988). In these areas, two absorption bands at 1392 and 1418 nm (1st overtone of OH stretching), due to the presence of kaolinite as filler, were also evident.

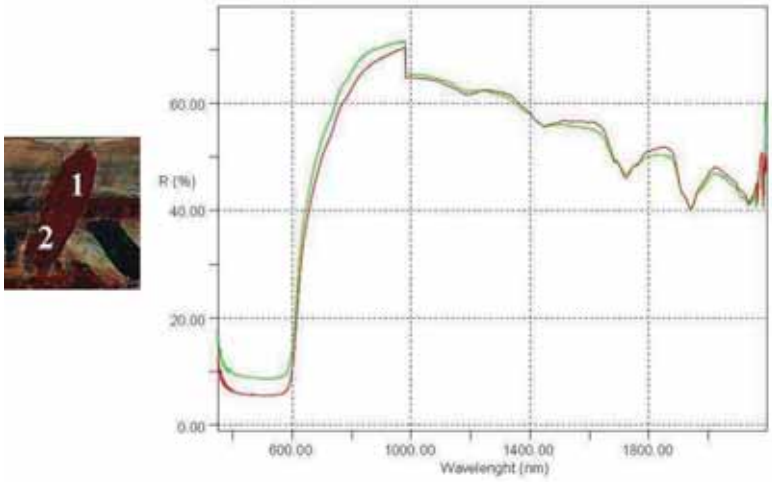

Fig. 5.60 - FORS spectra of area 1 (green line) and area 2 (red line)

5.5 Conclusion

In this chapter, the results of the spectroscopic analysis performed on the painting materials used by the Italian artist Fernando Melani (1907-1985) have been described.

The integrated use of FORS and FT-IR (with the aid, in some cases, of XRD and NMR) enabled us to successfully identify the artist's pictorial palette. The materials constituting each powder sample, with the main FT-IR and FORS absorption maxima as found in the acquired spectra are summarised in Table 5.1.

After examining the results obtained, it was possible to affirm that Melani usually used traditional inorganic pigments, such as chrome yellow, Mars yellow, Mars red, ultramarine blue, Prussian blue, and cinnabar, as well as modern organic dyes, such as Hansa yellows, toluidine red, Victoria Blue B, and phthalocyanine blue. Furthermore, he used calcite and barite as fillers. Sulphur and abrasive powder were also found, thus confirming Melani's use of non-conventional artists' materials.

Two of the artist's works were also studied using *in situ* UV-Vis-NIR reflectance spectroscopy (on *La Bandiera Italiana* and *N. Inv. 2625*) and FT-IR on samples (only on *La Bandiera Italiana*). The pigments/dyes identified with the main FORS absorption band positions,as found in the acquired spectra, are reported in Tables 5.2 and 5.3

From the data obtained, only the yellow areas in *N. Inv. 2625* were painted with the pure pigment (yellow lead chromate) and dye (arylide yellow, PY3) found in the artist's paint box

(FM5/ FM7 and FM1, respectively). Other materials, such as titanium white, phthalocyanine green, phthalocyanine blue, and toluidine red, were identified used both as pure or mixed paint or, in the case of *N. Inv. 2625*, as multiple superimposed layers.

Table 5.1– FT-IR and UV-Vis-NIR absorption band positions in the spectra acquired on the Melani powder samples

Sample	Identification	Main FTIR absorption bands (cm^{-1})	FORS absorption maxima (nm)[a]
FM1	Hansa Yellow (PY3)	3000-3150, 1666-1674, 1597,1500, 1337, 1036	λ<486 (ip) (s), 1130 (w), 1662 (sh), 2150
FM2	Hansa Yellow (PY1)	3000-3150, 2920, 2820, 1666-1674, 1600, 1500, 1346	λ <504 (ip) (s), 1130 (w), 1662 (br), 2150
FM3	Hansa Yellow (PY1)	3000-3150, 2920, 2820, 1666-1674, 1600, 1500, 1346	λ <504 (ip) (s), 1662 (w), 2150 (w)
	Calcite	2512, 1424, 875, 712	/
	Barite	1176, 1123, 1081, 635, 610	/
FM4	Lead chromate (PY34)	$PbCrO_4$: 870, 833 $PbSO_4$: 1180, 1103, 1060, 628, 600	λ <500 (ip) (s)
FM5	Lead chromate (PY34)	$PbCrO_4$: 870, 833 $PbSO_4$: 1180, 1103, 1060, 628, 600	λ <528 (ip) (s)
FM6	Yellow Iron Oxide (PY42)	3132, 904, 796, 613, 463	400 (s), 480 (s), 649 (m), 917 (m)
FM7	Lead chromate (PY34)	$PbCrO_4$: 870, 833 $PbSO_4$: 1180, 1103, 1060, 628, 600	λ <528 (ip) (s)
FM8	Toluidine red (PR3)	3150-3000, 2920, 2820, 1600, 1505, 1346	/
	Cinnabar	/	λ <600 (ip) (s)
	Calcite	2511, 1423, 875, 712	/
	Barite	1188, 1117, 1085, 611	/
FM9	Iron Oxide	544, 472 [Silicates 1096, 1200]	445 (s), 649 (sd), 870 (m)
FM10	Hansa Yellow (PY3)	3106, 1670, 1583, 1502, 1336, 1038, 810, 749, 620	λ <486 (ip) (s)
	Phthalocyanine Blue (PB15)	/	614 (m), 692 (m-sh), 1100 (w), 1660 (w), 2150 (w)
	Calcite	2511, 1425, 876, 712	/
	Barite	1178, 1103, 1083, 635, 610	/
FM11	Hansa Yellow (PY3)	3000-3150, 1666-1674, 1597,1500, 1337, 1036 [IOD00487]	λ <486 (ip) (s), 1130 (w), 1662 (w), 2150 (w)
	Phthalocyanine Blue (PB15)	/	614 (m), 692 (m-sh), 1100 (w), 1660 (w), 2150 (w)
	Calcite	2511, 1429-1492, 879, 706	/
	Barite	1185, 1120, 1082, 639, 612	/
FM12	Victoria Blue B (Basic Blue 26)	3150-3000, 2920, 2820, 1590, 1337	400 (s), 1140 (w), 1200 (w), 1440, 1680 (m), 1910(w),
FM13	Ultramarine Blue (PB29)	1010, 694, 659, 513, 451	600 (s)
	Prussian Blue (PB27)	2089	/
	Barite	1188, 1121, 1082, 983, 634, 610	/
FM14	Sulphur (S_8)	<500	400 (s)
FM15	Diaspore, α-AlO(OH) and Corundum, α-Al_2O_3	α-AlO(OH): 2910, 2117, 1984, 963, 753 α-Al_2O_3: 642 454 Both: 1080, 575-600, 520	/

[a]sh(sharp), br (broad), m (medium), s (strong), w (weak), sd (shoulder), ip (inflection point)

Table 5.2 –UV-Vis-NIR absorption band positions in the spectra acquired on the *La Bandiera Italiana*

Spot	Identification	FORS absorption maxima (nm)[a]
1	Toluidine red	λ < 620 (ip)
	Kaolinite	1382 (m), 1418 (m)
2	Toluidine red	λ < 620 (ip)
	Kaolinite	1382 (m), 1418 (m)
3	Toluidine red	λ < 620 (ip)
	Kaolinite	1382 (m), 1418 (m)
4	Toluidine red	λ < 620 (ip)
	Kaolinite	1382 (m), 1418 (m)
5		
6	Lead chromate	λ < 522 (ip), 555 (sd)
	Titanium white	λ < 400 (ip)
7	Lead chromate	λ < 522 (ip), 555 (sd)
	Titanium white	λ < 400 (ip)
8	Canvas	/
9	Titanium dioxide (rutile)	λ < 400 (ip)
10	Titanium dioxide (rutile)	λ < 400 (ip)
11	Titanium dioxide (rutile)	λ < 400 (ip)
12	Titanium dioxide (rutile)	λ < 400 (ip)
13	Titanium dioxide (rutile)	λ < 400 (ip)
14	Titanium dioxide (rutile)	λ < 400 (ip)
15	Ultramarine blue	600 (s)
	Kaolinite	1394(m),1418 (m)
16	Unidentified pigment/dye	/
17	Ultramarine blue	600 (s)
	kaolinite	1394(m),1418 (m)
18	Phthalo green	405 (s), 640 (s), 721 (s), 797 (s)
	kaolinite	1395 (m),1415 (m)
19	Phthalo green	405 (s), 640 (s), 721 (s), 797 (s)
	Kaolinite	1395 (m),1415 (m)
20	Phthalo green	405 (s), 640 (s), 721 (s), 797 (s)
	Kaolinite	1395 (m),1415 (m)
21	Phthalo green	405 (s), 640 (s), 721 (s), 797 (s)
	Kaolinite	1395 (m),1415 (m)
22	Phthalo green	405 (s), 640 (s), 721 (s), 797 (s)
	Kaolinite	1395 (m),1415 (m)
23	Unidentified pigment/dye	/
24	Carbazole violet (PV23)	530 nm, 569 nm, 627 nm and 697
	Titanium white (rutile)	λ < 400 (ip)
25	Carbazole violet (PV23)	530 nm, 569 nm, 627 nm and 697
	Titanium white (rutile)	λ < 400 (ip)
26	Titanium dioxide (anatase)	λ < 372 (ip)
27	Titanium dioxide (anatase)	λ < 372 (ip)

[a]sh (sharp), br (broad), m (medium), s (strong), w (weak), sd (shoulder), ip (inflection point)

Table 5.3 –UV-Vis-NIR absorption band positions in the spectra acquired on the *N. Inv. 2625*

Spot	Identification	FORS absorption maxima (nm)[a]
1	Toluidine red	λ < 620 (ip)
	Kaolinite	1382 (m), 1418 (m)
2	Toluidine red	λ < 620 (ip)
	Kaolinite	1382 (m), 1418 (m)
3	Phthalo green	405 (s), 640 (s), 721(s), 797(s)
4	Phthalo green	405 (s), 640 (s), 721(s), 797(s)
	Titanium white (rutile)	λ < 400 (ip)
	Kaolinite	1392 (m), 1418 (m)
5	Phthalo Blue	614 (s), 692 (s)
	Titanium white (rutile)	λ < 400 (ip)
6	Phthalo Blue	614 (s), 692 (s)
	Titanium white (rutile)	λ < 400 (ip)
7	Black pigment	/
8	Lead Chromate mixed lead sulphate	λ < 526 (ip)
9	Hansa yellow (PY1)	λ < 486 (ip)
	Phthalo green	614 (s), 726 (s), 786 (s)
	Kaolinite	1392 (m), 1418 (m)
10	Titanium dioxide (rutile)	λ < 400 (ip)
11	Hansa yellow (PY3)	λ < 486 (ip)
	Phthalo green	614 (s), 726 (s), 786 (s)
12	Phthalo green	405 (s), 640 (s), 721(s), 797(s)
	Hansa yellow (PY3)	λ < 486 (ip)
	Kaolinite	1392 (m), 1418 (m)
13	Hansa yellow (PY1)	λ < 486 (ip)
	Phthalo green	614 (s), 726 (s), 786 (s)
	Kaolinite	1392 (m), 1418 (m)
14	Hansa yellow (PY3)	λ < 486 (ip)
	Unidentified red pigment/dye	/
15	Hansa yellow (PY3)	λ < 486 (ip)
	Unidentified red pigment/dye	/
16	Hansa yellow (PY1)	λ < 486 (ip)
	Phthalo green	614 (s), 726 (s), 786 (s)
	Kaolinite	1392 (m), 1418 (m)
17	Phthalo green	405 (s), 640 (s), 721(s), 797(s)
	Hansa yellow (PY3)	λ < 486 (ip)
	Kaolinite	1392 (m), 1418 (m)
18	Unidentified pigment/dye	/
19	Phthalo Blue	614 (s), 692 (s)
	Titanium white (rutile)	λ < 400 (ip)
20	Phthalo Blue	614 (s), 692 (s)
	Unidentified red pigment/dye	/
21	Phthalo Blue	614 (s), 692 (s)
	Unidentified red pigment/dye	/
	Kaolinite	1392 (m), 1418 (m)
22	Phthalo Blue	614 (s), 692 (s)
	Titanium white (rutile)	λ < 400 (ip)
23	Titanium dioxide (rutile)	λ < 400 (ip)
24	Unidentified pigment/dye	/
25	Titanium dioxide (rutile)	λ < 400 (ip)
26	Lead Chromate mixed lead sulphate	λ < 526 (ip)
27	Phthalo green	405 (s), 640 (s), 721(s), 797(s)
	Kaolinite	1392 (m), 1418 (m)
28	Phthalo Blue	614 (s), 692 (s)
	Unidentified red pigment/dye	/

	Kaolinite	1392 (m), 1418 (m)
29	Phthalo Blue	614 (s), 692 (s)
	Unidentified red pigment/dye	/
30	Phthalo Blue	614 (s), 692 (s)
	Unidentified red pigment/dye	/
	Kaolinite	1392 (m), 1418 (m)
31	Hansa yellow (PY3)	$\lambda < 486$ (ip)
	Unidentified red pigment/dye	/

[a]sh(sharp), br (broad), m (medium), s (strong), w (weak), sd (shoulder), ip (inflection point)

CHAPTER 6 – KEITH HARING

"The best reason to paint is that there is no reason to paint.
I'd like to pretend that I've never seen anything, never read anything,
never heard anything…and then make something.
Every time I make something I think about the people who are going
to see it and every time I see something I think about the person who made it.
Nothing is important…so, everything is important"
Keith Haring, 25th June 1986

6.1 Keith Haring

6.1-1 Short biography

Keith Allen Haring was born on 4 May 1958 in Reading, Pennsylvania, the eldest of four children. He grew up nearby Kutztown, where he developed a love for drawing at a very early age. He learnt basic cartooning skills from his father[1], an amateur artist, and from the popular culture of that period (i.e. Walt Disney, Charles Schulz, the Looney Tunes characters, and so on).

Fig. 6.1 – Keith Haring in front of the *Tuttomondo* mural, Pisa, 1989
[Image from: http://www.haring.com/!/archives/in-his-own-words/transitions/attachment/pisa_keith; last access November 7, 2013]

After graduating from high school in 1976, Haring enrolled in the Ivy School of Professional Art in Pittsburgh, where he studied commercial graphic design. After just two semesters, however, he dropped out in order to devote himself exclusively to art. He then started to work on his own, and in 1978, at the age of only 19, had a solo exhibition at the Pittsburgh Arts and Crafts Center. Later that same year, Haring moved to New York and enrolled in the School of Visual Arts (SVA). The social scene in New York's East Village in the 1980s greatly influenced him and his art. There, he became a prominent figure in the underground art world, presenting his works on the streets, subways and in clubs, where everybody could see them.

[1] *"[…] My father made cartoons. Since I was little, I had been doing cartoons, creating characters and stories. In my mind, though, there was a separation between cartooning and being an 'artist'…"*(Sheff, 1989)

Indeed, Haring was of the opinion that art should be accessible to everybody, and not just to an exclusive elite (Haring, 2001; Kolossa, 2009).

In those years he established friendships with emerging artists such as Kenny Scharf and Jean-Michel Basquiat, as well as with musicians, performing artists, and graffiti writers who comprised the rapidly expanding art community. Between 1980 and 1989, Haring achieved international recognition and participated in numerous exhibitions. His first solo exhibition in New York was held at the Westbeth Painters Space in 1981. He also participated in international exhibitions such as Documenta 7 in Kassel, the São Paulo Biennial, and the Whitney Biennial (Barilli, 2000). Throughout his career, Haring devoted much of his time to public works, which often carried social messages. He produced more than 50 public artworks between 1982 and 1989, in dozens of cities around the world. Many of these were created for charities, hospitals, children's day care centres, and orphanages. *The Radiant Baby* became his symbol (Fig. 6.2).

Fig. 6.2 – *The Radiant Baby*
[Image from: http://www.graffiti-world.de/tag/radiant-baby/; last access November 8, 2013]

His artworks were easily identifiable by their characteristic bold lines, vivid colours, and active figures that carried strong messages of life and unity. By expressing universal concepts such as birth, death, love, sex and war, Haring attracted a wide audience, and his art became a universally recognised visual language of the 20th century (Clausen, 2010). For example, his famous *Crack is Wack* mural, created in 1986, has become a landmark on New York's FDR Drive (Fig. 6.3).

Fig. 6.3 – *Crack is wack* mural (1986) in FDR Drive (New York); front (A) and back (B)
[Images from: http://www.thingstoseenyc.com/tag/crack-is-wack-fdr; last access November 8, 2013]

In 1984, Haring visited Australia and painted wall murals in Melbourne and Sydney. He also visited and painted in Rio de Janeiro, Minneapolis, Phoenix, the borough of Manhattan, Amsterdam, Paris, and Berlin, on the Berlin Wall at the Brandenburg Gate. In April 1986, Haring opened his first *Pop Shop* in New York's Soho, a retail store which sold T-shirts, toys, posters, buttons and magnets bearing his figures. Haring considered the shop as a means to enabling people to have greater access to his work (Kolossa, 2009).

Haring was diagnosed with AIDS in 1988. In 1989, he established the foundation that bears his name. The purpose of the *Keith Haring Foundation* was and is to provide funding and imagery to AIDS research organisations and children's programs. In addition, its mandate is to expand the audience for Haring's work through exhibitions, publications and the loan of pictures (www.haring.com; last access November 8, 2013).

In the early hours of the morning of 16 February 16 1990, Keith Haring died of AIDS-related complications at the age of just 31 (Gruen, 2007). He left an enormous *œuvre* complet of drawings and paintings, murals and sculptures, as well as countless printed T-shirts and posters. Since his death, Haring has been the subject of several international retrospectives. The work of Keith Haring can be seen today in the exhibitions and collections of major museums around the world, including the Museum of Modern Art and the Whitney Museum of American Art (New York), the Los Angeles County Museum of Art, the Art Institute of Chicago, the Centre Georges Pompidou (Paris), and the Stedelijk Museum (Amsterdam).

6.2 Case study: *Tuttomondo*

6.2-1 The artwork

Tuttomondo (1989) is a large mural (Fig. 6.4) painted by Keith Haring (1958-1990) on the wall of the Church of Sant'Antonio Abate in Pisa (Italy), and is the artist's last public work (Bardelli, 2003).

Fig. 6.4 - *Tuttomondo* (image acquired by the ICCOM-CNR group of Pisa within the framework of the CoPAC Project)

This artwork project arose from a chance meeting between Keith Haring and Piergiorgio Castellani, a student of the University of Pisa. For the first time in Haring's artistic career, this mural was intended to be permanent. It thus entailed precise technical choices, with support from Caparol Italy GmbH & Co., which supplied free of charge the scaffolding and the long-lasting acrylic paints chosen specifically by Haring, together with the paint brushes (Fig. 6.5).

Fig. 6.5 - Haring's original paint brushes, stored at the headquarter of Caparol Italy GmbH & Co. at Lugnano,Vicopisano (Pisa) (image acquired on 29 August 2011)

Caparol also prepared the support of the painting using the "sistema a cappotto" ("overcoat system". Fig. 6.6) consisting of boards of polystyrene foam (which insulate the mural from dampness by blocking any direct contact with the plaster) coated with a white primer that contains quartz and calcite, with a styrene-acrylic resin as binding medium (Bardelli, 2003).

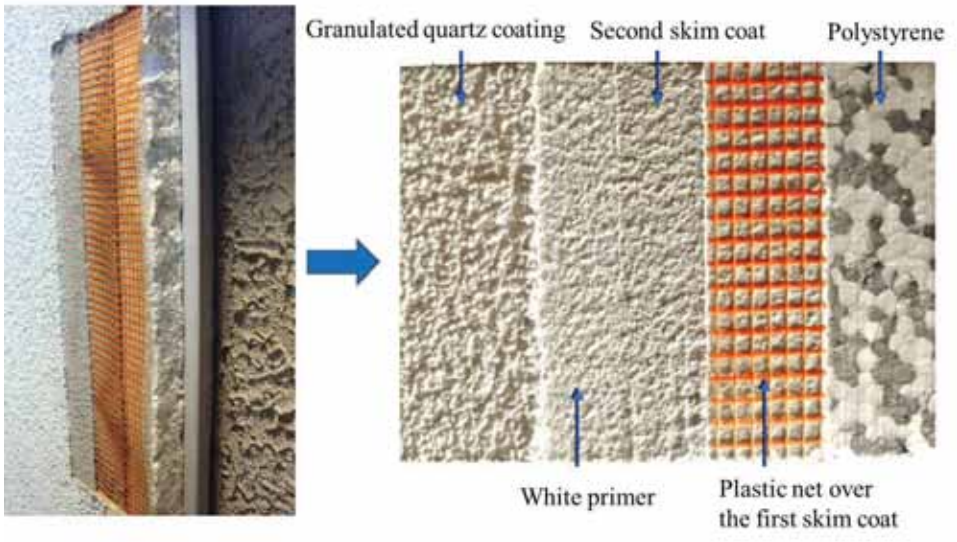

Fig. 6.6 - The Caparol "sistema a cappotto" ("overcoat system") on display at the headquarters of Caparol Italy GmbH & Co. at Lugnano,Vicopisano (Pisa) (image acquired on 29 August 2011)

The artist and his collaborators painted thirty figures, covering an area of approximately 180 m^2, in the space of one week (from June 14 to 20, 1989) without any preparatory sketches.

The figures represent the theme of “harmony and peace in the world”, and suggest the variety of aspects of human co-existence in society (Bardelli, A. 2003; Barilli, A. 2000).

Twenty-two years after its creation, the mural was in a relatively good state of conservation. Nevertheless, alterations and a fading of the colours, with a yellowing and darkening of the white background and losses in the black lines could be observed (Fig. 6.7).

Fig. 6.7 – *Tuttomondo*, darkening of a white background area

Therefore, a diagnostic survey[2] was started in September 2011 to evaluate the state of conservation of the mural, to support a scheduled conservation intervention for the cleaning of the surface, and, subsequently, to address several of the issues of its preventive conservation.

In particular, the FORS analysis was mainly focussed on obtaining preliminary information on the composition of the acrylic paints used by the artist. Colour measurements were used, instead, primarily to support the restorers in the choice of the best cleaning procedure. Subsequently, colour variations occurred during the cleaning treatment ,and the stability of the conservation intervention were monitored from time to time using a colorimeter. The results of the FORS and colorimetric analyses will be presented in the following sections.

6.2-2 Experimental

FORS

FORS measurements in the 350-2200 nm spectral range were acquired *in situ* on 67 small areas of the mural on the first floor of the scaffolding (Fig. 6.8), and provided useful information for the identification of the pigments/dyes present in the acrylic paints used by the artist. FORS spectra in the UV-Vis-NIR spectral range (350–2200 nm) were acquired thanks to two single-beam *Zeiss* spectroanalysers, model *MC601* (190-1015 nm range) and model *MC611 NIR 2.2WR* (910-2200 nm range), which were housed together in a compact and portable *chassis* for *in situ* analyses. The data acquisition step was 0.8 nm/ pixel for the 1024-element silicon photodiode array detector (*MCS601*) and 6.0 nm/pixel for the 256-element InGaAs diode array detector (*MCS611 NIR 2.2 WR*). The radiation between 320 nm

[2] The diagnostic campaign was performed within the framework of the CoPAC Project, with the support of the city of Pisa and the Friends of Heritage Preservation (USA).

and 2700 nm, which was provided by a voltage-stabilized 20W halogen lamp (mod. CLH600), was conveyed to the sample by means of a quartz optical fibre bundle that also transported the reflected radiation to the detectors. The geometry of the probe head was 8°/8°. Calibration was performed by means of a 99% Spectralon® diffuse reflectance standard. Each spectrum was the average calculated on three acquisitions. Spectra were processed using Aspect Plus® 1.80 software.

Fig. 6.8 - FORS measurement points

Colorimetry

Colorimetric analysis was used to help to select the most appropriate cleaning procedure and to monitor the state of the artwork during and after the conservation treatments. Colour data were acquired using two Konica-Minolta spectrophotometers: model *CM-2002* (for the choice of the best cleaning method) and model *CM-700d* (for the monitoring during and after the cleaning procedure). Both instruments were equipped with an integrating sphere. They had a d/8° measurement geometry, and operated in the 400-700 nm spectral range (acquisition step: 10 nm). The light source and detector consisted of a pulsed xenon lamp with UV cut filter and a silicon photodiodes array, respectively. The instruments were provided with their own white reference (100% reflective) and a zero calibration box (0% reference).

Colour data were calculated for D65 illuminant, 10° supplementary standard observer, and excluded the specular component of light. The results reported were based on an average of three measurements; colorimetric coordinates (L*, a*, b*) and chroma[3] (C*) were calculated for the CIEL*a*b* 1976 colour space. For each measurement, the instrument was positioned repeatedly on exactly the same spot (Ø 8 mm) using a repositioning mask, and was removed immediately afterwards. The total colour differences were calculated, on average values, as Δ(L*a*b*) and ΔE^*_{ab}[4].

[3] Chroma value was calculated by using this formula: $\mathbf{C^* = \sqrt{a^{*2} + b^{*2}}}$

[4] ΔE^*_{ab} was calculated by using this formula: $\mathbf{\Delta E^*_{ab} = \sqrt{\left(L^*_1 - L^*_2\right)^2 + \left(a^*_1 - a^*_2\right)^2 + \left(b^*_1 - b^*_2\right)^2}}$

6.2-3 Study of the artistic materials

FORS

The spectra collected on the whitish background support (Fig. 6.9) showed the typical absorption feature of titanium white in its rutile crystalline form, as demonstrated by its inflection point, which was positioned at around 400 nm, and it was due to an electronic band-gap transition (energy gap: 3.09 eV) (Hunt *et al.*, 1971; Bacci *et al.*, 2007; Picollo *et al.*, 2007). Rutile was also used by the artist in mixtures with pure colours in order to paint the coloured areas.

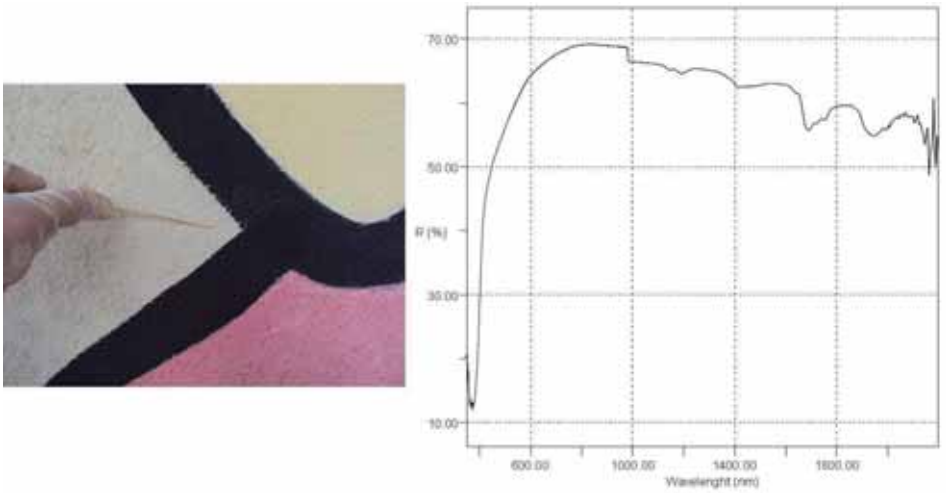

Fig. 6.9 - FORS spectrum of the background (spot 1)

Burgundy, red and pink areas were obtained using three different red pigments. In particular, the FORS spectra acquired on the burgundy spots (Fig. 6.10) showed two absorption bands at 530 nm (due to the charge transfer transition of the Fe-O bond.) and at 865 nm (due to ligand field transitions of the Fe^{3+} ion), characteristic of hematite (α-Fe_2O_3; Sherman and Waite, 1985; Cornell and Schwertmann, 1996). It is possible that a blue pigment was also present in the mixture, given that the spectra showed a maximum of reflectance at around 415 nm in the visible region.

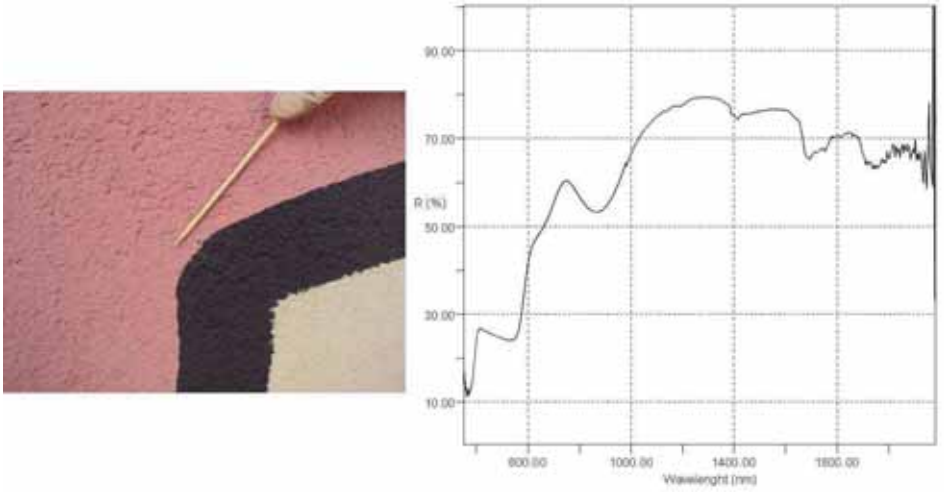

Fig. 6.10 - FORS spectrum of the burgundy area (spot 59)

The spectra collected on the red and pink areas presented the typical spectral shape of organic red dyes. The positions of the absorption bands, however, were not the same for the two colours, which were made with two different dyes. In fact, the spectra acquired on the red spots (Fig. 6.11) showed two absorption bands at 520 nm and 556 nm that could be attributed to the presence of a quinacridone red (Johnston-Feller, 2001). Instead, those acquired on the pink spots (Fig. 6.12) showed two absorptions at 498 nm and 535 nm, and these were attributable to the presence of another organic compound, perhaps an orange dye such as tetracene. The reflectance spectrum of tetracene should show another less intense absorption band at about 470 nm, which however was not visible in the spectra acquired on the wall. Possibly this was because it was partially covered by scattering due to dirt, which could have altered the spectral response in the visible region.

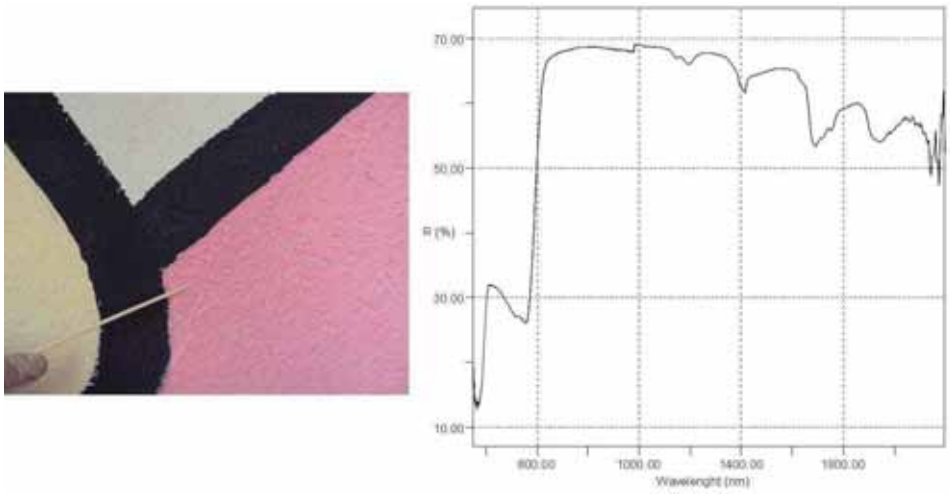

Fig. 6.11 - FORS spectrum of the red area (spot 5)

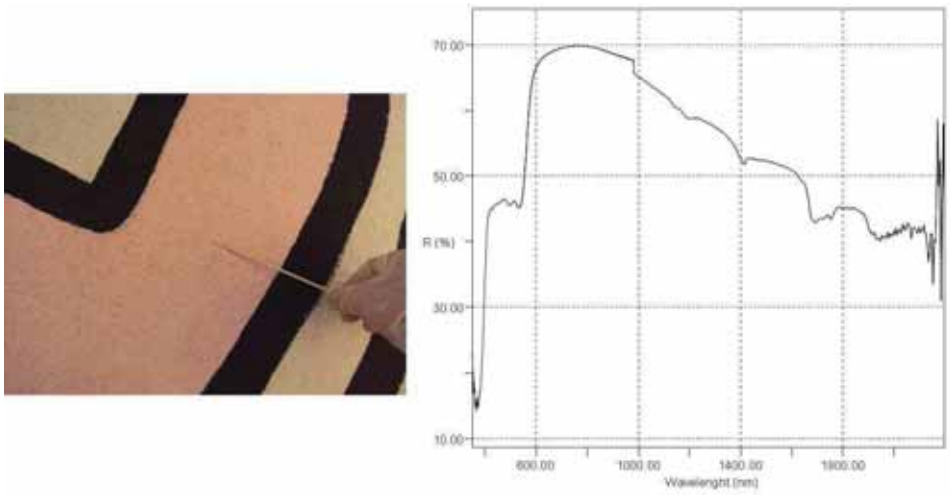

Fig. 6.12 - FORS spectrum of the pink area (spot 61)

The spectra acquired on the yellow areas (Fig. 6.13) showed an "S"-shape spectral feature with an inflection point at around 505 nm (2.45 eV), which was probably due to the presence of PY3 arylamide yellow pigment (Schunck and Hunger, 1988). If pure, this pigment should show an inflection point at about 486 nm, while its behaviour in a mixture with other

materials has not yet been determined by means of the FORS technique. It can therefore be assumed that the anomalous shift in the spectra acquired on the mural was due to the pigment's being mixed with titanium white, which increases reflectance in the visible range.

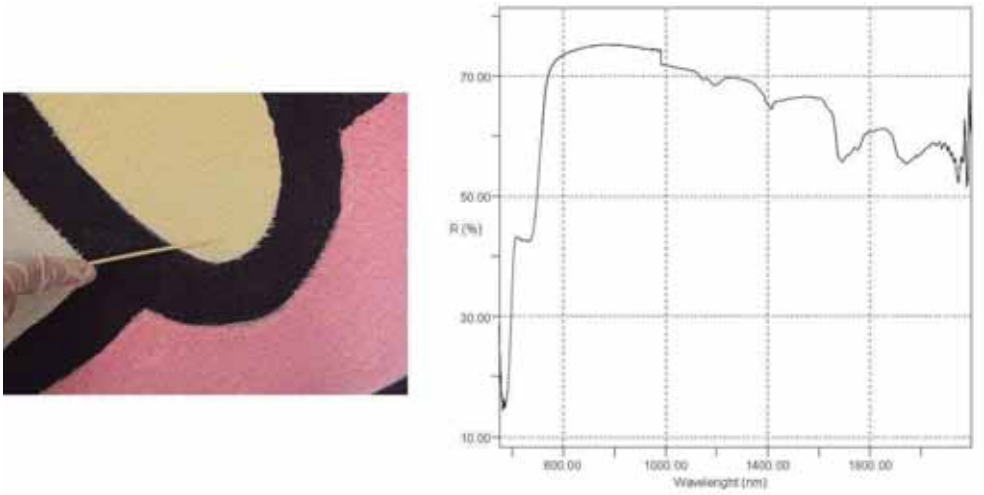

Fig. 6.13 - FORS spectrum of the yellow area (spot 3)

Green and blue areas showed the characteristic spectral features of phthalocyanine pigments. As regards the green area (Fig. 6.14), absorption bands at 450 nm, 650 nm, 730 nm and 780 nm (due to intense π–π* transitions) and attributable to a phthalo green pigment were observed (Johnston, 1967).

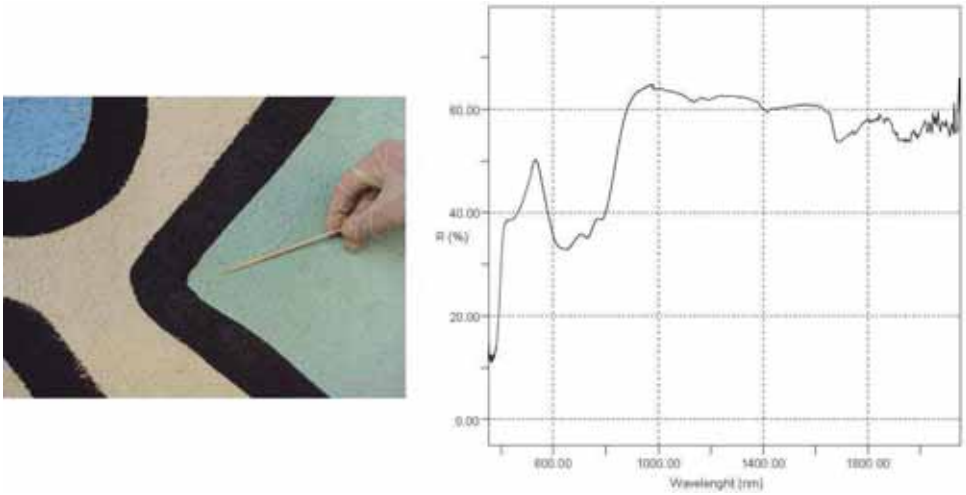

Fig. 6.14 - FORS spectrum of the green area (spot 55)

In the blue areas, a phthalo blue pigment was identified (Fig. 6.15). Its presence was confirmed by two absorption bands at 620 nm and 715 nm, with a shoulder at around 430 nm due to the intense π–π* transitions. Two other bands at about 910 nm and 1100 nm, which were due to the second overtone of the CH stretching group, were also present (Tomas Rubio, 2006).

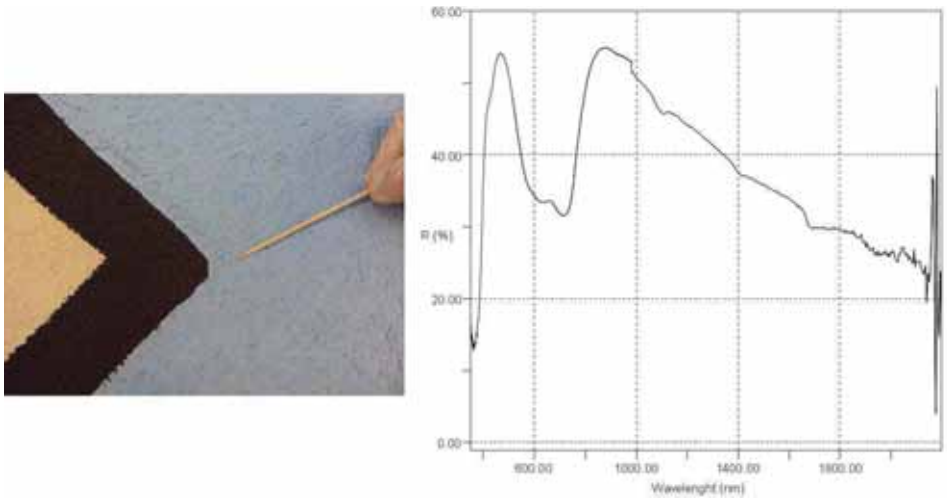

Fig. 6.15 - FORS spectrum of the blue area (spot 47)

Lastly, the FORS spectra acquired on the violet areas (Fig. 6.16) showed three absorption bands at around 540 nm, 567 nm and 627 nm, due to the presence of a carbazole dioxazine violet dye (Kaul and Wihan, 1988; Johnston-Feller, 2001).

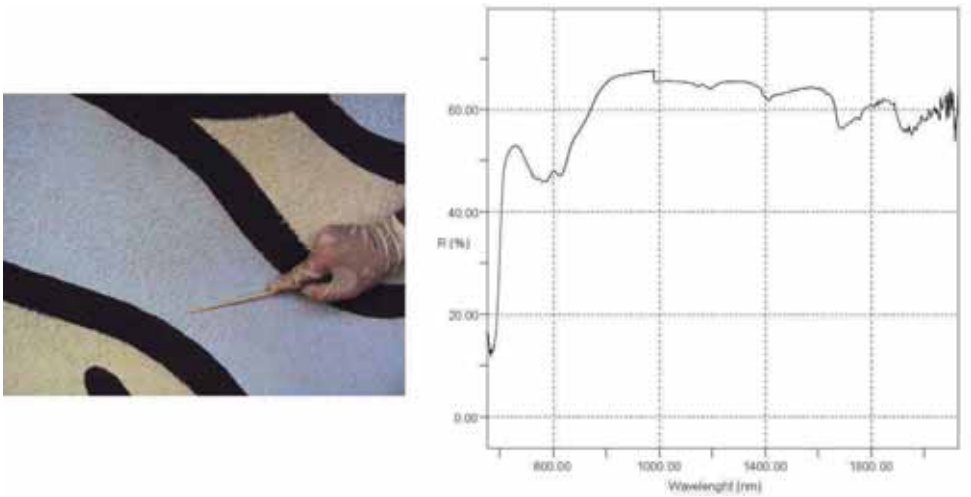

Fig. 6.16 - FORS spectrum of the violet area (spot 38)

UV-Vis-NIR reflectance spectra recorded on the black lines did not provide any specific information on the chemical composition of the pigments used by the artist. This was impossible because of the presence of a strong absorption band that covered the entire spectral range being investigated.

The spectra of all the coloured area also showed two absorption bands in the NIR region, at 1394 nm and 1414 nm, that were due to the presence of kaolinite (Bacci *et al.*, 2007). It can be assumed that the kaolinite was used as an inert in the paint formulation of the pure colours, whereas its absorptions were not present in the spectra acquired on the white background.

6.2-4 Colour measurements for the choice of the best cleaning method

The colorimetric survey was applied in order to identify a suitable cleaning system. A series of measurements were made over the entire surface of the painting. Different areas of the

mural were selected, under the supervision of the conservators, in order to carry out various cleaning tests. Measurements were acquired before and after each cleaning treatment in order to assess the effectiveness of the various systems. Brushes, sponges, rubbers, agar-agar, water solutions of EDTA (ethylenediaminetetracetic acid) and ammonium carbonate, and combinations of these solutions with agar-agar, were used in the said cleaning tests. The first survey regarded the colour variations due to a dry cleaning with the use of a brush, on the first floor of the scaffolding (6.17). The colorimetric values (L*, a*, b*, C*) and the ΔE_{ab} differences for each colour pattern are reported in Table 6.1.

Fig. 6.17 - Cleaning test carried out with the use of a brush (image acquired on 31 August 2011)

Table 6.1 - Colorimetric values (L*, a*, b*, C*) and ΔE_{ab} colour differences before (t_0) and after the cleaning test by brush (t_1) or with a damp sponge (t_2). Each value is the average of three measurements (± = max error)

Colour	**Spot**	**t_0**			**t_1**			**$\Delta E(t_1 - t_0)$**	**t_0**	**t_1**
		L*	**a***	**b***	**L***	**a***	**b***		**C***	**C***
burgundy	1	56.67 ± 0.07	15.52 ± 0.02	11.15 ± 0.05	58.62 ± 0.10	13.67 ± 0.02	8.46 ± 0.02	3.80 ± 0.08	19.11	16.08
red	2	66.70 ± 0.31	27.08 ± 0.10	12.63 ± 0.03	66.93 ± 0.08	26.57 ± 0.03	11.70 ± 0.04	1.11 ± 0.06	29.88	29.03
pink	3	80.81 ± 0.44	9.49 ± 0.05	13.32 ± 0.04	81.32 ± 0.29	8.99 ± 0.09	11.57 ± 0.02	1.93 ± 0.19	16.36	14.65
yellow	4	80.23 ± 0.34	0.30 ± 0.07	25.28 ± 0.20	80.19 ± 0.16	0.10 ± 0.04	21.81 ± 0.11	3.49 ± 0.32	25.28	21.81
orange	5	70.36 ± 0.32	7.08 ± 0.03	31.26 ± 0.11	71.82 ± 0.05	5.95 ± 0.01	27.49 ± 0.01	4.20 ± 0.11	32.06	28.13
green	6	73.65 ± 0.10	-10.64 ± 0.02	2.93 ± 0.01	74.39 ± 0.13	-10.58 ± 0.02	1.23 ± 0.01	1.86 ± 0.09	11.03	10.65
blue	7	64.84 ± 0.22	-6.25 ± 0.02	-13.43 ± 0.13	61.30 ± 0.14	-7.21 ± 0.05	-15.98 ± 0.04	4.47 ± 0.19	14.81	17.53
violet	8	74.57 ± 1.42	1.85 ± 0.01	-0.42 ± 0.05	76.58 ± 0.42	1.69 ± 0.01	-2.89 ± 0.07	3.32 ± 0.95	1.90	3.35
black	9A	28.65 ± 0.03	0.64 ± 0.03	0.71 ± 0.01	31.67 ± 0.11	0.49 ± 0.01	-0.10 ± 0.01	3.13 ± 0.14	0.96	0.50
background	10	79.63 ± 0.05	1.16 ± 0.01	12.41 ± 0.02	79.35 ± 0.28	1.05 ± 0.01	10.60 ± 0.04	1.85 ± 0.10	12.47	10.65
black	9B	33.13 ± 0.15	0.47 ± 0.01	0.72 ± 0.05	37.52 ± 0.03	0.25 ± 0.01	-0.23 ± 0.01	4.49 ± 0.17	0.86	0.34
		t_1			**t_2**			**$\Delta E(t_2 - t_1)$**	**t_1**	**t_2**
		37.52 ± 0.03	0.25 ± 0.01	-0.23 ± 0.01	36.01 ±0.07	0.15 ± 0.01	-0.34 ± 0.02	1.51 ± 0.11	0.34	0.37
		t_0			**t_2**			**$\Delta E(t_2 - t_0)$**	**t_0**	**t_2**
		33.13 ± 0.15	0.47 ± 0.01	0.72 ± 0.05	36.01 ±0.07	0.15 ± 0.01	-0.34 ± 0.02	3.09 ± 0.17	0.86	0.37

On a black area (spot 9B), the cleaning by means of a damp sponge (t_2) was performed after treatment with a brush (t_1). The data obtained demonstrated that the effectiveness of the cleaning using a brush was poor. In fact, the colour differences were low (ΔE max: 4.47 in the spot 7). Moreover, in all cases (except for the blue and violet areas) the chroma values decreased, resulting in a loss of saturation. This result enabled us to hypothesise that the said brush cleaning removed not only the dirt, but also the paint.

The second colorimetric survey was performed on the second floor of the scaffolding, where cleaning tests by means of a rigid rubber were carried out (Fig. 6.18).

Fig. 6.18 - Cleaning tests carried out by means of a rigid rubber in the green/pink areas (A) and in the yellow/blue areas (B) (images acquired on 8 September 2011)

The results are reported in Table 6.2. Since the black paint was very fragile and tended to lose materials even during soft contact procedures, it was necessary to consolidate it with an acrylic resin. The colour difference of this area was therefore calculated on the same spot before and after the consolidation treatment.

The data obtained demonstrated that the cleaning using rubber was more effective than the one using a brush (ΔE max: 15.08 in the blue area), which in many cases increased the colour saturation. In the burgundy and orange areas, however, the colour differences were mainly due to variations in the L* coordinate, and this decreased after the cleaning test. It thus seemed that the cleaning methodology selected, i.e. the one with the mechanical action of the rubber, partially removed these two pigments/dyes. In the black areas after consolidation, a decrease was registered in the L* value, which resulted in a more saturated/intense colour.

Chemical cleaning tests were carried out on the first floor of the scaffolding using agar-agar (a polysaccharidic gelling agent) alone or mixed with ammonium carbonate, together with solutions of ammonium carbonate/water or EDTA/water. As reported in Table 6.3, the best results were obtained with the solutions of ammonium carbonate and EDTA in water, while the use of agar was less effective.

Table 6.2 - Colorimetric values (L*, a*, b*, C*) and ΔE_{ab} colour differences before (t_0) and after the cleaning test by rubber (t_1). In the black area t_1 refers to the consolidation treatment with acrylic resin.
Each value is the average of three measurements (± = max error)

Colour	t_0			t_1			$\Delta E(t_1 - t_0)$	t_0	t_1
	L*	a*	b*	L*	a*	b*		C*	C*
burgundy	57.63 ± 0.04	16.85 0	10.36 0	57.30 ± 0.16	17.03 ± 0.08	9.31 ± 0.03	1.12 ± 0.09	19.78	19.40
red	70.47 ± 0.09	23.90 ± 0.02	10.10 ± 0.02	63.55 ± 0.07	32.76 ± 0.04	14.29 ± 0.03	12.00 ± 0.08	25.94	35.74
pink	79.33 ± 0.06	13.02 ± 0.01	13.18 ± 0.01	78.11 ± 0.03	18.19 ± 0.01	16.23 ± 0.01	6.13 ± 0.02	18.53	24.38
yellow	78.65 ± 0.11	1.42 ± 0.01	23.66 ± 0.03	83.83 ± 0.10	0.09 ± 0.01	35.71 ± 0.01	13.18 ± 0.09	23.70	35.71
orange	69.76 ± 0.18	6.77 ± 0.01	31.57 ± 0.05	72.90 ± 0.27	6.66 0	31.58 ± 0.05	3.14 ± 0.45	32.29	32.28
green	72.37 ± 0.08	-10.26 ± 0.01	4.10 ± 0.01	71.19 ± 0.09	-18.26 ± 0.02	-0.40 ± 0.01	9.26 ± 0.03	11.05	18.27
blue	65.15 ± 0.13	-5.78 ± 0.01	-13.97 ± 0.02	58.76 ± 0.22	-9.86 ± 0.01	-27.00 ± 0.05	15.08 ± 0.17	15.12	28.75
violet	75.58 ± 0.02	1.82 ± 0.01	-2.37 ± 0.01	74.20 ± 0.70	3.70 ± 0.02	-8.42 ± 0.08	6.49 ± 0.05	2.99	9.20
black	30.02 ± 0.05	0.61 ± 0.01	0.56 ± 0.02	24.71 ± 0.08	0.63 ± 0.01	0.40 ± 0.02	5.31 ± 0.10	0.83	0.75
background	77.96 ± 0.03	0.90 0	12.80 ± 0.01	84.63 ± 0.14	0.32 0	7.49 ± 0.01	8.55 ± 0.12	12.84	7.49

Table 6.3 - Colorimetric values (L*, a*, b*) and ΔE_{ab} colour differences before (t_0) and after (t_1) the cleaning tests.
Each value is the average of three measurements (± = max error)

Cleaning method	Colour	t_0			t_1			$\Delta E(t_1 - t_0)$	t_0	t_1
agar-agar		L*	a*	b*	L*	a*	b*			
spot 7A	blue	63.07 ± 0.24	-6.03 ± 0.02	-14.70 ± 0.03	60.43 ± 0.22	-8.57 ± 0.02	-19.84 ± 0.14	6.31 ± 0.13	15.89	21.61
agar + ammonium carbonate (1:1)										
spot 6A	green	72.83 ± 0.13	-10.85 ± 0.07	3.24 ± 0.03	71.78 ± 0.18	-15.35 ± 0.02	0.58 ± 0.01	5.34 ± 0.09	11.33	15.36
agar + ammonium carbonate (1:2)										
spot 2G	red	65.48 ± 0.17	26.33 ± 0.15	12.03 ± 0.15	66.15 ± 0.13	26.96 ± 0.17	11.97 ± 0.02	0.96 ± 0.14	28.95	29.50
spot 8A	violet	74.39 ± 0.06	1.79 ± 0.01	1.03 ± 0.02	73.83 ± 0.10	2.28 0	-4.48 ± 0.03	5.56 ± 0.06	2.07	5.03
ammoium carbonate + water										
spot 3A	pink	78.88 ± 0.26	12.95 ± 0.04	13.65 ± 0.04	77.28 ± 0.02	15.44 ± 0.01	15.59 ± 0.01	3.54 ± 0.07	18.81	21.94
spot 6G	green	71.50 ± 0.01	-10.97 ± 0.03	3.58 ± 0.01	68.89 ± 0.12	-19.89 ± 0.06	0.10 ± 0.01	9.93 ± 0.08	11.54	19.89
spot 10A	background	77.21 ± 0.10	1.13 ± 0.01	12.22 ± 0.01	81.88 ± 1.58	0.50 ± 0.07	9.79 ± 0.39	5.29 ± 0.77	12.27	9.81
EDTA + water										
spot 4A	yellow	82.90 ± 0.04	0.22 ± 0.01	25.81 ± 0.06	83.49 ± 0.13	-1.27 ± 0.01	34.73 ± 0.15	9.06 ± 0.17	25.81	34.75
spot 8 G	violet	74.52 ± 0.09	2.08 ± 0.01	-0.60 ± 0.01	71.54 ± 0.03	5.79 ± 0.04	-11.59 ± 0.32	11.98 ± 0.31	2.16	12.96

However, the agar tended to dry within just a few seconds after being applied, solidifying without wetting the surface and forming a layer that could easily be removed mechanically. For this reason, the final cleaning tests were carried out using a mixture of agar, ammonium carbonate and EDTA, in order to use polysaccharide as a medium in which the reactants were dispersed, thus limiting the amount of water that interacted with the mural surface (Fig. 6.19).
As reported in Table 6.4, after this cleaning test in all the coloured areas, the L* coordinate values decreased and the C* values increased, making all the colours more vivid and saturated after the treatment. Also in this case, the colour variations of burgundy ($\Delta E_{ab} \approx 2$) and orange ($\Delta E_{ab} \approx 1$) were less vivid than the other areas.
In the background, an increase in the L* coordinates and a decrease in the b* coordinates were registered, resulting in a whiter and more brilliant surface than before the cleaning.

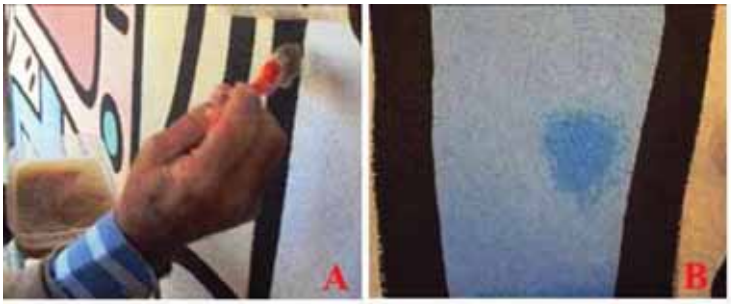

Fig. 6.19 - Application of the mixture of agar, EDTA and ammonium carbonate (A) and colour variation on a blue area after treatment (B)

Table 6.4 - Colorimetric values (L*, a*, b*) and ΔE_{ab} colour differences before (t_0) and after (t_1) the cleaning test with a mixture of agar, EDTA and ammonium carbonate.
Each value is the average of three measurements (± = max error)

Colour	t_0			t_1			$\Delta E(t_1 - t_0)$	t_0	t_1
	L*	a*	b*	L*	a*	b*		C*	C*
burgundy	58.99 ± 0.11	16.18 ± 0.01	10.45 ± 0.03	57.78 ± 0.13	17.88 ± 0.07	10.91 ± 0.03	2.14 ± 0.18	19.26	20.95
red	68.90 ± 0.13	22.52 ± 0.18	11.22 ± 0.06	65.17 ± 0.09	32.22 ± 0.15	14.98 ± 0.06	11.04 ± 0.25	25.17	35.53
pink	75.95 ± 0.10	13.25 ± 0.02	14.34 ± 0.02	76.43 ± 0.04	17.71 ± 0.01	15.98 ± 0.02	4.78 ± 0.03	19.52	23.86
yellow	82.89 ± 0.15	0.79 ± 0.02	23.66 ± 0.03	84.83 ± 0.35	-0.78 ± 0.01	32.04 ± 0.06	8.75 ± 0.20	23.67	32.05
orange	71.48 ± 0.11	6.42 ± 0.01	31.99 ± 0.04	71.64 ± 0.03	7.40 ± 0.02	32.89 ± 0.07	1.35 ± 0.10	32.63	33.71
green	72.53 ± 0.24	-10.72 ± 0.01	2.90 ± 0.01	69.87 ± 0.12	-19.53 ± 0.01	-0.27 ± 0.02	9.74 ± 0.09	11.11	19.53
blue	63.53 ± 0.15	-5.56 ± 0.04	-15.11 ± 0.15	55.37 ± 0.03	-9.98 ± 0.10	-28.03 ± 0.04	15.91 ± 0.25	16.10	29.75
violet	77.04 ± 0.11	1.68 ± 0.01	-1.88 ± 0.01	76.07 ± 0.07	3.54 ± 0.01	-7.49 ± 0.11	5.99 ± 0.10	2.52	8.28
background	76.71 ± 0.84	0.93 ± 0.01	12.32 ± 0.07	81.26 ± 0.18	0.41 ± 0.01	8.61 ± 0.02	5.91 ± 0.77	12.35	8.62

At the end of the cleaning tests, it was decided that the use of brushes and rubbers should be rejected. This decision was made in view of both the high risk of damaging the pictorial film and the long application times required by these dry-cleaning treatments.

In the end, the cleaning method selected to be applied to the entire mural surface, except for the black lines, was the treatment that employed a mixture of agar-agar gel in demineralised water (concentration of 5%, warmed in a microwave oven), 1% disodium EDTA (pH 4.5) with the addition of sufficient 0.2% ammonium carbonate to obtain a pH value of 7-8 in the mixture. The solution was applied in a thickness of about 1 mm. After drying, the film peeled off easily without leaving any residue. The presence of a thin white opaque layer adhering to the gel, with no trace of colour, showed the ability of the agar mixture to physically remove substances from the surface without dissolving them. The final result was a notable recovery of the original saturated colours.

On the other hand, the black linear elements of the composition showed a tendency to lose powder, leaving a veil of gray that was visible on the light background. Therefore, the black lines were not subjected to cleaning, but were consolidated with a micro-acrylic nanophase emulsion (Microacril® IMAR) diluted to 5% in water. The consolidation of these linear elements was very successful, as it perfectly retrieved the saturated tone of the black outlines.

6.2-5 Monitoring of *Tuttomondo* during and after the conservative intervention

After the selection of the most appropriate cleaning method, colour measurements were carried out to monitor the effectiveness of both the cleaning procedure (as applied to the coloured areas of the entire mural surface) and the consolidation treatment (applied to the black outlines). Analyses performed in the lower part of the mural (Fig. 6.20) were repeated soon after the application of an alkyl alcoxysilane protective resin (Hydrophase®) for the purpose of verifying the transparency of the treatment and, one year later, to monitor the state of conservation of the artwork. The results are shown in Tables 6.5 and 6.6.

All the coloured areas became more saturated after cleaning, except for the white and red areas, which did not present significant changes in colour. The pink and violet areas showed the same behaviour after the cleaning procedure: both the a* and b* parameters increased, while the L* parameters remained unchanged. For the burgundy spots, higher values of a* and b* were observed, but this colour was found to be darker ($\Delta L^* \approx -2$) than before the cleaning treatment. In the case of the blue and green areas, all three colorimetric coordinates decreased after cleaning. In particular, the most significant reductions were for the b* in the blue area ($\Delta b^* \approx -11$) and for the a* ($\Delta a^* \approx -8$) in the green one, resulting, as expected, in an

increase in the blueness and in the greenness, respectively. The yellow area showed an increase in the b* coordinate ($\Delta b^* \approx 8$) and a slight reduction in the reddish component. The black lines became darker and more saturated after the consolidation treatment.

As regards the protection treatment, the colour variations were very small after the application of the Hydrophase® protective treatment: ΔE_{ab} was approximately 1 (violet, blue, yellow, black and pink areas) or 2 (green, white and burgundy areas). A $\Delta E_{ab} \approx 5$ was registered only for the red area.

Furthermore, the colorimetric analysis repeated one year after the conservation procedure showed no significant changes, except in the red areas ($\Delta E_{ab} \approx 7$). This anomalous behaviour will need to be further investigated in order to justify the colorimetric values.

Table 6.5 – Average colour differences ΔE_{ab}

Area	**colour**	**ΔE_{ab} (t_1-t_0)**	**ΔE_{ab} (t_2-t_1)**	**ΔE_{ab} (t_3-t_2)**
Area 17	violet	9.4	0.6	0.9
Area 18	blue	13.7	0.7	0.8
Area 19	yellow	7.7	0.4	1.7
	black	3.8	0.6	0.2
	pink	5.5	1.4	0.4
Area 20	green	9.7	1.7	0.3
	background	0.8	1.6	0.3
	burgundy	4.8	2.2	0.8
Area 21	red	0.7	4.6	6.6

Fig. 6.20 –Detail of the investigated areas before, during, and after the conservation treatments

Table 6.6 – Colorimetric coordinates (L*, a*, b*) for each area before (t_0), during (t_1 and t_2), and after the conservation treatments

Area	colour	t_0 - before cleaning			t_1 – after cleaning			t_2 – after protection treatment			t_3 – after 1 year		
		L*	a*	b*	L*	a*	b*	L*	a*	b*	L*	a*	b*
Area 17	violet	73.8	1.7	-3.2	73.1	3.8	-12.3	72.6	3.9	-11.9	72.7	3.7	-11.1
Area 18	blue	62.6	-9.5	-15.5	57.5	-15.4	-26.8	56.8	-15.6	-26.4	56.1	-15.4	-26.2
Area 19	yellow	81.9	2.7	28.4	83.1	1.7	35.9	83.1	2.0	36.3	81.9	1.8	35.2
	black	28.8	0.5	0.2	25.1	0.5	-0.2	24.5	0.5	-0.1	24.3	0.5	0.0
	pink	74.5	18.1	13.5	73.9	23.2	15.4	73.1	24.1	16.1	72.9	23.9	16.3
Area 20	green	70.4	-14.4	4.8	67.7	-22.8	0.8	66.6	-21.8	1.6	66.7	-22.0	1.5
	background	78.1	0.9	11.0	78.2	1.0	10.2	79.6	0.8	9.7	79.3	0.9	9.7
	burgundy	54.7	17.4	7.7	52.4	21.4	9.3	50.7	20.1	8.8	51.1	20.4	9.4
Area 21	red	64.9	32.0	10.7	65.0	31.9	10.0	62.7	35.7	11.3	57.7	39.9	12.6

6.3 Conclusion

Within the conservation project of the *Tuttomondo* mural by Keith Haring, colorimetric and spectroscopic investigations were carried out in order to:

- identify the pigments in the acrylic paints used by the artist;
- identify the most appropriate cleaning treatment;
- check the chromaticity coordinates before, during, and after the cleaning process of the coloured areas and the consolidation of the black lines;
- check for any changes in the chromaticity coordinates as a result of the protective treatment;
- create a colorimetric mapping after the conservation treatment in order to provide colorimetric reference values for the future conservation processes.

The FORS results made it possible to tentatively characterise the artist's palette.

Table 6.7 – List of the materials detected using FORS analysis

Area	Identification	FORS absorption maxima (nm)[a]
white (background)	Titanium white	λ < 400 (ip)
	Kaolinite	1382 (m), 1418 (m)
burgundy	Hematite	530 (m), 865 (m)
	Titanium dioxide (rutile)	λ < 400 (ip)
	Kaolinite	1382 (m), 1418 (m)
red	Quinacridone red	520 (m), 556 (m)
	Titanium dioxide (rutile)	λ < 400 (ip)
	Kaolinite	1382 (m), 1418 (m)
pink	Tetracene	498 (m), 535 (m)
	Titanium dioxide (rutile)	λ < 400 (ip)
	Kaolinite	1382 (m), 1418 (m)
yellow	Hansa yellow (PY3)	λ < 505 (ip)
	Titanium dioxide (rutile)	λ < 400 (ip)
green	Phthalo green	450 (m), 650 (m), 730 (m),780 (m)
	Titanium white	λ < 400 (ip)
blue	Phthalo blue	620 (m), 715 (m), 430 (sd), 910 (w), 1100 (w)
	Titanium white	λ < 400 (ip)
violet	Carbazole dioxazine	540 (m), 567 (m), 627 (m)
	Titanium dioxide (rutile)	λ < 400 (ip)
black	Unidentified pigment	/

[a] sh(sharp), br (broad), m (medium), s (strong), w (weak), sd (shoulder), ip (inflection point)

Cleaning tests were carried out with a large variety of materials: brushes, hard rubbers, deionised water, ammonium carbonate, EDTA and agar gel (Table 6.8).

Table 6.8 – List of the cleaning methods used on the Tuttomondo mural anf their effects on the colour

Cleaning method	Effect on the colour	Remarks
brush	Loss of saturation	removal of dirt and pictorial film
rubber	Increase in saturation	removal of dirt and pictorial film (more effective than cleaning by brush)
water / ammonium carbonate	Increase in saturation	removal of dirt/ long application time and need for rinsing
water / EDTA	Increase in saturation	removal of dirt/ long application time and need for rinsing
agar /EDTA(1%)/ammonium carbonate (0.2 %)	Increase in saturation	removal of dirt/ very effective/ no need for rinsing

The best cleaning method was found to be a mixture of agar gel (5%) in demineralised water, applied as a liquid about 1 cm deep with the addition of 1% EDTA and 0.2% of ammonium carbonate, thanks to its ease of application and removal of the gel film, the possibility of intervening in the fields of each colour (evaluating the composition of the mixture and optimum contact times for each one), its optimal working time (a single step, without the need for subsequent rinsing), as well as the low cost of the products.

Furthermore, it was found that the cleaning treatment was very effective, inducing as it did significant colorimetric changes over the entire surface. In fact, all the colours of the painting, which had faded after twenty years of environmental exposure, appeared more saturated, vivid and brighter after the conservation. The protective treatment, instead, did not induce any significant changes on the colour surface, except in the red area, thus confirming the reported characteristic (good transparency) of the product. One year after the conservation procedure, the mural did not show any significant colorimetric changes, and this reconfirmed the effectiveness of the selected treatment.

CHAPTER 7– PINOT GALLIZIO

7.1 Pinot Gallizio

7.1-1 Short biography

Giuseppe (Pinot) Gallizio (Fig. 7.1) was born on 12 February 1902 in Alba (Cuneo, Italy). In 1912, his parents enrolled him at the Collegio San Giuseppe in Turin, where he earned a technical diploma. He then enrolled at the Faculty of Chemistry and Pharmacy of the University of Turin, from where he graduated in November 1924 (Roberto and Comisso, 2001).

Fig. 7.1 - Pinot Gallizio with a canvas of "Industrial Painting"
[Image from: http://auramagica.wordpress.com/2012/05/24/questionario-illegittimo/; last access: 7 August 2013)]

From October 1927 to March 1930 he worked in the Bosio Pharmacy in Via Garibaldi, Turin. After this experience, he moved to Alba where he opened his own pharmacy, the "Farmacia Gallizio", which he managed until January 1941. In 1933, Gallizio married Augusta Rivabella, and his son George was born two years later. In the 1940s Gallizio, who was keen on archaeology, unearthed, in the countryside of Alba, fragments of pottery and utensils dating back to the Neolithic age (Bertolino *et al.*, 2000).

In 1941, after closing the pharmacy in Alba, Gallizio began producing medicinal and pot herbs, chemical products, turpentine, and various types of pitch. In February 1944 he joined the partisan units of the "Divisione Alpi", and took part in the liberation struggle. He also worked for the Comitato di Liberazione Nazionale (Committee of National Liberation, or CLN, the group in which he started his political career as a Communist activist). After the war, he continued to experiment with herbal perfumes, first while teaching at the University of

Turin. He then founded a “Laboratorio Sperimentale” (Experimental Laboratory) near the Institute of Agriculture of Alba (Bandini, 1974).

Gallizio approached art only in adulthood. Indeed, he was already fifty when, in 1953, he met Piero Simondo, a young artist from Albisola (Savona), who introduced him to the world of modern painting. They became friends, and the following year Gallizio carried out his first experiments in painting, using natural resins. In 1955, together with Piero Simondo, he exhibited his first pictorial works in the “Restaurant Lalla” within the framework of the International Meeting on Pottery in Albisola. In that occasion, he made the acquaintance of several artists, such as Farfa and Fontana. He also met the Danish artist Asger Jorn, leader of the informal “International Movement for an Imaginist Bauhaus” (MIBI). On 29 September 1955, Gallizio, Jorn and Simondo founded the "First Laboratory of Imaginist Experiences”, which was immediately renamed “Alba Experimental Laboratory”. This was a sphere in which they could conduct artistic, scientific, and technological research programs while being free from the demands of the industrial market. The “Alba Experimental Laboratory” was located in the cellar of Gallizio’s home. There, Jorn, Gallizio and his son Giorgio (also known as Giors Melanotte), Piero Simondo, and their assistant Glauco Wuerich discussed science (especially chemistry and quantum physics) along with aesthetics, philosophy, and politics. The collaborative paintings that they produced in the laboratory, which were used mostly to decorate the walls, were called *peintures d’ensemble* (ensemble paintings). From that moment on, Gallizio worked in a hectic and relentless manner (Bandini, 1974; Poli, 1992; Vescovo, 1994; Fondazione Ferrero, 1998).

In 1957, Gallizio took part – together with Guy Debord, Michèle Bernstein, Asger Jorn, Constant Nieuwenhuys, Walter Olmo, Piero Simondo, Elena Verrone and Rulph Rumney – in founding the “Internazionale Situazionista” (International Situationist), which was born from the merger of the Lettrist movement with the MIBI. 1957 was a year of intense artistic production for Gallizio, who carried out the first experiments in “Pittura Industriale” (Industrial Painting), including *Antiluna* (Inventory number: 57 DT 34, 35), a roll measuring 9 meters (Busto, 2007).

On 10 November 1958, Gallizio started painting the canvas that would be used for the *Caverna dell’Antimateria* (Cavern of Anti-Matter), which he was to finish in January 1959 (§ 7.2-1).

The most important events of the following years were a solo exhibition at the Stedelijk Museum in Amsterdam (1960), the “Dalla Natura all’Arte” (From Nature to Art) exhibition organised at the Palazzo Grassi in Venice, and an invitation to the Venice Biennale from Maurizio Calvesi in 1964.

In 1964, Gallizio also worked on the *Anticamera della morte* (Antechamber of Death), a furniture-environment in which he arranged some of the objects that had accompanied him during his life (Fig. 7.2). Gallizio died on 13 February 1964 from a sudden heart attack. Thus, the exhibition room dedicated to him at the XXXII Venice Biennale took on the value of a posthumous retrospective exhibition (Roberto and Comisso, 2001).

Fig. 7.2 - *Anticamera della morte*, Pinot Gallizio (1964)
[Image from: http://www.discorsivo.it/magazine/2013/11/01/lanticamera-della-morte-opera-testamento-pinot-gallizio/]

Today, many of his works are exhibited in several important museums all over the world, including the Stedeljik Museum (Amsterdam), the Centre Georges Pompidou (Paris), the Museo Reina Sofia (Madrid), the "Luigi Pecci" Center for Contemporary Art (Prato), and the Gallery of Modern Art - GAM (Turin).

7.2 Case study: *Caverna dell'antimateria*

7.2-1 The artwork

In 1958, the writers Guy Debord and Michèle Bernstein, who were friends of Gallizio's and co-founders of the "International Situationist", invited Gallizio to give an exhibition at the "Galerie René Drouin" in Paris. The project was to cover the entire gallery space (from floor to ceiling) – the white walls of which were normally adorned with paintings – with about 150 meters of "Industrial Painting", thus converting the gallery into a synthetic environment. It was for this project that Gallizio created, in 1958-59, the *Caverna dell'antimateria* (inventory number: 58 DT 38) as a "work-environment" that provided a concrete representation of the theory of the Anti-World and gave a voice to the new concept of matter advanced by contemporary physics (Bertolino *et al.*, 2005). The work consisted of a nine-metre-long

painted canvas[1] that served to cover the ceiling, walls and floor, and six painted curtains to screen the front door and the staircase on the left wall (Fig. 7.3).

Fig. 7.3 – *Caverna dell'Antimateria*, Pinot Gallizio (1958-59)
[Image from: http://www.pinotgallizio.org/index.php?a=opere&b=3; last access: 26 November 2013]

All the canvases were painted with different colours that were mixed and/or overlaid with each other. As reported in his *Diario-Registro*[2] ("Diary-Register"), Gallizio used several pictorial techniques: "*olio tradizionale*" ("traditional oil"), "*soffitto […] resine soffiate a polvere, graffite ad umido*" ("ceiling [...]: ?powder-blown resins , wet-painted engraved"), "*pavimenti – tela di lino preparata con vinavil [...] tecnica delle aniline alla nitro*" ("floors: linen canvas prepared with vinavil [...] nitro aniline technique"), "*tecnica a fuoco, le grandi sacche vengono intaccate con ferro rovente e soffiate – si rompono le sacche con effetti grandi*" ("Fire technique: the large bags are burned with a red-hot iron tool and then blown up – the bags break with great effects") (Fig. 7.4). According to the testimony of Giorgio Gallizio[3], in fact, the canvases for the ceiling were made on the roof of the "Experimental Laboratory of Alba" (where Pinot Gallizio created his works). On that occasion, the artist sewed bags containing pigments and firecrackers, and these were blown up in order to randomly sprinkle colours on canvases that had previously been prepared with Vinavil® glue (Repetto and Balla, 2000; Roberto and Comisso, 2001).

[1] 2 canvases for the floor (each one measuring 1.80 x 10.50 m); 2 canvases for the ceiling (each one measuring 1.80 x 10.05 m); 5 canvases for the walls (the one for the right wall measured 10.00 x 2.05 m; for the left wall, one was 8.00 x 2.05 m and another of 5.00 x 2.05 mm;, the two for the back wall measured 3.80 x 2.05 m). Gallizio created the canvases for the ceiling in collaboration with his son Giorgio (alias Giors Melanotte). The canvases for the floor and the curtains were created by Giorgio Gallizio (Roberto and Comisso, 2001).
[2] Courtesy of the Archive Gallizio
[3] "*We smeared the canvases with a mixture of white glues [...]. We made up little bags of colour with petards inside, and set them in various places. We lit their fuses and they burst into clouds of colour*" (Giorgio Gallizio in Repetto and Balla, 2000).

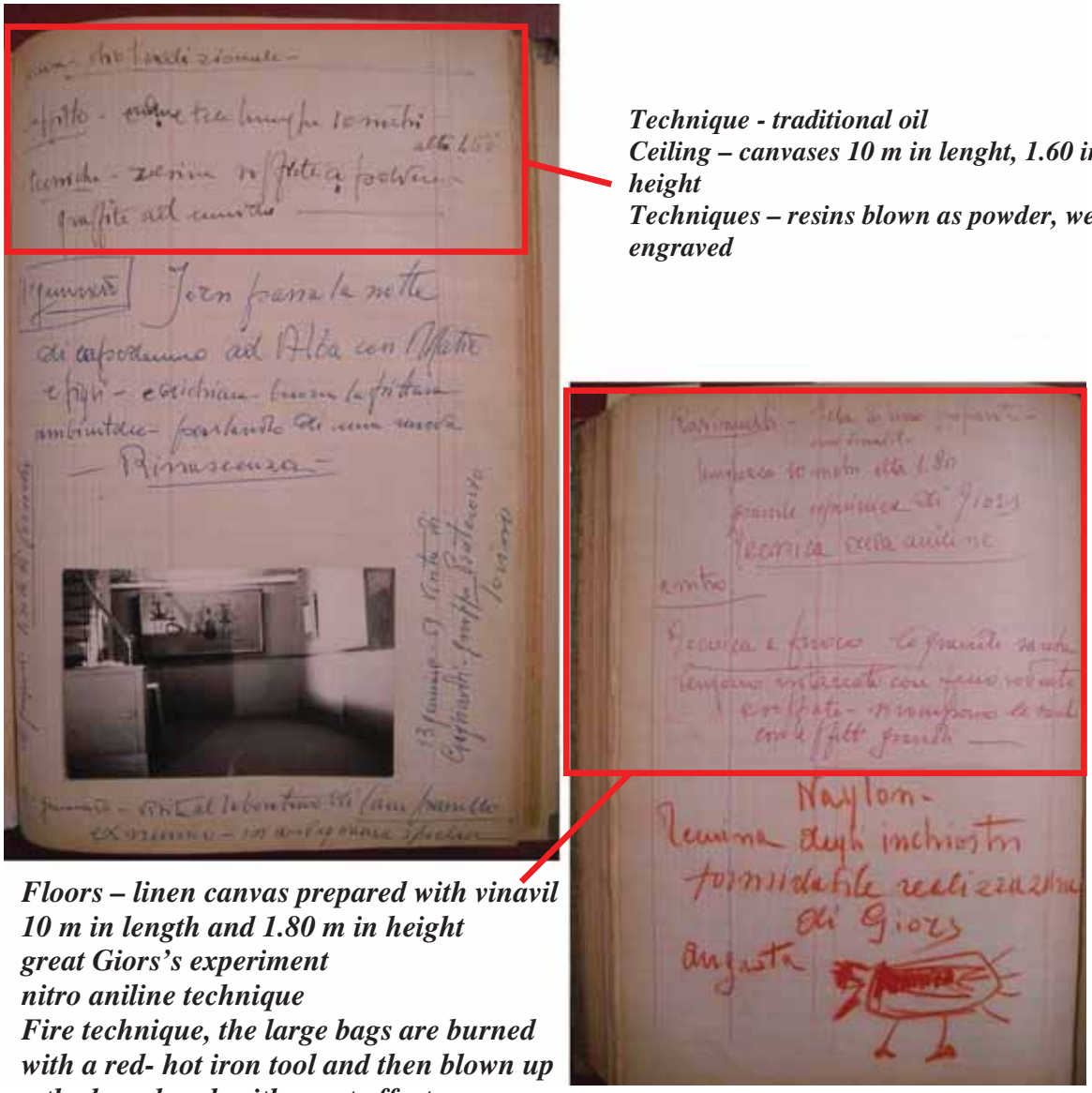

Fig. 7.4 - Pinot Gallizio, *Diario-Registro* Notes on *Caverna dell'antimateria* for its installation at the "Galerie René Drouin" in Paris (Courtesy of Archive Gallizio)

Today, the work consists of only seven canvases (all five canvases for the walls and two for the ceiling). The last installation of the *Caverna dell'Antimateria* was performed during the *In viaggio* ("En route") exhibition, which was held at the Pecci Museum in Milan from 16 December 2010 to 22 January 2011 (Fig. 7.5).

Fig. 7.5 – Caverna dell'Antimateria, Pinot Gallizio (1958-59),
last public exhibition at the Pecci Museum in Milan (2010-2011)
[Image from: http://www.undo.net/it/argomenti/1295361779; last access; 26 November 2013]

The work is currently stored in the warehouses of the "Luigi Pecci Center for Contemporary Art" (Prato, Italy). Each canvas is rolled up on cylindrical supports (Fig. 7.6A-B). Thanks to the courtesy of the curators of the museum, it was possible to have access to three canvases (two of the ceiling and one of the wall), which were unrolled (Fig. 7.6C-D) and then analysed using non-invasive *in situ* techniques (FORS and Optical Microscopy). As described in the following section, the canvases were also sampled (§ 7.2-2): the samples were analysed by means of FORS, FT-IR and Raman spectroscopies.

Fig. 7.6 – *Caverna dell'Antimateria*: cylindrical storage support (A, B), unrolling of the canvas of the wall (C, D)

7.2-2 Experimental

Canvases

The three unrolled canvases, the object of our diagnostic survey, are illustrated in Fig. 7.7. According to the curators of the museum, canvas A constitutes one of the walls of the *Caverna dell'antimateria*, while canvas B and canvas C are from the ceiling.

Fig. 7.7 - *Caverna dell'Antimateria*: canvas of the wall (A) and canvases of the ceiling (B, C)

Samples

During the diagnostic survey, 23 samples were collected. A list of the samples is reported in Table 7.1.

Table 7.1 - List of the samples analysed and a brief description of them

Sample	Canvas	Colour	Dimension
A1	A	white	3x5mm
A2	A	blue	3x7mm
A3	A	black	5x9mm
A4	A	white	4x7mm
A5	A	green	4x6mm
A6	A	blue	3x4mm
A7	A	green	5x6mm
A8	A	green	8x3mm
A9	A	green	5x4mm
B1	B	white	5x4mm
B2	B	blue	2x2mm
B3	B	yellow	3x2mm
B4	B	yellow	8x4mm
B5	B	blue	15x5mm
C1	C	blue	3x2mm
C2	C	green	3x2mm
C3	C	white	3x3mm
C4	C	blue	3x3mm
C5	C	yellow	5x4mm
C6	C	pink	5x3mm
C7	C	pink	4x3mm
C8	C	red	6x4mm
C9	C	black	3x3mm

Optical Microscopy

Some microscopic images of the several colored areas were acquired *in situ* on the canvases (Fig. 7.8). The instrument used was a *Scalar model DG-2A* portable digital microscope, which provided high-quality images with a magnification from 25x up to 200x. All the images were acquired with the 25x magnification, which corresponded to an area of 13x8 mm^2.

Fig. 7.8 – Acquisition of a microscopic image on the *Caverna dell'Antimateria*

FORS

FORS measurements were acquired both on different areas of the three canvases (*in situ*; Fig. 7.9) and on all the samples collected.

Fig. 7.9 - FORS instrumentation during the diagnostic survey of the *Caverna dell'Antimateria*

FORS spectra in the UV-Vis-NIR spectral range (350–2200 nm) were acquired by using two single-beam *Zeiss* spectroanalysers, model *MC601* (190-1015 nm range) and model *MC611 NIR 2.2WR* (910-2200 nm range), which were housed together in a compact and portable chassis for *in situ* analyses. The data acquisition step was 0.8 nm/ pixel for the 1024-element silicon photodiode array detector (*MCS601*), and 6.0 nm/pixel for the 256-element InGaAs diode array detector (*MCS611 NIR 2.2 WR*). The radiation between 320 nm and 2700 nm, which was provided by a voltage-stabilized 20W halogen lamp (mod. CLH600), was conveyed to the sample by means of a quartz optical fibre bundle that also transported the reflected radiation to the detectors. The geometry of the probe head was 8°/8°.

A *Zeiss* spectrum analyzer, model *CLX 500,* equipped with a xenon lamp was used to investigate the 270-800 nm (UV-Vis) range.

Calibration was performed by means of a 99% Spectralon® diffuse reflectance standard. Spectra were processed using Aspect Plus® 1.80 software.

FT-IR

Transmittance spectra on the samples mounted in KBr pellets were collected by means of a Nicolet spectrophotometer, model Nexus 470 E.S.P.™, equipped with a SiC Globar and a DTGS detector. The IR spectra were acquired in the 4000–400 cm^{-1} range (acquisition of 64 scans using a 4 cm^{-1} resolution).

ATR spectra were recorded using a *Perkin-Elmer System 2000* spectrometer equipped with a Golden Gate accessory. 32 scans were acquired on each sample in the 4000-600 cm^{-1} spectral range using a 2 cm^{-1} resolution.

Micro-Raman spectroscopy

Micro-Raman spectra of the samples were registered with a *Renishaw model Raman Invia* spectrometer, equipped with a *Leica* microscopy (50x lens), a diffraction grating of 1800 lines/mm, and a CCD detector. The source was a HeNe laser (λ = 633nm).

7.2-3 Study of the artistic materials

The three canvases under investigation appeared to be in a good state of conservation, although several craquelures were identified (Fig. 7.10). These were may be due to the mode of storage. It is possible, in fact, that less craquelures would have been found if the canvases had been stored stretched, instead of being rolled up.

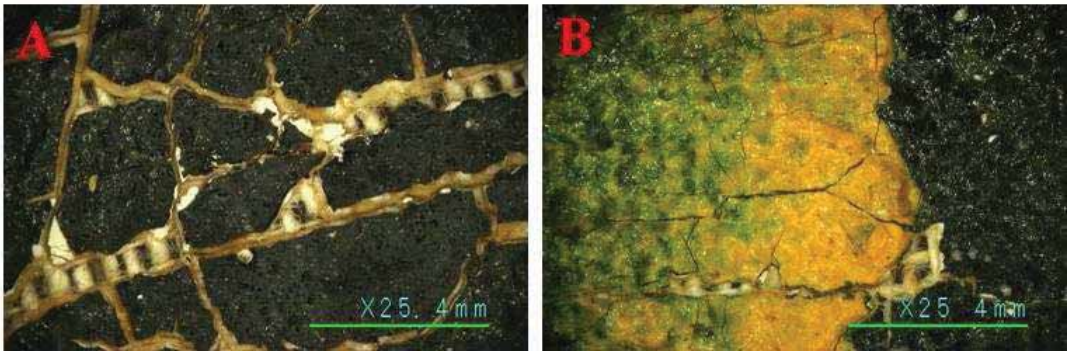

Fig. 7.10 – Microscopic images of missing pieces and craquelures found in the *Caverna dell'Antimateria*

In looking at the three selected stripes, a remarkable difference in the execution technique was noted. This was due to the different location inside the cave and to the different significance of each canvas. Many unconventional materials were detected in the canvases belonging to the ceiling: wires, sand, and a probable residue of gunpowder used to 'shoot' the colour onto the fresh binder, as described in § 7.2-1. The colours were unevenly distributed on the surface,

leaving it to shine through large areas of the white preparation below. Instead, no unconventional materials were found in, the strip of wall, and the paint was applied more evenly, giving a visibly darker colour cast.

The study of the data acquired *in situ* and on the samples made it possible to identify most of the materials used by the artist. In particular, all the FT-IR spectra showed the typical absorption bands of a polyvinylacetate resin: 2921 and 2852 cm^{-1} (aliphatic CH stretching), 1735 cm^{-1} (C=O stretching), 1427 cm^{-1} (asymmetric CH_2 bending), 1375 cm^{-1} (asymmetric CH_3 bending), 1240 cm^{-1} (CH in plane bending), 1125 cm^{-1} (C-O stretching) (Renuka Devi and Madivanane, 2012). The result obtained was confirmed unequivocally by means of Py-GC/MS, which was performed within the framework of the CoPAC Project at the SCIBEC[4] laboratory of the University of Pisa. In the pyrogram of samples A2 and A5, Vinavil® mixed with a siccative oil was also identified (Colombini, 2012). These results are in agreement with the notes of Gallizio himself, who, in his *Diario-Registro*, declared that he used Vinavil® and/or traditional siccative oils as binding media (§ 7.2-1).

The study of the coloured areas made it possible to affirm that Gallizio did not seem to have any specific preferences in his 'artistic materials', since he used both inorganic pigments and organic dyes for the creation of this work.

In considering the FT-IR spectra of the white samples (A1, A4, B1, C3), we were able to identify absorption bands of barite at *ca*. 1166, 1111, 1067 (SO_4^{2+} asymmetric stretching), 983 (ν_1 SO_4^{2+} in plane bending), 631 and 604 cm^{-1} (doublet, ν_4 SO_4^{2+} out of plane bending) (Ramaswamy *et al.*, 2010). In sample A1, absorptions at 3536 and 3398 cm^{-1} (OH stretching) due to the presence of gypsum were also found (Fig. 7.11).

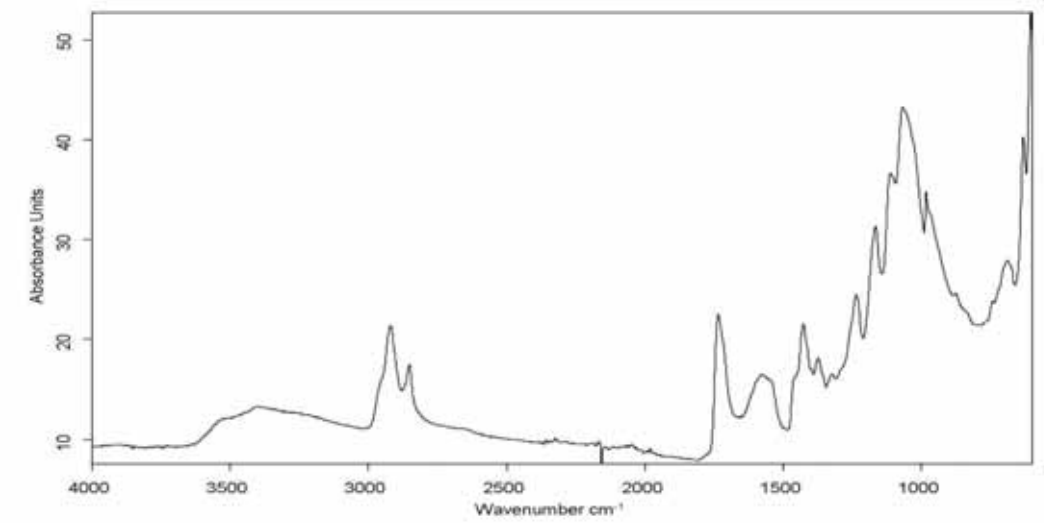

Fig. 7.11 – FT-IR spectrum of sample A1

[4] Chemical Science for the Safeguard of the Cultural Heritage

In the Raman spectra, the strong absorption at 986 cm^{-1} was attributable to the presence of barite (Bell *et al.*, 1997; Burgio and Clark, 2001) in the white samples (Fig. 7.12).

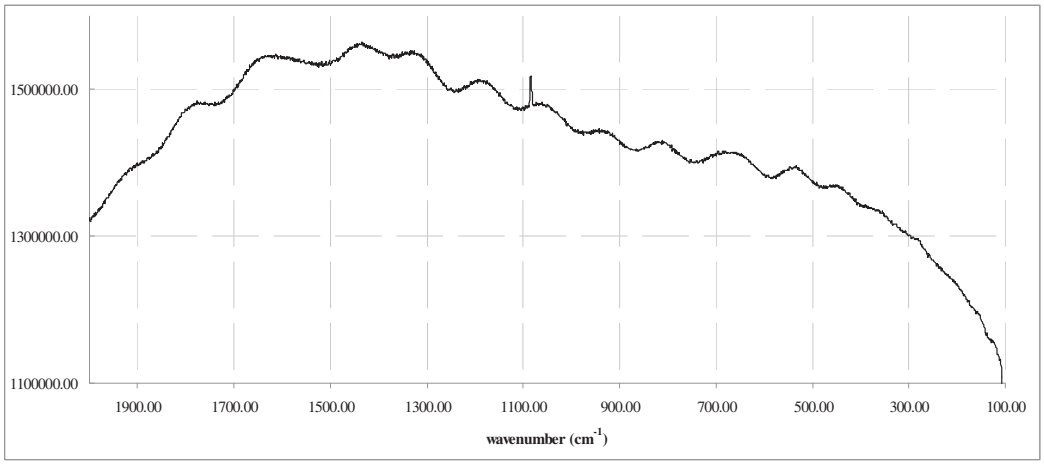

Fig. 7.12 – Raman spectrum of sample A1

In addition, FORS spectra showed two absorption bands at 670 nm and 728 nm, which are typical of Co^{2+} ion in pseudo-tetrahedral coordination as a vicariant of Zn^{2+} in the structure of ZnS. The presence of this ion has been associated with the lithopone pigment ($BaSO_4$ + ZnS) produced after the mid-1920s (Weakliem, 1962; Van Alphen, 1998). The presence of ZnS in these samples was confirmed by their FORS spectrum in the 270-800 nm range. The typical strong absorption in the UV region below 350 nm with an inflection point at 340 nm ascribable to ZnS was also observed (Picollo *et al*., 2007)(Fig.7.12).

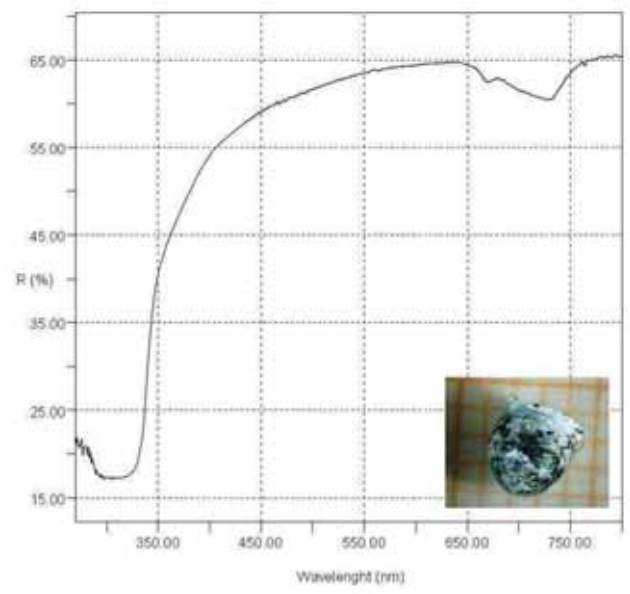

Fig. 7.13 – FORS spectrum of sample B1 (spectral range 270-800 nm)

It was not possible to identify the black pigment (samples A3 and C9) by means of FT-IR and FORS analysis. Only Raman spectra provided information on it. In fact, black areas were created using a black pigment based on amorphous carbon, with Raman absorptions at 1325 and 1580 cm^{-1} (Bell *et al.*, 1997) (Fig. 7.13).

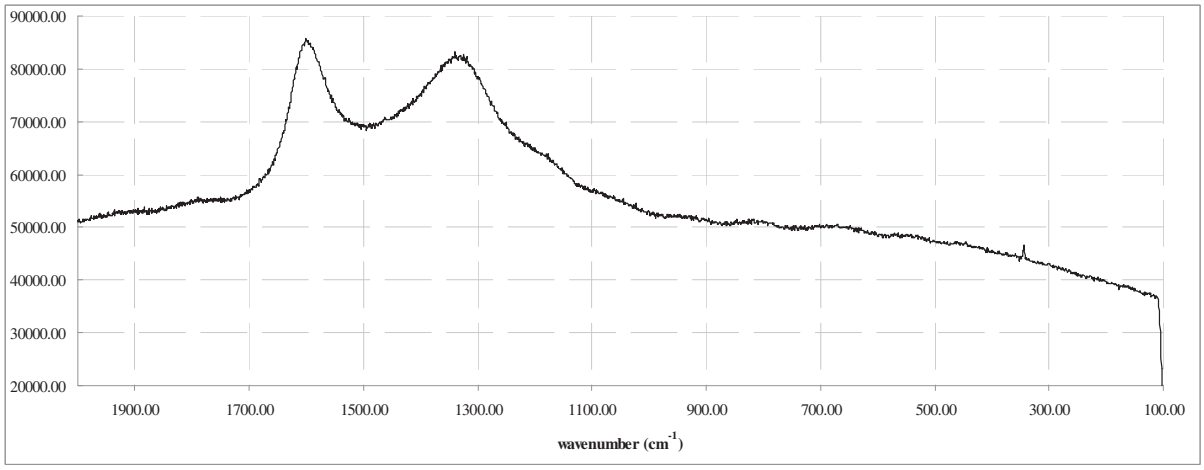

Fig. 7.14 – Raman spectrum of sample A3

Two different pigments were identified on the blue areas. In considering FT-IR spectra of the blue samples detached from the ceiling (B2, B5, C1, C4), we were able to identify the absorption bands of ultramarine blue. In particular, overlapping stretching bands of Si-O-Si and Si-O-Al between 1150 cm^{-1} and 950 cm^{-1} were present, as well as bands at 688 and 670 cm^{-1}, which were due to Si-O bond vibrations (Bruni *et al.*, 1999; Learner, 2004; Vahur *et al.*, 2010) (Fig. 7.15)

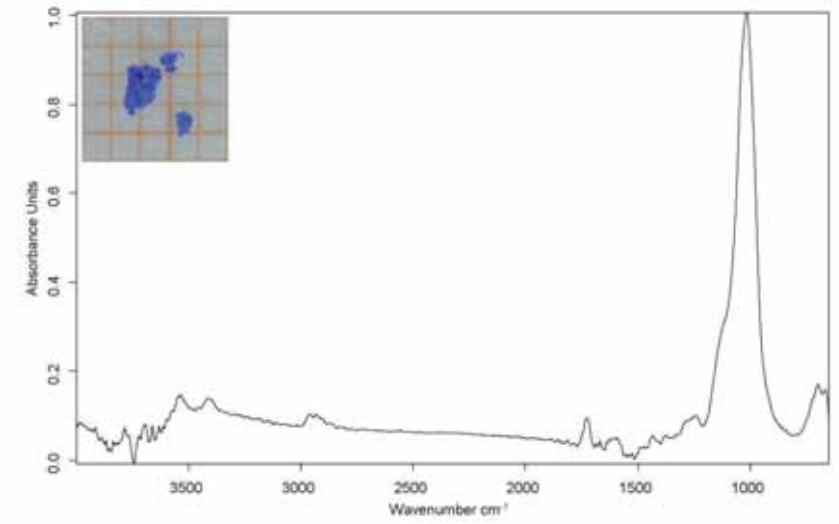

Fig. 7.15 – FT-IR spectrum of sample C1

Ultramarine blue was also identified in the Raman spectra (Fig. 7.16), where its typical absorptions at 1092, 814, 547 and 260 cm^{-1} were present (Bell *et al.*, 1997).

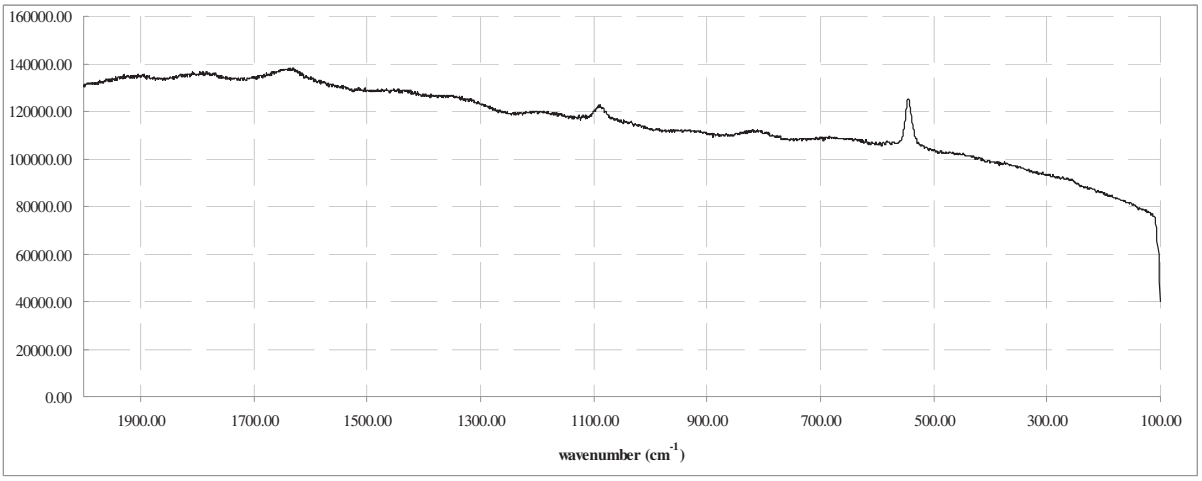

Fig. 7.16 – Raman spectrum of sample B2

Furthermore, the UV-Vis-NIR reflectance spectra showed a maximum of reflectance at about 447 nm and one around 770 nm, thus confirming the reddish component in the hue of this blue pigment as reported in the literature (Herbst and Hunger, 1993). The absorption centred around 600 nm was due to a charge transfer electronic transition that was related to the presence of the $\mathbf{S}_3^-$ ion in the crystal structure of the aluminosilicate (Bacci, 2000) (Fig. 7.17).

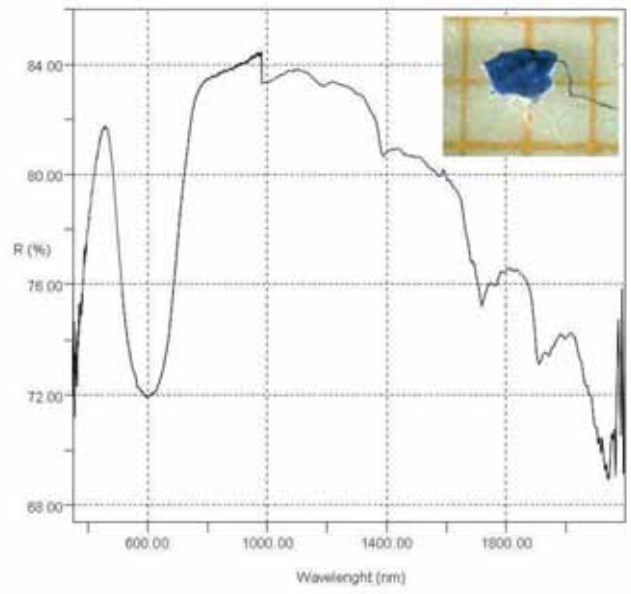

Fig. 7.17 – FORS spectrum of sample B2 (spectral range: 350-2100 nm)

Ultramarine blue was used in a mixture with phthalo blue on the canvas of the wall. As shown in the Raman spectrum of sample A2 (Fig. 7.18), in fact, we identified both absorptions of ultramarine blue at 1094, 539 and 255 cm^{-1} (Bell *et al.*, 1997) and of phthalo blue at 1524, 1448, 1335, 1301, 1138, 948, 744, 677, 484 cm^{-1} (Burgio and Clark, 2001; Scherrer *et al.*, 2009).

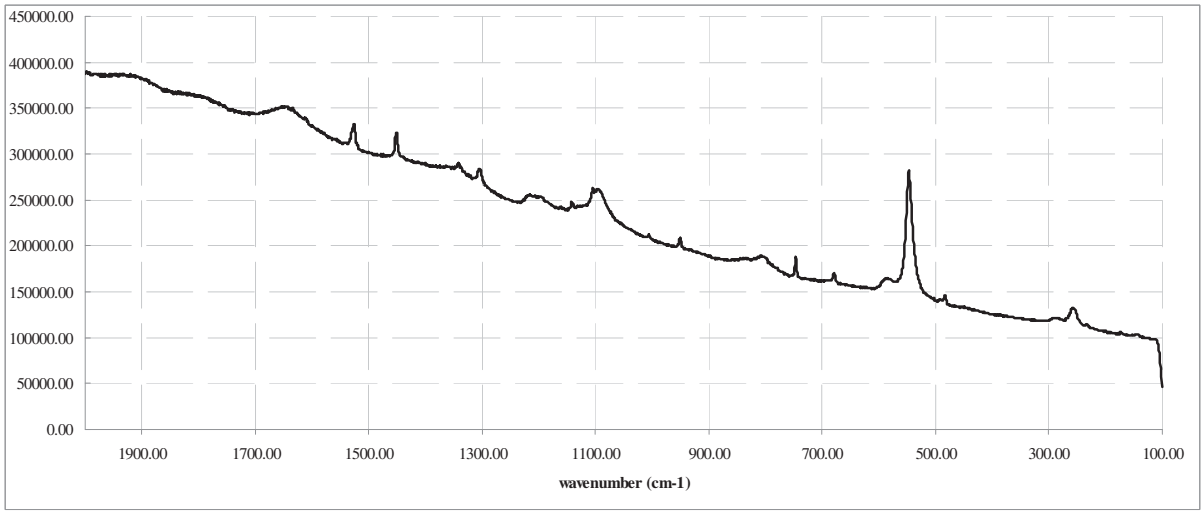

Fig. 7.18 – Raman spectrum of sample A2

Red areas were also created by using different pigments/dyes. In considering FORS spectra acquired *in situ*, for example, we could detect spectra with the typical spectral features of iron oxides (Fig. 7.19A) and also spectra with an "S"-shape absorption band and an inflection point at 600 nm (Fig. 7.19B).

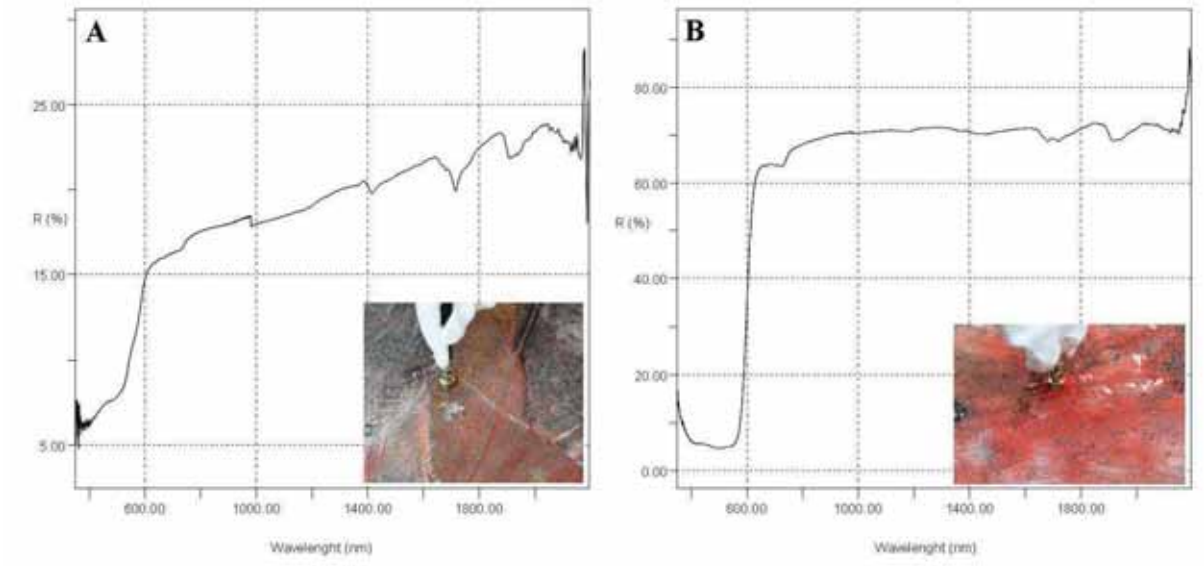

Fig. 7.19 – FORS spectra of an ochre red area (A) and a brilliant red area (B) in the 350-2100 nm spectral range

In the latter case, only the Raman analysis of the red sample (C8) enabled us to identify unequivocally the pigment/dye responsible for the colour. The Raman absorptions at 1620, 1560, 1499, 1447, 1397, 1334, 1258, 1221, 1187, 1131, 1080, 990, 845, 799, 726, 620, 459, 386 and 344 cm^{-1} were, in fact, attributable to a P3 monoazo pigment (Vandenabeele *et al.*, 2000; Scherrer *et al.*, 2009) (Fig. 7.20).

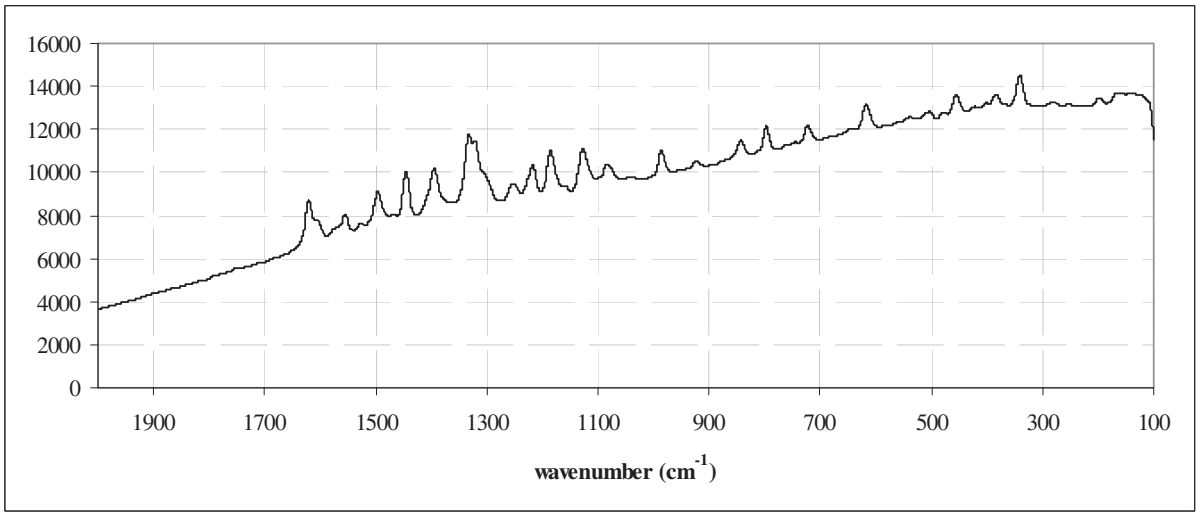

Fig. 7.20 - Raman spectrum of sample C8

Gallizio used different pigments/dyes for both the red colours and for the yellow ones. The FORS spectra acquired *in situ* on different yellow areas showed different spectral features. The brilliant yellow of canvas A (Fig. 7.21), for example, had an "S"-shape spectrum with an inflection point at 486 nm and an intense absorption band in the UV-Vis region, due to a n(azo) → π* transition of a monoazo PY3 yellow pigment (Christie *et al.*, 1988; Lake and Lomax, 2007).

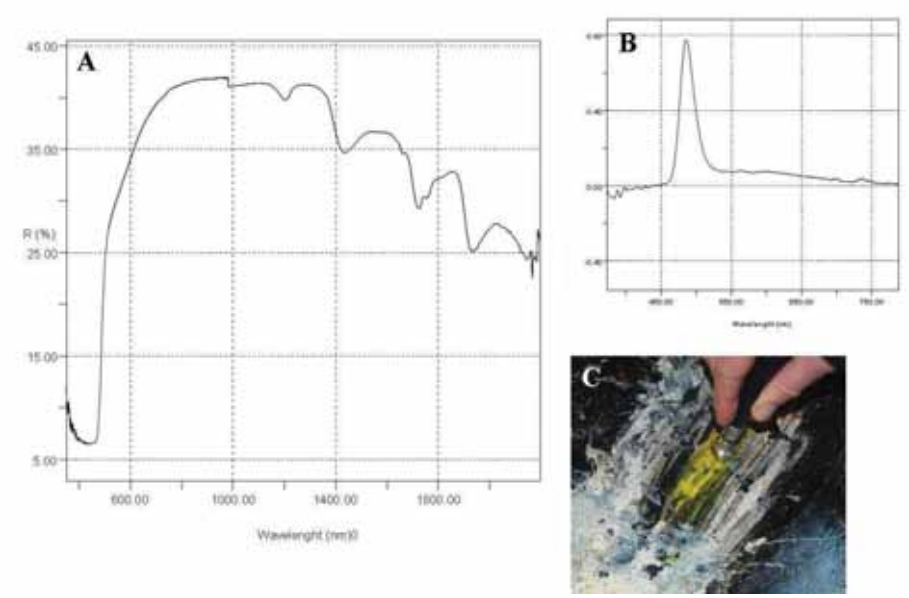

Fig. 7.21 - FORS spectrum (350-800 nm) of a brilliant yellow area of the canvas of the wall (A) with its 1st derivative spectrum (350-670 nm; B) and the image of the measured area (C)

Also the "S"-shape spectrum of the dark yellow (Fig. 7.22) had an intense absorption band in the UV-Vis region. In this case, however, the first derivative spectrum showed an intense maximum at 534 nm with a weak shoulder at 486 nm. These spectral features were possibly due to the presence of a mixture of a lead chromate yellow with a monoazo PY3 pigment (Christie *et al.*, 1988; Bacci, 2000; Lake and Lomax, 2007).

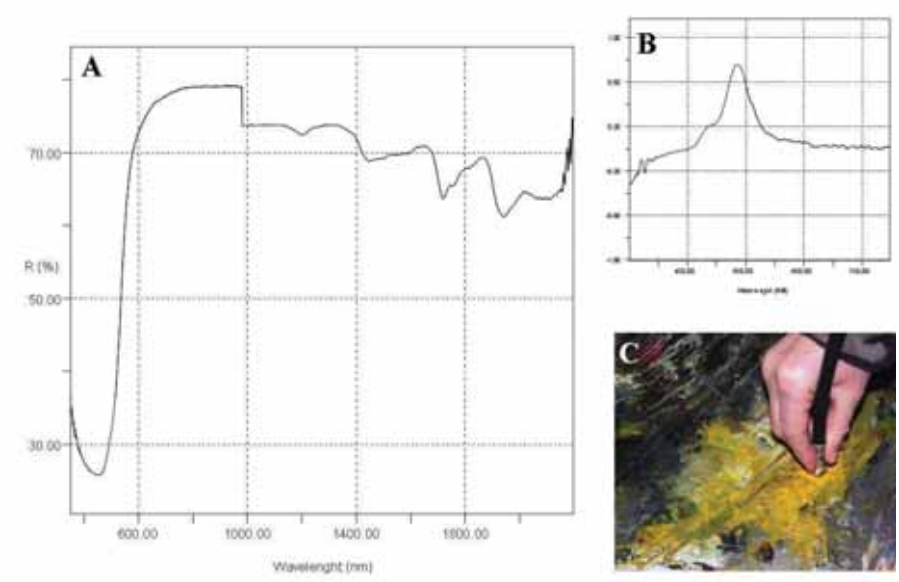

Fig. 7.22 - FORS spectrum (350-800 nm) of a dark yellow area of the canvas of the wall (A) with its 1st derivative spectrum (350-670 nm; B) and the image of the measured area (C)

In the case of the ochre yellow (e.g. samples B4 and C5), the FORS spectrum showed the absorption of a white pigment (at 364 nm) along with the absorption bands of goethite, α-FeOOH (Fig. 7.23). In fact, charge transfer transition absorption at 480 nm, as well as ligand field transition absorptions at 650 and 920 nm have been found (Sherman and Waite, 1985; Cornell and Schwertmann, 1996).

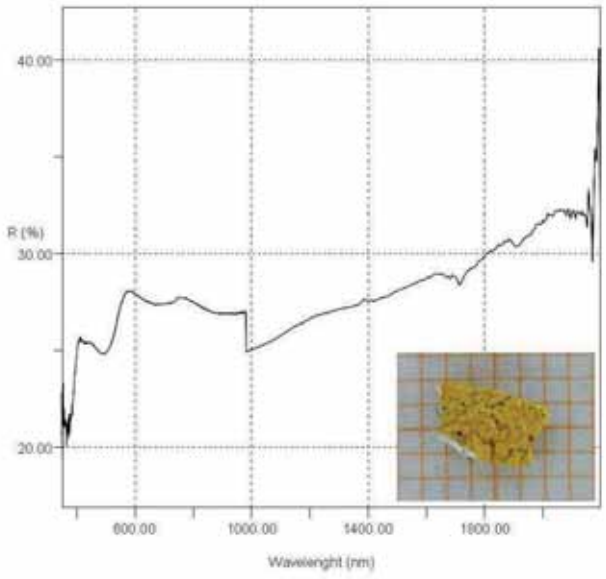

Fig. 7.23 - FORS spectrum of sample C5

In the FT-IR spectra of sample B4 and C5 (Fig. 7.24), the absorption bands at 3121, 898 and 797 cm^{-1} unequivocally confirmed the presence of goethite in the ochre yellow areas (Afremow and Vanderberg, 1966; Schwertmann *et al.*, 1985; Cambier, 1986).

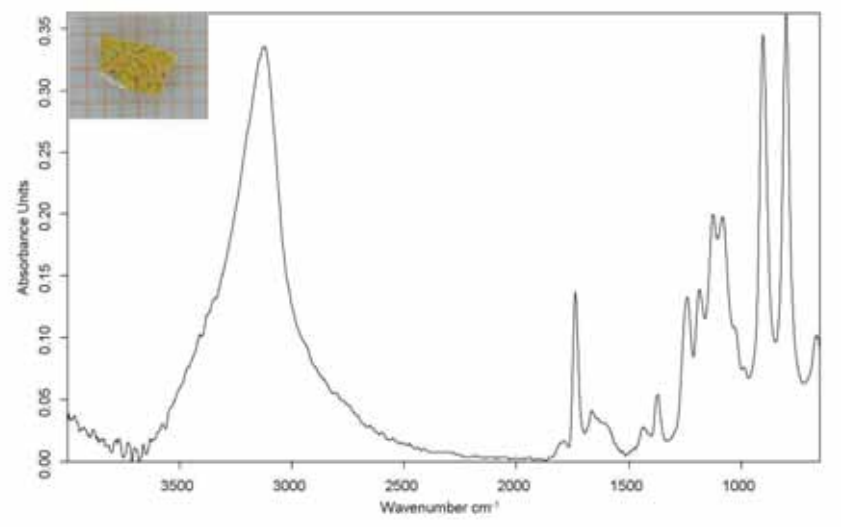

Fig. 7.24 – FT-IR spectrum of sample C5

Lastly, the green areas were created by mixing a blue pigment with a yellow one. FORS analysis (Fig. 7.25) enabled us to hypothesise the presence of a monoazo pigment (absorption under 480 nm) with a phthalocyanine blue (absorptions at 620 nm and 697nm) (Johnston and Feller, 1963; Johnston, 1967).

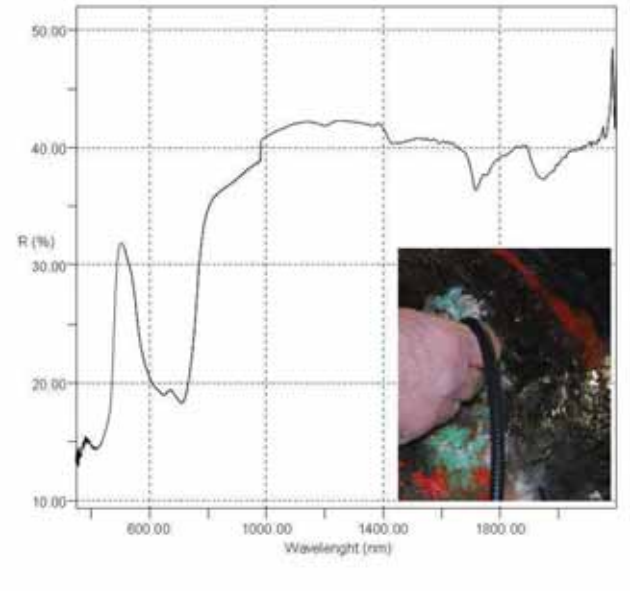

Fig. 7.25 – FORS spectrum of a green area (spectral range: 350-2100 nm)

In considering FT-IR spectra of samples A8 and A9, instead, we could identify only the absorption bands due to the binder and to the $BaSO_4$. Thus, no useful information on the coloured compounds was obtained. The proof that a blue-yellow mixture was used for the green areas was obtained by the Raman analysis. Raman spectra (Fig. 7.26) of green samples, in fact, showed both the absorptions of a phthalo blue PB15 pigment at 1530, 1450, 1139, 1106, 745 and 680 cm^{-1} (Scherrer *et al.*, 2009) and the peaks due to a monoazo PY3 pigment at 1613, 1543, 1494, 1425, 1385, 1337, 1310, 1189, 795, 395 and 142 cm^{-1} (Vandanbeel *et al.*, 2000; Scherrer *et al.*, 2009).

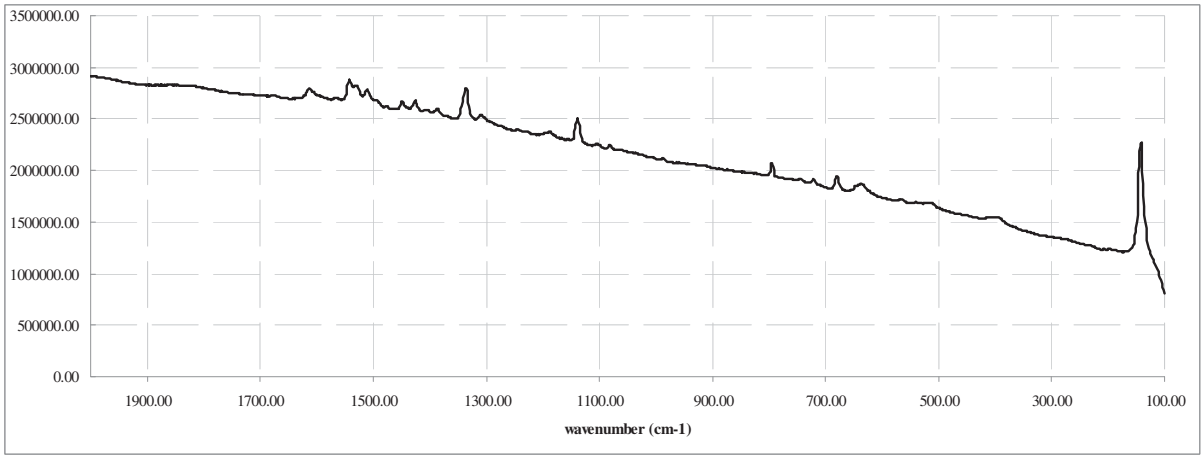

Fig. 7.26 - Raman spectrum of sample A8

7.3 Conclusion

The results of the spectroscopic analysis performed on the *Caverna dell'Antimateria* have been described in this chapter.

The integrated use of FORS, FT-IR and Raman spectroscopy was successfully employed to identify the artist's pictorial palette. The materials constituting each sample, with the main FT-IR and FORS absorption maxima as found in the acquired spectra, are summarised in Table 7.2.

The results obtained made it possible to affirm that, for the *Caverna dell'Antimateria*, Gallizio used traditional inorganic pigments, such as ultramarine blue, lithopone, and carbon black, as well as modern organic dyes, such as Hansa yellow, toluidine red, and phthalocyanine blue. Wires, sand and gunpowder were also found, thus confirming Gallizio's use of unconventional artists' materials.

Table 7.2 – FT-IR, Raman and FORS absorption band positions in the spectra acquired on the *Caverna dell'Antimateria* samples

Sample	Identification	Main FT-IR absorption bands (cm^{-1})	Main Raman absorption bands (cm^{-1})	FORS absorption maxima (nm)
A1	lithopone	$BaSO_4$: 1166, 1111, 1067, 983 631, 604	$BaSO_4$: 986	ZnS: 368 (s) 670 (m) 728 (m)
	gypsum	3536, 3398	/	/
	polyvyinylacetate	2921, 2852, 1735, 1427, 1375, 1240, 1125	/	/
A2	Ultramarine blue	1150-950, 688, 670	1094, 539, 255	600 (s)
	Phthalo blue	/	1524, 1448, 1335, 1301, 1138, 948, 744, 677, 484	/
	Barite	$BaSO_4$: 1166, 1111, 1067, 983 631, 604	$BaSO_4$: 986	/
	gypsum	3536, 3398	/	/
	polyvyinylacetate	2921, 2852, 1735, 1427, 1375, 1240, 1125	/	/
A3	carbon black	/	1325, 1580	/
	polyvyinylacetate	2921, 2852, 1735, 1427, 1375, 1240, 1125	/	/
A4	lithopone	$BaSO_4$: 1166, 1111, 1067, 983 631, 604	$BaSO_4$: 986	ZnS: 368 (s) 670 (m) 728 (m)
	polyvyinylacetate	2921, 2852, 1735, 1427, 1375, 1240, 1125	/	/
A5	phthalo blue (PB15)	/	1530, 1450, 1139, 1106, 745, 680	614 (m) 690 (m)
	barite	1171, 1116, 1073, 983, 633, 607	/	/
	polyvyinylacetate	2926, 2854, 1738	/	/
A6	phthalo blue (PB15)		1530, 1450, 1139, 1106, 745, 680	/
	calcite	1416, 873, 712	/	/
	polyvyinylacetate	2926, 2853, 1738	/	/
A7	phthalo blue (PB15)	/	1530, 1450, 1139, 1106, 745, 680	/
	hansa yellow (PY3)	/	1613, 1543, 1494, 1425, 1385, 1337, 1310, 1189, 795, 395 and 142	/
	barite	1166, 1111, 1067, 983 631, 604	986 (BaSO4)	/
	polyvyinylacetate	2921, 2852, 1735, 1427, 1375, 1240, 1125	/	/
A8	phthalo blue (PB15)	/	1530, 1450, 1139, 1106, 745, 680	614 (m) 690 (m)
	hansa yellow (PY3)	/	1613, 1543, 1494, 1425, 1385, 1337, 1310, 1189, 795, 395 and 142	
	barite	1166, 1111, 1067, 983 631, 604	986	/
	polyvyinylacetate	2921, 2852, 1735, 1427, 1375, 1240, 1125	/	/
A9	phthalo blue (PB15)	/	1530, 1450, 1139, 1106, 745 and 680	614 (m) 690 (m)
	hansa yellow (PY3)	/	1613, 1543, 1494, 1425, 1385, 1337, 1310, 1189, 795, 395 and 142	
	barite	1166, 1111, 1067, 983 631, 604	986 (BaSO4)	/
	polyvyinylacetate	2921, 2852, 1735, 1427, 1375, 1240, 1125	/	/

B1	lithopone	$BaSO_4$: 1166, 1111, 1067, 983 631, 604	$BaSO_4$: 986	ZnS: 368 (s) 670 (m) 728 (m)
	polyvyinylacetate	2921, 2852, 1735, 1427, 1375, 1240, 1125	/	/
B2	ultramarine blue	1150-950, 688, 670	1092, 814, 547, 260	600 (s)
	polyvyinylacetate	2921, 2852, 1735, 1427, 1375, 1240, 1125	/	/
B3	calcite	2515, 1798, 1427, 878, 714	/	/
	barite	1185, 1125, 1080, 637, 610	/	/
	polyvyinylacetate	2924, 2844, 1741	/	/
	Unidentified yellow	/	/	425 (m)
B4	goethite	3121, 910, 795, 466	/	655 (m) 950 (m)
	calcite	2515, 1798, 1427, 878, 714	/	/
	polyvyinylacetate	2921, 2852, 1735, 1427, 1375, 1240, 1125	/	/
B5	ultramarine blue	1019, 446	1092, 814, 547, 260	600 (s)
	barite	1180, 1119, 1076, 636, 607	/	/
	polyvyinylacetate	2920, 2850, 1740, 1433, 1374, 1242	/	/
C1	ultramarine blue	1016	1092, 814, 547, 260	600 (s)
C2	lithopone	$BaSO_4$: 1166, 1111, 1067, 983 631, 604	$BaSO_4$: 986	ZnS: 368 (s) 670 (m) 728 (m)
	polyvyinylacetate	2934, 2875, 1737, 1434, 1373, 1242	/	/
C3	lithopone	1166, 1111, 1067, 983 631, 604	$BaSO_4$: 986	ZnS: 368 (s) 670 (m) 728 (m)
	polyvyinylacetate	2921, 2852, 1735, 1427, 1375, 1240, 1125	/	/
C4	ultramarine blue	1015, 452	1092, 814, 547, 260	600 (s)
	barite	1180, 1122, 1077, 638, 608	/	/
	polyvyinylacetate	2924, 2854, 1738, 1434, 1375, 1244, 792	/	/
C5	goethite	3121, 898, 797	/	400, 480, 649, 917 (w)
	barite	1182, 1122, 1078, 635, 609	/	/
	polyvyinylacetate	2924, 2854, 1736, 1434, 1373, 1243	/	/
C6	unidentified	/	/	/
C7	unidentified	/	/	/
C8	Monoazo pigment (PR3)	/	1620, 1560, 1499, 1447,1 397, 1334, 1258, 1221, 1187, 1131, 1080, 990, 845, 799, 726, 620, 459, 386, 344	l < 600 (ip)
	polyvyinylacetate	2921, 2852, 1735, 1427, 1375, 1240, 1125	/	/
C9	carbon black	/	1325, 1580	/
	polyvyinylacetate	2921, 2852, 1735, 1427, 1375, 1240, 1125	/	/

[a]sh(sharp), br (broad), m (medium), s (strong), w (weak), sd (shoulder), ip (inflection point)

CONCLUSIONS

This research was mainly focussed on the application of spectroscopic techniques in the UV-Vis-IR range to the study of the materials used in contemporary art. Since preservation of the integrity of the object is a priority in the art conservation field, non-invasive or micro-invasive analytical techniques were applied to identify the main compounds that constitute both mock-ups and artworks. The standard procedure is to examine small representative fragments taken from areas of the artwork in the proximity of losses and cracks in order to avoid damaging its appearance and physical structure. Nevertheless, this research establishes the use of non-invasive and portable instrumentation *in situ* as a preferred procedure.

UV-Vis-NIR spectroscopy was one of the analytical methods reported on in this thesis project. It is a well established and non-invasive technique commonly used to obtain diagnostics on traditional artworks, such as paintings, frescoes, and polychrome surfaces. Here, it was successfully applied to identify many contemporary pigments/dyes. In fact, this technique made it possible to identify various white pigments (e.g. titanium white, both in rutile and in anatase crystalline forms, and lithopone), blue pigments/dyes (e.g. ultramarine blue, phthalo blue), green pigments/dyes (e.g. viridian, phthalo green) and yellow pigments/dyes (arylide and arylamide yellows, chromium yellow, mars yellow) by observing the differences in the spectral features, in the absorption bands, and in the position of the inflection point of the spectral shapes. Some fillers and extenders, such as kaolinite and other aluminum-silicates, were also identified. Unfortunately, UV-Vis-NIR spectroscopy did not provide accurate results when complex mixtures were investigated. In fact, in these cases, the absorption bands often were shifted a few nanometers or reduced in intensity. Thus, it was impossible to unequivocally identify, with this method only, all the pigments/dyes used. Examples are some orange or violet areas of the *N.Inv.2625* by Fernando Melani and some green areas of the *Caverna dell'Antimateria* by Pinot Gallizio. Furthermore, not all the pigments/dyes could be identified with this technique. An example is the black pigments, which presented a strong absorption band that covered the entire spectral range under investigation. In all these cases, only the integration of the data obtained with UV-Vis-NIR spectroscopy with other methods, such as FT-IR, Raman, XRD and/or XRF spectroscopies, made it possible to completely reconstruct the pictorial palette used by each artist. The main advantage of UV-Vis-NIR spectroscopy is the ability to use easily transportable devices to perform *in situ* analysis on unmoveable objects (e.g. the *Tuttomondo* mural) and on works that could not be transported because of their large size. (e.g. *Caverna dell'Antimateria*), their fragility (e.g. *N.inv. 2635*), or museum constraints (e.g. *La Bandiera Italiana*).

Since FT-IR spectroscopy is a routine method for the analysis of artworks, it was used in this thesis project as both an invasive method (in the transmittance and ATR configuration) and as a non-invasive one (in the total reflectance mode). The main advantage of this technique was the possibility of identifying both inorganic and organic materials. Not only natural/synthetic pigments/dyes, but also fillers/extenders and binders were recognised by this methodology. As did UV-Vis-NIR spectroscopy, the FT-IR method also had some limitations in the identification of complex matrices, especially when the single components had absorption bands that overlapped. For instance, it was very difficult to distinguish between the Naphtol carbamide and the Naphtol A reds found in the *Winsor red Griffin Alkyd Oil Colour* because these dyes have similar spectral features. Another limitation was the higher infrared absorption of inorganic materials compared with some of the organic ones. This limitation is also due to the general low concentration of organic materials in the paint formulations. For example, it was possible to identify some yellow (PY1 and PY3), blue (PB15) and red (PR3) dyes in the pictorial palette of Fernando Melani only after extraction with acetone. As a result, problems in interpreting the IR data, due to the presence of inorganic fillers (such as calcite and barite), which partially masked the absorption bands of the dyes, were avoided. However, not all the pigments could be identified with this technique. For instance, pigments based on cadmium (such as those found in *Winsor red* and *Winsor lemon Griffin Alkyd Oil Colour*) did not present any absorption band in the mid-IR spectral range. In this case, IR data were integrated with an XRF analysis. A possible alternative could have been the study of the IR spectrum in the far-IR range.

Also, as a totally non-invasive preliminary investigation technique, a TR FT-IR analysis was successfully performed on plastic objects. In sum, a series of tests were performed on a set of synthetic polymeric reference samples, and the results provide a useful archive of the TR FT-IR reference spectra for the selected polymers. Although the research was performed in the TR mode, where some of the acquired spectra presented large distortions in their band-shape and position, the results proved that this non-invasive and *in situ* method has significant potential for developing new tools for diagnostics studies of plastics.

Although it is a destructive technique, the principal advantage of Py-GC/MS is the possibility of its use to study both natural and synthetic organic materials. In this thesis project the Py-GC/MS method was performed on reference alkyd paints, and the results accurately described their chemical characterisation. This technique was also used to recognise the degradation products formed during the artificial ageing of the alkyd paints themselves.

Since Py-GC/MS provides information on the overall composition of the micro-samples, it provided information about all of the organic materials present in the samples whether they

were on the surface or in the bulk of the samples. Thus, it was not always possible to determine whether the identified compounds were present in the surface only, in the inner layers of the samples, or in both areas. This was the case for the polyvynilacetate and the polystirenic resins found in a sample from *La Bandiera Italiana*, where it was not possible to determine if both compounds were used as binding media or, instead, if one was used as binder and the other as final varnish.

Lastly, colorimetric analysis was successfully used to obtain information about the colour of painted surfaces. In particular, this method allowed checking colour variations due to artificial ageing of alkyd paints and highlighting the differences in behaviour between the various pigments/dyes present in the paints. Colorimetry was also applied *in situ* on the *Tuttomondo* mural painting to evaluate the colour variations of the surface during the cleaning intervention by scheduling measurement campaigns at different times on the same spots.

In conclusion, as is true of traditional art, non-invasive analytical techniques can be successfully applied to the study of contemporary artists' materials. However, the application of non-invasive methods is not always sufficient for the identification of all of the analysed materials, which means that micro-samples taken from the artwork could be necessary to obtain more exhaustive information about the composition of the object under examination.

The multi-analytical approach used in this thesis project made it possible to study and identify the principal materials constituting some contemporary artworks, which were chosen within the framework of the CoPAC Project. Thus, it was possible to reconstruct the "material palette" used by each selected artist. All of the results found in this study are available to the conservators, curators, and institutions/museums involved in the CoPAC Project. Finally, the collected data can be used to evaluate the conservation-state of the investigated artworks and to identify their risk factors in order to select the most appropriate preservation practices.

REFERENCES

Aceto M., Agostino A., Fenoglio G., Picollo M. (2013) – "Non-invasive differentiation between natural and syntheticultramarine blue pigments by means of 250-900 nm FORS analysis", *Analytical Methods*, 5:4184-4189

Afremow L.C., Vanderberg J.T. (1966) – "High resolution spectra of inorganic pigments and extenders in the mid-infrared region from 1500 cm^{-1} to 200 cm^{-1}", *Journal of Paint Technology*, 38:169–202

Ahmed N.M., Selim M.M. (2010) – "Anticorrosive performance of titanium dioxide-talc hybrid pigments in alkyd paint formulations for protection of steel structures", *Anti-Corrosion Methods and Materials*, 57(3):133-141

Ahmed N.M., Selim M.M. (2011) – "Innovative titanium dioxide-kaolin mixed pigments performance in anticorrosive paints", *Pigment & Resin Technology*, 40(1):4-16

Albano A.P. (1998) – "Reflections on painting, alchemy, nazism: visiting with Anselm Kiefer", *JAIC*, 37(3): 348-361

Albus S., Bonten C., Keßler K., Rossi G., Wessel T. (2007) - *Plastic Art – A Precarious Success Story,* AXA Art Versicherung eds., Cologne, Germany

Aldrovandi A., Picollo M. (2007) - *Metodi di documentazione e indagini non invasive sui dipinti*, Padova, Collana I Talenti, Il Prato eds., 67-83

Alferj P., Cernia F. (1983) – "Gli anni di plastica", Electa Editrice, Milano

Althöfer H. (1991) – *Il restauro delle opera d'arte moderne e contemporanee*, Firenze, Nardini Editore

Athawale V.D., Chamnker A.V. (1997) - "The effect of driers on film properties of alkyd resins", *Pigment & Resin Technology*, 26(6):378-381

Ávár L., Bechtold K. (1999) – "Studies on the interaction of photoreactive light stabilizers and UV-absorbers", *Progress in Organic Coatings*, 35(1-4):11-17

Aydin S., Akçay H., Özkan E., Seniha Güner F., Tuncer Erciyes A. (2004) - "The effects of anhydride type and amount on viscosity and film properties of alkyd resin", *Progress in Organic Coatings*, 51(4):273-279

Bacci M. (2000) - "UV-VIS-NIR, FT-IR and FORS spectroscopies", *Modern Analytical Methods in Art and Archaeology*, edited by E. Ciliberto and G. Spoto, Chemical Analysis Series, Vol.155, Chapter 12:321-361

Bacci M. (2001) - "La misura del colore", *La matiére picturale: fresque et peinture murale*, *Cycle de cours intensif sur les "Sciences at Matériux du Patrimoine Culturel"* Villa Ruffolo-Ravello, 15-20 settembre 1997, 101-109

Bacci M., Bellucci R., Cucci C., Frosinini C., Picollo M., Porcinai S., Radicati B. (2005) - "Fiber Optics Reflectance Spectroscopy in the Entire VIS-IR Range: a Powerful Tool for the Non-invasive Characterization of Paintings," in *Proc. Mat. Res. Soc. Symp*. 852**,** OO.2.4.1-6

Bacci M., Boselli L., Picollo M., Pretzel B. (2008) - "Colour measurement on paintings" in *New trends in Analytical, Environmental and Cultural Heritage Chemistry Developments*, L. Tassi and M. P. Colombini, Eds., RESEARCH SIGNPOST, Trivandrum, 333-344

Bacci M., Boselli L., Picollo M., Radicati B., (2009) - "UV, VIS, NIR Fibre Optic Reflectance Spectroscopy (FORS)" in *Scientific examination for the investigation of paintings. A handbook for conservator restorers*, D. Pinna, M. Galeotti and R. Mazzeo, Eds., European Project ARTECH, Centro Di, Firenze, 197-200

Bacci M., Casini A., Cucci C., Picollo M., Radicati B., Vervat M. (2003) – "Non invasive spectroscopic measurements on the Il ritratto della figliastra by Giovanni Fattori: identification of pigments and colorimetric analysis", *Journal of Cultural Heritage*, 4:329-336

Bacci M., Picollo M., Trumpy G., Tsukada M., Kunzelman D. (2007) – "Non-invasive identification of white pigments on 20th-century oil paintings by using fiber optic reflectance spectroscopy", *Journal of the American Institute for Conservation*, 46(1):27-37

Ballard M.W. (1991) - *Important early synthetic dyes, chemistry, constitution, date, properties*, Conservation analytical Laboratory, Smithsonian Institution, Washington

Bandini M. (1974) - *Pinot Gallizio e il Laboratorio sperimentale d'Alba del Movimento internazionale per una Bauhaus immaginista, 1955-57, e dell'Internazionale situazionista, 1957-60*: Torino, Galleria civica d'arte moderna, 28 maggio-15 luglio 1974

Bardelli A. (2003) - *Keith Haring a Pisa: cronaca di un murales*, Pisa, ETS eds.

Barilli R. (2000) - Haring. Art Dossier, Firenze, Giunti ed.

Bell I.M., Clark R.J.H., Gibbs P.J. (1997) – "Raman spectroscopic library of natural and synthetic pigments (pre- ~1850 AD)", *Spectrochimica Acta Part A: Molecular and Biomolecular Spectroscopy*, 53(12):2159-2179

Berrie B. (1997) – "Prussian blue" in E. West Fitzhugh (Ed.), *Artists' Pigments. A Handbook of Their History and Characteristics*, vol. 3, National Gallery of Art, Oxford University Press, Washington, 191-217

Bertolino G., Comisso F., Dematteis L. Roberto M.T. (2000) – *Pinot Gallizio: l'uomo, l'artista e la città (1902-1964)*, Milano, Mazzotta

Bertolino G., Comisso F., Roberto M.T. (2005) - *Pinot Gallizio. Il laboratorio della scrittura*, Milano, Charta eds

Bonaduce I., Andreotti A. (2009) – "Py-GC/MS of organic paint binders", *Organic Mass Spectrometry in Art and Archeology*, M.P. Colombini and F. Modugno eds., John Wiley and sons

Bonaduce I., Colombini M.P. (2004) – "The characterisation of beeswax in works of art by gas chromatography-mass spectrometry and pyrolisis- gas chromatography-mass spectrometry procedures, *Journal of cromatography A*, 1028:297-306

Bonaduce I., Colombini M.P., Gautier G. (2003) – "Molecular pattern recognition of fresh and aged shellac", *Chromatographia,* 58(5-6):357-364

Bordini S. (2007) – *Arte contemporanea e tecniche. Materiali, procedimenti, sperimentazioni,* Carocci ed., Roma

Borgioli L., Cremonesi P. (2005) – *Le resine sintetiche usate nel trattamento di opere policrome*, Il Prato, Collana I Talenti, Padova

Boulet-Audet M., Buffeteau T., Boudreault S., Daugey N., Pézolet M. (2010) - "Quantitative determination of band distortions in diamond attenuated total reflectance infrared spectra", *The Journal of Physical Chemistry B*, 114(24):8255-61

Brommelle N. (1955) – "Colour and Conservation", *Studies in Conservation*, 2(32):76-85

Bruni S., Caglio S., Poldi G. (2011) – "Ftalocianine e gialli Hansa. Contributo per l'identificazione di pigmenti del XX secolo, anche di restauro, mediante analisi non invasive", *Proceedings of the conference "La scienza per l'arte contemporanea. AIAr 2011"*, Ferrara, March 1-4, 2011

Bruni S., Cariati F., Casadio F., Toniolo L. (1999) – "Spectrochemical characterization by micro-FTIR spectroscopy of blue pigments in different polychrome works of art", *Vibrational Spectroscopy*, 20(1):15-25

Burgio L., Clark R.J.H. (2001) – "Library of FT-Raman spectra of pigments, minerals, pigment media and varnishes, and supplement to existing library of Raman spectra of pigments with visible excitation", *Spectrochimica Acta Part A: Molecular and Biomolecular Spectroscopy*, 57(7):1491-1521

Busto A. (2007) - *Pinot Gallizio e il suo tempo 1953-1964*, Milano, Silvana

Buxbaum G., Ed. (1993) – *Industrial Inorganic Pigments*, VCH, Weinhem

Cacciari M., Celant G. (1997) - *Anselm Kiefer. Catalogo della mostra (Venezia, Museo Correr 1997)*, Milano, Charta

Caki S.M., Risti I.S., Vladislav J.M., Stamenkovi J.V., Stojiljkovi D.T. (2012) – "IR-change and colour changes of long-oil air drying alkyd paints as a result of UV irradiation", *Progress in Organic Coatings*, 73(4):401-40

Calabrese O., Corà B. (2007) - *Anselm Kiefer. Die Grosse Fracht*, Gli Ori, Pistoia

Cambier P. (1986) – "Infrared study of goethite of varying cristallinity ad particle size. I. Interpretation of OH and lattice vibration frequencies", *Clay Minerals*,. 21:191–200

Cappitelli F. (2004) - "THM-GCMS and FTIR for the study of binding media in *Yellow Islands* by Jackson Pollock and *Break Point* by Fiona Banner", *Journal of Analytical and Applied Pyrolysis*, 71(1):405-415

Cappitelli F., Koussiaki F. (2006) - "THM-GCMS and FTIR for the investigation of paints in Picasso's *Still Life, Weeping Woman and Nude Woman in a Red Armchair* from the Tate Collection, London", *Journal of Analytical and Applied Pyrolysis*, 75 (2):200-204

Cappitelli F., Learner T. T.J.S., Cummings A. (2002) - Thermally assisted hydrolysis and methylation-gas cromatography-mass spectrometry for the chemical characterization of

traditional and synthetic binders, in R. Vontobel ed., *Preprints of the 13th Triennial Meeting of the ICOM Committee for Conservation*, *Rio de Janeiro, September 22-27, 2002*, vol. 1:231-237, London; James and James

Casadio F., Toniolo L. (2001) - "The analysis of polychrome works of art: 40 years of infrared spectroscopic investigations", Journal of Cultural Heritage, 2(1):71-78

Celant G., 2008. *Kiefer e Mao: che mille fiori fioriscano*, Skira, Milano

Celant G. (2011) - *Arte Povera. History and stories*, Electa, Milano

Challinor J.M. (2001) - Review: the development and applications of thermally assisted hydrolysis and methylation reactions, *Journal of Analytical and Applied Pyrolysis*, 61 (1-2):3-34

Chalmers J.M., Everall N. J., Ellison S. (1996) - "Specular Reflectance: A Convenient Tool for Polymer Characterisation by FTIR-Microscopy?", *Micron*, 27(5):315-328

Chang J.C.S., Guo Z. (1998) – "Emissions of odorous aldehydes from alkyd paint", *Atmospheric Environment*, 32(20):3581-3586

Chen L. W., Kumanotani J. (1965) - "Effect of method of synthesis of unsaturated fatty acid-modified alkyd resin on the crosslinking behavior of prepolymer: Correlation of molecular weight distribution of prepolymer and degree of crosslinking of the derived film", *Journal of Applied Polymer Science*, 9(11): 3649–3660

Chércoles Asensio R., San Andrés Moya M., de la Roja J. M., Gómez M. (2009) - "Analytical characterization of polymers used in conservation and restoration by ATR-FTIR spectroscopy", Analytical and Bioanalytical Chemistry, 395(7):2081–2096

Chiantore O. (1994) – "Le materie plastiche dell'arte contemporanea e la loro rasformazione e decadimento", in *Arte Contemporanea. Conservazione e Restauro*, Angelucci S. ed., Proceedings of the Conference "Colloquio sul restauro dell'arte moderna e contemporanea", Prato, 4-5 November 1994, Firenze, Nardini, 131-1557

Chiantore O., Rava A. (2005) - *Conservare l'arte contemporanea. Problemi, metodi, materiali, ricerche*, Milano, Electa

Chiavari G., Fabbri D., Mazzeo R., Bocchini P., Galletti G.C. (1995) – "Pyrolisis gas chromatography-mass spectrometry of natural resins used for artistic objects",*Chromatographia*, 41:273-281

Chiavari G., Prati S. (2003) - Analytical pyrolysis as diagnostic tool in the investigation of works of art, *Chromatographia*, 58 (9/10):543-554

Christie R.M., Freer B.G. (1994) – "Colour and constitution relationships in organic pigments: Part 3 – Phtalocyanines", *Dyes and Pigments*, 24(2):113-124

Christie R.M., Standring P.N., Griffiths J. (1988) - "Colour and constitution relationships in organic pigments: Part 1 – Monoazoacetoacetanilides", *Dyes and Pigments*, 9(1):37–56

Ciardelli F., Farina M., Giusti P., Cesca S. (1983) – "Macromolecole, scienza e tecnologia" Vol. I, Pacini Editore, Pisa

Cipriani G., Salvini A., Dei L., Macherelli A., Cecchi F.S., Giannelli C. (2009) – "Recent advances in swollen-state NMR spectroscopy for the study of drying oils", *Journal of Cultural Heritage*, 10(3):388-395

Chittavanich P., Miller K., Soucek M.D. (2012) – "A photo-curing study of a pigmented UV-curable alkyd", *Progress in Organic Coatings*, 73(4):392-400

Clark R.J.H., Cobbold D.G., (1978) – "Characterization of sulfur radical anions in solutions of alkali polysulfides in dimethylformamide and hexamethylphosphoramide and in the solid state in ultramarine blue, green, and red", *Inorganic Chemistry*, 17(11):3169-3174

Clausen C. (2010) – *The universe of Keith Haring*, Milano, Feltrinelli

Coates J. (1998) - "A review of sampling methods for infrared spectroscopy," in *Applied spectroscopy. A compact reference for practitioners*, J. Workman and A. Springsteen, Eds. , Academic Press, San Diego, 50-91

Coe J.T. (2000) – *Unlikely Victory: How General Electric Succeeded in the Chemical Industry*, American Institute of Chemical Engineers, New York, ISBN 0-8169-0819-2

Colombini M.P. (2012) – Private communication

Colombini M.P., Modugno F. (2004) – "Characterisation of proteinaceous binders in artistic paintings by chromatographic techniques", *Journal of Separation Science*, 27:147-160

Colombini M.P., Modugno F., Fuoco R., Tognazzi A. (2002) - "A GC-MS study on the deterioration of lipidic paint binders", *Microchemical Journal*, 73(1-2):175-185

Colombini M.P., Modugno F., Menicagli E., Fuoco R., Giacomelli A. (2000) - "GC-MS characterization of proteinaceous and lipid binders in UV aged polychrome artefacts", *Microchemical Journal*, 67(1-3): 291-300

Corà B. (1990) - Fernando Melani - la casa-studio, le esperienze, gli scritti dal 1945 al 1985, Electa, Milano

Cornell R.M., Schwertmann U. (1996) - *The Iron Oxides Structure, Properties, Reactions, Occurrence and Uses*, VCH, Verlagsgesellschaft, Weinheim

Crowley J. K., Vergo N. (1988) – "Near-Infrared reflectance spectra of mixtures of kaolin-group minerals: use in clay mineral studies", *Clays and Clay Minerals*, 36(4): 310-316

Cucci C., Bigazzi L., Picollo M. (2013) - "Fibre Optic Reflectance Spectroscopy as a non-invasive tool for investigating plastics degradation in contemporary art collections: A methodological study on an expanded polystyrene artwork". *Journal of Cultural Heritage*, 14(4): 290-296

Derrick M.R., Landry J.M., Stulik D.C. (1991) – *Methods in scientific examination of works of art:Infrared Microspectroscopy*, The Getty Conservation Institute, Los Angeles

Derrick M., Stulik D., Ordonez E. (1993) - "Deterioration of cellulose nitrate sculptures made by Gabo and Pevsner", *Saving the twentieth century: The conservation of modern materials* edited by D. Grattan, Ottawa: Canadian Conservation Institute, 169–82

Demichelis R., Noel Y., Zicovich-Wilson C.M., Roetti C., Valenzano L., Dovesi R. (2008) – "*Ab initio* Quantum Mechanical Study of Akdalaite ($5Al_2O_3 \cdot H_2O$: Structure and Vibratonal Spectrum", in *Ab initio Simulation of Crystalline Solids: History and Prospects*, Journal of Physics: Conference Series 117, 012013

Di Bernardo A., Resnick P. (1959) – "Anomalous spectrophotometric behavior of copper phthalocyanine-benzedine yellow misture", *Journal of the Optical Society of America*, 49:480–484

Ebert Jr. A.A., Gottlieb H. B. (1952) - Infrared Spectra of Organic Compounds Exhibiting Polymorphism, *Journal of the American Chemical Society*, 74 (11):2806–2810

Eccher D. (1999) – "Un'anima oscura"*, Art e Dossier*, Firenze, Giunti , 146:40-45

Enlow E., Kennedy J. L., Nieuwland A. A., Hendrix J. E., Morgan S. L. (2005) - "Discrimination of nylon polymers using attenuated total reflection mid-infrared spectra and multivariate statistical techniques", *Applied Spectroscopy*, 59(8):986-992

Erich S.J.F., Laven J., Pel L., Huinink H.P., Kopinga K. (2005) – "Dynamics of cross linking frots in alkyd coatings", *Applied Physics Letter*, 86(12):134105 (3 pages)

Fabbri M., Picollo M., Porcinai S., Bacci M. (2001a) - "Mid-infrared fiber optics reflectance spectroscopy: a non-invasive technique for remote analysis of painted layers. Part I - technical set up", *Applied Spectroscopy*, 55(4):420-427

Fabbri M., Picollo M., Porcinai S., Bacci M. (2001b) - "Mid-infrared fiber optics reflectance spectroscopy: a non-invasive technique for remote analysis of painted layers. Part II – statistical analysis of spectra", *Applied Spectroscopy*, 55(4):428-433

Feller R.L. (1986) – "Barium sulfate-natural and synthetic" in: R.L. Feller (Ed.), *Artists' pigments. A Handbook of Their History and Characteristics*, vol. 1, Cambridge University Press, Cambridge, 1986, 47-64

Fondazione Ferrero (1998) - *Le Langhe e i loro pittori: da Cabutti a Pinot Gallizio e oltre*, Milano, Electa

Gadsden J.A. (1975) - The infrared spectra of minerals and related inorganic compounds, London, Butterworths

Galeotti M., Joseph E., Mazzeo R., Prati S. (2009) - "Fourier Transform Infrared Spectroscopy (FTIR)," in *Scientific examination for the investigation of paintings. A handbook for conservator restorers*, D. Pinna, M. Galeotti and R. Mazzeo, Eds., European Project ARTECH, Centro Di, Firenze, 151-156

Giuntoli D. (1987-1991) – *Schede tecniche* of Casa-Studio Fernando Melani, Comune di Pistoia

Giuntoli D. (2004) - *Fernando Melani – la casa studio*, Gli Ori, Pistoia

Giuntoli D. (2010) - *Fernando Melani - un'esperienza bio-artistica*, Gli Ori, Pistoia

Gori G., Serafini G. (2009) – *Anselm Kiefer. Cette obscure clarté qui tombe des étoils*, Prato, Gli Ori

Gruen J. (2007) – *Keith Haring: la biografia*, Milano, Baldini Castoldi-Dalai

Haring K. (2001) – *Diari* (Diaries) translation by G. Amadasi and G. Picco, Milano, Mondadori

Helwig K. (2007) – "Iron oxide pigments, natural and synthetic" in: Barbara H. Berrie (Ed.), *Artists' pigments, A Handbook of Their History and Characteristics*, vol. 4, Archetype publications, London, 39–109

Herbst W., Hunger K. (1993) - *Industrial Inorganic pigments. Production, properties, applications*, New York, Edited by Gunter Buxbaum, Weinheim

Hodson J., Landert J.A. (1987) – "The analysis of cured paint media and a study of the weathering of alkyd paints by *FT*i.r./PAS", *Polymer* 28(2):251-256

Hofland A. (2012) - "Alkyd resins: From down and out to alive and kicking", *Progress in Organic Coatings*, 73(4):274-282

Hubert J.C., Venderbosch R.A.M., Muizebelt W.J., Klaasen R.P., Zabel K.H. (1997) – "Singlet oxygen drying of alkyd resins and model compounds", *Journal of Coatings Technology*, 69(869):59-64

Hunt C. P., Moskovitz B. Banerjee S. K. M. (1995) – "Magnetic properties of rocks and minerals", *Rock Physics and Phase Relations, A Handbook of Physical* Constants, T. J. Ahrens eds, Washington, USA, 189-205

Hunt G. R., Salisbury J. W., Lenhoff C. J. (1971), "Visible and near-infrared spectra of minerals and rocks: Oxides and Hydroxides", Modern Geology, 2:195-205

Johnston R.M. (1967) – "Spectrophotometry for the analysis and description of color", *Journal of Paint Technology*, 39:346-354

Johnston R.M., Feller R.L. (1963) – "The use of differential spectral curve analysis in the study of museum objects", *Dyestuffs*, 44:1–10

Johnston-Feller R. (2001) - *Color science in the examination of museum objects: non-destructive procedures*, Oxford University Press

Kalenda P., Veselý D., Kalendová A., Šťáva V. (2010) - "Ferrocene-based catalyst systems for alkyd paint drying", *Pigment & Resin Technology*, 39(6):342-347

Kalendová A., Veselý D., Kalenda P. (2010) - "Contribution of inorganic pigments to the formation of paint films from oxypolymerising drying paints", *Pigment & Resin Technology*, 39(5):255-261

Karayannidis G.P., Achilias D.S., Sideridou I.D., Bikiaris D.N. (2005) - "Alkyd resins derived from glycolized waste poly(ethylene terephthalate)", *European Polymer Journal*, 41(2):201-210

Kaul B. L., Wihan L. (1988) - "Carbazole Dioxazine Violet" in Lewis P. A. (1988), *Pigment Handbook*, vol. 1, John Wiley and sons, New York

Keneghan B. (1998) - "Assessing plastic collections in museums by FTIR spectroscopy", *Postprints of IRUG2*, September 1995, Victoria & Albert Museum, London, 21-24

Kienle R.H., Ferguson C.S. (1929) - "Alkyd Resins as Film-Forming Materials", *Industrial and Engineering Chemistry*, 21(4):349-352

Knudsen B.I. (1966) – "Copper phthalocyanine. Infrared absorption spectra of polymorphic modifications", *Acta Chemica Scandinavica*, 20:1344-1350

Kolossa A. (2009) – *Keith Haring. 1958-1990 A life for art*, Köln, Taschen

Kortüm G. (1969) - *Reflectance spectroscopy*, New York, Springer Verlag

Kühn H., Curran M. (1986) – "Chrome yellow and other chromate pigments" in: R.L. Feller (Ed.), *Artists' pigments. A Handbook of Their History and Characteristics*, vol. 1, Oxford University Press, New York, 187–200

Kulesza P.J. (1996) – "In situ FT-IR/ATR spectroelectrochemistry of Prussian blue in the solid state", *Analytical Chemistry*, 68(14):2442-2446

La Nasa J. (2011) – *Studio dell'invecchiamento di resine sintetiche utilizzate nell'arte contemporanea mediante tecniche cromatografiche e spettroscopia infrarossa*, Master degree thesis; University of Pisa

La Nasa J., Degano I., Modugno F., Colombini M.P. (2013) – "Alkyd paints in art: Characterization using integrated mass spectrometry", *Analytica Chimica Acta*, 797:64-80

Laganà A., Keneghan B. (2012) - "Which plastics are in my collectiuons? The need for a plastic reference sample collection (SamCo)" in: B. Lavédrine, A. Fournier, G. Martin eds, *Preservation of Plastic artefacts in museum collections*. Comité des travaux historiques et scientifiques, France, CTHS, 37-42

Lake S., Lomax S.Q. (2007) – "Arylide (Hansa) yellow pigments", in: B.H. Berrie (Ed.), *Artists' Pigments. A Handbook of Their History and Characteristics*, vol. 4, Archetype publications, London, 179–222

Lattuati-Derieux A., Egassea C., Thao-Heu S., Balcar N., Barabant G., Lavédrine B. (2013) - "What do plastics emit? HS-SPME-GC/MS analyses of new standard plastics and plastic objects in museum collections", *Journal of Cultural Heritage*, 14(3): 238-247

Laver M. (1997) – "Titanium Dioxide Whites" In: E. West Fitzhugh (Ed.), *Artists' Pigments. A Handbook of Their History and Characteristics*, vol. 3, National Gallery of Art, Oxford University Press, Washington, 295-355

Lazzari M., Chiantore O. (1999) – "Drying and oxidative degradation of linseed oil", *Polymer degradation and stability*, 65:3003-3013

Learner T.J.S. (2001) - The analysis of synthetic paints by pyrolysis-gas chromatography-mass spectrometry (PyGCMS), *Studies in Conservation*, 46(4):225-241

Learner T.J.S. (2003) - "Modern paints", *Sackler NAS Colloquium-Scientific examination of Art: Modern Techniques in Conservation and Analysis*, National Academy of Sciences, Washington, D. C., March 19-21, 2003:137-151

Learner T.J.S. (2004) - *Analysis of modern paints*, Los Angeles, Getty Conservation Institute

Learner T.J.S. (2007) - "Modern paints: uncovering the choices", in *Modern Paints Uncovered*: Proceedings From the Modern Paints Uncovered Symposium, (May 16-19, 2006, Tate Modern, London), ed. Thomas J. S. Learner, Patricia Smithen, Jay W. Krueger, and Michael R. Schilling, 129-39. Getty Conservation Institute Symposium Proceedings Series. Los Angeles: Getty Conservation Institute

Leona M. Winter J. (2001) – "Fiber optics reflectance spectroscopy: a unique tool for the investigation of Japanese paintings", Studies in conservation, 46(3):153-162

Lewis P.A. (1987). *Pigment Handbook. Application and markets* 1,2, John Wiley and Sons Ltd, United States.

Lin K.F. (2005) - "Paints, Varnishes, and Related Products" in *Bailey's industrial oil and fat products*, sixth edition, edited by Shahidi Fereidoon, John Wiley & Sons, Vol. 6, Chapter 9, 307-351

Lindner S., Vitoria A., Alba L. (2004) – "Anselm Kiefer at the Guggenheim Museum Bilbao: towards a new methodology for the preventive conservation of contemporary artworks", *Modern Art, New Museums*, Contributions to the XX IIC Congress, Bilbao September 13-17, 2004, 21-24

Littlejohna D., Pethrick R. A., Quye A., Ballany J.M. (20139 - "Investigation of the degradation of cellulose acetate museum artefacts", *Polymer Degradation and Stability*, 98 (1):416–424

Loan L.D. (1972) – "Peroxide crosslinking reactions of polymers", *Pure and Applied Chemistry*, 30(1-2):173-180

Lucarini V., Saarinen J. J., Peiponen K. E., Vartiainen E. M. (2005) - "Kramers Kronig relations in optical materials research" in: *Springer Series in Optical Sciences* 110, ISBN 3-540-23673-2. ISSN 03242-4111

Luo M.R., Cui G., Rigg B. (2001) – "The development of the CIE 2000 colour-difference formula CIEDE2000", *Color research and application*, 26(5):340-350

Madejová J. (2003) – "FTIR techniques in clay mineral studies", *Vibrational Spectroscopy* 31(1):1–10

Mallégol J., Gardette J.L., Lemaire J. (1999) – "Long-term behavior of oil-based varnishes and paints. I. Spetroscopic analysis of curing drying oils", *Journal of the American Oil Chemists' Society*, 76(8):967-976

Mallégol J., Gardette J.L., Lemaire J. (2000) – "Long-term behavior of oil-based varnishes and paints. Photo- and thermooxidation of cured linseed oil", *Journal of the American Oil Chemists' Society*, 77(3):257-263

Mallégol J., Gonon L., Commereuc S., Verney V. (2001) – "Thermal (DSC) and chemical (iodometric titration) methods for peroxides measurements in order to monitor drying extent of alkyd resins", *Progress in Organic Coatings*, 41(1-3)-176

Mallégol J., Barry A.M., Ciampi E., Glover P.M., McDonald P.J. (2002) – "Influence of drier combination on through-drying in waterborne alkyd emulsion coatings observed with magnetic resonance profiling", *Journal of Coatings Technology*, 74(933):113-124

Marshall G.L., Lander J.A. (1985) – "The characterisation of alkyd paint binders using ^{13}C-NMR spectroscopy", *European Polymer Journal*, 21(11):949-958

Marshall G.L. (1986) – "A ^{13}c-NMR study of stoving alkyd systems" *European Polymer Journal*, 22(3):217-230

McIntire J.E. (2003) - "The Historical Development of Polyesters" in *Modern Polyesters: Chemistry and Technology of Polyesters and Copolyesters*, edited by J. Scheirs and T. E. Long, John Wiley & Sons, Chapter 1, 3-28

McQuarrie D., Rock P.A., Donald A. (1991) - *General Chemistry*, 3rd ed., WH Freeman & Co, New York

Melani F. (1971) - autobiographical note in Flash Art, V (27):8

Miliani C., Rosi F., Brunetti B. G., Sgamellotti A. (2010) - "In Situ Noninvasive Study of Artworks: The MOLAB Multitechnique Approach", *Accounts of Chemical Research*, 43(6):728–738

Mohammed Noori Z.T. (2011) – "Optical Characteristics of CdSSe Films Prepared by Thermal Evaporation Technique", Baghdad Science Journal, 8(1):155-160

Mukhopadhyay R. (2004) -"Portable FTIR spectrometers get moving" , *Analytical Chemistry*, 76(19): 369A–372A

Muizebelt W.J., Hubert J.C., Venderbosch R.A.M. (1994) – "Mechanistic study of drying of alkyd resins using ethyl linoleate as a model substance, *Progress in Organic Coatings*, 24(1-4):263-279

Muizebelt W.J., Hubert J.C., Venderbosch R.A.M., Lansbergen A.J.H. (1998) – "Aluminum compounds as additional crosslinkers for air-drying high-solids alkyd paints", *Journal of Coatings Technology*, 70(882):53-59

Muizebelt W.J., Hubert J.C., Nielen M.W.F., Klaasen R.P., Zabel K.H. (2000) – "Crosslink mechanisms of high-solids alkyd resins in the presence of reactive diluents", *Progress in Organic Coatings*, 40 (1-4):121-130

Nakamoto K. (1978) - *Infrared and Raman Spectra of Inorganic and Coordination Compounds*, John Wiley & Sons, Inc., Publication, New York

Naranjo A. C., Osswald T. A., Sierra J.D. (2008) - *Plastics Testing and Characterization: Industrial Applications*, Munich, Germany, Hanser Verlag Pubs.

Newman R. (1979) – "Some applications of infrared spectroscopy in the examination of painting materials", *Journal of the American Institute for Conservation*, 19(1):42-62

Oleari C. editor (2008) - *Misurare il colore. Fisiologia della visione a colori. Fotometria - Colorimetria e norme internazionali*, Milano, Hoepli

Paris C., Lecomte S., Coupry C. (2005) - "ATR-FTIR spectroscopy as a way to identify natural protein-based materials, tortoiseshell and horn, from their protein-based imitation, galalith", *Spectrochimica Acta Part A: Molecular and Biomolecular Spectroscopy*, 62(1-3):532–538

Pastorelli G., Trafela T., Taday P. F., Portieri A., Lowe D., Fukunaga K., Strlič M. (2012) - "Characterisation of historic plastics using terahertz time domain spectroscopy and pulsed imaging", *Analytical and Bioanalytical Chemistry*, 403(5):1405–1414

Picollo M., Bacci M., Magrini D., Radicati B., Trumpy G., Tsukada M., Kunzelman D. (2007) - "Modern white pigments: their identification by means of non invasive ultraviolet, visible and infrared fiber optic reflectance spectroscopy", in *Modern Paints Uncovered*: Proceedings From the Modern Paints Uncovered Symposium, (May 16-19, 2006, Tate Modern, London), ed. Thomas J. S. Learner, Patricia Smithen, Jay W. Krueger, and Michael R. Schilling, 129-39. Getty Conservation Institute Symposium Proceedings Series. Los Angeles: Getty Conservation Institute

Picollo M., Porcinai S. (1999) – "Non destructive spectroscopic investigations of artworks", *Recent research developments in applied spectroscopy*, 2:125-135

Plesters J. (1993) – "Ultramarine blue, natural and artificial", in R. Ashok (Ed.), *Artists' Pigments. A Handbook of Their History and Characteristics*, vol. 2, National Gallery of Art, Oxford University Press, Washington, 37-65

Ploeger R., Chiantore O. (*in press*) - "Characterization and Stability Issues of Artists' Alkyd Paints", *Smithsonian contributions to museum conservation*, 3:89-95

Ploeger R., Chiantore O., Scalarone D., Poli T. (2011) - "Mid-Infrared Fiber-Optic Reflection Spectroscopy (FORS) Analysis of Artists' Alkyd Paints on Different Supports", *Applied Spectroscopy*, 65(4):429-435

Ploeger R., Musso S., Chiantore O. (2009a) - "Contact angle measurements to determine the rate of surface oxidation of artists' alkyd paints during accelerated photo-ageing", *Progress in Organic Coatings*, 65(1):77-83

Ploeger R., Scalarone D., Chiantore O. (2007) – "Ageing properties and stability of artists' alkyd paints", *Conservation Science 2007* Papers from the conference held in Milan, Italy May 10-11, 2007, edited by Joyce H. Townsend, Lucia Toniolo and Francesca Cappitelli, 272-273

Ploeger R., Scalarone D., Chiantore O. (2008) - "The characterization of commercial artists' alkyd paints", *Journal of Cultural Heritage*, 9(4):412-419

Ploeger R., Scalarone D., Chiantore O. (2009b) - "Thermal analytical study of the oxidative stability of artists' alkyd paints", *Polymer Degradation and Stability*, 94(11):2036-2041

Poli F. (1992) - *Pinot Gallizio nell'Europa dei dissimmetrici*, Milano, Mazzotta

Potdar S. (1988) – "Toluidine, para, and chloronitroaniline reds", in P.A. Lewis (Ed.), *Pigment Handbook, Properties and Economics*, second ed., vol. 1, Wiley Interscience, John Wiley & Sons, Inc., Publication, New York, 441–452

Pugliese M. (2006) – *Tecnica mista. Materiali e procedimenti nell'arte del XX secolo*, Milano, Paravia Bruno Mondadori Editori

Pyle D., Pearce E. eds (2001) - *The oil colour book*, Published by Winsor & Newton, Middlesex, Colart Fine Art and Graphics Limited

Quillen Lomax S., Schilling M.R., Learner T.J.S. (2007). "The identification of synthetic organic pigments by FTIR and DTMS", in *Modern Paints Uncovered*: Proceedings From the Modern Paints Uncovered Symposium, (May 16-19, 2006, Tate Modern, London), ed. Thomas J. S. Learner, Patricia Smithen, Jay W. Krueger, and Michael R. Schilling, 129-39. Getty Conservation Institute Symposium Proceedings Series. Los Angeles: Getty Conservation Institute

Ramaswamy V., Vimalathithan R.M., Ponnusamy V. (2010) – "Synthesis of well dispersed, elliptical shaped Barium Sulphate nanoparticles via Water-Chloroform mixed solvent", *Archives of Physics Research*, 1(4):217-226

Ranaldi R., Giuntoli D., Landini L., Chiavacci G. (2009) - "Fernando Melani – L'uomo e l'artista", Via del vento eds, *periodico quadrimestrale Le Streghe*, Pistoia

Rava A. (1994) – "Il restauro dell'arte contemporanea dal dopoguerra, nuovi materiali e nuovi criteri d'intervento", in *Arte Contemporanea. Conservazione e Restauro*, Angelucci S. ed., Proceedings of the Conference "Colloquio sul restauro dell'arte moderna e contemporanea", Prato, 4-5 November 1994, Firenze, Nardini

Rawlins I.F.G. (1936) – "Studies in the colorimetry of paintings, I", *Technical studies in the field of the fine arts*, 4(4):179-186

Rawlins I.F.G. (1937) – "Studies in the colorimetry of paintings, II", *Technical studies in the field of the fine arts*, 5(3),150-156

Renuka Devi K.B., Madivanane R. (2012) – "Normal coordinate analysis of poly vinyl acetate", IRACST-Engineering Science and Technology: An International Journal (ESTIJ), 2(4):795-799

Repetto M., Balla P. (2000) - *Dèrive Gallizio*, documentary film, written and directed by Monica Repetto and Pietro Balla, Monica Repetto and Fondazione Ferrero Onlus production

Roberto M.T. and Comisso F. (2001) – Pinot Gallizio. Catalogo generale delle opere 1953 – 1964, Milano, Gabriele Mazzotta eds

Robin M.B., Simpson W.T. (1962) – "Assignment of Electronic Transitions in Azo Dye Prototypes", *The Journal of Chemical Physics*, 36(3):580-588

Rumma L., Belpoliti M., Andreotti R., De Melis F. (2006) - *Anselm Kiefer. Merkaba*, Milano, Charta

Sacchi R., Addeo F., Paolillo P. (1997) – "^{1}H and ^{13}C NMR of virgin olive oil. An overview", *Magnetic Resonance in Chemstry*, 35(13):S133-S145

Saikia B.J., Parthasarathy G., Sarmah N.C. (2008) – "Fourier transform infrared spectroscopic estimation of cristallinità in SiO_2 based rocks", *Bullettin of Material Science*, 31(5):775-779

Saunders D. (1986) - "The measurement of colour change in paintings;" *European Spectroscopy News* 67:10–18

Scalarone D., Chantore O. (2009) – "*Py-GC/MS of Natural and Synthetic Resins", Organic Mass Spectrometry in Art and Archeology*, M.P. Colombini and F. Modugno eds., John Wiley and sons

Scherrer N.C., Zumbuehl S., Delavy F., Fritsch A., Kuehnen R. (2009) – "Synthetic organic pigments of the 20th and 21st century relevant t artist's paints: Raman spectra reference collection", *Spectrochimica Acta Part A:Molecular and Biomolecular Spectroscopy*, 73(3):505–524

Schunck R.P., Hunger K. (1988) – "Hansa® Yellows and Oranges" in P.A. Lewis, *Pigment Handbook*, Whiley-Interscience, 1, 535-546

Schwertmann U., Cambier P., Murad E. (1985) - "Properties of goethites of varying cristallinity", Clays and Clay Minerals, 33(5):369–378

Scicolone G.C. (1993) – *Il restauro dei dipinti contemporanei.. Dalle tecniche d'intervento tradizionali alle metodologie innovative*, Firenze, Nardini Editore

Sharma G., Wu W., Dalal E.N. (2005). "The CIEDE2000 color-difference formula: implementation notes, supplementary test data, and mathematical observations", *Color research and application*, Vol.30-1, pp.21-30

Shashoua Y. (2008) - *Conservation of plastics. Materials science, degradation and preservation*, Butterwoth-Heinemann Editors

Shearer C. L. (1990) – "Use of FT-IR in the Conservation of Twentieth Century Objects", *MRS Spring meeting Proceedings*, Doyal, 1990, doi:10.1557/PROC-185-813

Sheff D. (1989), "Keith Haring: An Intimate Conversation", *Rolling Stone*, August 10, p. 61

Sherman D.M., Waite T.D. (1985) – "Electronic spectra of Fe(III) oxides and oxides hydroxides in the near IR to near UV", *American Mineralogist*, 70:1262–1269

Schilling M.R., Mazurek J., Learner T.J.S. (2007) - "Studies of modern oil-based artists' paint media by gas chromatography/mass spectrometry", in *Modern Paints Uncovered*: Proceedings From the Modern Paints Uncovered Symposium, (May 16-19, 2006, Tate Modern, London), ed. Thomas J. S. Learner, Patricia Smithen, Jay W. Krueger, and Michael

R. Schilling, 129-39. Getty Conservation Institute Symposium Proceedings Series. Los Angeles: Getty Conservation Institute

Sharma G., Wu W., Dalal E.N. (2005) – "The CIEDE2000 color difference formula: implementation notes, supplementary test data, and mathematical observations", *Color research and application*, 30(1):21-30

Socrates G. (1998) – *Infrared characteristic group frequencies, tables and charts*, 2nd edition, John Wiley and Sons, New York

Sonoda N. (1999) – "Characterization of organic azo-pigments by pyrolysis-gas chromatography", *Studies in Conservation*, 44(3):195 – 208

Soucek M.D., T. Khattab T., Wu J. (2012) - "Review of autoxidation and driers", *Progress in Organic Coatings*, 73(4):435-454

Springsteen A. (1998) - "Reflectance Spectroscopy: an overview of classification and techniques," in *Applied spectroscopy. A compact reference for practitioners*, J. Workman and A. Springsteen, Eds. (Academic Press, San Diego), 194-224

Spyros A. (2003) – "Characterization of unsaturated polyester and alkyd resins using one- and two-dimensional NMR spectroscopy", *Journal of Applied Polymer Science*, 88(7):1881-1888

Spyros A., Anglos D. (2004) – "Study of Aging in Oil Paintings by 1D and 2D NMR Spectroscopy", *Analytical Chemistry*, 76(17):4929-4936

Spyros A., Anglos D. (2006) – "Studies of organic paint binders by NMR spectroscopy, *Applied Physics A* 83(4):705-708

Thanamongkollit N., Soucek M.D. (2012) - "Synthesis and properties of acrylate functionalized alkyds via a Diels–Alder reaction", *Progress in Organic Coatings*, 73(4):382-391

Tomas Rubio M. (2006) - *UV-Vis-IR spectroscopic characterization of two modern blue pigments: blue phthalocyanine and blue indanthrene*, 1st level Master thesis in "Materials and diagnostic techniques for Cultural Heritage", University of Pisa

Vahur S., Teearu A., Leito I. (2010) – "ATR-FT-IR spectroscopy in the region of 550–230cm^{-1} for identification of inorganic pigments", *Spectrochimica Acta Part A: Molecular and Biomolecular Spectroscopy*, 75(3):1061-1072

Van Alphen M. (1998) - *Paint Film Components*, Monograph, general series 2, National Environmental Health Forum, Australia

van den Berg J.D., van den Berg K.J., Boon J.J. (2001) - "Determination of the degree of hydrolysis of oil paint samples using a two-step derivatisation method and on-column GC/MS", *Progress in Organic Coatings*, 41(1-3):143-155

van den Berg J.D., van den Berg K.J., Boon J.J. (2002) - "Identification of non-cross-linked compounds in methanolic extracts of cured and aged linseed oil-based paint films using gas chromatography-mass spectrometry", *Journal of Chromatography A*, 950(1-2):195-211

van der Marel H.W., Beutelspacher H. (1976) - *Atlas of infrared spectroscopy of clay minerals and their admixtures*, Elsevier, Amsterdam

van Gorkum R., Bouwman E. (2005) – "The oxidative drying of alkyd paint catalysed by metal complexes", *Coordination Chemistry Reviews*, 249(17–18):1709-1728

Van Oosten T. (2012), coordinated by - "Identification and characterization of plastic artefacts" in: B. Lavédrine, A. Fournier, G. Martin eds, *Preservation of Plastic artefacts in museum collections*. Comité des travaux historiques et scientifiques, France, CTHS, 29-109

Vareckova D., Podzimek S., Lebduska J. (2006) - "Characterization of alkyd resins by size exclusion chromatography coupled with a multi-angle light scattering photometer", *Analytica Chimica Acta*, 557(1–2):31-36

Van Alphen M. (1998) - *Paint Film Components*, Monograph, general series 2, National Environmental Health Forum, Australia

Vandenabeele P., Moens L. Edwards H.G.M. Dams R. (2000) – "Raman spectroscopic database of azo pigments and application to modern art studies", *Journal of Raman spectroscopy*, 31(6):509-517

Veaute M., Cottrer C. (2010) – "Promote the memory of the future contemporary art and its conservation", *Conservazione dell'arte contemporanea: temi e problemi, un'esperienza didattica-Conservation of contemporary art: themes and issues. A didactic experience*, Iazurlo P. and Valentini F. eds, Il Prato, Padova, 69-72

Vescovo M. (1994) - *Pinot Gallizio: immoralità del perimetro*, Milano, Mazzotta

Vicente J.P., Baumer U., Stege H., Lutzenberger K., Gimeno Adelantado V. (2009) – "Characterization of Commercial Synthetic resins by Pyrolysis-Gas Chromatography/Mass Spectrometry: Application to Modern Art and Conservation*", Analitical Chemistry*, 81(8): 3180-3187

Waenting F. (2008) - "Plastics in art", M. I. Verlag, GmBH & Co, Petersberg, eds. Germany

Wang X., Luo X. (2004) - "A polymer network based on thermoplastic polyurethane and ethylene–propylene–diene elastomer via melt blending: morphology, mechanical properties, and rheology", *European Polymer Journal*, 40(10):2391-2399

Weakleim H. (1962) - Optical spectra of Ni^{2+}, Co^{2+}, and Cu^{2+} in tetrahedral sites in crystals, *Journalof Chemical Physics*, 36:2117-2140

Wexler H. (1964) – "Polimerization of drying oils", *Chemical Reviews*, 64(6):591-611

Wyszecki G., Stiles W.S. (1982) – *Color science. Concepts and methods, Quantitative data and Formulae*, John Wley and Sons, 2nd edition

Wutticharoenwong K., Dziczkowski J., D. Soucek M.D. (2012) - "Tung based reactive diluents for alkyd systems: Film properties", *Progress in Organic Coatings*, 73(4):283-290

Ye G., Courtecuisse F., Allonas X., Ley C., Croutxe-Barghorn C., Raja P., Taylor P., Bescon G. (2012) - "Photoassisted oxypolymerization of alkyd resins: Kinetics and mechanisms", *Progress in Organic Coatings*, 73(4):366– 373

Zendri E. (2010) – "Future developments and issues in the studing of contmporary works", *Conservazione dell'arte contemporanea: temi e problemi, un'esperienza didattica-Conservation of contemporary art: themes and issues. A didactic experience*, Iazurlo P. and Valentini F. eds, Il Prato, Padova, 52-54

ACKNOWLEDGMENTS

I would like to thank the many people and institutions that helped me in my PhD research.

At first, I would like to acknowledge my tutor, Dr. Marcello Picollo, for giving me the possibility to develop this research with autonomy but never alone, and my co-tutor, Prof. Antonella Salvini, for her support.

Special thanks also to Giovanni Bartolozzi and Dr. Costanza Cucci for their help and assistance.

I also greatly acknowledge Prof. Manfred Schreiner, and his collaborators Dr. Valentina Pintus and Dr. Wilfried Vetter, for having me for three months at the Institute of Science and Technology in Art-Academy of Fine Arts (Vienna, Austria) where they introduced me with the THM-GC/MS technique.

A special thanks to the researchers and conservators that shared with me information about the materials studied within the framework of the CoPAC Project: Prof. MariaPerla Colombini, Dr. Vincenzo Palleschi, Prof. Vincenzo Barone and their research groups, Antonio Rava, Will Shank and Mauro Matteini.

A great acknowledge to the museum and institutions that permitted to analyse the artworks studied in this research activity: the Pisa City Council for the study of the Keith Haring *Tuttomondo* mural; the "Luigi Pecci Center for Contemporary Art" of Prato for the study of the *Caverna dell'Antimateria* by Pinot Gallizio; the S.Giorgio Library of Pistoia for the study of *Die Grosse Fracht* by Anselm Kiefer; the Fernando Melani's Studio-Home for the study of Melani's artworks. Thanks also to Archive Gallizio for having provide useful information about Gallizio's artistic technique and to the artist Patrizia Zara for having open the doors of her atelier.

I would like to thanks all the researches who helped and supported me in performing part of my research at their laboratories: Susanna Bracci, Dr. Emma Cantisani and Dr. Donata Magrini (ICVBC-CNR); Maurizio Peruzzini and Dr. Vincenzo Mirabello (ICCOM-CNR); Dr. Benedetto Pizzo (IVALSA-CNR); Monica Galeotti (OPD);Prof. Donatella Giomi and Dr. Giacomo Cipriani (Department of Chemistry "Ugo Schiff" of the University of Florence).

Many thanks also to Prof. Oscar Chiantore, Dr. John K. Delaney and Marvin Gore for their helpful comments and background information.

Thanks to everyone because all of you have been important in supporting this research.

E dopo i ringraziamenti formali finalmente posso ringraziare di cuore tutti coloro che mi hanno supportato in questi tre intensi anni (e non c'è bisogno dei cognomi, tanto sapete a chi mi riferisco).
Il primo grazie, di cuore, all'insostituibile Marcello per aver sempre creduto in me, per la stima e l'affetto reciproco, per avermi sopportato sempre e comunque, perché un tutor così dove lo ritrovo?
Un grazie immenso a Giovanni, perché senza di lui gran parte di questa tesi non sarebbe stata scritta.
Grazie per l'assistenza, la sopportazione, l'amicizia, le risate, la scelta della musica da ascoltare in ufficio, le news dal mondo rosso-nero e per tutto il resto che in poche righe non entra.
Grazie a Costanza, Bruno, Lorenzo, Andrea, Marco, Donatella, Ago, Roberto e a tutti gli altri ricercatori, tecnici e amministrativi che mi hanno fatto sentire in IFAC come in una grande famiglia.
Grazie anche alle "compagne di sventura" Roberta, Floriana, Elisa e Anna per le chiacchiere, i pranzi, i gossip, le risate ... perché solo se fai un dottorato al CNR puoi capire certe cose.
Ringrazio anche Valentina, Marta, Monica e Irene perché senza di loro la mia lunga estate austriaca non sarebbe stata la stessa.
Un grazie immenso, di cuore, anche alle mie più care amiche Valentina, Maria e Lavinia per essermi state vicine sempre, con cui da anni ormai condivido gioie e dolori e che spero di continuare ad avere al mio fianco anche in futuro, perché non c'è tesoro più grande dell'amicizia vera. Infine grazie ai miei genitori, per quella che sono e per dove sono arrivata, senza di loro tutto questo non sarebbe stato possibile. Dimenticavo ... stavolta voglio ringraziare anche me stessa, per non aver mollato mai anche quando la vita voleva mettermi i bastoni tra le ruote.
Grazie a tutti per essere parte della mia vita. Comunque vada sarà un successo anche solo per il fatto di avervi incontrato.